

qQB
723
.H2
I54
1988

Infrared Observations of Comets Halley and Wilson and Properties of the Grains

*Summary of a workshop held at
Cornell University,
Ithaca, New York
August 10-12, 1987*

The NASA logo, consisting of the word "NASA" in a bold, sans-serif font, is positioned at the bottom right of the page. A thick horizontal line runs across the page just above the logo.

Infrared Observations of Comets Halley and Wilson and Properties of the Grains

Martha S. Hanner, *Editor*
Jet Propulsion Laboratory
California Institute of Technology
Pasadena, California

Summary of a workshop sponsored by the
National Aeronautics and Space Administration
Washington, D.C., and held at
Cornell University
Ithaca, New York
August 10-12, 1987



National Aeronautics
and Space Administration

Scientific and Technical
Information Division



The nucleus of Comet Halley taken by the Halley Multicolour Camera on the ESA Giotto spacecraft. This picture is a composite of 60 of the images of Comet Halley that were taken when the spacecraft flew to within 600 km of the nucleus at 00:03:02 UT on March 14, 1986. Photo courtesy of the Max Planck Institut für Aeronomie, Federal Republic of Germany.

PREFACE

Comet Halley provided an unprecedented opportunity not only to observe a comet with a variety of modern techniques but also to compare remote observations with *in situ* sampling. Many of the exciting new discoveries, such as the detection of a $3.4\mu\text{m}$ signature of organic material, were made at infrared wavelengths. The Kuiper Airborne Observatory yielded the first spectrophotometry of a comet at infrared wavelengths inaccessible from the ground.

It became clear at the 1986 Heidelberg Symposium that the synthesis and interpretation of the infrared observations required an interdisciplinary approach, drawing on our knowledge of dust composition from the Halley probes, interplanetary and interstellar grains, as well as laboratory studies of grain properties.

The aim of this Workshop, then, was to bring together a group with varied expertise to review the infrared observations and relate them to optical properties and composition of the cometary grains.

The Workshop was held at Cornell University, August 10-12, 1987, hosted by the Astronomy Department. The program consisted of informal summary talks and discussion directed towards key questions in each of the five sessions. Contributed papers were presented as poster papers. The scope of the Workshop was restricted to the infrared, and primarily to the dust, in order to focus on a limited number of issues.

It was felt that formal Proceedings for this workshop were not appropriate, for the interpretation of the infrared data is only beginning. Instead, this report has been prepared by the Organizing Committee as a working paper, highlighting the new results and the unsolved puzzles and suggesting directions for future research. Relation to NASA programs is discussed and recommendations are made for future infrared observations of comets and supporting laboratory investigations.

Each of the five chapters covers one of the sessions and was written by the session chairs, with contributions from many participants. Extended abstracts of presented papers are appended.

We hope that readers will view this report not as a complete treatment of the subjects, but rather as a summary reflecting the discussions that took place. The ultimate product of the Workshop will be the scientific papers resulting from the ideas explored during three days of lively debate.

Martha S. Hanner
Workshop Organizer and Editor

ACKNOWLEDGEMENTS

It is a pleasure to thank Dr. Terry Herter and Sylvia Corbin of the Cornell Astronomy Department for the local arrangements that made the Workshop so pleasant. Sylvia Corbin efficiently carried out the final typing and editing of the report. Tables 2-3 and 2-4 were drawn by CRSR's illustrator, Barbara Boettcher. We thank Dr. Jurgen Rahe, Planetary Astronomy Discipline Specialist, NASA Solar System Exploration Division, for his support. The success of this workshop depended on the enthusiasm and hard work of the Organizing Committee: Jesse Bregman, Humberto Campins, Robert Gehr, Terry Herter, Ray Russell, and Alan Tokunaga. Roger Knacke, Discipline Specialist for the Infrared Net of the International Halley Watch, generously contributed his ideas, although he was unable to attend. Finally, I would like to thank all the participants for their ideas and lively discussion and for their contributions to this report.

Martha Hanner

PARTICIPANTS

Organizing Committee

Jesse D. Bregman
Mail Stop 245-6
NASA-Ames Research Center
Moffett Field, CA 94035

Humberto Campins
Planetary Science Institute
2030 East Speedway, #201
Tucson, AZ 85719

Robert D. Gehrz
Department of Astronomy
University of Minnesota
116 Church Street, S.E.
Minneapolis, MN 55455

Martha S. Hanner
Mail Stop 183-401
Jet Propulsion Laboratory
4800 Oak Grove Drive
Pasadena, CA 91109

Terry L. Herter
Department of Astronomy
226 Space Sciences Building
Cornell University
Ithaca, NY 14853

Ray W. Russell
The Aerospace Corporation
M2-266, P.O. 92957
Los Angeles, CA 90009

Alan Tokunaga
Institute for Astronomy
University of Hawaii
2680 Woodlawn Drive
Honolulu, HI 96822

* * * * *

Vincent Anicich
Mail Stop 183-601
Jet Propulsion Laboratory
4800 Oak Grove Drive
Pasadena, CA 91009

Paul Bernhardt
Code 4780
National Research Laboratory
Washington DC 20375

Timothy Y. Brooke
Department of Earth Sciences
SUNY at Stony Brook
Stony Brook, NY 11794

Louis J. Allamandola
Mail Stop 245-6
NASA-Ames Research Center
Moffett Field CA 94035

Joseph Burns
328 Space Sciences Building
Cornell University
Ithaca, NY 14853

Donald E. Brownlee
Department of Astronomy
University of Washington
Seattle, WA 98285

Christopher Chyba
320 Space Sciences Building
Cornell University
Ithaca, NY 14853

Michael R. Combi
A&ER Inc.
840 Memorial Drive
Cambridge, MA 02139

Anthony Danks
Applied Research Corporation
8201 Corporate Drive, Suite 920
Landover, MD 20785

Louis D'Hendecourt
University of Paris 7
U Pl. Iussieu, 75251
Paris Cedex 05, FRANCE

Neil Divine
Mail Stop 301-460
Jet Propulsion Laboratory
4800 Oak Grove Drive
Pasadena, CA 91109

Bertram Donn
Astrochemistry Branch
NASA-GSFC
Code 691
Greenbelt, MD 20771

Therese Encrenaz
Observatoire de Meudon
F-92195 Meudon
FRANCE

William J. Forrest
Dept. of Physics and Astronomy
Bausch & Lomb Building
University of Rochester
Rochester, NY 14627

William Glaccum
NASA-GSFC
Code 685
Greenbelt, MD 20771

Simon F. Green
Unit for Space Science, Physics Lab
University of Kent
Canterbury, Kent CT2 7NR
UNITED KINGDOM

Thomas L. Hayward
Box 3905
University of Wyoming
University Station
Laramie, WY 82071

Donald Huffman
Department of Physics
University of Arizona
Tucson, AZ 85721

Anuradha Koratkar
Dept. of Earth and Space Sciences
SUNY at Stony Brook
Stony Brook, NY 11794

Philippe L. Lamy
Lab. d'Astronomie Spatiale
Les Trois Lucs
Marseille 13012, FRANCE

David J. Lien
Department of Physics
Cardwell Hall
Kansas State University
Manhattan, KS 66506

David K. Lynch
The Aerospace Corporation
P.O. Box 92957
Los Angeles, CA 90009

Larry Mason
Martin Marrietta
Mail Stop 0560
P.O. Box 179
Denver, CO 80201

Brian B. McGuinness
Dept. of Earth & Space Sciences
SUNY at Stony Brook
Stony Brook, NY 11794

Karen Meech
Institute for Astronomy
University of Hawaii
2680 Woodlawn Drive
Honolulu, HI 96822

Tadashi Mukai
Kanazawa Institute of Technology
Nonoichi, Ishikawa 921
JAPAN

Michael J. Mumma
Code 693
NASA-GSFC
Greenbelt, MD 20771

Eileen V. Ryan
Planetary Science Institute
2030 East Speedway, Suite #201
Tucson, AZ 85719

Carl Sagan
302 Space Sciences Building
Cornell University
Ithaca, NY 14853

Scott Sandford
Mail Stop 245-6
NASA-Ames Research Center
Moffett Field, CA 94035

Kristen Sellgren
Institute for Astronomy
University of Hawaii
2680 Woodlawn Drive
Honolulu, HI 96822

John R. Stephens
Los Alamos National Laboratory
P.O. Box 1663
Los Alamos, NM 87545

K. S. Krishna Swamy
Mail Stop 245-6
NASA-Ames Research Center
Moffett Field, CA 94035

Wm. Reid Thompson
307 Space Sciences Building
Cornell University
Ithaca, NY 14853

Joseph Veverka
312 Space Sciences Building
Cornell University
Ithaca, NY 14853

Robert M. Walker
McDonnell Center for Space Science
Washington University
Box 1105
St. Louis, MO 63130

Russell G. Walker
Jamieson Science/Engineering, Inc.
P.O. Box F1
Felton, CA 95018

INFRARED OBSERVATIONS OF COMETS HALLEY AND WILSON AND PROPERTIES OF THE GRAINS

SUNDAY, AUGUST 9, 1987

Arrival at Townhouse Residence

5:00 – 7:00 PM	Dinner – Robert Purcell Union
6:00 – 10:00	Registration – Robert Purcell Union
8:00 – 10:00	Reception – Robert Purcell Union

MONDAY, AUGUST 10, 1987

7:00 –	Breakfast – Robert Purcell Union
8:00 – 8:30	Registration – Mudd Building
8:30	Workshop Begins – Mudd Building

INTRODUCTION

M. Hanner

Session I: Infrared Observations of the Dust Coma

Chairs: A. Tokunaga & H. Campins

8:45	Ground-based 1–20 μm Observations	Short Presentations
9:05	Airborne Observations of Halley & Wilson	H. Campins
9:25	Latest Results from the Vega Infrared Spectrometer	T. Encrenaz
9:45	Spectral Appearance of Comets from 5–20 μm	J. Bregman
10:15	Coffee Break and Posters	

10:45	Spatial Variations	Short Presentations
11:05	Changes in Grain Properties during Outbursts	Short Presentations
11:25	Near-Infrared Polarization and Color	T. Brooke
11:40	General Discussion	All

12:15 – 1:30

LUNCH

Session II: Grain Optical Properties

Chair: M. Hanner

2:00	Applicability of Optical Constants for Interpreting Astronomical Data	D. Huffman
2:30	Optical Properties of Rough Particles	Ph. Lamy
2:55	Thermal Properties of Heterogeneous Grains	D. Lien

3:15 Coffee Break and Posters

3:45	Dust Grains in Reflection Nebulae	K. Sellgren
4:05	Cometary Dust Size Distributions from Flyby Spacecraft	N. Divine
4:25	Models Fit to Halley & Wilson Data	Short Presentations
4:50	General Discussion	All
5:15	Organize Working Groups	All

5:30 – 7:00

DINNER

7:30 – 9:00 Working Groups meet at Townhouses

TUESDAY, AUGUST 11, 1987

Session III: Cometary Dust Composition

Chair: R. Gehrz

- | | | |
|--------------|----------------------------------------------------------------------|----------------------------|
| 8:45 | PIA/PUMA <i>In Situ</i> Dust Measurements | L. Mason/
D. Brownlee |
| 9:05 | Comparison of Halley Dust with Meteorites and
Interplanetary Dust | D. Brownlee |
| 9:50 | Infrared Spectral Features in Interplanetary Dust
Particles | S. Sandford |
| 10:15 | Coffee Break and Posters | |
| 10:30 | The Nature of Interplanetary Dust in Comparison with
Comet Halley | R. Walker |
| 11:15 | The 3 Micron Emission Features in Halley | T. Brooke &
A. Tokunaga |
| 11:30 | IR Emission from Organic Grains in P/Halley | C. Chyba/
C. Sagan |
| 11:45 | Discussion and Summary | |

12:15 – 1:30

LUNCH

Session IV: Laboratory Investigations

Chair: R. Russell

- | | | |
|-------------|---------------------------------------------------|---------|
| 1:45 | Survey of Experiments Relating to Cometary Grains | B. Donn |
| 2:30 | Discussion | |
| | ★ Sample preparation | |
| | ★ Measurement Techniques | |
| | Reflectivity vs. emissivity vs. transmissivity | |
| 3:15 | Coffee Break and Posters | |

- 3:45 Discussion
- ★ Measurements of single particles
 - ★ Optical constants and the real world
 - ★ Organic materials and the 3 micron features
- 5:15 Adjourn

BANQUET

WEDNESDAY, AUGUST 12, 1987

Session V: Focus on the Future

- 8:45 Status Report on the Halley Watch Infrared Net B. McGuinness
- 9:15 Panel Discussion
 (to be followed by general discussion of each topic)
- ★ How to achieve a consistent interpretation of Halley infrared data
 - ★ Effectiveness of International Halley Watch
 - ★ Plans for infrared observations, new instrumentation
 - ★ Recommendations for laboratory studies
 - ★ Outlook for NASA Programs

12:00-1:00 LUNCH

Session VI: Preparation of Summary Report and Recommendations

- 1:15 Working Groups meet
- 3:00 Workshop Adjourns
- 4:00 Organizing Committee meets

TABLE OF CONTENTS

Preface	iii
Acknowledgements	iv
List of Participants/Organizing Committee	v
Workshop Program	ix
Table of Contents	xiii
Introduction	xv
CHAPTER 1 - INFRARED OBSERVATIONS OF THE DUST COMA . . .	1
1.0 What We Learned from Comet Halley	1
2.0 The Infrared Observations	2
3.0 Recommendations	15
Comet Wilson World-Wide Observation Log	19
CHAPTER 2 - GRAIN OPTICAL PROPERTIES	22
1.0 Introduction	22
2.0 Optical Constants	23
3.0 Application of Optical Constants	28
4.0 Dust-Size Distribution	39
5.0 Comparison of Infrared Data with Models	42
6.0 Comparison with Interstellar Dust in Reflection Nebulae	44
CHAPTER 3 - COMETARY DUST COMPOSITION	50
1.0 Introduction	50
2.0 <i>In Situ</i> Measurements	50
3.0 Interplanetary Dust Particles	51
4.0 Infrared Spectra of IDPs and Identification of Silicates	51
5.0 The 3.4-Micron Feature	52
Manuscripts:	
Comparison of Laboratory Determined Properties of Interplanetary Dust	
Dust with Those of Comet Halley Particles: What are Comets Made Of?	53
PIA Update: Correlation Analyses of Mass Spectra	64
A Comparison of Halley Dust with Meteorites,	
Interplanetary Dust and Interstellar Grains	66
The Spectral Properties of Interplanetary Dust Particles	68
DISCUSSION	72
Aromatic Components in Cometary Materials	73
The 3.4 μ m Emission Feature in Comet Halley	75
DISCUSSION	78
Comparison of the 3.36 μ m Feature to the ISM	79
A Two-Component Model for Thermal Emission	
from Organic Grains in Comet Halley	83

On the Carbon Abundance in Comet Halley Derived from the 3μ Feature: Comparison with Interstellar Dust	85
Possible Identifications of the $3.4\mu\text{m}$ Feature	86
DISCUSSION AND RECOMMENDATIONS	89
CHAPTER 4 - LABORATORY INVESTIGATIONS	91
1.0 Introduction	91
2.0 Spectral Studies	91
3.0 Sample Preparation	96
4.0 Grain Processing	99
5.0 Laboratory Groups	100
CHAPTER 5 - FOCUS ON THE FUTURE	105
1.0 Achieving a Consistent Interpretation of Halley Data	105
2.0 International Halley Watch/Infrared Net	106
3.0 Supporting Laboratory Studies	107
4.0 Strategy for Future Comet Observations	110
5.0 Relation to NASA Programs	112
6.0 The Comet Rendezvous/Asteroid Flyby Mission	115
Current Status of the International Halley Watch Infrared Net Archive	117
EXTENDED ABSTRACTS	123

INTRODUCTION

The study of small solid grains in astrophysics involves understanding physical and chemical processes: How do grains form? What is their chemistry? How do different environments affect processes of grain growth? Are these equilibrium or non-equilibrium processes? How are grains subsequently altered by ultraviolet radiation or charged-particle flux?

The study of the solid grains in comets is one aspect of this larger investigation. By studying their structure and composition we would like to learn: How are interstellar grains incorporated into comets? What has been the effect of cosmic-ray processing in the Oort Cloud? What organic materials are present? How are grains emitted from the nucleus and what changes occur during heating? Can we recognize interstellar grains in comet grains today?

We are just beginning to unravel the story that comet grains have to tell. Our understanding rests on three types of research: remote sensing of the comet dust coma, *in situ* sampling from spacecraft, and laboratory investigations to interpret the remote sensing data and to simulate physical and chemical processes.

A quantum jump in our knowledge has resulted from Comet Halley. The first *in situ* sampling of a comet from the Halley flyby spacecraft has shown that the comet is rich in hydrocarbons. Earth-based observations of the dust show puzzling differences from the spectra of interstellar sources in the organic signatures near 3 microns and in the silicate band structure at 10 microns, as well as many previously unobserved spectral features.

Moreover, recent advances in techniques to analyze interplanetary dust particles at the submicron level are yielding exciting new discoveries about their composition and their relationship to cometary and interstellar grains.

In the next decade, we look forward to the Comet Rendezvous mission, with its opportunity for directly sampling the elemental and isotropic composition of the grains, their mineralogy, size distribution and structure, and the organic components present in both the gas and solid phases.

It is an exciting time to be working in this field. We hope that some of the excitement is conveyed in this Report.

CHAPTER 1

INFRARED OBSERVATIONS OF THE DUST COMA

Humberto Campins
Planetary Science Institute

and

Alan Tokunaga
Institute for Astronomy, University of Hawaii

with contributions by J. Bregman, T. Brooke, T. Encrenaz,
R. Gehrz, S. Green, T. Hayward, D. Lynch, K. Meech,
T. Mukai, M. Mumma, R. Russell, K. Sellgren, R. Walker

1.0 WHAT WE LEARNED FROM COMET HALLEY

The main infrared observational results were briefly reviewed at the start of the session. No attempt was made for completeness; instead the speakers (Bregman, Brooke, Campins, Encrenaz, Gehrz, Lynch, and Tokunaga) concentrated on the final results and the new questions they raised. These new results are summarized below. Further discussion of these results is given in the abstracts at the end of this report (with references to the primary publications).

All of these results have yet to be synthesized into a self-consistent picture of the dust grain composition, dust production history, outburst mechanisms, and composition of the nucleus. The workshop discussion was helpful in pointing out problems faced by theorists, such as data of variable quality, the lack of the proper theory for computing the scattering and emission of irregular particles, and in some cases the lack of optical constants of "realistic" materials. We may expect, however, that the gross spectral and dynamical properties of Comet Halley can be understood in time, even if the details of the observations and the theoretical calculations continue to vex us into the future.

SUMMARY OF NEW RESULTS

(Unless indicated, these results refer only to Comet Halley)

- New emission features ascribed to C-H vibrations in organic material were detected at 3.36 and $3.52\mu\text{m}$ by Vega IKS and subsequently observed out to $r=2$ AU post perihelion. Emission at $3.29\mu\text{m}$, the position of the interstellar unidentified feature, may also be present.
- First cometary spectra at $5 - 8\mu\text{m}$ showed none of the expected organic features, but a possible emission feature at $6.8\mu\text{m}$, which is attributed to carbonates.
- Structure (at least one sharp peak) was detected for the first time in the broad $10\mu\text{m}$ emission; this structure and shape is interpreted as indicating anhydrous crystalline olivine and pyroxene particles.
- New emission features were detected in the $16 - 68\mu\text{m}$ spectral region, at 28.4 and tentatively at 23.8 , 34.5 , and $45\mu\text{m}$; these are possibly due to olivine.
- Changes in dust optical properties (polarization, color, temperature, silicate emission) were well documented and seem to be associated with outbursts.
- New infrared imaging techniques applied to Halley detected radial trends in the optical

properties of the coma dust.

Although this workshop concentrated on dust, there was some discussion of infrared observations of gaseous species. We point out the most significant discoveries in this area.

- The H₂O molecule was directly detected for the first time at 2.65 μ m and the ortho/para ratio measured.
- Vega IKS spectrometer shows evidence for emission by the following gases: H₂O, CO₂, CO, H₂CO, OCS, as well as the C-H features and possibly C \equiv N.

2.0 THE INFRARED OBSERVATIONS

2.1 Photometric Monitoring

Several observatories carried out regular monitoring programs of 1 - 20 μ m filter photometry. These data are valuable for defining the activity level and temporal changes in dust properties, as well as giving a photometric reference for the higher resolution spectral studies. The monitoring programs known to us are compiled in Table 1.1. For this purpose, a monitoring program is defined as at least four data sets taken in a consistent manner through standard infrared filters. A complete listing of infrared observations is available from the International Halley Watch (IHW) Infrared Net.

2.2 New Spectral Features

One of the most significant aspects of the Comet Halley observations was the detection of many new molecules, solid-state features, and new unidentified features. Table 1.2 gives a summary of these spectral features; for further information, refer to the abstracts and the references.

One of the primary observational difficulties was the limited opportunity to confirm the presence of new spectral features. This is most important for the features which are weak and difficult to identify. In spite of the best efforts, there are spectral features for which only a single observation is available or for which the existence of the feature remains uncertain because of possible instrumental effects. This is particularly true for spectral regions inaccessible from the ground. In such cases, the feature is indicated as "tentative" in the Table.

In the case of Comet Halley, it is difficult to be sure of the existence of some features as they may be (1) present only in Comet Halley and not in other comets; (2) present in comets generally, but variable; and (3) spurious. This underscores the importance of synoptic observations of comets and continued observations of more comets with adequate spectral resolution and signal to noise to observe rarely seen features. Whether the spectral features we see in Comet Halley are typical or not is not known at the present time (with the exception of the H₂O fluorescence emission).

The difficulties discussed so far should not obscure the fundamental discoveries obtained through infrared spectroscopy of Comets Halley and Wilson: (1) the observation of H₂O fluorescence for the first time, (2) the discovery of a hydrocarbon feature at 3.4 μ m, (3) the discovery of structure in the 10 μ m silicate feature, (4) the discovery of CO₂ at 4.3 μ m and possibly H₂CO at 3.5 μ m, and (5) the discovery of new emission features at 2.8 and 28.4 μ m in Comet Halley and at 12.2 μ m in Comet Wilson. These discoveries are a quantum leap in the number of spectral features observed and demonstrate the importance of infrared observations for cometary studies.

The 3.4 μ m feature is discussed in detail in Section 2.3. This feature probably arises

TABLE 1.1

HALLEY INFRARED PHOTOMETRIC MONITORING PROGRAMS

Telescope	Location	Field of View (arc sec)	Inclusive Dates	Filters	Ref.
0.76m O'Brien	U. Minn.	19.5	12 Dec 85– 6 May 86	V – 18.5 μ m	Gehrz & Ney 1986
2.3m WIRO	U. Wyoming	5, 8	12 Jan 86 30 Apr 86	2.3 – 23 μ m	Gehrz & Ney 1986
3.0m IRTF	Mauna Kea	7	18 Jan 85 10 Mar 87	1.2 – 20 μ m	Tokunaga et al 1986
3.0m IRTF	Mauna Kea	7	16 Jan 86 5 Mar 86	2–20 μ m 7.5–13 CVF	Campins & Ryan 1987
3.8m UKIRT	Mauna Kea	5	20 Dec 84 3 May 86	1.2 – 20 μ m	Green et al 1986
1.5m Steward Observatory	Mt. Lemmon	15	8 Nov 85 13 Jan 86	2 – 13 μ m	Lynch et al 1986
3.0m IRTF	Mauna Kea	8, 10	21 Sept 85 27 Apr 86	JHK polarimetry	Brooke et al 1986
1.3m KPNO	Kitt Peak	11, 15, 33	22 Nov 85 28 May 86	JHK polarimetry	Brooke et al 1986
1m ESO	La Silla	5–30	4 Nov 85 June 86	JHK LM	Bouchet et al 1987
0.75m SAAO	Sutherland South Africa	36	19 Oct 85 13 June 86	JHKL	Whitelock et al
1.25m Sternberg	Crimea USSR	12	2 Oct 85 21 June 86	JHK LM	Taranova & Shenavrin
1.5m TIRGO	Gornergrat Switzerland	10–25	14 Oct 85 23 Mar 86	JHK LM	Stanga et al 1986

from a hydrocarbon material, but the identification is uncertain (see Chapter 3). The $2.8\mu\text{m}$ feature is not securely identified, but OH infrared fluorescence, hydrated silicate emission, and LTE H_2O emission can be ruled out (Tokunaga *et al.*, 1987; Table 1.2). Similarly, only a tentative identification exists for the $28.4\mu\text{m}$ feature, but LTE H_2O and OH emission have been ruled out (Herter *et al.*, 1987).

The 2.63 and $2.7\mu\text{m}$ features were observed by Weaver *et al.* (1986). Mumma reported at this conference the likely existence of these features and that they may arise from clusters of molecules, although no firm identification could be made at this time.

2.3 The $3.4\mu\text{m}$ Hydrocarbon Feature

The most plausible identification of the $3.4\mu\text{m}$ emission feature (centered at $3.36\mu\text{m}$) is that it arises from C-H molecular bonds, although the composition of the emitting material cannot be specified. The intensity of the $3.4\mu\text{m}$ feature was observed by the Vega spacecraft to vary with distance from the nucleus (within a few thousand km) in the same manner as a parent molecule (Combes *et al.*, 1986, Encrenaz *et al.*, this report). The feature-to-continuum ratio was found to be constant with distance from the nucleus from ground-based observations (Knacke *et al.*, 1986). A $3.29\mu\text{m}$ emission feature, associated with PAHs in the interstellar medium, may also have been detected (Baas *et al.*, 1986; Encrenaz *et al.* 1987).

Brooke reviewed the emission mechanism theories for the $3.4\mu\text{m}$ feature (Brooke and Knacke, Chapter 3; see also abstracts by Danks and Lambert, Encrenaz *et al.*, and Chyba and Sagan). One of the main conclusions is that the abundance of carbon in Comet Halley depends greatly on the assumed emission mechanism, from less than 1% to about 30% of H_2O . Thus it is crucial to understand the emission mechanism in order to understand the carbon budget of the comet.

A discussion of how to understand better the emission mechanism yielded the following observational approaches:

- 1) The further study of the 3.4 and $6-8\mu\text{m}$ spectral regions in bright comets should help to determine whether or not some of the C-H bonds are attached to PAHs, and whether another hydrocarbon feature can be observed in the $6-8\mu\text{m}$ region. This may lead to an understanding of whether the $3.4\mu\text{m}$ feature could arise from thermal emission or not. A detection of a longer wavelength hydrocarbon feature could also lead to an identification. It was suggested that a $6-8\mu\text{m}$ feature, if it exists, should be observed from as large a heliocentric distance as possible ($r > 2 \text{ AU}$?). This is desirable so as to avoid overwhelming the potentially weak hydrocarbon features by the strong thermal emission of the grains. Only comets as bright or brighter than the past Comet Halley apparition can be studied effectively with current instrumentation.
- 2) Study of the feature/continuum ratio vs. heliocentric distance. More complete data similar to that obtained by Knacke *et al.* (1986) and Baas *et al.* (1986) may help to distinguish more clearly whether or not the $3.4\mu\text{m}$ feature strength follows that of the continuum thermal emission, or is dependent on the solar flux. In such a study, repeated observations are required of both the feature and the thermal continuum to remove the effects of variability.
- 3) Measurement of the feature intensity vs. distance from the nucleus. The best study thus far comes from the Vega-IKS experiment. Additional work could determine with greater certainty whether or not the $3.4\mu\text{m}$ feature is always a primary substance, rather than a daughter product.
- 4) Further spectroscopy. The $3.4\mu\text{m}$ feature appears very similar in Comets Halley and Wilson, but is it the same in all comets? In addition, high-resolution and high signal-

to-noise observations are necessary. The minimum spectral resolution for useful work is 400, such as that obtained by Baas *et al.* (1986). The “ideal” spectral resolution is 2,000-3,000 with good signal to noise. In general, it is more important to achieve high- signal to noise rather than high-spectral resolution to aid in the identification.

We await the arrival of the next bright comet!

2.4 Airborne Observations of Comets Halley and Wilson

Because a significant fraction of the infrared spectrum is not available to ground-based telescopes, airborne infrared observations played a key role in the study of the dust in Comets Halley and Wilson. A coordinated effort aimed at obtaining the maximum possible spectral coverage of Comet Halley yielded excellent results. A more modest effort (because of the severe time constraints associated with new comets) aimed at Comet Wilson also proved very fruitful.

For convenience, we will divide the airborne observations into the four spectral regions covered by the instruments used. Following is a summary of the main results from each region.

The 5 to 9 μ m Region in Comet Halley

Spectrophotometry from 5 to 9 μ m (spectral resolution = 2%, see Fig. 1.4) was obtained from the Kuiper Airborne Observatory (KAO) on 12.1 Dec. 1985 and on 8.6 and 10.5 April 1986 (Campins *et al.*, 1986; Bregman *et al.*, 1987). Photometry was carried out from the Lear Jet Observatory (LJO) on 7.6, 8.6, 9.6 and 11.6 April 1986 (Russell *et al.*, 1986).

- Except for the possible detection of a feature at 6.8 μ m (also observed by the Vega IKS instrument (Encrenaz, this report) and tentatively attributed to carbonates) none of the features expected in this region were found. Analogies with interplanetary dust particles and circumstellar dust had suggested the presence of features at 6.2, 7.7 and 8.6 μ m (Campins *et al.*, 1986). Thus, any attempt to link the 3.4 μ m emission features to organic materials must explain the absence of these longer wavelength features.
- A new and unidentified feature observed to rise from 5.5 to 5.24 μ m (the shortest wavelength observed) is present in all but one of the Halley spectra, after normalization to a 325 K black body (Bregman *et al.*, 1987).
- The onset of a strong, broad silicate emission feature is observed, consistent with the emission observed in the 8 to 13 μ m spectrum obtained from the ground on 17.2 Dec (Bregman *et al.*, 1987). The onset of the emission seems to occur at a shorter wavelength than previously believed, beginning between 7.5 and 8 μ m, depending on how the continuum is defined. The strength of the feature relative to the continuum was higher on 8 April than 10 April.
- The 5 - 7 μ m color temperature is significantly higher than an equilibrium black body, indicating the presence of small hot dust grains. This color temperature is higher than that observed at longer wavelengths, where the emission arises from larger, somewhat cooler grains (but still warmer than an equilibrium black body). This dependence of the color temperature on wavelength is the main reason why it is difficult to define the continuum under the broad silicate emission.
- Spatial variations in the color temperatures were found in April between the photo-center and other coma observations one beamwidth away.
- Temporal variability of the overall brightness equal to that described in Section 2.7 was observed between flights.

The 5 to 13 μ m Region in Comet Wilson

Spectrophotometry was obtained from the KAO on 23.6 and 25.6 April 1987 (Lynch *et al.*, this report). Preliminary results are:

- The observations are consistent with a weak silicate emission, apparently different from that in Comet Halley at the same heliocentric distance (1.2 AU).
- A new and unidentified feature was found at 12.2 μ m which has not been observed in any other astronomical source.
- The color temperatures from the 5 to 8 μ m region are very high, a behavior similar to that found in Comet Halley.
- No measurable short-term variability was displayed by this comet, in sharp contrast to Comet Halley.

The 16 to 30 μ m Region in Comet Halley

The Cornell University 16 to 30 μ m spectrometer (spectral resolution = 1%, see Fig. 1.1) was used from the KAO on 14.2 December 1985 (R=1.28 AU preperihelion; Herter *et al.*, 1987). Only one observation with this instrument was obtained, and hence no information on spatial or temporal variability is available.

- No strong, or sharply peaked, silicate emission feature was evident near 20 μ m. Without simultaneous data at shorter wavelengths it is difficult to know where to draw the continuum (particularly in light of the large brightness fluctuations observed on timescales shorter than a day); thus a broad, relatively weak feature cannot be ruled out.
- Excess emission in broad and narrow-band 20 μ m photometry is clearly present when the comet was closer to the sun. Hence, the lack of an obvious feature in the 20 μ m airborne spectrum may be due to uncertainties in the level of the continuum and unfortunate timing. The 10 μ m silicate feature was clearly present, but still relatively weak, in filter photometry on 13.3 Dec (Tokunaga *et al.*, 1986).
- A new feature was found at 28.4 μ m. This finding has been confirmed in one of the 20 to 68 μ m unpublished spectra (Glaccum, *et al.*, this report). Theoretical models have ruled out LTE emission by OH and H₂O as the source of this feature (Herter *et al.*, 1987).
- Possible new features were observed at 23.8 (also observed in a 20-68 μ m spectrum) and at 26.7 μ m. The 23.8, 28.4 μ m and two more features in the 20 to 68 μ m region (see below), have been tentatively identified with olivine particles.

The 20 to 68 μ m Region in Comet Halley

The NASA-Goddard spectrometer (spectral resolution = 2 to 3%, see Fig. 1.2) was flown on the KAO on 17.1 and 20.1 December 1985 and 15.6 and 17.7 April 1986 (Glaccum *et al.*, 1987).

- No strong features were found; however, a series of weak (7% above the continuum), but repeatable features have been found near 24, 28, 35, and 45 μ m, and tentatively identified with olivine particles, in agreement with conclusions obtained from the structure of the 10 μ m silicate feature (Table 1.2 and Glaccum *et al.*, this report). This identification suggests that, similarly to the 10 μ m region, there may be a broad (but much weaker) 20 μ m silicate feature with structure (narrower peaks) characteristic of olivine (see discussion in 2.5).

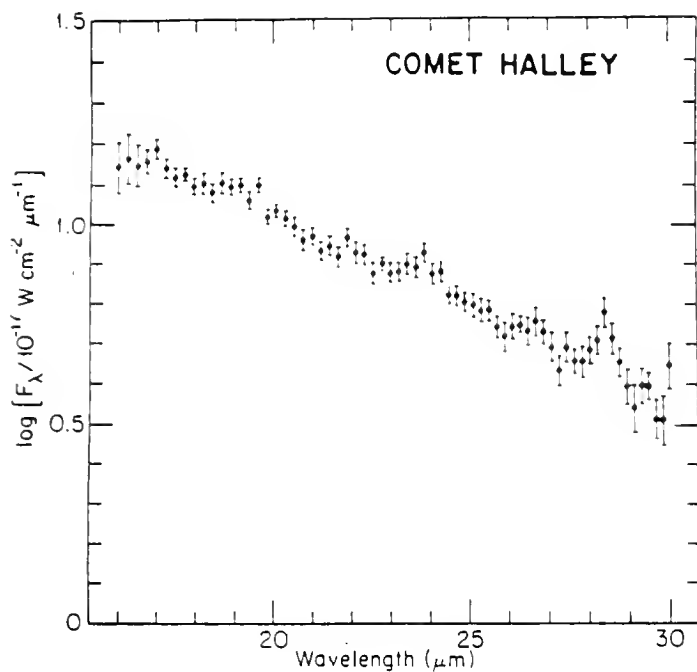


Figure 1.1 - The 16 to 30 μm spectrum of Comet Halley (December 1985). A sharp new feature was discovered at 28.4 μm and two ones at 23.8 and 26.7 μm . The 23.8 and 28.4 μm features have been tentatively identified with crystalline olivine (see Fig. 1.2). No strong, broad silicate emission is evident in this spectrum; however, without simultaneous data at shorter wavelengths it is difficult to know where to draw the continuum particularly in light of the large brightness fluctuations observed in Comet Halley on timescales shorter than a day. Figure adapted from Herter, Gull and Campins (1986).

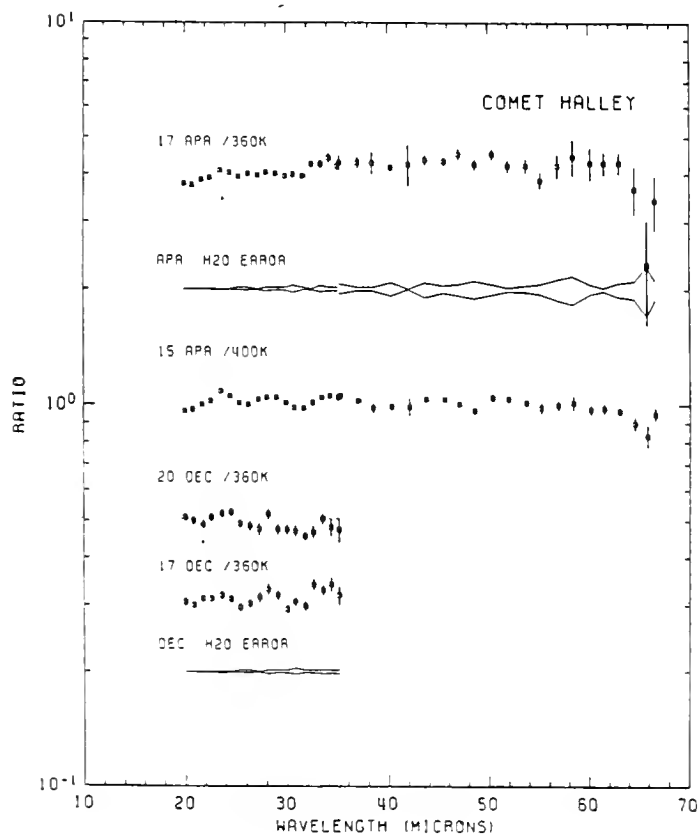


Figure 1.2 - The 20 to 36 μm and 20 to 68 μm spectra of Comet Halley (December 1985 and April 1986) relative to blackbody fits to the continuum. The emission features near 24 and 28 μm discovered by Herter, Campins, and Gull (1987) are confirmed, and most clearly seen in the December 20, 1985, spectrum. These two features along with two more features peaking near 35 and 45 microns (in the April 15, 1986, spectrum) have been tentatively identified with crystalline olivine, in excellent agreement with the identification of the structure of the 10 μm silicate emission (see Figs. 1.3 and 1.4). Also shown (solid lines labeled H₂O error) is the effect on the errors of a change of $\pm 20\%$ in the ratio of boresight water vapor for observations of the comet and calibration stars. Figure adapted from Glaccum *et al.* (1986) and Glaccum *et al.*, this report.

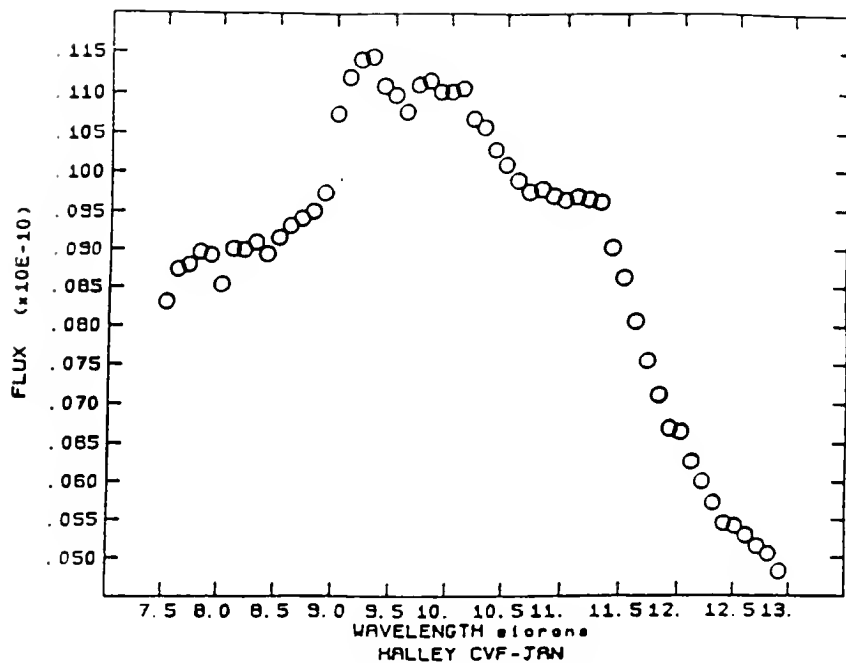


Figure 1.3 - The 7.5 to 13 μ m spectrum of Comet Halley obtained on 16.0 January 1986. The one sigma errors are smaller than the symbols except in the 7.5 to 8.0 μ m and 9.3 to 10.0 μ m regions where the errors can be several times the size of the symbols. The continuum is not well defined but can be approximated by a straight line joining the first and last data points. The flux is in units of Watts cm⁻² μ m⁻¹ (from Campins and Ryan, this report).

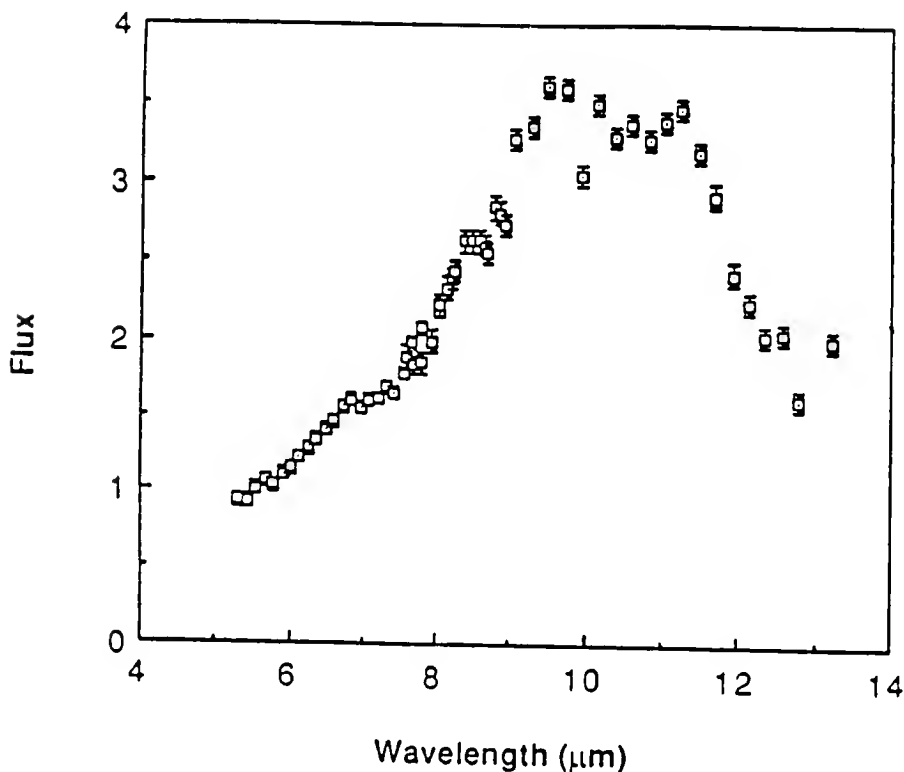


Figure 1.4 - The 5 to 13 μ m spectrum of Comet Halley obtained on 12.1 (8 to 13 μ m) and 17.2 (5 to 9 μ m) December 1985. The low datapoint at 9.7 μ m is due to a mis-correction for the terrestrial ozone. The flux is in units of 10⁻¹⁶ Watts cm⁻² μ m⁻¹ (from Bregman *et al.*, 1987).

Table 1.2

Spectral Features Observed in Comets Halley and Wilson

Wavelength(μm)	Species	References	Remarks
1-2.5	CN, H ₂ O	25	
2.6, 2.7(?)	?	31, 40	Broad emission features
2.7(?)	H ₂ O gas	11, 14, 29, 40	Obs. in Halley & Wilson
≈ 2.8	?	30, 39	Obs. in Halley & Wilson
3.0	H ₂ O ice	3, 11, 14, 38	Tentative
3.15	?	14	Tentative
3.29	PAHs(?)	1, 14	Tentative
3.36	CH features	1,11,12,13,14,23,27	Obs. in Halley & Wilson
3.52		39, 41	
3.6	H ₂ CO	11, 13, 14, 27	ID not confirmed
4.3	CO ₂	11, 13, 14, 27	First detection
4.44	C N	14	Tentative
4.6	CO	11, 14, 27	Tentative
4.84	OCS	14	Tentative
5.2	?	6	Tentative
6.8	Carbonates	4, 6	Tentative
9.8, 10.5, 11.3	Silicates	4, 10, 14	Olivine and pyroxene?
12.2	?	24	Variable Observed in Wilson; tentative
≈ 20	Silicates	15, 16, 22	Shape uncertain
23.8	Olivine?	16, 22	Tentative
26.7	?		Tentative
28.4	Olivine?	16, 22	Variable strength
34.5	Olivine?	16	Tentative
45	Olivine?	16	Tentative

- The continuum has been modeled and the derived particle-size distribution is consistent with that measured by the spacecraft.
- Temporal variability of the overall brightness was observed.
- No spatial variability of the color temperature was observed between the photocenter and observations one and two beamwidths away.

The 40 to 160 μ m Region of Comet Halley

Because of the rapidly dropping flux level with wavelength, this region could only be observed using broadband photometry, and hence there is information on the shape of the continuum but not on any spectral features. The University of Texas far-infrared photometer was used on the KAO on 15.7 and 16.7 March 1986 (Campins *et al.*, 1987b).

- Modeling of the shape of the continuum is consistent with the results obtained from the 20 to 68 μ m region.
- A color temperature gradient was found with the hottest point at the photocenter.
- Observations on two consecutive days show brightness variability of a factor of two; lower color temperatures were observed when the comet was fainter.

2.5 Silicate Features

Until recently, these features were the only solid state spectral features observed in comets and one of the few observational clues to the composition of cometary solids. The Comet Halley observations have shown these features to be more complex and more diagnostic of the dust's composition than previously believed.

Circumstellar and Interstellar Sources

A broad emission or absorption feature which peaks near 10 μ m and is generally associated with oxygen-rich stars has been attributed to the stretching vibration of Si-O bonds in silicate grains. This identification is strengthened by the presence of a feature in the 16 to 24 μ m region produced by the O-Si-O bending mode. Because of its width and lack of a sharply defined structure (peaks), the 10 μ m feature has been generally explained as due to amorphous silicate grains, and hence, not very diagnostic of the specific type of silicate producing the feature.

Previous Comets

There is a large body of filter photometry showing that the 10 μ m feature is present in most (but not all) comets within 1 AU of the sun (Ney 1982 and references therein).

Before Comet Halley it had been thought that the cometary 10 μ m feature was similar in shape to the interstellar feature and thus also due to amorphous grains. Prior to Halley, few spectra of the cometary silicate feature had been obtained; the one with the best spectral resolution and signal to noise was of Comet Kohoutek (Merrill, 1974). This spectrum showed a broad, structureless feature; thus, it was thought that comets must also have amorphous silicates. A number of other spectra taken of comets beyond 1 AU from the sun (Churyumov-Gerasimenko, IRAS-Araki-Alcock, Grigg-Skjellerup and Wilson) are consistent with either no emission feature or a very weak structureless one. On the other hand, interplanetary dust particles (IDPs), which are believed to be mostly of cometary origin, show clear structure in the 10 μ m region due to the presence of crystalline olivine, pyroxene and hydrated silicates (Sandford and Walker, 1985; Sandford, Chapter 3).

No published spectra of the 20 μ m region of comets existed before Comet Halley's

apparition. The presence of this feature in comets was determined from filter photometry (Ney, 1982, Rieke and Lee, 1974).

Halley

a) The 10 μ m Feature

There are four published spectra of the 10 μ m region of Comet Halley (Bouchet *et al.*, 1987; Bregman, *et al.*, 1987; Campins and Ryan, this report; Encrenaz, this report). All these spectra show some structure in the band and are roughly consistent with each other. The structure is clearest in the spectra of Bregman *et al.* and Campins and Ryan which are shown in Figures 1.1 and 1.2. These spectra show a clear peak near 11.3 μ m with possible structure between 9 and 10 μ m which is difficult to define due to the presence of the telluric ozone absorption. The width and structure observed in Halley's 10 μ m emission has been reproduced using a sample of IDP spectra (Sandford, Chapter 3). A good fit requires a combination of anhydrous, crystalline olivine and pyroxene particles. This is radically different from the case of Comet Kohoutek (Sandford and Walker, 1985) and in excellent agreement with the results from the Vega and Giotto mass spectrometer observations (Brownlee, Chapter 3) which suggest, based on a comparison with the mass spectra of meteoritic particles, that the Si-bearing particles are indeed anhydrous.

Comet Halley's silicate particles are, thus, different from those in Comet Kohoutek (at least based on the comparison between several spectra of Halley taken at different heliocentric distances, ranging from 0.8 to 1.2 AU, and a single spectrum of Kohoutek, taken at 0.3 AU) and from those so far observed in interstellar and circumstellar dust. However, they appear to be similar to the anhydrous IDPs studied in the laboratory.

b) The 20 μ m Feature

Evidence for the presence of this feature in Comet Halley when the comet was within 1 AU of the sun comes from filter photometry which shows this spectral region to be significantly above extrapolations of the continuum at shorter wavelengths. The only published spectrum of any comet in this region is discussed in Section 2.4. Although no evidence was found for a strong 20 μ m silicate emission at the time the spectrum was obtained (heliocentric distance = 1.3 AU), four weak emissions observed near 24, 28, 35, and 45 μ m have been tentatively identified with olivine, in agreement with the same identification in the 10 μ m spectrum.

Spatial and Temporal Variations

The 10 and 20 μ m emission features were observed to have temporal variability on timescales as short as a few hours, and spatial variability in the coma. This variability makes very difficult the combination of different data sets (taken at different times or with different apertures). More detailed discussions of these variations are given in Sections 2.6 and 2.7; however, the mechanisms for the observed variability are not understood.

Recommendations for Observations of Future Bright Comets

It is clear from the case of Comet Halley that observations of the silicate features are potentially very diagnostic of the composition of the dust. Furthermore, observations of other comets are essential to determine how typical (or unusual) the silicates in Comet Halley are. In order to maximize the effectiveness of future observations one must consider the following recommendations:

- a) Comets at heliocentric distances smaller than 1 AU are most likely to show well-developed 10 and 20 μ m features.
- b) Simultaneous observations of the 10 and 20 μ m regions as well as of the continuum (shortward of 7.5 μ m) are essential for the determination of the relative and absolute

strengths of these features.

- c) Observations at a variety of heliocentric distances are necessary to de-couple the behavior of the feature from that of the continuum.

2.6 Spatial Variations

Two-dimensional detector arrays at infrared wavelengths are coming into use, and several groups obtained infrared images of Halley's dust coma. The importance of these arrays for comet study lies in their ability to image the dust coma relatively quickly at several wavelengths, in order to map spatial variations in the optical properties of the grains.

JHK Colors

Rieke and Campins (1987) reported on J,H,K images taken 3.5 Nov. 1985 which show well-defined J-H and H-K color gradients within 7,000 km of the nucleus, with bluest colors at the photocenter. Radial brightness gradients were steeper than the $1/d$ expected for a steady-state isotropic outflow of dust, where "d" is the projected distance from the nucleus. These authors pointed out that both of these phenomena are consistent with a coma of volatile (dirty ice) grains; however, other explanations, such as recent emission of small (Rayleigh scattering) grains, are also possible.

Albedo Maps

Thermal images were combined with nearly simultaneous CCD visible images to obtain albedo maps. A map obtained on 18.4 Nov. 1985 shows an increase in albedo away from the nucleus, except in the anti-solar direction where the albedo decreases (Hammel *et al.*, 1987). A similar spatial structure was found in an albedo map obtained for Comet Giacobini-Zinner on 4.4 Aug. 1985 (Telesco *et al.*, 1986). However, the absolute value of the albedo in Comet Halley was about three times greater than that in Comet GZ, attributed to the fact that Halley was near opposition (phase angle 2° on 18.4 Nov). This interpretation is supported by the albedo map of Halley obtained on 13.7 March 1986, which shows the absolute level of the albedo to be roughly equal to that of Comet GZ when observed at a similar phase angle (Hayward *et al.*, 1987b).

Spatial Structure

Both thermal images and single-detector maps obtained in early 1986 show sunward fans and radial surface brightness profiles more complex than the "canonical" $1/d$, as would be expected for patterns of variable dust emission. (Campins and Ryan, this report; Campins *et al.*, 1987b; Hayward *et al.*, 1987; Hanner *et al.*, 1987).

Silicate Features

The strengths of the 10 and $20\mu\text{m}$ silicate features, and their ratio, were observed to vary with location in the coma. The features were usually – but not always – strongest at the photocenter (Campins and Ryan, this report; Campins *et al.*, 1987b; Hanner *et al.*, 1987b).

Polarimetric Images

Broad-band polarimetric images taken on 5.7 and 7.7 Jan 1986 show maximum polarization in dust jets and not at the photocenter (Eaton *et al.*, this report).

2.7 Temporal Variations

The comet showed frequent and possibly periodic infrared brightness variations. On timescales shorter than or equal to a day, brightness changes greater than a factor of 3 were observed. Because of their frequency and regularity, these brightness variations may not fit the classical definition of outbursts. However, for lack of a better term, we will refer to them as outbursts.

JHK - Color Correlation with Outbursts

A possible correlation between bluer J-H colors and brightness maxima was reported by Hanner. It is interesting to note that in the spatial trends discussed earlier, the bluest J-H and H-K were found on the brightest point in the coma.

Tokunaga (this report) reports systematically bluer JHK colors after July 1986 in the IRTF monitoring data and suggests that the composition of the grains may have changed.

Albedo Changes During Outbursts

A sudden drop in the $2.2\mu\text{m}$ (reflected light) brightness of Comet Halley was observed within a few hours; the $10\mu\text{m}$ brightness stayed roughly constant during this period, indicating a sudden change in the effective albedo of the coma (Lynch *et al.* 1986).

A correlation between higher albedo and brightness peaks is reported by Green *et al.* (this report), Gehrz and Ney (1986), and Tokunaga *et al.* (1986).

Variability in the Silicate Emission

Gehrz and Ney (1986) report the disappearance and reappearance of the 10 and $20\mu\text{m}$ silicate emission features on a timescale of a few days. (See also Green *et al.*, 1986 and Hanner *et al.*, 1987b).

A change in the shape and strength of the $10\mu\text{m}$ emission on a timescale of three hours on 3.8 March 1986 has been observed (Campins and Ryan, this report).

Broad- and narrow-band photometry show stronger 10 and $20\mu\text{m}$ features when the comet was brighter (Hanner *et al.*, 1987b; Campins and Ryan, this report).

High Temperature Correlation with Outbursts

A higher color temperature, based on the $40\text{--}160\mu\text{m}$ photometry, was found when the comet was brightest (Campins *et al.*, 1987a).

Further analysis is necessary to determine if a brightness - color temperature correlation is present in the filter photometry sets of Campins and Ryan, Gehrz and Ney and Tokunaga *et al.*

Polarization Increases During Outbursts

Mukai (this report) reported increases in the polarization during brightness maxima observed by the Suisei spacecraft. He has modeled and interpreted these as an increase in the abundance of small particles.

To summarize, there is evidence that, at times of enhanced dust production, the J-H color may be bluer, the $1 - 2\mu\text{m}$ albedo increases, silicate features are stronger, and the polarization is higher. All of these optical properties are consistent with a shift in the observed size distribution toward smaller grain sizes at times of dust outbursts, although changes in the composition of the dust are not ruled out.

2.8 Problems in Comparing Separate Data Sets

In order to obtain the most complete picture of the infrared activity of Comet Halley, it is necessary to combine data sets of different observers. Most data sets will be eventually found in the archives of the IHW (and for this reason all observers are encouraged to submit Comet Halley data to the IHW).

However, there are significant problems in comparing such data sets. As an illustration of the difficulties, consider the problems in the straightforward case of comparing two photometric data sets. It is first necessary to resolve differences in the photometric system: standard star magnitudes, and flux densities, beam size, filter sets, effective wavelengths, and sky chop amplitude. An additional major complication is that even with a resolution of such problems, the variability of the comet may preclude a direct comparison unless it is known that the comet was quiescent at the time the comparison is made.

Nevertheless, there are cases where the comparing of data sets is important. Examples include the joining of data sets (1) to construct the infrared photometric history of the comet, (2) to obtain more complete wavelength coverage, (3) to search for color or color temperature variations during outbursts, and (4) to confirm the detections of spectral features.

In view of the relatively subtle problems involved with the comparing of data sets, such work should be accomplished by the observers themselves whenever it is possible. In general it will not be meaningful to compare data sets taken directly from the IHW archive without considering in detail the differences in the photometric system, method of data reduction, and considering the possibility of variability.

From the above considerations, it is highly desirable that the comparing of data sets be undertaken as soon as possible, so that the primary sources of data can be consulted with the benefit of fresh memories.

2.9 Polarization

The near-infrared polarization of Halley is similar to the visible polarization in this and other comets in showing a negative branch of a few percent at small phase angles, a neutral point at $\theta = 20$ deg, and an approximately linear rise toward larger phase angles (Brooke *et al.*, abstract this report). However, the polarization increases with wavelength at large phase angles, contrary to the available polarimetry of asteroids, interplanetary dust, and Comet West. Visible polarization of Halley also shows a slight increase with wavelength, from 0.365 to $1\mu\text{m}$ (Mukai, *et al.* 1986). Mukai also reported an increase in polarization associated with brightness maxima (outbursts). Polarimetric images show maximum polarization in dust jets, not at the photocenter (Eaton *et al.*, this report).

The interpretation of these results in terms of physical characteristics and composition of the particles is complicated because Mie theory calculations are valid only for smooth perfect spheres. Laboratory experiments and theoretical studies of rough particles should help in the interpretation of the observations (see Chapter 2).

2.10 Comet Wilson

Comet Wilson provided the opportunity to compare a new comet with Halley. Already active at a heliocentric distance greater than 3 AU, it was predicted to be as bright as Halley when it reached perihelion at 1.2 AU in April 1987. The comet did not quite live up to the predictions, and its southern declination and small elongation made observations difficult. Thus, fewer observations than originally anticipated were obtained. A log of observations of Comet Wilson, compiled by D. Lynch, is presented in Table 1.3. These

include four KAO flights. The preliminary infrared results are summarized here:

A new spectral feature was discovered at $12.2\mu\text{m}$ ($\text{FWHM} = 0.2\mu\text{m}$). This emission was present in all the KAO spectra on 23.6 and 25.6 April 1987 (Lynch *et al.*, this report).

A $3.36\mu\text{m}$ feature similar to that observed in Comet Halley was detected on 24 May 1987 (Brooke *et al.*, 1987).

There was no evidence for a strong $10\mu\text{m}$ silicate emission in early March (Bregman *et al.*, this report), late April (Lynch *et al.*, this volume) and late May (Hanner and Newburn, this report). The KAO spectra are consistent with a weak $10\mu\text{m}$ silicate emission.

No significant day-to-day variability was found in thermal infrared images obtained on 13, 14, and 15 March 1987 (Campins *et al.*, 1987c).

The emission from gaseous H_2O at $2.65\mu\text{m}$ was also detected in this comet using the KAO. The ortho/para ratio in the H_2O gas was measured (Mumma *et al.*, this report).

3.0 RECOMMENDATIONS

Interpreting Halley Observations

- 1) Observers should clearly state standard star magnitudes, flux calibration, filter-effective wavelength, beam size, and sky-chop amplitude and direction when reporting observations. Comments on the weather or other factors affecting data quality are also helpful. Because the comet varied on timescales of a few hours, the time of the observations should be given.
- 2) Modelers should contact observers to assess potential problems with data, such as the reality of features, reproducibility, unconfirmed results, etc. This is an important "no-cost" mechanism to enhance the quality of interpreted results.

Observations of Future Comets

- 1) The 10 and $20\mu\text{m}$ silicate features need to be observed with good temporal coverage, to ascertain whether spectral structure indicative of crystalline grains is present for other comets and to document changes with heliocentric distance (i.e., with grain temperature). The $10\mu\text{m}$ region can be observed from the ground with either circular variable filters (CVF) or spectrometers at resolution of $\sim 1\%$, while the $20\mu\text{m}$ region requires airborne observations. Ground-based photometry indicates that the $20\mu\text{m}$ emission is strongest when comets are less than 1 AU from the sun.
- 2) Basic photometric monitoring is essential to define the thermal emission continuum and its variability. This can be done with intermediate-sized telescopes (~ 1 m), ideally telescope(s) dedicated for that purpose. The goal is to obtain uniform, moderate- to high-time resolution coverage. The broad-band spectral energy distribution allows the grain size distribution and the total cross section of emitting grains to be estimated.
- 3) Correlations between the 3.4 , 10 , and $20\mu\text{m}$ emission features need to be established with simultaneous observations. Coordinated observations among telescopes is required, as single telescopes cannot be expected to have all the instrumentation or to undertake observations at all of these wavelengths simultaneously (variations on time scales of a few hours can be expected).
- 4) Better spectral resolution of the broad-emission features at 3.4 and $10\mu\text{m}$ is required.

The continuum must be measured as well as possible.

- 5) Complete 5 - 13 μ m spectra and/or both 10 and 20 μ m spectra should be obtained during a KAO flight, in order to define the continuum level and to correlate spectral features. Lack of such coverage complicates the interpretation of Halley spectra.
- 6) More airborne data are required to confirm the presence of the 5.2, 26.7, 34.5, and 45 μ m emission features in comets. Additional laboratory work is needed to help identify these features.
- 7) A higher priority should be given to simultaneous airborne and ground-based data-taking. Some of the important airborne data on Comet Halley did not have corresponding ground-based data taken at the same time. In practice, this has been difficult to achieve because of the inevitable changes in flight schedules versus the long-lead time for scheduling observations at major telescopes. Coordinated KAO and Lear jet flights would be valuable for observing two spectral regions simultaneously.
- 8) There is a need for ground-based and airborne instrumentation which can observe more than one feature at a time (i.e., 3.4 and 10 μ m, or 10 and 20 μ m).

REFERENCES

1. Baas, F., Geballe, T.R., and Walther, D.M. 1986, *Ap.J.*, **311**, L97.
2. Bouchet, P., Chalabaev, A., Danks, A., Encrenaz, T., Epchtein, N., and LeBertre, T., 1987, *Astron. and Astrophys.*, **174**, 288.
3. Bregman, J.D., Witteborn, F.C., Rank, D.M., Wooden, D. 1986, *Bull. Am. Astron. Soc.*, **18**, 634.
4. Bregman, J.D. et al, 1987, *Astron. and Astrophys.*, **187**, 616.
5. Bregman, J.D. 1987, abstract this report.
6. Campins, H., Bregman, J.D., Witteborn, F.C, Wooden, D.H., Rank, D.M., Allamandola, L.J., Cohen, M., and Tielens, A.G.G.M. 1986, ESA SP-250, vol. 2, p. 121.
7. Campins, H., Joy, M., Harvey, P.M., Lester, D.F., and Ellis, H.B. Jr., 1987, *Astron. and Astrophys.*, Nov. 1987, in press.
8. Campins, H., Telesco, C.M., Decher, R., and Ramsey, B.D., 1987b, *Astron. and Astrophys.*, Nov. 1987, in press.
9. Campins, H., Decher, R., Telesco, C.M., and Clifton, R.S., 1987c, *Bull. Am. Astron. Soc.*, **19**, 893.
10. Campins, H. and Ryan, E.V. 1987, this report, Part II.
11. Combes, M. *et al.*, 1986, *it Nature*, **321**, 266.

12. Danks, A., Encrenaz, T., Bouchet, P., Le Bertre, T., Chalabaev, A., Epchtein, N. 1986, ESA SP-250, vol. 3, p. 103.
13. Encrenaz, Th., Puget, J.L., Bibring, J.P., Combes, M., Crovisier, J., Emerich, C., d'Hendecourt, L., and Rocard, F. 1987, Proc. of the Brussels Conf., in press.
14. Encrenaz, Th. *et al.*, 1987, this report, Part II.
15. Gehrz, R.D., and Ney, E.P. 1986, ESA SP-250, vol. 2, p. 101.
16. Glaccum, W., Moseley, S.H., Campins, H., and Loewenstein, R.F. 1986, ESA SP-250, vol. 2, p. 111; and this report.
17. Hammel, H.B., Telesco, C.M., Campins, H., Decher, R., Storrs, A.D., and Cruikshank, D.P., 1987, *Astron. and Astrophys.*, Nov. 1987, in press.
18. Hanner, M.S., Kupferman, P.N., Bailey, G., and Zarnecki, J.C., 1987, in *Infrared Astronomy with Arrays* (eds. C.G. Winn-Williams and E.E. Becklin, U. of Hawaii), p. 205.
19. Hanner, M.S., Tokunaga, A.T., Golisch, W.F., Griep, D.M., and Kawinski, C.D., 1987b, *Astron. and Astrophys.*, in press.
20. Hayward, T.L., Gehrz, R.D. and Grasdalen, G.L., 1987, *Nature*, **326**, 55.
21. Hayward, T.L., Grasdalen, G.L., and Gren, S.F., 1987b. Preprint.
22. Herter, T. Gull, G.E., and Campins, H. 1987, ESA SP-250, vol. 2, p. 117.
23. Knacke, R.F., Brooke, T.Y., and Joyce, R.R. 1986, *it Ap.J.*, **310**, L49.
24. Lynch, D., *et al.* 1987, this volume.
25. Maillard, J.P., Crovisier, J., Encrenaz, T., and Combes, M. 1986, ESA SP-250, vol. 1, p. 359
26. Merrill, K.M., 1974, *Icarus*, **23**, 566.
27. Moroz *et al.* 1987, *Astron. Astrophys.*, in press.
28. Mukai, T., Mukai, S., and Kikuchi, S., 1987, ESA SP-250, Vol. II, 59.

29. Mumma, M.J., Weaver, H.A., Larson, H.P., Davis, D.S., and Williams, M. 1986, *Science*, **232**, 1523.
30. Mumma, M. 1987, private communication.
31. Ney, E.P., 1974, *Icarus*, **23**, 551.
32. Rieke, G.M. and Lee, T.A., 1974, *Nature*, **248**, 737.
33. Rieke, M.J. and Campins, H., 1987, ESA SP-278, in press.
34. Russell, R.W., Lynch, D.K, Rudy, R.J., Rossano, G.S., Hackwell, J.A. and Campins, H., 1986, ESA SP-250, Vol. 2, p. 125.
35. Sandford, S.A. and Walker, R.M., 1985, *Astrophys. J.*, **291**, 838.
36. Telesco, C.M., *et al.*, 1986, *Astrophys. J.*, **310**, L61.
37. Tokunaga, A. T., Golisch, W. F., Griep, D. M., Kaminski, C. D., and Hanner, M. S. 1986, *Astron. J.*, **92**, 1183.
38. Tokunaga, A.T., Smith, R.G., Nagata, T., DePoy, D.L., Sellgren, K. 1986, *Ap. J.*, **310**, L45.
39. Tokunaga, A.T., Nagata, T., and Smith, R.G. 1987, *Astron. Astrophys.*, in press.
40. Weaver, H.A., Mumma, M.J., Larson, H.P., and Davis, D.S. 1986, *Nature*, **324**, 441.
41. Wickramasinghe, D.T., and Allen, D.A. 1986, *Nature*, **323**, 44; Allen D. A. and Wickramasinghe, D. T. 1987, *Nature*, **329**, 615.

COMET WILSON WORLD-WIDE OBSERVATION LOG

David K. Lynch
The Aerospace Corporation
P.O. Box 92957, M2-266
Los Angeles, CA 90009

The following is an abbreviated list of observations of Comet Wilson compiled up through January 20, 1988. The purpose is to allow people working on Comet Wilson to make contact with other observers who may have supporting data. No claim of completeness is made. More information can be obtained by contacting the observers noted. For brevity, only the name of the observing team leader or person reporting the observations is listed. Visual magnitude estimates can be obtained from the IAU circulars. A four-digit number in brackets (e.g., [4241] refers to the IAU circular reporting the observations. UT may be rounded to the nearest 0.1 day.

Observers are encouraged to send a brief summary of their observations to the author for inclusion in future editions of this log. Information can be sent to the above address or to DIRAC2::LYNCH on the SPAN network.

TABLE 1.3

DATE (UT)	Type of Observation		Observer
<u>1986</u>			
Aug 4-6	Palomar 1.2 m Schmidt - DISCOVERY	[4241]	C. Wilson
	Precise Positions		various
Aug 6-10	Precise Positions	[4243]	various
Aug 25-31	Nancay 1667 MHz OH		E. Gerard
Sept 2.3	LPL Catalina 1.5 m 300-930 nm spectra	[4253]	S. Larson
Sept 3.3	"		"
Sept 5.0-5.3	IUE 195-340 nm		P. Feldman
Sept 6.3	IRTF 10.8 μ m bolometer array	[4258]	R. Decher
Oct 8.9-9.2	IUE 115-340 nm		P. Feldman
Oct 10-18	Nancay 1667 MHz OH	[4271]	E. Gerard
Oct 31.5	KPNO 2.1 m CCD R filter images		K. Meech
Nov 6-8	Nancay 1667 MHz OH	[4271]	E. Gerard
Nov 11-12	"	[4271]	"
Nov 16.8-17.1	IUE 115-340 nm		P. Feldman
<u>1987</u>			
Feb 6-7	VLA OH emission	[4314]	P. Palmer
Mar 13.8	IRTF 10.8 μ m imaging		H. Campins
Mar 14.5-21.8	Pioneer Venus UV spectrometer		I. Stewart
Mar 14.8	IRTF 10.8 μ m imaging		H. Campins
Mar 15.8	IRTF 10.8 μ m imaging		H. Campins
Mar 17.1-19.8	Pioneer Venus UV spectrometer image		I. Stewart
Mar 17.7	Lick 1 m, 8 - 14 μ m CVF spectra		J. Bregman
Mar 30.8-	Pioneer Venus UV spectrometer		I. Stewart
May 2.8			
Mar 28.8-29.1	IUE 115-340 nm		P. Feldman
Mar 29.8	UK Schmidt J plate 20 ^m	[4372]	C. Humphries
Apr 3.7-4.7	IUE 115-340 nm		P. Feldman
Apr 10.7-11.4	"		"

Apr 12.7	KAO 1.5 - 3.0 μm	FTS	[4403]	H. Larson
Apr 14.7	"	"	"	"
Apr 16	CTIO 0.6 m photometry/molecules		[4371/2]	J. Ducati
Apr 17.7	KAO 1.5 - 3.0 μm	FTS	[4403]	H. Larson
Apr 18	CTIO 0.6 m photometry/molecules		[4371/2]	J. Ducati
Apr 19	"	"	"	"
Apr 22.9	IUE 115-340 nm			P. Feldman
Apr 23.4	CTIO .6 m photometry/molecules		[4375]	J. Ducati
Apr 23.6	KAO 5.2 - 13 μm array spectra			D. Lynch
Apr 24.4	CTIO 1.5 Schmidt IIIa-J			K. Meech
Apr 24.4	CTIO .6 m photometry		[4375]	J. Ducati
Apr 25.4	"	"	"	"
Apr 25.6	KAO 5.2 - 13 μm array spectra			D. Lynch
Apr 26.4	CTIO 1.5 Schmidt IIIa-J			K. Meech
Apr 27.4	"	IIa-O		"
Apr 27.4	El Leoncito 0.8 m	CCD NB filters		P. Bernhardt
Apr 28.3	"	0.5 m " "	H_2O^+	"
Apr 28.4	Siding Spring 2.3 m	CCD images		T. Rettig
Apr 29.3	El Leoncito 0.3 m	CCD NB filters	CO^+	P. Bernhardt
Apr 29.4	"	0.5 m " "	CO^+	"
Apr 30.4	Siding Spring 2.3 m	CCD images		T. Rettig
Apr 30.5	Siding Spring 2.3 m	CCD spectra 380-700 nm		T. Rettig
May 1.2	El Leoncito 0.5 m	CCD NB filters	H_2O^+	P. Bernhardt
May 2.0	CTIO 1.5 m	Many short N/B CCD images		K. Meech
May 2.5	Siding spring 2.3 m	CCD images		T. Rettig
May 3.3	El Leoncito 0.5 m	CCD NB filters	H_2O^+	P. Bernhardt
May 4.2	"	0.5 m " "	H_2O^+	"
May 4.17	U. Toronto/Las Campanas photo	103a-O 5 ^m		C. Aikman
May 4.38	CTIO Schmidt	103a-0 10 ^m		A. Gomez
May 4.5	Siding springs 2.3 m	CCD images		T. Rettig
May 4.5	Siding spring 2.3 m	CCD spectra 380-700 nm		T. Rettig
May 5.15	U. Toronto/Las Campanas photo	IIa-O, 098 5 ^m		C. Aikman
May 5.4	Siding Springs 2.3 m	CCD spectra 380-700 nm		T. Rettig
May 5.5	Siding Spring 2.3 m	CCD images		T. Rettig
May 5.6-6.0	IUE 115-340 nm			P. Feldman
May 6.3-7.0	"	"		P. Feldman
May 6.5	Siding Springs 2.3 m	CD images		T. Rettig
May 7.4	AAO 3.9 m	CCD spectra 390-690 nm		T. Rettig
May 8.04	U. Toronto/Las Campanas photo	IIIa-J 5 ^m		C. Aikman
May 9.1	U. Toronto/Las Campanas photo	IIIa-J, 098 5 ^m		C. Aikman
May 10.5	"	IIIa-J, 098		"
May 10.5	AAO 3.9 m	IPCS spectra 370-620 nm		T. Rettig
May 12.6-27.0	IUE 115-340			P. Feldman
May 16.1	CTIO 0.6 m	NB photometry/308-700 nm		W. Osborn
May 20.0	"	"		"
May 21.0	"	"		"
May 24	IRTF 2.8 - 3.4 μm spectra		[4399]	T. Brooke
May 26.6-27.0	IUE 115-340 nm			P. Feldman
May 29.2	IRTF photometry M,N,8.7,10.3,12.5 μm			M. Hanner
Jun 1.2	"	M,N,7.8,8.7,10.3,11.6,12.5 μm		"
Jun 1.2	"	J,H,K,L		"
Jun 2.2	"	N,Q,18 μm		"
Jun 8.5-8.9	IUE 115-340 nm			P. Feldman

Jun 16.8	IRAM 30 m HCN J-1-0 88.6 GHz	[4411]	J. Crovisier
Jun 17.7	"		"
Jun 18.7	"		"
Jun 19.7	"		"
Nov	CCD Images at R		K. Meech
 <u>1988</u>			
Jan 10.5	IRTF Photometry N, 18 μ m		M. Hanner
Jan 11.5	IRTF Photometry J, H, K		"
Jan 12.5	IRTF Photometry N, 18 μ m		"
Jan 13.5	IRTF Photometry N, 18 μ m		"
Jan 14.5	IRTF Photometry J, H, K		"

CHAPTER 2

GRAIN OPTICAL PROPERTIES

Martha Hanner
Jet Propulsion Laboratory

with contributions from D. R. Huffman, N. Divine,
S. Green, P.L. Lamy, D. Lien, and K. Sellgren

1.0 INTRODUCTION

The optical properties of small grains provide the link between the infrared observations presented in Chapter 1 and the dust composition described in Chapter 3. In this session, the optical properties were discussed from the viewpoint of modeling the emission from the dust coma and the scattering, at $\lambda \leq 2.5\mu\text{m}$, in order to draw inferences about the dust-size distribution and composition.

The optical properties are applied to the analysis of the infrared data in several ways, and these different uses should be kept in mind when judging the validity of the methods for applying optical constants to real grains.

1) Computing grain temperature:

The equilibrium temperature of a grain in the solar radiation field is computed by equating the total energy absorbed to the total energy radiated

$$\pi s^2 \left(\frac{R_o}{R} \right)^2 \int_0^\infty Q_{\text{abs}}(s, \lambda) S(\lambda) d\lambda = 4\pi s^2 \int_0^\infty \pi B(\lambda, T) Q_{\text{abs}}(s, \lambda) d\lambda$$

where $S(\lambda)$ is the solar flux, $B(\lambda, T)$ the Planck function at grain temperature T , R is the heliocentric distance, and $Q_{\text{abs}}(s, \lambda)$ the wavelength-dependent absorption efficiency factor for grain radius s . For this purpose the Q_{abs} are required from the ultraviolet through the infrared for any grain size; however, the accuracy required is not stringent. In fact, for absorbing grains, the resulting grain temperatures depend primarily on grain size, not on the detailed wavelength dependence of the complex refractive index.

From the computed temperatures (as a function of grain size) and the grain size distribution, the infrared flux can be calculated and compared with the observed flux to derive the dust production rate.

2) Predicting the infrared spectral energy distribution:

Here, the interest lies in identifying the physical nature of the grains – their composition, size and other attributes such as degree of crystallinity. Spectral features are of particular interest. For this purpose, one needs not only good optical constants, but also a means of applying them to real grains, with all their bumps and blemishes.

3) Analyzing the scattered light and polarization:

At wavelengths $\lambda \leq 2.5\mu\text{m}$, scattered light dominates the radiation from the coma. Here, the angular scattering functions $i_1(\phi)$, $i_2(\phi)$ are required, and these are strongly affected by grain shape and surface irregularity.

Although simpler than the case of circumstellar dust in the sense that the geometry is known and the optical depth is low, the comet analysis is complicated by the range of grain sizes, which tends to obscure the band structure diagnostic of composition. Moreover, the large range of grain sizes means that the Rayleigh approximation is never valid, in contrast to interstellar grains in the far infrared.

Our discussion at this workshop focused on the availability of appropriate optical constants and the adequacy of theories to apply them to real grains. Some first attempts to fit the infrared data with models based on optical constants were reported. The grain-size distribution, as measured by the spacecraft, and its compatibility with the infrared data were also discussed. The analysis of comet dust was contrasted with the case of interstellar dust in reflection nebulae.

2.0 OPTICAL CONSTANTS

To interpret the infrared observations, optical constants are required not only in the infrared, but also in the visible and near-uv in order to compute the equilibrium temperature of small grains in the solar radiation field. By optical constants we mean the complex dielectric functions, or equivalently the complex refractive indices, as a function of wavelength.

Huffman stressed the amount of effort required to determine optical constants correctly in the laboratory. Optical measurements, such as reflectance and/or transmittance must be performed as a function of wavelength on a polished bulk sample and an appropriate theory (such as Fresnel's equations) is then used to compute the optical constants as a function of wavelength. The optical constants cannot adequately be measured directly on small particles, in part because of the problems of clustering, as discussed in Section 2.5.

Among the materials relevant for cometary dust are silicates, various forms of carbon, magnetite, and organic materials. All of these have at least some measured optical constants. While ices are also of interest, they were not addressed at this workshop.

2.1 Silicates

As described in Chapter 1, spectra of Halley's dust coma exhibit a prominent 8- to 12.5 μm emission feature with peaks indicative of crystalline olivine and pyroxene. This is in contrast to earlier comet spectra and almost all relevant spectra of interstellar and circumstellar sources, which show a broad, structureless feature, leading to the conclusion that the grains must be amorphous. However, the Halley spectra are consistent with the composition and infrared spectra of interplanetary dust particles (IDPs), which clearly show signatures of crystalline olivine and pyroxene minerals (Sandford and Walker 1985; Sandford, Chapter 3, this report).

It was emphasized at the Workshop that one should not think only of two end states, but rather a continuous range of structural order. Indications of crystallinity will be evident in the 10 μm stretching mode vibrations for a greater degree of disorder than in the 20 μm bending mode vibration. This is a possible explanation for the lack of a distinct peak in the 20 μm Halley spectrum. An example of the changing 10 μm spectrum during annealing is given by Day (1974). Thus, optical constants for silicates with differing degrees of structural order are desirable.

Refractive indices of crystalline silicates are tabulated by Pollack *et al.* (1973) for natural samples of obsidian, basalt, and andesite from 0.2 to 0.50 μm . Steyer (Ph.D. thesis 1974) determined the optical constants of several silicates from 0.2 to 50 μm , including

the three major polarization directions of crystalline olivine, $[\text{Mg,Fe}]_2 \text{SiO}_4$. Mooney and Knacke (1985) have measured refractive indices from 2.5 to $50\mu\text{m}$ for natural samples of the hydrated silicates chlorite and serpentine.

Kratschmer and Huffman (1979) derived the optical constants for a disordered olivine by irradiating polished crystals of olivine with high-energy neon ions until the crystal structure in the optically active surface layer was destroyed. In this way, the smooth surface was preserved for reflectance measurements. Classical dispersion theory was used to derive the optical constants from 8 to 25 microns. The extinction of amorphous silicate smokes from 7 to 300 microns has been measured by Day (1976, 1979, 1981), but optical constants approximated from Day's extinction measurements and those extrapolated from Kratschmer and Huffman's work are badly discrepant. A direct determination of optical constants for disordered olivine at long wavelengths is desirable.

2.2 Carbon

Graphitic carbon (as opposed to diamond-like carbon) can occur in a complete range of structural order from totally amorphous on one end to single-crystal graphite on the other. Graphite was originally suggested as a component of interstellar grains because it shows a feature near the position of the 2200\AA interstellar feature. However, recent laboratory work has shown that less structured forms of carbon can produce a similar feature (e.g., Borghesi *et al.* 1985; Sakata *et al.* 1983). Furthermore, graphite is rarely seen in interplanetary dust particles, although carbonaceous material is common.

Single-crystal graphite is anisotropic. Reliable optical constants exist for the easy-to-measure $E \perp c$ direction (Taft and Philipp 1965; Philipp 1977). The $E \parallel c$ is much more difficult because of the difficulty of preparing a polished sample for the reflectance measurements, and existing measurements are quite discrepant. But modeling using only the $E \perp c$ optical constants overestimates the absorption in the ultraviolet, for example, compared to an ensemble of randomly oriented graphite grains.

In choosing a material representative of partially disordered carbon, Edoh (1983) selected for study the homogeneous bulk material called glassy or vitreous carbon. It is available commercially and is capable of being highly polished to permit proper optical measurements to be made. The ultraviolet region had already been well measured by Williams and Arakawa (1972).

Edoh prepared polished samples of glassy carbon and performed specular reflectance measurements, overlapping and agreeing well with the previous measurements. The usual Kramers-Kronig analysis of the combined reflectance data set produced the optical constants contained in Table 2-1 and plotted in Figure 2.1. These may prove useful to modelers needing optical constants for a type of carbon having a partial degree of order intermediate between single-crystal graphite and completely disordered carbon. Details of these measurements are found in the 1983 Ph.D. thesis of Edoh, which can be cited as the source reference until the measurements appear in a published journal article.

2.3 Magnetite

Magnetite is a candidate cometary material which is present in meteorites. It has the interesting property that infrared optical constants change with temperature. Steyer (1974) determined the optical constants from 2 to 100 microns for the same samples which Huffman and Stapp (1973) measured in the ultraviolet (see Huffman 1977, Fig. 33); these refer to room temperature.

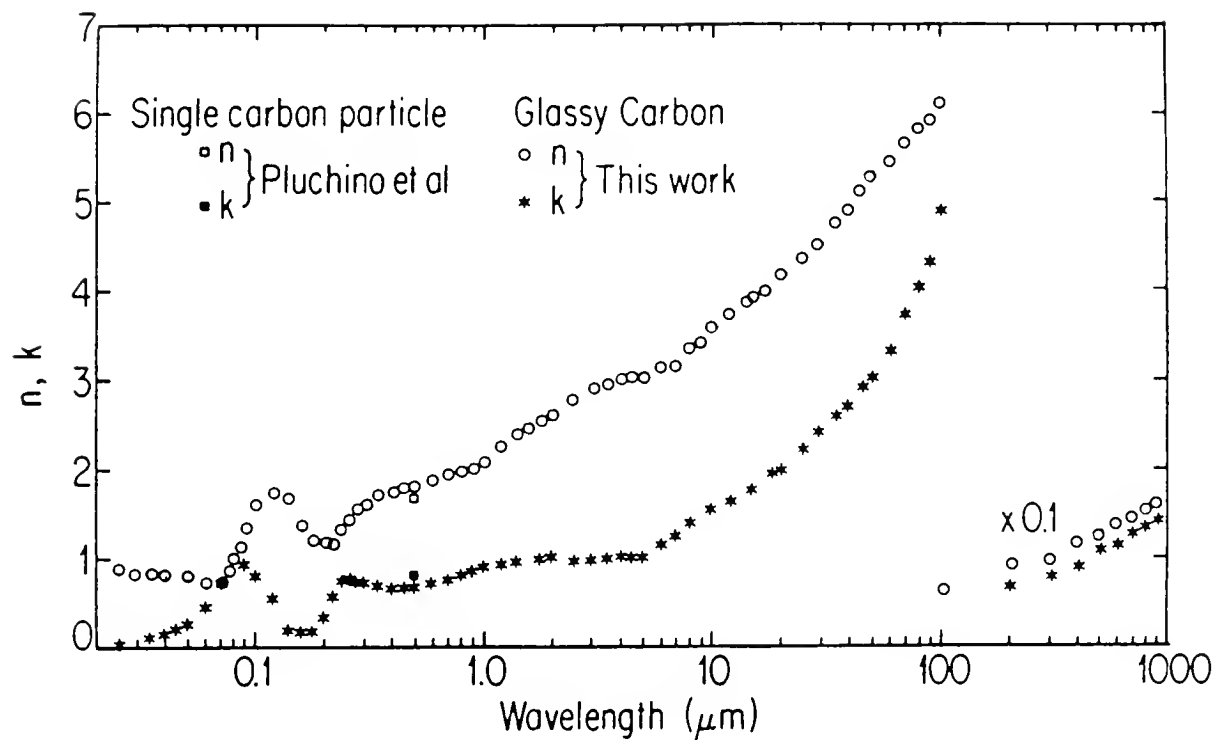


Figure 2.1 - Optical constants n and k of glassy carbon as computed by the Kramers-Kronig method (Edoh 1983).

Table 2-1

OPTICAL PROPERTIES OF CARBON FROM THE FAR INFRARED TO THE FAR ULTRAVIOLET

$\lambda(\mu\text{m})$	n	k	$\lambda(\mu\text{m})$	n	k
.04	.84	.108	11.	3.63	1.60
.05	.74	.177	12.	3.70	1.63
.06	.69	.380	13.	3.75	1.69
.07	.76	.66	14.	3.84	1.74
.08	.93	.90	15.	3.88	1.78
.09	1.26	.95			
.10	1.53	.84	16.	3.96	1.83
.12	1.74	.56	17.	3.99	1.89
.14	1.70	.202	18.	4.1	1.95
.16	1.39	.151	19.	4.14	1.95
.18	1.24	.180	20.	4.18	1.98
.20	1.22	.321			
			21.	4.22	2.03
.22	1.19	.57	23.	4.31	2.08
.24	1.34	.74	25.	4.36	2.19
.26	1.46	.74	27.	4.47	2.27
.28	1.54	.73	29.	4.53	2.37
.30	1.60	.72			
.30	1.60	.72	31.	4.61	2.42
.35	1.70	.69	33.	4.67	2.52
.40	1.75	.67	35.	4.77	2.60
.45	1.79	.67	37.	4.82	2.67
.50	1.82	.68	39.	4.91	2.72
.60	1.88	.71	41.	4.96	2.81
.70	1.94	.77	43.	5.04	2.85
.80	2.00	.80	45.	5.11	2.92
			50.	5.25	3.00
.90	3.45	.85			
.92	2.04	.86	55.	5.32	3.18
.94	2.04	.87	60.	5.44	3.31
.96	2.06	.89	65.	5.49	3.50
.98	2.06	.90	70.	5.67	3.70
1.0	2.11	.90	75.	5.71	3.80
1.2	2.24	.95	80.	5.85	4.00
1.4	2.38	.97	85.	5.90	4.15
1.6	2.46	.99	90.	5.99	4.30
1.8	2.55	1.00	95.	5.94	4.48
2.0	2.63	1.02	105.	6.7	4.7
2.5	2.80	1.00	205.	8.6	6.5
3.0	2.86	.99	305.	10.2	8.0
3.5	2.95	1.01	405.	11.6	9.5
4.0	3.03	1.04	505.	12.6	10.5
5.0	3.04	1.03	605.	13.4	11.6
			705.	14.1	12.5
6.0	3.15	1.15	805.	15.0	13.4
7.0	3.16	1.25	905.	16.5	14.1
8.0	3.35	1.42			
9.0	3.42	1.47			
10.	3.55	1.54			

2.4 Organic Materials

Optical constants from 0.02 to 1000 μm have been determined by Khare *et al.* (1984) for a dark organic solid produced by electrical discharge in a gas mixture of 0.9 N₂ and 0.1 CH₄ ("Titan tholin"). The imaginary part of the refractive index, k is ~ 0.04 at 0.5 μm and decreases to 4×10^{-4} at 1.5 microns, causing a reddish color and classifying this as a "slightly absorbing" material. The real part of the refractive index at visible wavelengths is ~ 1.68 , similar to silicates; thus, this tholin resembles the "dirty silicate" in the visible.

Recently, Khare *et al.* (1987) have measured optical constants in the visible and near-infrared (0.35-2.5 μm) for several other tholins produced by electrical discharge in pure methane gas and in H₂ gas with varying methane abundance. The synthesized products have similar optical properties, with n in the range 1.56 - 1.67 and $10^{-4} < k < 10^{-2}$ at $\lambda > 0.5\mu\text{m}$, similar also to the Titan tholin. Refractive indices for various carbonaceous materials at $\lambda = 0.5\mu\text{m}$ are summarized in this reference.

Optical measurements are in progress for another organic residue produced by irradiating gas and ice mixtures similar to cometary ices in initial composition (Khare *et al.* 1987b). For a product synthesized from a gas mix of equal parts methane and water, they find $n = 1.48 - 1.58$ and $k = 2 \times 10^{-3}$ to 4×10^{-2} at 0.5 μm .

While there are many infrared spectra of organic residues showing features near 3.4 μm , optical constants are needed for this region, to allow modeling as a function of grain-size distribution and temperature.

In general, one would expect the optical constants (especially the absorptivity) to depend on the radiation dose, which determines the C/H ratio of the material. Coloration and progressive darkening with increasing irradiation are noted by almost all experimenters.

2.5 Relating Extinction Measurements to Optical Constants: The Problem of Clustering

One would think that optical constants could be derived from measured extinction, scattering, absorption directly on small particles. However, in cases where extinction has been computed, based on the optical constants measured on bulk samples, and compared with extinction measured in the laboratory for small particles, the results are disconcertingly discrepant. Much of this problem is apparently due to particle-clustering (Bohren & Huffman 1983, Huffman 1987 and abstract, this report). Huffman proposed that the shape distribution for randomly oriented ellipsoids in the Rayleigh limit is an appropriate way to treat the problem of clustering (see Section 3.3).

2.6 Optical Constants in the Far Infrared

Carbon: The optical constants of Edoh may be satisfactory to represent disordered carbon at wavelengths $\leq 100\mu\text{m}$. The effects of clustering are expected to become increasingly important in carbon at longer wavelengths ($> 100\mu\text{m}$) because of the increasing values of both real and imaginary parts of the dielectric functions.

Silicates: Pollack *et al.* present optical constants of crystalline silicates out to 50 μm , while Steyer's measurements extend to 300 microns. No reliable optical constants exist for amorphous silicate beyond $\sim 25\mu\text{m}$. Several general trends of optical constants for insulators such as silicate are expected at long wavelength (Huffman 1977; Mitra and Nudelman 1970):

- (1) In single crystals, absorption should decrease steeply with a magnitude that is quite temperature-dependent (lower absorption at low temperatures).

- (2) In disordered (amorphous) insulators absorption is generally much higher than for single crystals, is less steep in wavelength dependence, and much less dependent on temperature.
- (3) Impurities will lead to higher absorption.
- (4) The effects of clustering are expected to become constant in insulators at long wavelength.

Organic Materials: A slightly absorbing material, such as the "Titan tholin," will follow the general behavior of an insulator. For the Titan tholin, the real part of the refractive index increases slightly and the imaginary part decreases from 0.2 to 0.002 from 100 to 1000 microns.

2.7 Recommendations for Further Measurements

Measurements of optical constants for disordered silicates from 25 to 100 μ m are needed, not only to define the wavelength dependence, but also to indicate any features in the 24 to 40 μ m region.

Because both silicates and carbon can occur with a range from complete disorder to fully crystalline, it is important to document the degree of disorder in the measured samples.

Measurements are desirable that would help to define the structure in both the 10- and 20-micron silicate bands for olivine and pyroxene as a function of the degree of disorder.

Optical constants, as opposed to transmission and reflectance spectra, are needed for appropriate organic materials in the 3 μ m region.

One needs to be aware of the discrepancies that can be caused by particle clustering, in particular when attempting to deduce optical constants from extinction measurements.

3.0 APPLICATION OF OPTICAL CONSTANTS

Once the optical constants as a function of wavelength have been specified, an appropriate theory must be applied to predict the observable radiation from the ensemble of cometary particles. While we have many reasons to believe that cometary dust particles are not perfect spheres (one has only to look at the IDPs), most interpretations rely on the theory of spheres to solve for the interaction of light with the particles. Generalization of this theory to non-spherical particles is a formidable task which is being approached slowly from the theoretical and experimental viewpoints.

It does not appear, at the present time, that the problem can be treated in a unified way; as a consequence, we have to distinguish different situations for which we have some understanding of the interaction. We discuss here examples of theoretical approaches which were presented at the Workshop; other approaches exist in the literature.

3.1 Smooth Spheres

The interaction of light with a smooth, homogeneous spherical particle can be computed from Mie theory. Descriptions are given by Kerker (1969), van de Hulst (1957), Bohren and Huffman (1983). For our purposes, we need to understand the extent to which Mie theory is useful in predicting the behavior of non-spherical particles, specifically in predicting grain temperatures, infrared emissivity (continuum, features) and scattering.

The problem also has been solved analytically for other smooth, geometric shapes, such as spheroids and infinite cylinders, by expressing the boundary conditions in the

appropriate coordinates.

3.2 Rough Non-Spherical Particles

Particles Smaller than the Wavelength

For particles smaller than the wavelength, but larger than the Rayleigh limit, the best approach appears to rely on the representation of the particle by a network of interacting dipoles, as pioneered by Purcell and Pennypacker (1973). This has recently been improved by Chiapetta, Perrin, and Torresani (1987) and their model is able to reproduce the phase functions $i_1(\theta)$ and $i_2(\theta)$ of a perfect sphere as given by Mie theory. It remains to be seen how the model will behave when more complex shapes are introduced. It is important to realize that, in this case, the roughness is much less than the wavelength.

Large Rough Particles ($s > \lambda$)

When the roughness scale is comparable to or larger than the wavelength, several effects, such as diffraction, multiple reflection, and shadowing enter the interaction. Perrin and Lamy (1986) have obtained a solution for this problem in the framework of the potential theory, introducing a statistical description of the roughness. In its most elaborate form, a vectorial description is obtained enabling one to calculate not only the efficiency factors but also the polarization. This theory is able to produce remarkably well the experimental data of Weiss-Wrana (1983) for non-absorbing as well as absorbing material (see Fig. 2.4).

It must be kept in mind that this solution holds for large rough particles, with a conservative lower limit of particle radius $s/\lambda \geq 6$.

The effect of the roughness in terms of optical properties is illustrated in Figure 2.2, where the efficiency factors for a $50\mu\text{m}$ astronomical-silicate grain (Draine 1985) are plotted as a function of the mean roughness for various wavelengths ($0.25, 0.5, 3, 10\mu\text{m}$). Of importance is the substantial rise in the efficiency factors with respect to the "canonical" Mie values (roughness = 0), the differing behavior as a function of wavelength resulting from the complex index of refraction. Note that the Q_{abs} is less affected than Q_{scat} and Q_{ext} , a trend noted also in an analytic treatment by Wiscombe and Mugnai (1980).

A direct consequence is that rough grains of this "dirty" silicate absorb more energy in the visible than spheres, therefore reaching a somewhat higher equilibrium temperature. A preliminary calculation (Lamy, in preparation) is shown in Figure 2.3, where the temperature of "dirty" silicate grains at 1 AU is plotted versus their radius; for $s = 100\mu\text{m}$, the increase reaches 30 K, or about 10%.

Other consequences concern the phase function, which generally exhibits a broader diffraction lobe, and the polarization. Figure 2.4 compares the predictions from this theory with scattering by a $14\mu\text{m}$ slightly absorbing particle from the Allende meteorite measured by Weiss-Wrana (1983). One sees that the theory correctly predicts the width of the forward-scattering peak and the rise toward 180 deg, as well as the magnitude of polarization. The observed polarization of the dust coma of Halley can be matched approximately by a mixture of rough silicate and graphite particles, as illustrated in Figure 2.5 (Lamy *et al.* 1987). It is important to emphasize that, in this theory, the negative polarization branch is caused by the surface roughness of the absorbing grains, which does not exist for absorbing spheres; the surface roughness reduces the large (both positive and negative) polarization of the (dielectric) silicate grains.

3.3 Treatment of Shape Effects

Shape effects can be important, even in very small particles, in regions where surface modes are important (Bohren & Huffman Chapter 12). Two cases of direct relevance to

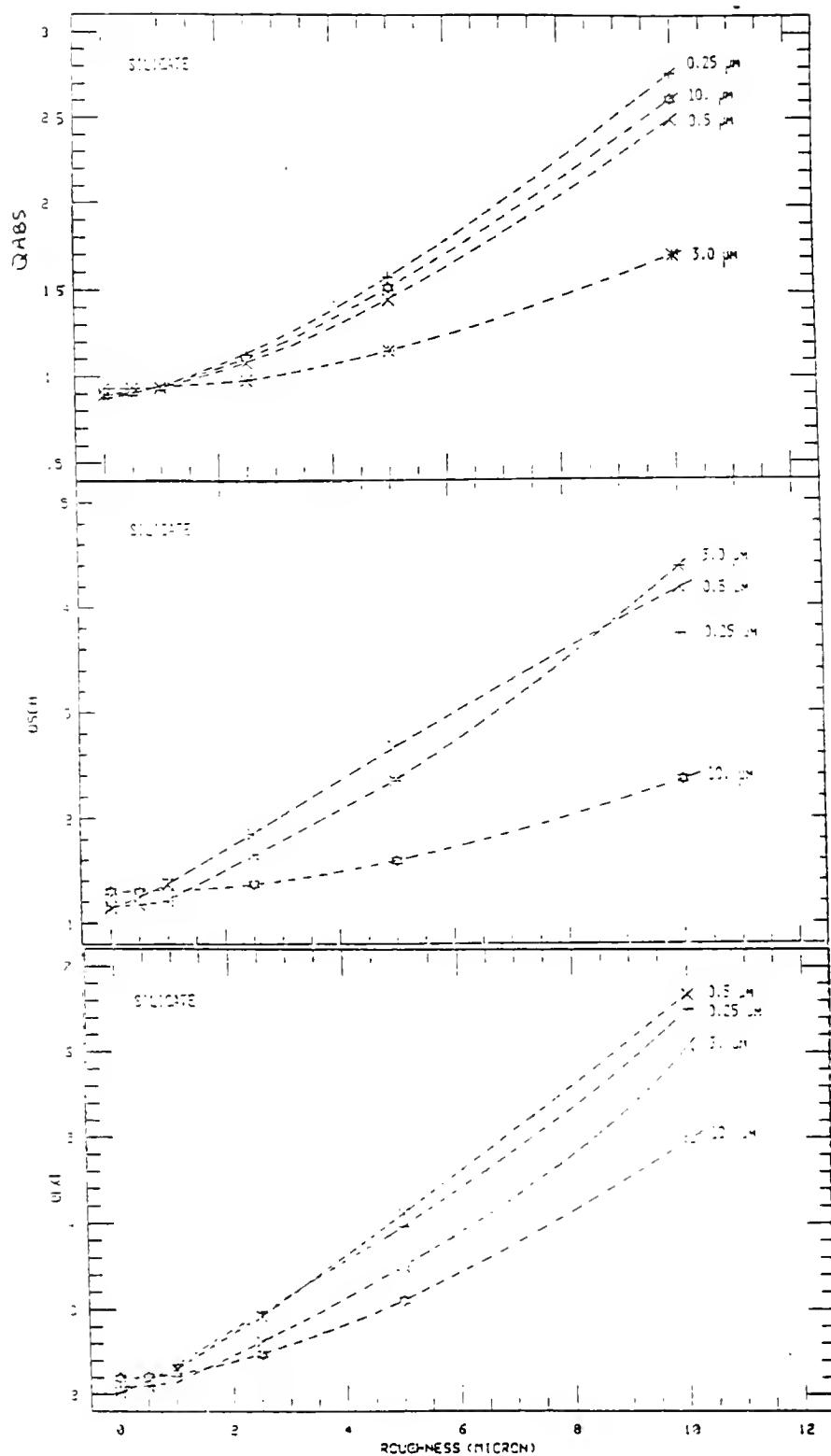


Figure 2.2 - Efficiency factors as a function of roughness for a $50\mu m$ silicate particle at various wavelengths (Lamy, abstract this report).

TABLE : TSIL

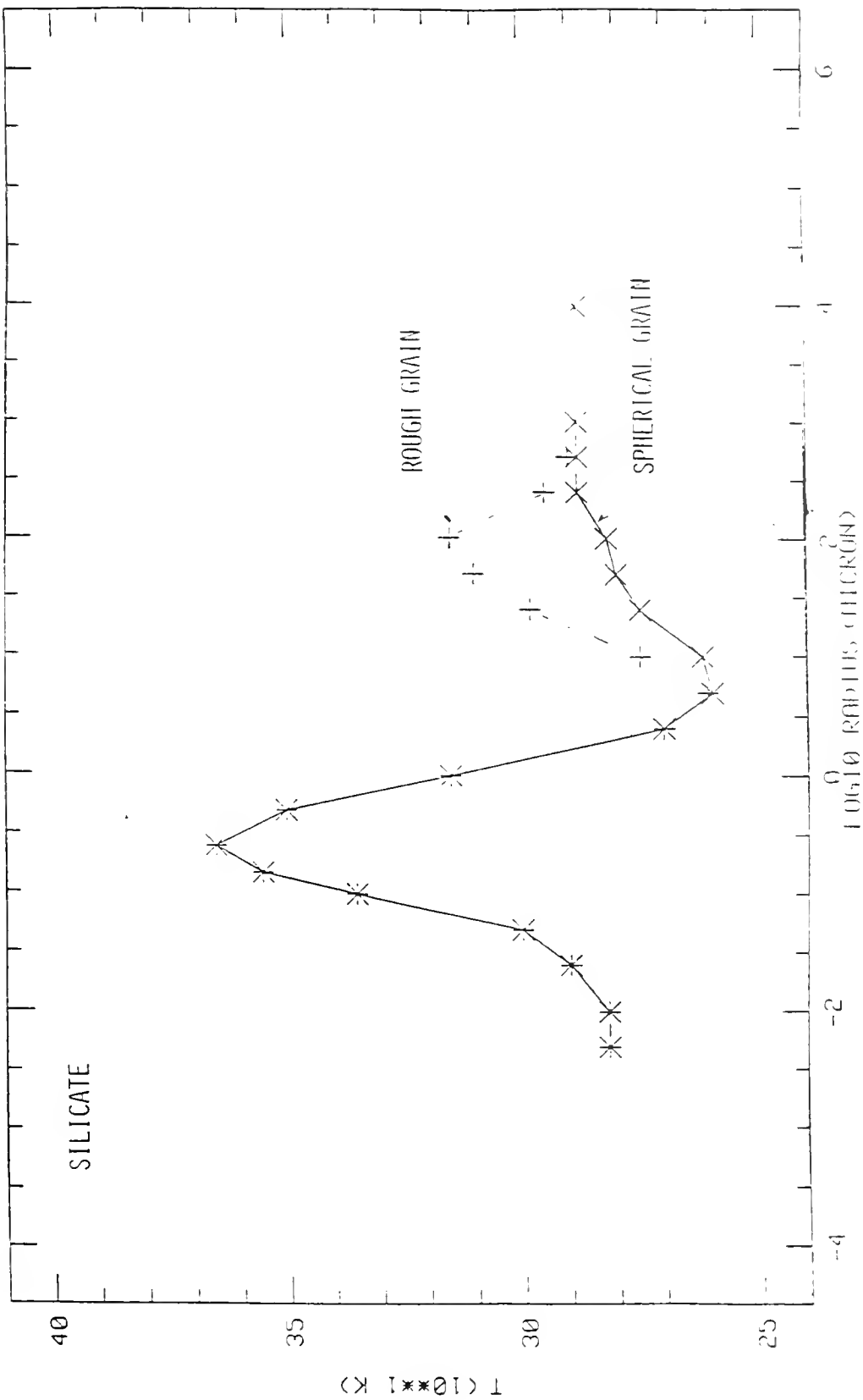


Figure 2.3 - Temperature of "astronomical" silicate grains at 1 AU, as a function of particle size for the spherical and rough cases.

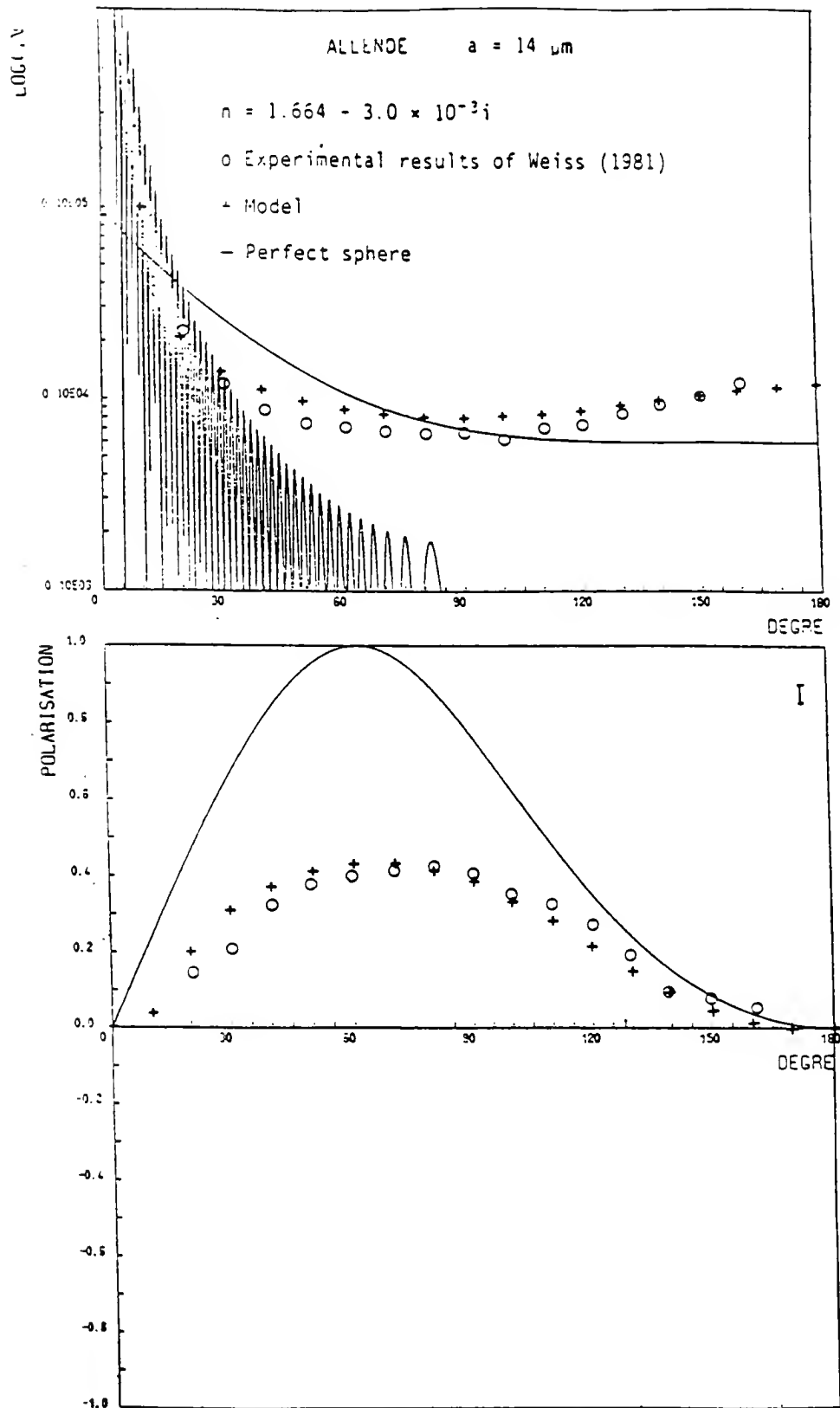


Figure 2.4 - Comparison of theory for rough particles (+) with optical measurements on a particle from the Allende meteorite (Perrin and Lamy 1983).

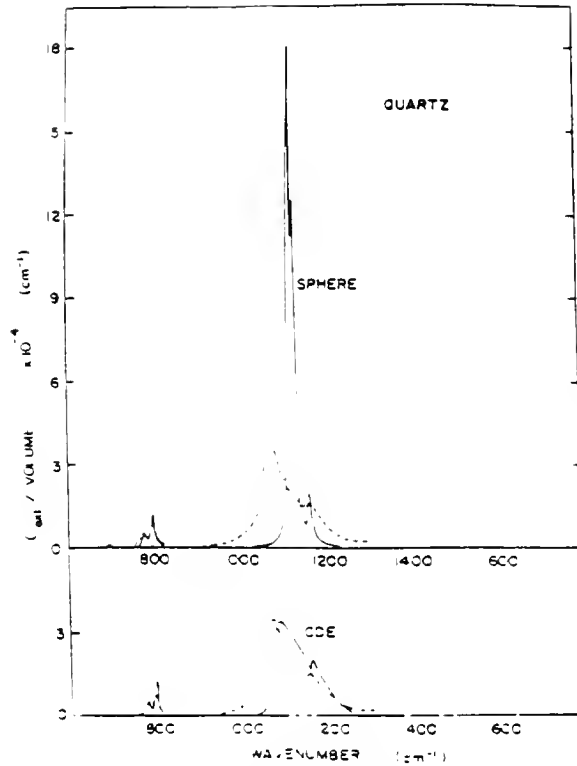


Figure 2.6 - Measured extinction of crystalline quartz particles compared with calculations for spheres and CDE (Bohren and Huffman 1983).

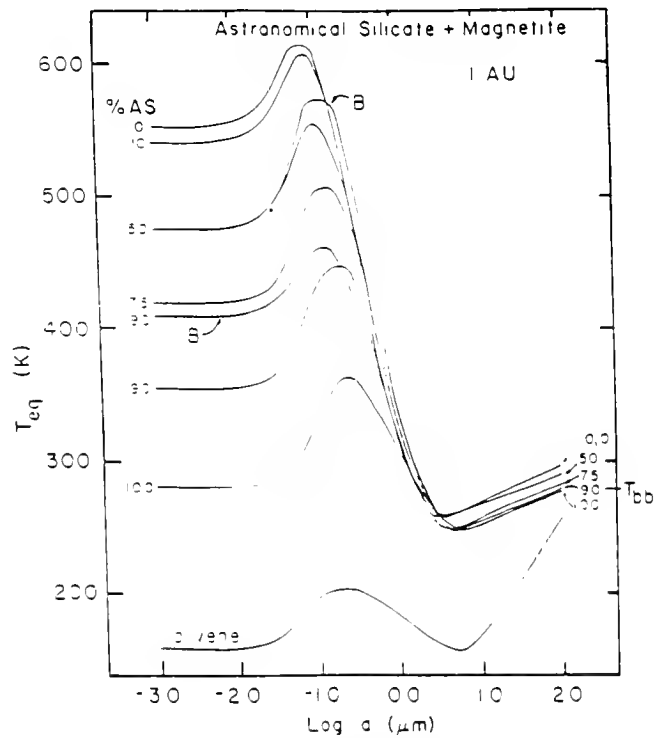


Figure 2.7 - Equilibrium grain temperatures at 1 AU computed for blends of "astronomical" silicate and magnetite, based on Maxwell-Garnett theory and Bruggeman theory (B) (Lien 1987).

the infrared data were discussed in which shape effects can cause significant deviation from the predictions of Mie theory. One case is the $10\mu\text{m}$ silicate resonance, the other the behavior of the far-infrared emissivity.

Huffman described a relatively simple approach which seems to permit reasonable calculations to be made for clustered particles. Known as the CDE model, this method treats the particles as a continuous distribution of ellipsoidal shape parameters, in the Rayleigh limit. The expression for the volume-normalized absorption cross section, averaged over all ellipsoid orientations and all possible shape parameters, reduces to:

$$\frac{\langle\langle C_{\text{abs}} \rangle\rangle}{v} = k \operatorname{Im} \frac{(2\epsilon \log \epsilon)}{\epsilon - 1}$$

where ϵ is the complex dielectric constant. An example for the $9\mu\text{m}$ resonance in crystalline quartz is displayed in Figure 2.6 (Bohren & Huffman 1983; Huffman, abstract this report). One sees that the CDE theory comes far closer to predicting the correct height, width, and central wavelength of the measured extinction feature. However, the CDE theory has been less successful when applied to measurements of an olivine smoke; thus, its usefulness for relating the cometary $10\mu\text{m}$ spectrum-to-optical properties of silicate minerals is not clear. (See Section 3.5).

The Far-Infrared

Most crystalline materials exhibit a $1/\lambda^{-2}$ falloff in extinction at long λ , while various interstellar measurements suggest a less steep decrease, perhaps $1/\lambda$. Laboratory measurements of carbon by Koike *et al.* (1980) also seem to show a falloff more like $1/\lambda$. Huffman (1987) explains this discrepancy as caused by particle clustering and shows (see abstract this report) that the CDE treatment, using the optical constants of glassy carbon measured by Edoh (1983), duplicates the slope of the laboratory-smoke measurements.

Thus, particle shape appears to be a significant factor in determining the long-wavelength emissivity. Further comparisons with laboratory measurements for well-defined particle shape distributions (fractals?) are clearly important. A more detailed discussion, and further examples, can be found in Bohren & Huffman, Chapter 12, and Huffman (1987).

3.4 Non-Homogeneous Particles

Two conceptual models for computing the average dielectric functions of nonhomogeneous grains were discussed. In the Bruggeman theory the composite grain is considered to be a mixture of small grains randomly packed together, while in the Maxwell-Garnett theory the composite grain consists of small inclusions ($x \ll 1$) embedded in a matrix material. The theories can be generalized to more than two components. Their limitations have been discussed by Bohren (1986).

Lien reported on calculations performed using these two theories for composite grains consisting of "astronomical" silicate (Draine 1985) and magnetite. Temperatures computed for spherical grains at 1 AU are plotted in Figure 2.7 as a function of the percent silicate included in a magnetite matrix (Lien 1987). (The "astronomical" silicate already has a higher absorption at visible wavelengths than pure silicate, leading to a warmer temperature than pure olivine.)

It is evident that even the addition of 10% of an absorbing material such as magnetite raises the temperature significantly, and a 50-50 mix is almost indistinguishable from pure magnetite, except at the smallest grain sizes. (Note that for larger grains, $s > 10\mu$, the temperature dip is reversed in rough particles – see Fig. 2.3).

Strictly, these effective medium theories assume that the component particle sizes are much smaller than the wavelength. These theories suffer from the same problems already discussed when near a resonance in the optical constants of one component.

3.5 10-Micron Silicate Feature

The 10-micron region in the Halley spectra is extremely difficult to treat analytically. There are two serious problems, either one of which alone could be fatal to a quantitative model. First, Mie theory does not adequately predict the structure and strength of the $10\mu\text{m}$ feature in irregularly-shaped crystalline silicate particles. Second, it is likely that the comet grains have varying degrees of crystallinity, which are not adequately represented by the optical constants for the end members alone. Complicating the picture further, it appears that more than one kind of silicate is present and contributing to the observed feature. While the optical constants for olivine have been measured rather well, the same cannot be said for other silicates, such as enstatite, a pyroxene mineral known to be present in IDPs. Moreover, the silicate grains in the comet seem likely to be embedded in carbonaceous material.

No easy answers emerged from this workshop. Analogy with the spectra of IDPs, as discussed by Sandford (this report), may be the best approach available to identify the kinds of silicates present. A detailed quantitative analysis of the Mg:Fe:Si ratios, relative abundances and size distribution of the silicates in comet dust, will be possible by direct sampling from the Comet Rendezvous mission.

3.6 Core-Mantle Particles

Although not discussed specifically at this workshop, calculations for layered spheres, while still suffering from the limitations of Mie theory, may be of some use in predicting the general effects of absorbing material overlying silicate particles, for example.

3.7 Laboratory Studies

Laboratory measurements of the interaction of irregular particles are an important means of testing the validity of analytical treatments. Their drawback is that it is difficult to generalize from the specific laboratory experiment to particles in astrophysical contexts, as the above discussion of clustering effects illustrated.

Considerable work has been done on measurement of the scattering and polarization of irregular particles of relevance to cometary grains. Much of this has been accomplished by scaling the particle size and wavelength to microwave frequencies (e.g., Schuerman 1980a; Zerull *et al.* 1980). Larger particles have been suspended and studied with lasers. These studies support the results of Lamy and Perrin regarding the shape of the phase function and the negative polarization branch. Obtaining the efficiency factors, Q_{scat} and Q_{ext} from these scattering measurements is not always possible, however, because the laboratory setup often does not allow measurement of the forward scattering lobe where much of the energy is concentrated.

Many extinction measurements have been made at infrared wavelengths. These are useful to the extent that the measured particle ensemble resembles that in the comet (size distribution, shape distribution, composition, degree of crystallinity). One should also be aware that extinction is not equal to absorption in cases where scattering may be important, since $Q_{\text{ext}} = Q_{\text{abs}} + Q_{\text{scat}}$.

Interplanetary dust particles are an important resource for understanding optical/ir grain properties. Their composition can be directly related to their infrared spectra and

their measured optical properties can be compared with predictions based on optical constants.

3.8 Other Sources

Considerable theoretical and experimental research is taking place for other applications of particle optical properties which may be relevant for interpreting the optical and infrared observations of comet dust (see for example Schuerman (1980)).

Each year, for about ten years now, the U.S. Army Chemical Research Development and Engineering Center (CRDEC) has sponsored a conference called the "Scientific Conference on Obscuration and Aerosol Research." These have brought together an impressive group of workers in the field of small-particle optical research. Both theory and experiments relating to spherical and nonspherical particles have been presented. Numerous measurements of optical constants have been reported, including natural silicates and carbons. It may be of value for astronomical studies of particles to become familiar with the results of this annual conference, as reported in the publications listed in Table 2-2.

3.9 Summary

These points emerged from the discussion:

- For a compact, homogeneous particle with surface irregularity smaller than the wavelength, the absorption efficiency, Q_{abs} , is not badly approximated by Mie theory, provided the wavelength is not near a strong feature. As the roughness increases, the Q_{abs} will increase.
- The temperature of a large rough particle under solar illumination will be somewhat higher than that of an equivalent smooth sphere, because of the higher Q_{abs} .
- The CDE model for a random distribution of ellipsoids shows promise for treating the far-infrared emissivity; further laboratory comparisons are desirable.
- Effective medium theory for deriving optical constants of heterogeneous material can be useful for investigating the approximate optical and thermal properties of composite grains (e.g., silicates + absorbing material; crystalline + amorphous silicates).
- An adequate analytical treatment for predicting the shape of the 10- and 20-micron silicate features does not exist.
- Particle roughness is particularly important for polarization, and the polarization versus phase angle for an irregular particle is not well represented by Mie theory.
- Polarization can be treated by a theory for rough particles; surface roughness introduces a negative polarization branch for absorbing particles and reduces the polarization in silicates.
- Surface roughness can explain the observed scattering phase function, including the enhanced backscattering.
- The Q_{abs} and scattering for a fractal grain model should be explored.
- Analytical methods can be tested by attempting to reproduce measured infrared spectra of IDPs.
- Astronomers should not ignore the considerable research on light interaction with irregular particles being conducted in other fields, for example the research funded by the Army.

TABLE 2-2
 Previous Proceedings
 of the CSL/CRDC* Scientific Conference
 on Obscuration and Aerosol Research
 Chemical Research, Development and Engineering Center
 Aberdeen Proving Ground, Maryland 21010-5423

Year of Conference	Report Number
1979	ARCSL - CR - 81023
1980	ARCSL - SP - 82021
1981	ARSCL - SP - 82022
1982	ARCSL - SP - 83011
1983	CRDC - SP - 84009
1984	CRCD - SP - 85007
1985	CRDEC - SP - 86019

*The U.S. Army Chemical Research, Development and Engineering Center (CRDEC) was known as the Chemical Research and Development Center (CRDC) prior to March 1986 and as the Chemical Systems Laboratory (CSL) prior to July 1983.

4.0 DUST-SIZE DISTRIBUTION

4.1 *In-Situ*-Mass Distribution

The Vega and Giotto spacecraft carried detectors to record the impact rate and mass distribution of dust particles. Since the spacecraft velocity of ~ 70 km/s was far larger than the outflow velocity of the dust, the sensors sampled the spatial density of the dust, a quantity needed for modeling the infrared emission. While a generally consistent picture emerges, all of the sensors detected changes in the mass distribution along the trajectory, with steeper slope (more small particles) generally associated with higher impact rates (dust jets). The abundant small particles ($\sim 0.01\mu\text{m}$) discovered by the flyby missions contribute negligibly to the infrared thermal continuum or scattered light.

Divine described the cumulative mass distributions from the spacecraft data and the analytical expressions he has applied to them. He has fit the various integral mass distributions with a function which approximates two power-law segments, using the parameters and formulae specified in Table 2-3. These are discussed further in his abstract, this volume, and Divine and Newburn (1987). Some additional useful quantities are defined in Table 2-4.

The Giotto Dust Impact Detector (DIDSY) used momentum sensors attached to the spacecraft dust shield to detect particle masses $\geq 4 \times 10^{-10}$ g. The sensor response to impacts on the shield was calibrated pre-flight by several techniques. A momentum enhancement factor of 11 was used to account for the ejected target material, based on prior experimental and analytical studies (McDonnell *et al.* 1984). To form a complete mass curve, the DIDSY fluences were joined to those recorded by the Particle Impact Analyzer at masses 10^{-12} to 10^{-16} g (McDonnell *et al.* 1987). This composite distribution and Divine's curve are displayed in Figure 2.8. The cumulative mass exponent is equal to 0.94.

The fluences recorded by the SP-2 instruments on Vega 1 and 2 are shown in Figure 2.9, along with Divine's analytical curve. SP-2 utilized impact plasma sensors for the mass range 10^{-16} – 10^{-11} g and momentum sensors for 3×10^{-13} to 10^{-6} g (Mazets *et al.* 1986). In-flight calibration was performed by comparing the two data sets in the overlapping mass range and assuming a momentum enhancement factor of 5. For the impact velocity of 78 km/s, the momentum enhancement is probably closer to 11 (McDonnell *et al.* 1984); thus the curves in Figure 2.9 should probably be shifted toward smaller mass by a factor 2 (factor of 1.3 in radius). It can be seen that Vega 1, which encountered stronger jet activity than Vega 2, measured a steeper mass distribution. The SP-1 experiment, an impact plasma sensor with different geometry, gave similar slope and impact rate for $m < 10^{-10}$ g (Vaisberg *et al.* 1986).

On the other hand, the DUCMA experiment, which used a PVDF detector, recorded steeper slopes in the mass range 10^{-13} to 10^{-11} g (Simpson *et al.* 1986). This discrepancy remains unresolved.

4.2 Large Particles

The DIDSY sensors effectively used the entire dust shield as a sounding board, thus enabling the detection of large particles, including those that penetrated the front shield. The mass distribution for these large particles shows a very flat slope (McDonnell *et al.* 1987). Crifo (1987) has pointed out that this flat slope is inconsistent with the observed thermal emission spectrum. Green reported on the efforts to understand this enhancement of large particles and reconcile the DIDSY data with the Giotto radio science experiment and earth-based infrared observations (Perry, Green, McDonnell abstract this report).

Giotto DIDSY and radio-science data represent observations of dust originating from a narrow track along the nucleus, the smallest observed grains being emitted \sim one hour pre-

TABLE 2-3
DUST SIZE DISTRIBUTION

QUANTITY	SYMBOL / FORMULA	UNITS
Particle Mass (variable)	m	(kg)
Transition Mass (parameter)	m_t	(kg)
Dummy Variable	$x = (m/m_t)^{1/\gamma}$	
Exponent for Large Mass	a	
Exponent Ratio, Small/Large Masses	β	
Transition Sharpness Parameter	γ	
Distribution Coefficient	F_t	(m^{-2})
Integral Number Fluence (mass > m, or size > a)	$F = F_t \left[\frac{(1+x)^{\beta-1}}{x\beta} \right]^{a\gamma}$	(m^{-2})
Differential Number Fluence (per mass interval)	$f_m = \left(\frac{a F_t}{m_t} \right) \frac{(\beta+x)(1+x)^{(\beta-1)a\gamma-1}}{x(a\beta+1)\gamma}$	($m^{-2}kg^{-1}$)
Radius	$a = \left(\frac{3m}{4\pi\rho} \right)^{1/3} = a_t x^{\gamma/3}$	(μm)
Differential Number Fluence (per radius interval)	$f_a = \left(\frac{3a F_t}{a_t} \right) \frac{(\beta+x)(1+x)^{(\beta-1)a\gamma-1}}{x(a\beta+1/3)\gamma}$	($m^{-2}\mu m^{-1}$)

RELATIONS: $f_m = -\frac{dF}{dm} = -\frac{dx}{dm} \frac{df}{dx}$, $f_a = \frac{dm}{da} f_m$, and $F = \int_m^\infty dm f_m = \int_a^\infty da f_a$

TABLE 2-4
SIZE DISTRIBUTION: LIMITING DEPENDENCES $[x = (m/m_t)^{1/\gamma} = (a/a_t)^{3/\gamma}]$

<p style="text-align: center;">For $\beta = 1$ (any x) or Large $x \gg 1$ (any β) ($m \gg m_t$ and $a \gg a_t$)</p> $F = F_t x^{-a\gamma} = F_t \left(\frac{m_t}{m} \right)^a = F_t \left(\frac{a_t}{a} \right)^{3a}$ $f_m = \frac{a F_t}{m_t} x^{-(a+1)\gamma} = \frac{a F_t}{m_t} \left(\frac{m_t}{m} \right)^{a+1}$ $f_a = \frac{3a F_t}{a_t} x^{-(a+1/3)\gamma} = \frac{3a F_t}{a_t} \left(\frac{a_t}{a} \right)^{3a+1}$	<p style="text-align: center;">For $\beta \neq 0$ and Small $x \ll 1$ (any $\beta > 0$) ($m \ll m_t$ and $a \ll a_t$)</p> $F = F_t x^{-a\beta\gamma} = F_t \left(\frac{m_t}{m} \right)^{a\beta} = F_t \left(\frac{a_t}{a} \right)^{3a\beta}$ $f_m = \frac{a\beta F_t}{m_t} x^{-(a\beta+1)\gamma} = \frac{a\beta F_t}{m_t} \left(\frac{m_t}{m} \right)^{a\beta+1}$ $f_a = \frac{3a\beta F_t}{a_t} x^{-(a\beta+1/3)\gamma} = \frac{3a\beta F_t}{a_t} \left(\frac{a_t}{a} \right)^{3a\beta+1}$
--------------------------------------------------------------------------------------------------------------------------------------------------------------------------------------------------------------------------------------------------------------------------------------------------------------------------------------------------------------------------------------------------------------------------------------------------------------------------------------------------------------------	-------------------------------------------------------------------------------------------------------------------------------------------------------------------------------------------------------------------------------------------------------------------------------------------------------------------------------------------------------------------------------------------------------------------------------------------------------------------------------------------------------------------------------------------------------------------

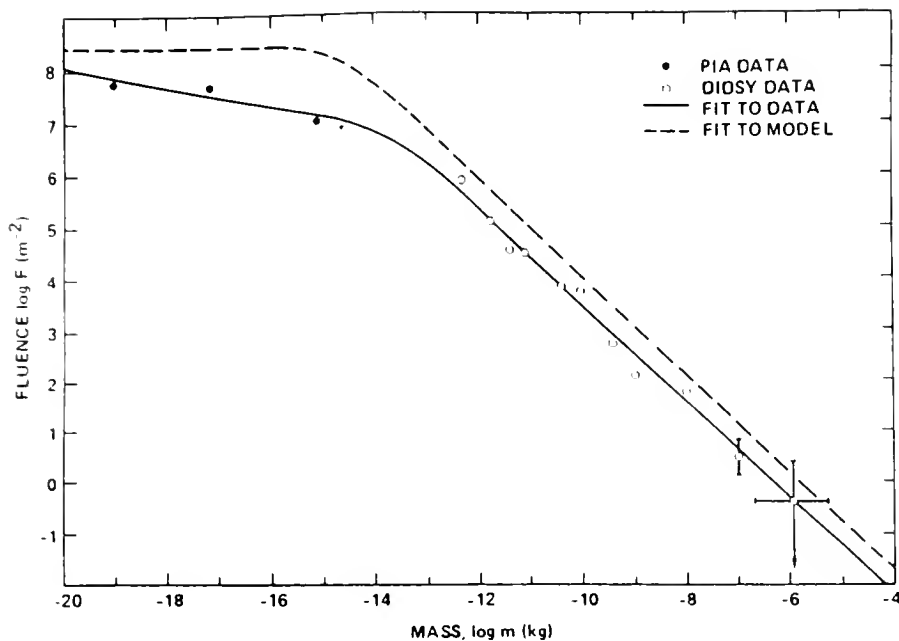


Figure 2.8 - Cumulative fluence versus particle mass from the Giotto DIDSY and PIA experiments, with analytical fit (solid line) from Divine and Newburn (1987). Dashed line is the model with the pre-Halley size distribution (arbitrary fluence or normalization).

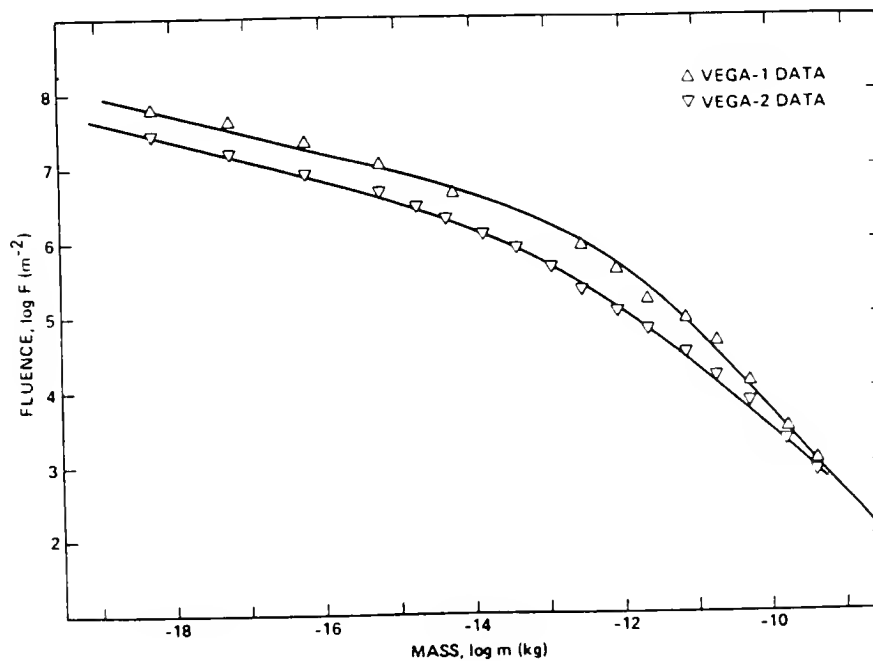


Figure 2.9 - Cumulative mass distribution (fluence) recorded by SP-2 detectors on Vega 1 and Vega 2 with analytical fit by Divine (abstract this report).

encounter and the largest, with their lower velocity, about six hours prior to the encounter. Green proposed that the rate of dust emission decreased, beginning about six hours before Giotto's flyby. Thus, the sensors would sample the higher flux of larger grains from the earlier emission.

The actual size distribution that should be used for modeling the whole coma should not include the excess of large particles measured by DIDSY, since this appears to be a consequence of the velocity dispersion of the grains rather than indicative of the actual mass distribution. According to Green, an extrapolated index of $\alpha \sim 0.9$ would be more representative and would be consistent with the infrared data. However, the Giotto data illustrate that there can be a large dispersion around the average mass-distribution function in the coma.

4.3 Dust Velocity Distribution

To relate the dust density in the coma – whether derived from *in situ* measurements or remote sensing – to the dust production rate from the nucleus requires knowledge of the dust particle velocities, which depend on the gas flux and the mass loading as well as on the particle area/mass ratio. A computed velocity distribution is given by Gombosi (1986) for Halley at 0.8 AU post-perihelion, using a dusty gas dynamic calculation and a mass distribution approximating the *in situ* data. Similar calculations for Halley at several heliocentric distances, based on pre-encounter data, are tabulated by Gombosi *et al.* (1986).

4.4 Dust Particle Density

To convert from the measured mass distribution to the size distribution needed for modeling the optical and infrared remote sensing data, some assumptions about the density of the dust grains are needed. Most likely, the coma contains both compact and fluffy [porous] particles. Table 2-4 summarizes the conversion from power-law-mass distribution to the equivalent size distribution if the density is independent of particle size. The chondritic aggregate IDPs, which seem to be our closest analog to cometary dust, have a filling factor of the order of 0.5, giving a density of $\leq 1 \text{ g/cm}^3$.

Information on the particle density can be derived from the dust-composition experiment on Vega (PUMA) and on Giotto (PIA). The density of pure mineral grains was almost always $> 1 \text{ g/cm}^3$, while that of organic grains (CHON particles) was within the limits 0.2 to 1.2 g cm^{-3} (Krueger and Kissel 1987). However, these results refer to small ($\leq 10^{-12} \text{ g}$) particles.

Assuming a constant value of 1 g/cm^3 for the average density of the particles is probably not wrong by more than a factor of two in either direction over the size range contributing most of the infrared emission, although larger grains may have lower density.

Donn described a fractal aggregate model for the dust; this model leads to a density inversely proportional to particle radius (Donn and Meakin 1987). The fractal model also predicts higher velocities for the larger grains than the models referred to in Section 4.3, because the ratio of mass to cross section for gas drag interaction is smaller than that of spherical grains (Meakin and Donn, abstract this report).

5.0 COMPARISON OF INFRARED DATA WITH MODELS

Various model calculations to fit the observed infrared data were presented at the Workshop. Given the caveats discussed in Sections 1-4, these models have to be considered preliminary.

5.1 Size Distribution

Although one would like simply to adopt the measured mass distribution to apply to all our observations, it is known from both the *in situ* detectors and the infrared observations that the size distribution varied with time and location in the coma. Moreover, the infrared emission is particularly sensitive to the abundance of roughly micron-sized grains. Yet, this is the region of the inflection in the slope of the mass distribution, whose position is both uncertain and probably variable (SP-1 vs DUCMA on board Vega; Vega 1 vs Vega 2; the gap between DIDSY and PIA on Giotto). If there is more than one dust component, each one may not separately follow the average size distribution (e.g., Clark *et al.* 1986).

In practice, one approach is to adopt Divine's function and vary the parameters as needed to fit the observations, in particular the transition mass, m_t .

5.2 Thermal Emission

Hanner reported on comparisons with the IRTF data taken in March 1986 (Hanner *et al.* 1987). She applied the mass distribution from Giotto, assuming $\rho = 1\text{g/cm}^{-3}$ and omitting the large particle enhancement, to compute via Mie theory the thermal energy distribution (excluding features). Agreement with the data was achieved by shifting m_t by a factor of 2 to 3 toward smaller masses, well within the uncertainties described above.

Mukai (abstract this report) presented models using the Vega 2-size distribution and a "dirty" silicate, whereby the observations of Herter and Tokunaga at 1.3 AU could be matched.

Krishna Swamy reported on two-component models, based on Mie theory, for carbonaceous and coated silicate grains for the full wavelength range from 3 to $160\mu\text{m}$ (Krishna Swamy *et al.*, abstract this report). He stressed that the low albedo of comet dust and the lack of an obvious $10\mu\text{m}$ silicate feature in some comets does not necessarily imply a composition dominated by dark carbonaceous material.

Lien (1987 and abstract, this report) has modeled the thermal emission using effective medium theory to compute optical constants for a mixture of silicate and absorbing grains, as described in Section 3.

Glaccum reported on modeling of the long-wavelength infrared data (Glaccum *et al.* 1986). The slope of the spectrum changed from one day to the next, requiring a change in the relative number of small grains. The size distribution fitting the long-wavelength data depends on the assumed emissivity of the grains, which is uncertain due to the problems of clustering discussed in Section 3.

5.3 The 3.4-Micron Emission

At present, it is not known whether the emission feature near $3.36\mu\text{m}$ arises from gas molecules or small solid grains. Chyba and Sagan (Chapter 3) proposed that thermal emission from dark organic grains can explain this feature and presented calculations for the thermal emission from small, hot grains having emissivity derived from the transmission spectrum of an irradiated methane ice clathrate residue.

5.4 Polarization

Mukai *et al.* (1987) performed a study of the n, k domain, using Mie theory, to match the observed phase angle and wavelength dependence of polarization. They concluded that $n = 1.39 - 1.37$ and $k = 0.024 - 0.042$ at $\lambda = 0.37 - 2.2\mu\text{m}$ provided a good match. (See also Mukai, abstract this report).

Brooke *et al.* (1987 and abstract this report) analyzed the near-infrared polarization, using Mie theory, and concluded that both "dirty" silicate and a more absorbing material were needed.

Lamy *et al.* (1987) concluded that the observed polarization can be reproduced by rough particles, including both dirty silicates and absorbing grains. The negative polarization is introduced by the surface roughness, in contrast to the Mie models, where the negative polarization is caused by silicate spheres (see Section 3.2).

It remains to be shown how valid are the general conclusions about the refractive index deduced from Mie theory for the case of rough, irregular grains.

6.0 COMPARISON WITH INTERSTELLAR DUST IN REFLECTION NEBULAE

As an example of infrared radiation from interstellar grains, Sellgren (abstract this report) summarized the infrared observations of reflection nebulae and the inferences about grain properties from them.

Because the grains are observed at much larger distance from the central star, the equilibrium grain temperatures of ~ 50 K are much colder than the case of comet dust. However, the ultraviolet flux is proportionately higher than in the solar radiation field. Thus, in the near infrared it is possible to observe radiation from non-thermal processes in very small grains or large molecules normally masked by thermal emission.

Strong continuum emission is observed at $1 - 13\mu\text{m}$, corresponding to $T \sim 1000$ K. Sellgren explains the emission as arising from a component of very small (10 \AA) particles, temporarily heated by the absorption of a single UV photon (Sellgren 1984). These particles must be refractory enough to survive the occasional (~ 100 yr) heating from absorbing two UV photons simultaneously.

Reflection nebulae also exhibit the set of six unidentified interstellar emission features, including a strong emission peak at $3.3\mu\text{m}$ and a broader emission feature extending to $3.4\mu\text{m}$. These are thought to arise by ultraviolet pumped fluorescence from polycyclic aromatic hydrocarbon molecules (PAHs) (Leger and Puget 1984; Allamandola *et al.* 1985). These authors propose that overlapping vibrational states in PAH molecules can produce the infrared continuum radiation.

Why the $3.3\mu\text{m}$ emission is strong in reflection nebulae and other interstellar sources, while it appears as only a weak component compared to the $3.36\mu\text{m}$ emission in the comet is not yet understood. Further discussion of the 3-micron region in interstellar sources is given by Tokunaga and Brooke, Chapter 3.

REFERENCES

- Allamandola, L. J., Tielens, A. G. G. M., and Barker, J. R. (1985). Polycyclic aromatic hydrocarbons and the unidentified infrared emission bands: auto exhaust along the Milky Way! *Astrophys. J.*, **290**, L25.
- Bohren, C.F. (1986). Applicability of effective-medium theories to problems of scattering and absorption by nonhomogeneous atmospheric particles. *Jour. Atmos. Sci.* **43**, 468.
- Bohren, C.F. & Huffman, D.R. (1983). Absorption and Scattering of Light by Small Particles. Wiley & Sons, New York.
- Borghesi, A. Bussoletti, E. and Colangeli, L.(1985). Amorphous carbon grains: laboratory measurements in the 2000Å - 40 micron range. *Astron Astrophys* **142**, 225-231.
- Brooke, T. Y., Knacke, R. F. and Joyce, R. R. (1987). The near-infrared polarization and color of Comet Halley. *Astron. Astrophys.*, in press.
- Chiapetta, P., Perrin, J. M., Torresani, B. (1987). Low energy light scattering: multiple scattering description. *Nuovo Cimento D*, in press.
- Clark, B.C., Mason, L.W., Kissel, J. (1986). Systematics of the "CHON" and other light-element particle populations in Comet Halley ESA SP-250, III, 353.
- Crifo, J. F. (1987). Optical and hydrodynamic implications of Comet Halley dust size distribution. Brussels Symposium, April 1987, ESA SP-278, in press.
- Day, K.L. (1974). A possible identification of the 10 μm "silicate" feature, *Astrophys. J.* **192**, L115.
- Day, K.L. (1976) Further measurements of amorphous silicates. *Astrophys. J.* **210**, 614-17.
- Day, K.L. (1979). Mid-infrared optical properties of vapor-condensed magnesium silicates. *Astrophys. J.* **234**, 158-161.
- Day, K.L. (1981). Infrared extinction of amorphous iron silicates. *Astrophys. J.* **246** 110-112.
- Divine, N. and Newburn, R.L. (1987). Modeling Halley before and after the encounters *Astron. Astrophys.* in press.
- Donn, B. (1985). Experimental investigations related to the properties and formation of cosmic grains. NASA Conf. Publ. 2403: Interrelationships among Circumstellar, Interstellar, and Interplanetary Dust.

- Donn, B. and Meakin, P. (1987). Aerodynamics of fractal grains: implications for the primordial solar nebula. *Bull. AAS* **19**, 847.
- Draine, B.T. (1985). Tabulated optical properties of graphite and silicate grains. *Astrophys. J. Suppl.* **57**, 587-594.
- Edoh, O. (1983). Optical properties of carbon from the far infrared to the far ultraviolet. Ph.D. dissertation, Dept. of Physics, University of Arizona. (Available through University Microfilms.)
- Glaccum, W. Moseley, S. H., Campins, H. and Loewenstein, R. F. (1986). Airborne spectrophotometry of P/Halley from 20 to 65 microns. *ESA SP-250*, II, 111.
- Gombosi, T.I. (1986). A heuristic model of the Comet Halley dust size distribution *ESA SP-250 II*, 167.
- Gombosi, T.I., Nagy, A.F. and Cravens, T.E. (1986). Dust and neutral gas modeling of the inner atmospheres of comets. *Rev. Geophys.* **24**, 667.
- Hanner, M. S., Tokunaga, A. T., Golisch, W. F., Griep, D. M. and Kaminski, C. D. (1987). Infrared emission from Halley's dust coma during March 1986. *Astron. Astrophys.*, in press.
- Huffman, D.R. (1977). Interstellar grains: the interaction of light with a small-particle system. *Adv. in Physics* **26**, 129-230.
- Huffman, D.R. (1987). Methods and difficulties in laboratory studies of cosmic dust analogues. *Proc. Capri Workshop on Laboratory Studies of Cosmic Dust Analogues*, Sept. 1987.
- Huffman, D.R. and Stapp, J.L. (1973). Optical measurements on solids of possible interstellar importance. *IAU Symp. 52 Interstellar Dust and Related Topics*, p. 297-301.
- Kerker, M. (1969). *The Scattering of Light and Other Electromagnetic Radiation*. Academic Press, New York
- Khare, B.N. et al (1984). Optical constants of organic tholins produced in a simulated Titanian atmosphere: from soft xray to microwave frequencies. *Icarus* **60**, 127.
- Khare, B.N., Sagan, C., Thompson, W. R., Arakawa, E. T., and Votan, P. (1987a). Solid hydrocarbon aerosols produced in simulated Uranian and Neptunian stratospheres. *Jour. Geophys. Res.*, in press.

- Khare, B.N., Arakawa, E. T., Thompson, W. R. and Sagan, C. (1987b). Optical constants and spectra of tholins from H₂O - CH₄ gas and H₂O hydrocarbon ices. *Bull. AAS* **19**, 897.
- Koike et al (1980). Extinction coefficients of amorphous carbon grains from 2100Å to 340 microns. *Astrophys. Space Sci.* **67**, 495-502.
- Kratschmer, W. and Huffman, D.R. (1979). Infrared extinction of heavy ion irradiated and amorphous olivine with application to interstellar dust. *Astrophys. Space Sci.* **61**, 195
- Krueger, F. R. and Kissel, J. (1987). The chemical composition of the dust of Comet P/Halley as measured by PUMA on board Vega-1. *Naturwissenschaften* **74**, 312.
- Lamy, P.L. (1978). Optical properties of silicates in the far ultraviolet. *Icarus* **34**, 68.
- Lamy, P.L., Gruen, E., and Perrin, J.M. (1987). Implications of the mass distribution function for the photopolarimetric properties of the dust coma. *Astron. Astrophys.* in press.
- Leger, A. and Puget, J. L. (1984). Identification of the unidentified IR emission features of interstellar dust? *Astron. Astrophys.* **137**, L6.
- Lien, D.J. (1987). Dust in comets I. Thermal properties of homogeneous and heterogeneous grains. *Astrophys J.* in press.
- Mazets, E.P. et al (1986). Dust in Comet Halley from Vega observations. ESA SP-250 II, 3.
- McDonnell, J.A.M. et al (1984). The impact of dust grains on fast-flyby spacecraft: momentum multiplication, measurements and theory. *Adv. Space Res.* **4**, No. 9, 297.
- McDonnell, J.A.M. et al (1986). Giotto's dust impact detection system DIDSY and particulate impact analyzer PIA: interim assessment of the dust distribution and properties within the coma. ESA SP-250 II, 25.
- McDonnell, J.A.M. et al (1987). The dust distribution within the inner coma of comet P/Halley 1982i: encounter by Giotto's impact detectors *Astron. Astrophys.* in press.
- Mitra, S.S. & Nudelman, S., eds. (1970). Far Infrared Properties of Solids, Plenum Press, New York.
- Mooney, T. and Knacke, R.F. (1985). Optical constants of chlorite and serpentine between 2.5 and 50 microns. *Icarus* **64**, 493-502.

- Mukai, T., Mukai, S. and Kikuchi, S. (1987). Complex refractive index of grain material deduced from the visible polarimetry of Comet Halley. *Astron. Astrophys.*, in press.
- Perrin, J.M. & Lamy, P.L. (1983). Light scattering by large rough particles. *Optica Acta* **30**, 1223.
- Perrin, J.M. & Lamy, P.L. (1986) Light scattering by large particles II. a vectorial description in the eikonal picture. *Optica Acta* **33**, 9.
- Perry, C. H. et al. (1972). Infrared and raman spectra of lunar samples from Apollo 11, 12 and 14. *The Moon* **4**, 315.
- Philipp, H.R. (1977). Infrared optical properties of graphite. *Phys. Rev. B* **16**, 2896-2900.
- Pollack, J.B. Toon, O.B., Khare, B.N. (1973). Optical properties of some terrestrial rocks and glasses. *Icarus* **19**, 372-389.
- Purcell, E.M. and Pennypacker, C.R. (1973). Scattering and absorption of light by non-spherical dielectric grains. *Astrophys. J* **186**, 705.
- Sakata, A., Wada, S., Okutsu, Y., Shintani, H., Nakada, Y. (1983). Does a 2,200 Å hump observed in an artificial carbonaceous composite account for UV interstellar extinction? *Nature* **301**, 493.
- Sandford, S.A. and Walker, R.M. (1985). Laboratory infrared transmission spectra of individual interplanetary dust particles from 2.5 to 25 microns. *Astrophys. J.* **291**, 838.
- Schuerman, D.W., Editor (1980). Light Scattering by Irregularly Shaped Particles. Plenum Press New York.
- Schuerman, D.W. (1980). The microwave analog facility at SUNYA: capabilities and current programs. In Light Scattering by Irregularly Shaped Particles. ed. Schuerman, Plenum Press New York, p. 227.
- Sellgren, K. (1984). The near-infrared continuum emission of visual reflection nebulae. *Astrophys. J.*, **277**, 623.
- Simpson, J.A., Rabinowitz, D, Tuzzolino, A.J., Ksanfomality, L.V. and Sagdeev, R.Z. (1986). Halley's comet coma dust particle mass spectra, flux distributions and jet structures derived from measurements on the Vega-1 and Vega-2 spacecraft. *ESA SP-250 II*, 11.
- Steyer, T.R. (1974). Infrared optical properties of some solids of possible interest in astronomy and atmospheric physics. Ph.D. dissertation, Dept. of Physics, University of Arizona. Available through University Microfilms.

- Taft, E.A. and Philipp, H.R. (1965). Optical properties of graphite. *Phys. Rev.* **138** A197-202.
- Vaisberg, O., Smirnov, V. and Omelchenko, A. (1986). Spatial distribution of low-mass dust particles ($m < 10^{-10}$ g) in Comet Halley coma. ESA SP-250 II, 17.
- Van de Hulst, H.C. (1957). Light Scattering by Small Particles. Dover Publ. New York.
- Weiss-Wrana, K. (1983). Optical properties of interplanetary dust: comparison with light scattering by larger meteoritic and terrestrial grains. *Astron. Astrophys.* **126**, 240.
- Williams M.W. and Arakawa, E.T. (1972). Optical properties of glassy carbon from 0 to 82 ev. *J. Appl. Phys.* **43**, 3460-63.
- Wiscombe, W. and Mugnai, A. (1980). Exact calculations of scattering from moderately nonspherical T_n - particles: comparisons with equivalent spheres. In Light Scattering by Irregularly Shaped Particles, Ed: Schuerman, Plenum Press, New York, p. 141.
- Zerull, R., Giese, R.H., Schwill, S., Weiss, K. (1980). Scattering by particles of non-spherical shape. In Light Scattering by Irregularly Shaped Particles, Ed. Schuerman, Plenum Press New York, p. 273.

CHAPTER 3

COMETARY DUST COMPOSITION

R. D. Gehrz
University of Minnesota

and

M. S. Hanner
Jet Propulsion Laboratory

with contributions from Session III speakers

1.0 INTRODUCTION

The earth-based measurements and *in situ* sampling of Comet Halley have provided intriguing new data about the chemical composition of cometary grains. Recent progress in laboratory studies of interplanetary dust particles (IDPs) complements the comet data, allowing inferences about the mineralogy and physical structure of the comet dust to be drawn from the observed elemental composition and infrared spectra.

Seven speakers presented talks in this session, discussing the *in situ* dust composition measurements at Halley, the composition of IDPs and their relation to comet dust, and the origin of the 3.4 μ m hydrocarbon feature. They were requested to prepare written versions of their talks, which are included here in this chapter. Related poster papers on aromatic components in comets (Allamandola *et al.*) and the 3.4 μ m feature (Danks *et al.*, Encrenaz *et al.*) are also included here for completeness.

The topics discussed in the session are briefly summarized below. Further discussion and recommendations for future research are included at the end of the chapter. How well the conclusions from independent research techniques fit together was one of the exciting aspects of the Workshop.

2.0 *IN SITU* MEASUREMENTS

A time-of-flight mass spectrometer was carried on board the Vega (PUMA) and Giotto (PIA) spacecraft to record the composition of impacting dust particles (Kissel *et al.*, 1986). Particles striking the target generated a cloud of ions which were accelerated down a drift tube and counted by the detector, as a function of mass/charge ratio. Several thousand mass spectra of dust particles in the mass range 10^{-16} to 10^{-12} g were recorded by the three instruments.

From a sample of PUMA spectra, the relative abundances of the major rock-forming elements are chondritic within a factor of 2 (Jessberger *et al.* 1986, 1987). Carbon, however, is enhanced by a factor of ~ 10 in this sample, compared to CI carbonaceous chondrites. A class of particles containing primarily H,C,N,O was discovered ("CHON" particles; Kissel *et al.* 1986), supporting the evidence from the infrared spectra that Halley was rich in organic materials.

At the Workshop, Mason reported on correlation analyses of elemental abundances in over 8,000 PIA spectra (Mason and Clark, this Chapter). Carbon is the most abundant element, appearing in 74 percent of all the spectra, while highest correlation occurs for the pair C,O. The presence of molecular ions, such as MgOH⁺ and CN⁺ is suggested by the data.

Initially, it was thought that molecular ions would not be formed during particle impact. The appearance of the spectra, however, particularly the peaks at large amu,

has caused a reconsideration of the theoretical model for the impact process. Kissel and Krueger (1987) have concluded that molecular ions are present in the data and have constructed a model for the ion chemistry and the kinds of organic molecules present. They argue that their model is indicative of the silicate cores with organic refractory mantles, predicted for interstellar grains by Greenberg.

Further analysis of the PUMA and PIA data is in progress by several groups, and we can expect interesting new results to emerge in the next few years. However, it must be kept in mind that the instruments sampled only the smallest grains in the coma, whereas most of the mass in the comet grains lies in particles larger than 10^{-11} g (see Chapter 2).

3.0 INTERPLANETARY DUST PARTICLES

For more than 15 years, IDPs collected in the stratosphere have been available for laboratory study. Recent advances in techniques for analyzing submicron sections of these grains and for obtaining infrared spectra make possible a comparison with Halley data. These techniques, including thin sections, EDX spectra, and ion-probe imaging, are reviewed in the paper by Walker, along with a discussion of results relevant to the comparison with comet dust.

Using a different approach, Brownlee compared the degree of variability in the mineral composition for the Halley dust, carbonaceous chondrites, and IDPs. The CI and CM meteorite samples contain primarily hydrated silicates, with a narrow range in Mg/Si ratio, in contrast to the broad dispersion in composition and prevalence of pure Mg silicates in the Halley particles. Hydrated IDPs show a narrow range of Mg/Si similar to the meteorite samples. The anhydrous chondritic aggregate IDPs, on the other hand, display a broad compositional dispersion similar to that seen in the Halley spectra. These IDPs even look like plausible cometary particles, perhaps with ice originally filling the voids. Walker cautioned that one should not rule out other kinds of IDPs as potential cometary grains, for example the Ca and Al rich refractory particles and FSN particles as well as hydrated silicates.

Relationships between CHON particles and IDPs were also discussed. The chondritic aggregate IDPs contain dark, carbon-rich matrix material. Some IDPs may have a $3.4\mu\text{m}$ absorption feature, although possible contamination is difficult to rule out (see discussion by Walker). Raman spectra of IDPs, described by Allamandola and by Sandford, exhibit bands characteristic of aromatic molecular units of size $\leq 25\text{\AA}$, and some showed red luminescence as well. The band positions are similar to the interstellar infrared emission features. Some IDPs have strong D/H enrichment in localized areas correlated with high carbon concentration. Allamandola *et al.* associate the high D/H enrichment with polycyclic aromatic hydrocarbons in the grains and suggest that these may be only slightly modified interstellar grains. Walker presented an ion image of an IDP containing a fragment rich in C,H,N, perhaps related to a subset of the "CHON" particles seen in Halley. Thus, laboratory evidence regarding hydrocarbons in IDPs seems to be consistent with what we have learned about the organic material in Comet Halley, although further investigations of both IDPs and comets are clearly important. Better understanding of the organic material in the grains is one goal of the CRAF mission.

4.0 INFRARED SPECTRA OF IDPs AND IDENTIFICATION OF SILICATES

Sandford reviewed the $5\text{--}20\mu\text{m}$ infrared spectra of IDPs. These fall into three groups, identified respectively with terrestrial olivine, pyroxene and hydrated silicates. Composition analysis of the IDPs confirms the spectral identifications. A $6.8\mu\text{m}$ feature seen in hydrated IDPs is associated with carbonate; a weak $6.8\mu\text{m}$ emission may have been present in the spectrum of Halley (Chapter 1). The silicate feature observed in Halley can be fitted with a combination of the three spectral types, primarily olivine and pyroxene. This result is in agreement with Brownlee's conclusion that anhydrous silicates dominate

the dust composition. In contrast, the $10\mu\text{m}$ spectrum of Comet Kohoutek at 0.3 AU showed a broad smooth silicate feature, resembling the hydrated silicates and inconsistent with more than a small per cent crystalline olivine.

Caution should be exercised, however, in attempting to make a detailed fit of laboratory transmission spectra to cometary emission spectra. As discussed in Chapter 4, a transmission spectrum generally includes scattering as well as absorption, which can distort the shape of the band. The temperature and size of the emitting grains also have to be taken into account. One also has to consider the processing history of IDPs since their ejection from a parent body and the extent to which they may have been altered by heating. Nevertheless, given the difficulty of predicting accurately the band shape for a mixture of inhomogeneous, irregular particles (Chapter 2), the direct laboratory comparison is a valuable first step, and it is significant that crystalline silicates seem to be present in Halley.

5.0 THE 3.4-MICRON FEATURE

The observed spectrum of the $3\mu\text{m}$ region was described in Chapter 1. The main emission peak occurs at $3.36\mu\text{m}$, with weaker features at 3.29 and $3.52\mu\text{m}$. Tokunaga and Brooke stressed that the $3.36\mu\text{m}$ feature seen in Halley and Wilson is not matched by any interstellar source. Although the Galactic Center has a feature centered near $3.4\mu\text{m}$, the detailed shape differs and the feature is seen in absorption, not emission. Of the set of unidentified infrared emission features usually occurring together in interstellar sources, only the $3.29\mu\text{m}$ band seems to be present in Halley. Thus, the task for theoreticians is to explain not only the origin of the $3.36\mu\text{m}$ cometary emission, but also why it differs from that seen in the ISM and why no corresponding emission bands are present at longer wavelengths.

Moreover, it appears that not all comets exhibit $3.4\mu\text{m}$ emission (Tokunaga and Brooke), and Danks pointed out that no feature was evident in a preperihelion CVF spectrum of Halley in December 1985.

While the consensus is that the emission probably arises from C-H vibrations in organic molecules, the specific molecule(s) and emission mechanism are unknown, and it is not even clear whether the carrier is in the gas or solid phase. Several possible emission mechanisms were discussed at the Workshop and are described in the papers in this chapter. These include resonance scattering by gas molecules, UV-pumped fluorescence in gas molecules or small grains, and thermal emission from small grains. Because the derived carbon abundance depends strongly on the emission mechanism, clarification of the $3.36\mu\text{m}$ feature is necessary for understanding the carbon budget of the comet.

References

1. Kissel *et al.* 1986, *Nature*, **321**, 280, 336.
2. Jessberger, E. K., Kissel, J., Fechtig, H. and Krueger, F. R. 1986, *The Comet Nucleus Sample Return*, ESA SP-249, p. 27.
3. Jessberger, E. K., Christoforidis, A., Kissel, J. 1987, submitted to *Nature* (Dec 1987).
4. Kissel, J. and Krueger, F. R. 1987, *Nature*, **326**, 755.

COMPARISON OF LABORATORY DETERMINED PROPERTIES OF INTERPLANETARY DUST WITH THOSE OF COMET HALLEY PARTICLES: WHAT ARE COMETS MADE OF?

Robert M. Walker
McDonnell Center for the Space Sciences
Physics Department
Washington University
St. Louis, MO 63130

Introduction

In recent years, Interplanetary dust particles (IDPs) collected in the stratosphere have been the object of increasingly sophisticated laboratory studies.^(1,2) In this talk, I will briefly describe some of the main properties of IDPs, and then address the question of whether any of them appear similar to the dust from Comet Halley.

The importance of answering this question is clear; laboratory measurements give much more information on the properties of the dust than can be obtained by either remote observations or by fly-by space missions. If a reasonable case can be made that some of the IDPs are similar to comet dust, then we can use measurements on them to address some of the fundamental questions concerning comets. Specifically, we can ask whether the popular view that comet dust consists of simple assemblages of interstellar grains is consistent with the measured properties of IDPs.

Short of going to a comet and returning with a sample, we are not likely to prove that a given class of IDPs is identical to comet dust. Thus, when I describe this work as "cost effective" comet sample research, it is done partially with tongue-in-cheek -- but not totally. For one thing, it is not clear that a single comet sample return mission would properly solve the problem. I consider it likely that not all comets are the same; nor even, that a given comet is identical from place to place.

For me, the most interesting aspect of extraterrestrial materials research is the mounting evidence that they contain bits of pre-existing interstellar material that survived the processes of planet formation. Apart from photons of different wavelengths, only galactic cosmic rays give a direct sample of interstellar material. But these are individual nuclei whose origin cannot be uniquely specified. Study of ensembles of nuclei found in interstellar dust could, in principle, give new insights into a number of astrophysical questions. The prospect of bootstrapping our way out of the solar system provides a powerful motivation for work on comets, IDPs, and meteorites.

Lest they get lost in the details of the presentation, let me first state the major conclusions of my talk:

- 1) Some types of IDPs do appear to be similar to dust from Comet Halley.
- 2) Both IDPs and Halley dust appear to differ in important respects from primitive meteorites.
- 3) IDPs do not appear to be simple assemblages of material that is demonstrably interstellar in origin.

- 4) Notwithstanding, some surviving interstellar material does appear to be present. The volume fraction of this material is small and, further, occurs in the form of isotopically distinct sub-grains $\leq 1 \mu\text{m}$ in size that are difficult to characterize.
- 5) Much more work is possible, both in the analysis of the Comet Halley fly-by data and in laboratory studies of IDPs, to elucidate the relationship of IDPs to comet dust.

Experimental Methods Used To Study IDPs

Most IDPs have masses of several nanograms and are invisible to the naked eye. Notwithstanding their small sizes, developments in microanalytic techniques make it possible to perform a variety of measurements on single particles. In our laboratory, IDPs are first examined in a scanning electron microscope and pictures are taken to document their morphologies which range from, "fluffy reentrant" to "solid compact." Characteristic X-rays generated by the scanning electron beam are measured with a Si Li detector (EDX) to determine the abundances of major elements in the particles. In the past, most such measurements have been made with a Be window covering the detector and only elements with $Z \geq 12$ have been determined. Recently, however, several groups, including our own, have obtained data with ultra-thin window detectors which permit measurement of elements with $Z \geq 6$. Following the initial characterization, several different analysis schemes can be followed. If the particle is compact, it is transferred to a quartz plate and crushed against another quartz plate. Material adhering to one plate is then pressed into a KBr crystal and its whole-particle IR transmission spectrum is measured using a Fourier transform IR spectrometer (FTIR) equipped with an auxiliary microscope. Material on the other quartz plate is pressed into a sputter-cleaned, Au foil for isotopic analyses using an ion probe mass spectrometer. The ion probe is a relatively new instrument that uses an ion beam to sputter ions from a surface; the ions are then mass analyzed in a high resolution double focusing mass spectrometer. Images of specific isotopes can be obtained at a spatial resolution of $\sim 1 \mu\text{m}$. A Raman microprobe is used to obtain spectra on the fragments found on either the Au or KBr substrates. Any material still adhering to the quartz plate is used to make mounts for transmission electron microscopy (TEM). If no remaining material is available, TEM mounts are made by evaporating a carbon film on the KBr. The film, with its imbedded fragments, is then floated off in water and transferred to a TEM grid.

Recently, Bradley and Brownlee⁽³⁾ have developed an experimental technique that greatly enhances quantitative analytical electron microscopic (AEM) studies of IDPs. The particles are first mounted in epoxy and then sliced into wafers $\sim 1000 \text{ \AA}$ thick. Examination of a sequence of slices permits a complete three dimensional characterization of a particle using a combination of AEM methods including EDX, electron diffraction, and electron energy loss spectroscopy (EELS). Some IDPs are quite fragile and break into a number of distinct chunks. In such cases, different fragments can be independently studied, and, in particular, some of them mounted for thin-sectioning in addition to the other studies.

Other measurements can also be made. For example, Flynn and Sutton (1987)⁽⁴⁾ have used synchrotron X-ray fluorescence to measure certain minor and trace elements in IDPs. On larger particles, or on ensembles of smaller particles, it has also proven possible to measure the contents and isotopic composition of noble gases in IDPs.^(5,6,7)

Because a given particle, or fragments thereof, can have a complex analysis history, we have developed the practice of giving names to individual IDPs. After using several ad hoc schemes, we have finally settled on a formal procedure; a road map of Missouri and a set of darts are the essential elements of this new nomenclature system.

Some First Order Results

Contrary to the claims of early investigators, attempts made several decades ago to collect cosmic dust on earth were unsuccessful. The pioneering work of D. Brownlee and his colleagues at the University of Washington, Seattle,⁽⁸⁾ set the field on its modern course. Subsequent measurements of isotopes⁽⁹⁾ and fossil nuclear tracks⁽¹⁰⁾ proved that many stratospheric dust particles come from interplanetary space.

We now know that different kinds of interplanetary dust particles exist. Most work has concentrated on the "chondritic" subset of particles whose "cosmic" major element abundances made them the most likely candidates for an extraterrestrial origin. However, recent oxygen isotopic measurements have shown that some refractory stratospheric grains, which are rich in Ca and Al, are also extraterrestrial.⁽¹¹⁾ The enrichment of deuterium seen in one particle of another type rich in iron, sulphur, and nickel (FSN), indicates that these too are extraterrestrial.⁽¹²⁾

The chondritic set of IDPs can also be broken down into different categories. The broadest separation is between particles whose crystalline components are dominated by mafic minerals (anhydrous) and those in which layer-lattice silicates dominate (hydrous). In turn, as shown originally by Sandford and Walker,⁽¹³⁾ and described further in the paper by Sandford at this conference, IR spectroscopy shows a division of the anhydrous particles into "olivine" or "pyroxene" types. Electron diffraction studies show that most of the hydrous particles have lattice parameters similar to terrestrial smectites, but a few particles have spacings characteristic of terrestrial serpentine minerals. Thus, there are at least two types of layer-lattice silicate particles. Some IDPs which appear to have IR spectra intermediate between the various end members have also now been found.

It is beyond the scope of this talk to review in detail the considerable information that has been obtained from TEM studies of IDPs.^(2,14) Suffice to say that many chondritic particles consist of complex, unequilibrated assemblages of a variety of (mostly) crystalline and amorphous phases which range in grain size from tens of angstroms to microns. Fine whiskers and thin platelets are common features and have been interpreted as being due to the growth of crystals directly from the vapor phase.⁽¹⁵⁾ Still other microstructures appear to have been formed by catalytic reduction of CO to form carbonaceous phases.^(16,17) Overall, the anhydrous IDPs, which also are generally porous and fluffy, appear to consist of less altered, thus more primitive, materials than have yet been found in the matrices of primitive meteorites.

Isotopic measurements also demonstrate that chondritic particles are primitive in the sense that they contain material that is greatly enriched in deuterium relative to hydrogen compared to the terrestrial values. Figure 1 shows the range of δD^* values measured in different fragments of several IDPs. The δD variations in IDPs are correlated with carbon but not with OH, showing that the (as yet) unidentified carrier is carbonaceous in nature. In Fig. 2 taken from McKeegan *et al.* (1987),⁽¹²⁾ we show ion images of a fragment of the IDP, Butterfly. It can be seen that the deuterium signal is concentrated in a small "hot spot" $\leq 1 \mu m$ in size. The small size of the carrier grains explains the wide variation in δD values shown in Fig. 1.

In contrast, with one exception, carbon isotopic measurements do not vary from place to place in a given particle although differences between particles are seen.⁽¹⁸⁾ Although small, the intraparticle differences are probably real. No deviations from average solar system isotopic

$$^* \delta D \equiv \left[\frac{(D/H)_{\text{unknown}}}{(D/H)_{\text{standard}}} - 1 \right] \times 1000$$

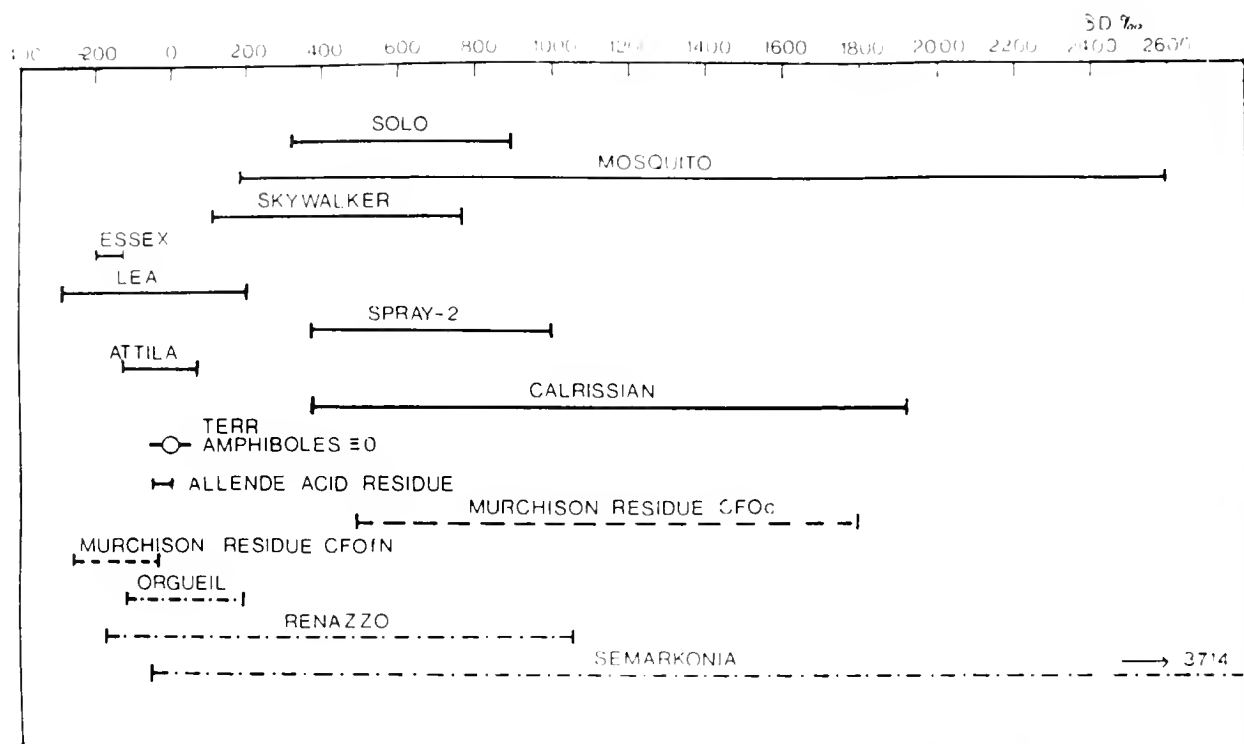


Figure 1: δD values for several IDPs. The horizontal lines show the full range of measured values for different fragments of a given particle. Since the measurement errors are ≤ 200 ‰, the large spread shows that the deuterium enrichments are inhomogeneously distributed. Data are taken from McKeegan *et al.* (1985). Similar data for meteorites are shown on bottom.

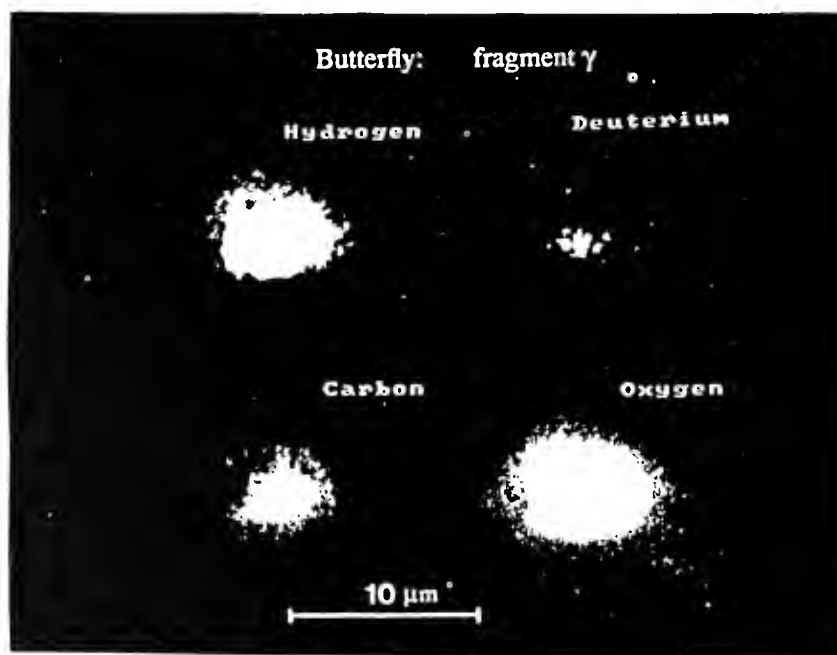


Figure 2: Ion images of a fragment of the IDP Butterfly taken with the Washington University ion probe. It can be seen that the deuterium is concentrated in a local "hot spot" whose extent is less than the limit of spatial resolution of the ion probe ($\sim 1 \mu m$). The δD for this spot is estimated at $\geq 9,000$ making it the most deuterium-enriched sample yet found in natural solar system materials. Taken from McKeegan *et al.* (1987).

values have been found for Mg, Si, or O, although the number of measurements is quite limited. In this sense, IDPs are less primitive than certain sub-samples of primitive meteorites.

Points of Comparison Between IDPs and Halley Dust

There are four main points of comparison between IDPs and Halley dust: 1) the infrared spectral properties, 2) the presence of CHON components, 3) the distribution of elemental abundances for elements with $Z \geq 12$ measured at a spatial resolution of $\sim 1000 \text{ \AA}$, and 4) isotopic properties. These are discussed separately below.

In a companion paper at this conference, Sandford compares the IR observations of Comet Halley dust with different combinations of laboratory spectra and, I will not treat the subject further here. Suffice to say that a satisfactory match can be made between the Halley data and spectra from IDPs.

One of the new findings resulting from the intensive study of Comet Halley is the discovery of a structured $3.4 \mu\text{m}$ emission band.^(19,20,21) Because it is not certain that the $3.4 \mu\text{m}$ band is due to dust, its presence in IDPs is not a necessary condition for the equivalence of IDPs and Halley dust. However, as shown in Fig. 3, taken from Swan *et al.* (1986),⁽²²⁾ some IDPs do indeed show a structured $3.4 \mu\text{m}$ feature attributable to aliphatic hydrocarbons. Several sources of possible terrestrial contamination exist and we cannot be completely sure that the species responsible for the $3.4 \mu\text{m}$ absorption is indigenous to the particles in space. Some contaminants can be ruled out including silicone oil used to collect the particles, the xylene used to clean them, and hydrocarbons introduced during SEM examination. However, we know that terrestrial particles are present on the collectors and that IDPs can move around in the collecting medium. Dry particle collection methods need to be developed to finally eliminate the contamination problem.

Abundance of Light Elements: CHON'S

One of the more striking results of the PIA-PUMA dust analyzers flown on the Giotto and Vega missions,^(23,24) was the discovery that many of the dust particles were composed primarily of carbon, hydrogen, oxygen, and nitrogen in various proportions. I wish now to demonstrate that similar assemblages of light elements occur in IDPs.

The paper at this conference by Allamandola, Sandford and Wopenka shows the Raman spectra of several IDPs. Double peaks at $\sim 1360 \text{ cm}^{-1}$ and 1600 cm^{-1} have been found in 16 of 20 particles so far measured. These peaks are characteristic of "disordered graphite" and their presence demonstrates that IDPs typically contain an abundance of carbonaceous material. Secondary ion images of the IDP, Mosquito, previously published by McKeegan *et al.* (1985),⁽⁹⁾ further show that regions rich in C and H, but depleted in silicon, are present in this particle.

In Fig. 4, we show previously unpublished ion images of fragments of the olivine type IDP, Tyson, taken in our laboratory by K. McKeegan.⁽¹⁸⁾ It can be seen that there is a central region of the particle which is rich in H, C, and N, similar to a number of the impact events seen in the PIA-PUMA data. That some IDPs are very carbon rich can also be seen in Fig. 5 which shows an EDX spectrum taken with a thin window detector of a fragment of the IDP, Smash. About two-thirds of the subgrains of Smash had similar high carbon contents; in contrast, only occasional fragments of the carbonaceous meteorites, Murchison and Ivuna showed measurable carbon peaks.

The above results show that IDPs contain sub-units that correspond, at least qualitatively, to the CHON type events seen in the Comet Halley fly-by experiments. However, more detailed work needs to be done to quantify the comparisons. Part of the difficulty in making such

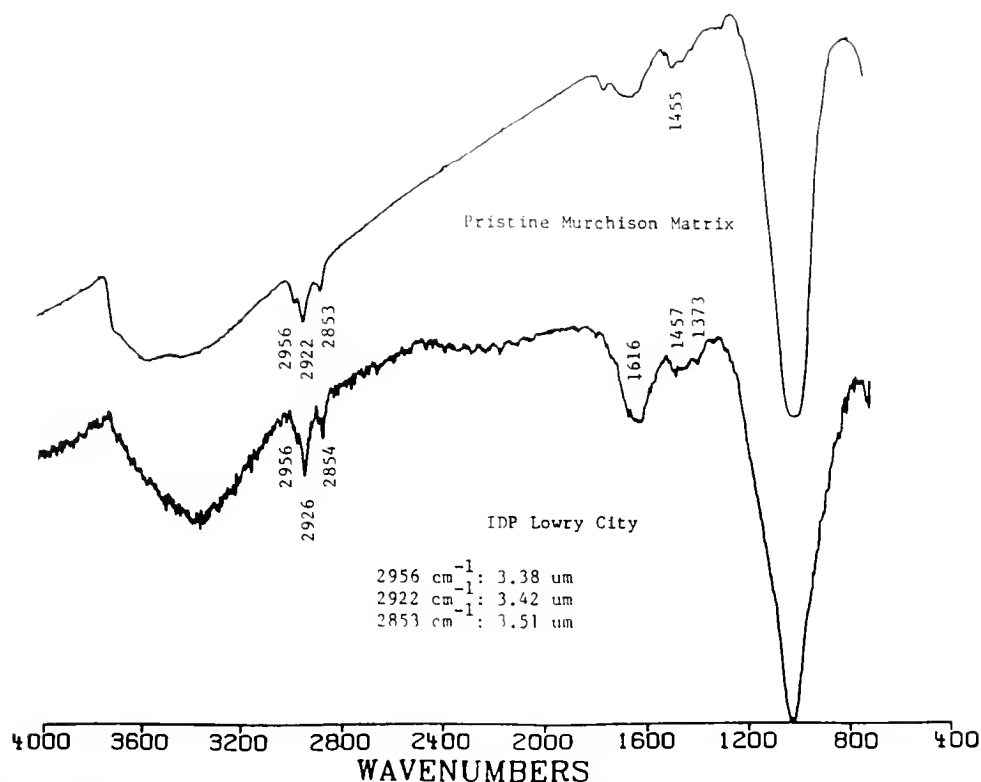


Figure 3: Infrared absorption of the IDP, Lowry City, as measured by Fourier transform microspectrometry. In addition to the typical major $10\ \mu\text{m}$ feature identifying this particle as a layer-lattice silicate type, there is a prominent triplet at $3.4\ \mu\text{m}$. Data from Swan *et al.* (1987).

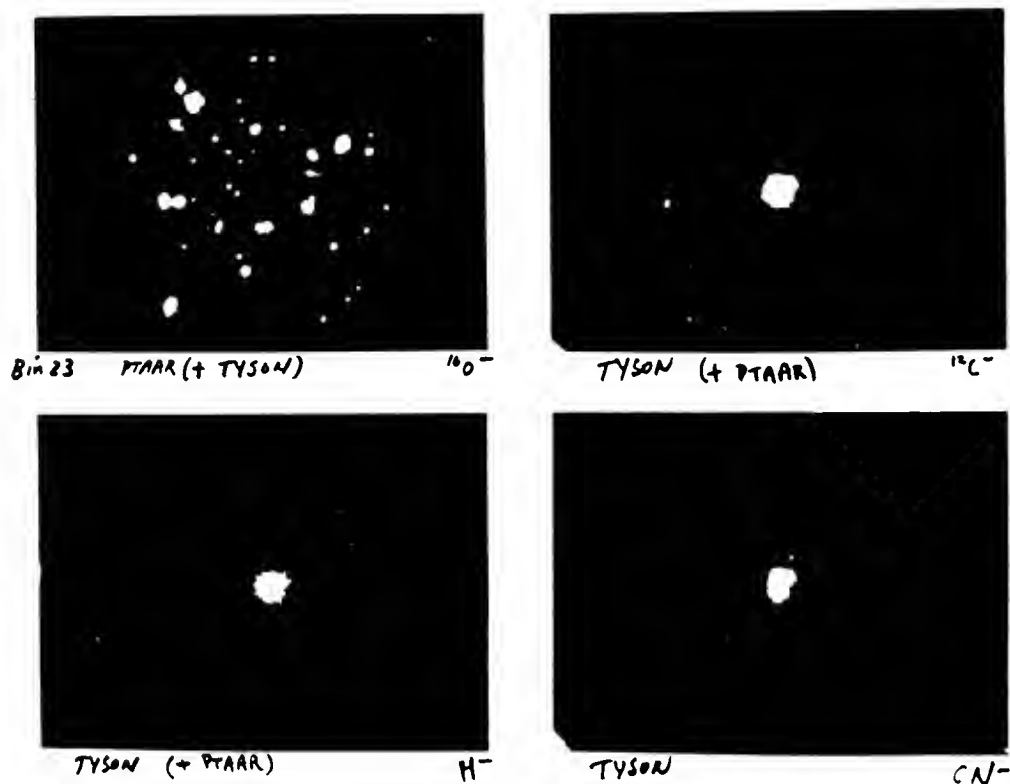


Figure 4: Ion images of fragments of the IDP, Tyson. The O^- image on the upper left shows a cluster of small silicate grains. The other images taken in H^- , C^- , and CN^- show a central fragment, missing in the O^- image, that is rich in C, H, and N. Taken from K. McKeegan (1987).

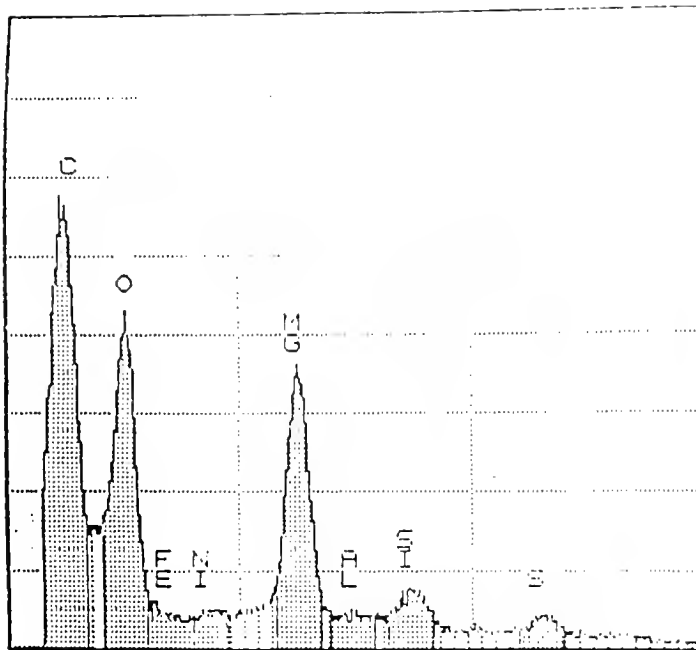


Figure 5: EDX spectrum of a C-rich fragment ($\leq 1 \mu\text{m}$ in size) of the crushed IDP, Smash (U2033M1), taken with an ultra-thin window detector. In contrast, only an occasional fragment from the carbonaceous meteorites Murchison and Ivuna, shows a discernible C peak.

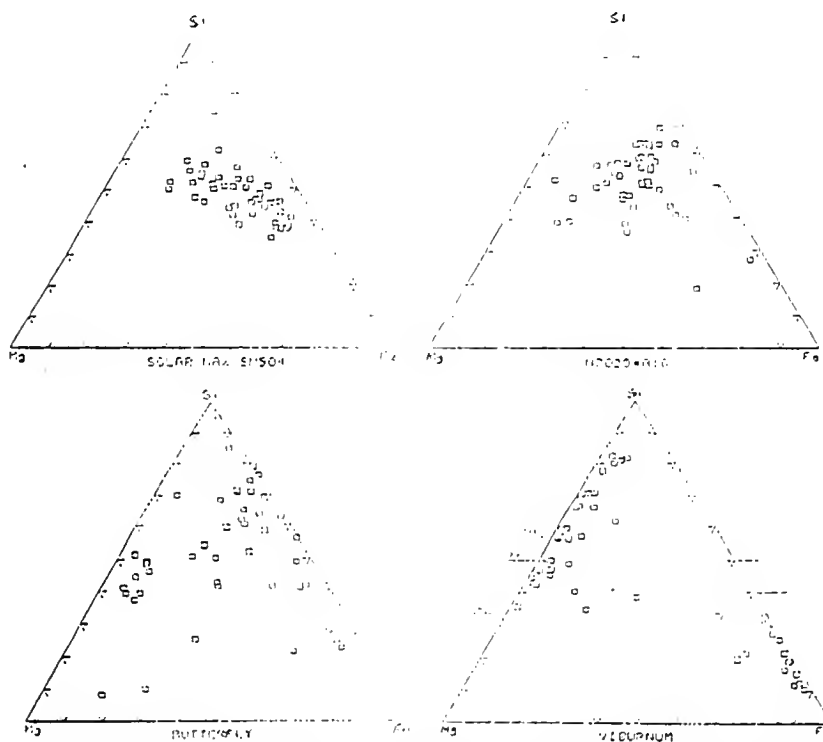


Figure 6: Distribution of the relative abundances of Mg, Fe, and Si in several IDPs of different spectral classes. The data were obtained from EDX measurements on thin sections $\sim 1000 \text{ \AA}$ thick. The particles in the upper two diagrams are both layer lattice silicates (Solar Max-serpentine, W7029A16-smectite) and those in the bottom are dominated by mafic minerals (Butterfly-pyroxene, Viburnum-olivine).

comparisons lies in the fact that the Halley encounter data have so far only been published in preliminary form. Hopefully, a definitive version of the Halley results will be published soon so that the proper comparisons can be made.

Distribution of the Abundances of Mg, Si, and Fe

In addition to the CHON's, the PIA-PUMA experiments recorded events containing heavier elements, some of them with relative abundances suggestive of single mineral phases that have previously been seen in IDPs. A key point to realize in making comparisons is that the mass of a typical impacting Halley particle was $\leq 3 \times 10^{-15}$ gms; the total mass of all the impacts recorded was less than the mass of a single IDP. Comparisons with impact results must therefore be made using measurements on IDPs at a spatial resolution of $\sim 1000 \text{ \AA}$.

Elemental determinations using EDX techniques on thin sections of IDPs $\sim 1000 \text{ \AA}$ thick provide such a base for comparison. This subject is treated in detail in the paper by D. Brownlee, who pioneered this technique, and will not be discussed in detail here. I simply wish to show Fig. 6 which summarizes data taken by W. Carey in our laboratory, in collaboration with J. Bradley of McCrone & Associates, on the distribution of Mg, Fe, and Si. Two IDPs that fall in the anhydrous IR classes show patterns of element abundances that differ significantly from those of two other particles of the layer-lattice type. The data base amassed by D. Brownlee show that the latter patterns are similar to primitive meteorites while the former patterns more closely resemble those found in the PIA-PUMA results.

Isotopes

The most distinctive isotopic signature yet found in IDPs is the large D/H enhancements found in small carbonaceous carriers. Unfortunately, the PIA-PUMA instruments are apparently incapable of measuring D/H ratios⁽²⁵⁾ and thus the most interesting comparison cannot be made. Analysis of results from the neutral gas mass spectrometer give a value of D/H between 0.4 and 3.0 times the terrestrial value for the volatile component of Halley.⁽²⁶⁾ This is consistent with what one would expect from the results on IDPs. However, the same is true for primitive meteorites.

Some of the PIA-PUMA events have been interpreted as indicating low values of $^{13}\text{C}/^{12}\text{C}$ in individual impacts.⁽²⁷⁾ This could be a crucial point of comparison since no such regions have yet been found in IDPs. However, private conversations with some members of the Halley team suggest that the result should be viewed with caution at this time. The isotopic patterns of Halley dust appear to be terrestrial for the elements Mg, Si, O, S, and Fe. This is consistent with what is known about IDPs.

All in all, the isotopic data obtained to date do not appear to provide decisive points of comparison between IDPs and Halley dust. This situation might change if it became possible to measure isotopic ratios in smaller regions of IDPs.

Discussion

For a variety of good reasons (e.g., mass balance arguments) and some bad, it has become widely accepted in certain circles that IDPs come predominantly from comets. However, some IDPs must come from asteroids and Flynn 1986^(28,29) has recently pointed out several factors, based on orbital considerations, that would favor the collection of asteroidal particles over cometary particles by the earth. The true fractional contribution of each source should be considered as an open question at this time.

Chondritic IDPs fall into several distinct categories and it is possible that one of these subtypes consists uniquely of cometary particles. This is the point of view that has been taken by Bradley and Brownlee 1987 in a recent paper.⁽³⁾ They point out that particles of high porosity, i.e., the anhydrous fluffy particles, would be mechanically weak and thus similar to the fragile particles observed in certain meteor showers. As discussed earlier, the microscopic Fe, Mg, Si abundance patterns of anhydrous IDPs appear to be similar to the PIA-PUMA Halley results and dissimilar from those obtained in primitive meteorites; this provides powerful support for the proposed cometary origin of the anhydrous component of IDPs.

However, I believe that it is probably premature to associate one type of IDP with cometary material. For one thing, the best IR spectral fit to the Halley data is obtained with an admixture of the laboratory spectra of both anhydrous and hydrous types of particles. Further, from an isotopic standpoint, the hydrous particles appear to be as anomalous as their anhydrous counterparts. Both types of particles may be present in a given comet, and further, all comets may not be the same. It is also possible that the surficial layers of certain asteroids closely resemble the nonvolatile component of comets.

However, there can be no doubt that at least some IDPs come from comets. With this in mind, what of the popular view that comet dust consists of simple assemblages of interstellar grains? Greenberg⁽³⁰⁾ has proposed a specific model for comet dust grains in which the particles consist of randomly arranged stacks of elongated silicate cores mantled by carbonaceous coatings. Certain features of the model may be partially valid. Elongate grains (whiskers) are seen in IDPs and many IDPs contain abundant amounts of carbonaceous material which coats and imbeds small crystalline grains. However, nothing resembling the Greenberg model has been seen in the study of several hundred IDPs. We therefore doubt that it is a valid picture for typical cometary particles.

If morphology is an uncertain guide, what about isotopic composition? Any grain with an isotopic composition distinctly different from that of average solar system material is certainly a candidate for interstellar material. But such grains represent only a small fraction by mass of a typical IDP and, further, are themselves quite small. In IDPs the isotopic compositions of all elements except hydrogen and, to a limited extent, carbon, are normal within measurement errors.

However, "normal" isotopic composition for an IDP as a whole, does not preclude it being composed of interstellar grains. Many IDPs consist of assemblages of large numbers of tiny mineral phases. Each 100 Å crystal might have a distinct isotopic signature, but the ensemble of many such grains might have a composition close to the solar system average. Further, the subgrains could be material that survived the formation of the solar system yet still not be isotopically distinct. Interstellar grains can be vaporized in the interstellar medium⁽³¹⁾ and later reconstituted after mixing. It is perhaps important to note that the one true sample of interstellar material that we know of - the galactic cosmic radiation - has (with the exception of Ne) an average isotopic composition that is not strikingly different from that of the solar system.

All things considered, the simplest picture of IDPs, and, by inference, comet dust, is that they consist of solid materials that were formed mostly in the solar nebula. Some interstellar material is present but the volume fraction is small and the interstellar grains themselves exceedingly tiny.

References

1. Fraundorf P., Brownlee D. E. and Walker R. M. (1982) Laboratory studies of interplanetary dust. In *Comets*, (L. L. Wilkening, ed.), University of Arizona Press, 383-409.
2. Bradley J. P., Scott Sandford and R. M. Walker (1987) Interplanetary dust particles. In *Meteorites and the Early Solar System*, Chapter 11.2, (J. Kerridge, ed.) Univ. Arizona Press (in press).
3. Bradley J. P. and Brownlee D. E. (1986) Cometary particles: Thin sectioning and electron beam analysis. *Science* **231**, 1542-1544.
4. Flynn G. and Sutton, S. (1987) First cosmic dust trace element analysis with the Synchrotron XRF microprobe. *Lunar Planet. Sci. XVIII*, 296-297.
5. Rajan R. S., Brownlee D. E., Tomandl D., Hodge P. W., Farrar H. and Britten R. A. (1977) Detection of ^4He in stratospheric particles gives evidence of extraterrestrial origin. *Nature* **267**, 133-134.
6. Hudson B., Flynn G. J., Fraundorf P., Hohenberg C. M. and Shirck J. (1981) Noble gases in stratospheric dust particles: Confirmation of extraterrestrial origin. *Science* **211**, 383-386.
7. Nier A. O., Schlutter D. J. and Brownlee D. E. (1987) Helium and neon isotopes in extraterrestrial particles. *Lunar Planet. Sci. XVIII*, 720-721.
8. Brownlee D. E., Tomandl D., Blanchard M. B., Ferry G. V. and Kyte F. T. (1976) An atlas of extraterrestrial particles collected with NASA U-2 aircraft: 1974-1976. *NASA TMX-73,152*.
9. McKeegan K. D., Walker R. M. and Zinner E. (1985) Ion microprobe isotopic measurements of individual interplanetary dust particles. *Geochim. Cosmochim. Acta* **49**, 1971-1987.
10. Bradley J. P., Brownlee D. E. and Fraundorf P. (1984a) Discovery of nuclear tracks in interplanetary dust. *Science* **226**, 1432-1434.
11. McKeegan K. D. (1987) Oxygen isotopic abundances in refractory stratospheric dust particles: proof of extraterrestrial origin. *Science* (in press).
12. K. D. McKeegan, P. Swan, R. M. Walker, B. Wopenka, and E. Zinner (1987) Hydrogen isotopic variations in interplanetary dust particles. (Abstract) *Lunar Planet. Sci. XVIII*, 627-628.
13. Sandford S. A. and Walker R. M. (1985) Laboratory infrared transmission spectra of individual interplanetary dust particles from 2.5 to 25 microns. *Ap. J.* **291**, 838-851.
14. For recent reviews see Ref. 2 and Mackinnon I. D. R. and Rietmeijer F. J. (1987) Mineralogy of chondritic interplanetary dust particles. *Rev. Geophysics*, in press.
15. Bradley J. P., Brownlee D. E. and Veblen D. R. (1983) Pyroxene whiskers and platelets in interplanetary dust: evidence for vapour phase growth. *Nature* **301**, 473-477.
16. Bradley J. P., Brownlee D. E. and Fraundorf P. (1984b) Carbon compounds in interplanetary dust: evidence for formation by heterogeneous catalysis. *Science* **223**, 56-58.
17. Christoffersen R. and Buseck P. R. (1983) Epsilon carbide: a low-temperature component of interplanetary dust particles. *Science* **222**, 1327-1329.
18. McKeegan K. D. (1987) Ion microprobe measurements of H, C, O, Mg, and Si isotopic abundances in individual interplanetary dust particles. Ph.D. Thesis, Washington University.
19. Wickramasinghe D. T. and Allen D. A. (1986) Discovery of organic grains in comet Halley. *Nature* **323**, 44-46.

20. Knacke R. F., Brooke T. Y. and Joyce R. R. (1986) Observations of 3.2-3.6 micron emission features in comet Halley. *Ap. J.* **310**, L49-L53.
21. Danks A., Encrenaz T., Bouchet P., Le Bertre T., Chalabaev A. and Epchtein N. (1987) Observation of an emission feature at 3.4 μ m in the spectrum of comet Halley. *Proc. 20th ESLAB Symposium on the Exploration of Halley's Comet III*, ESA S-250, 103-106.
22. Swan P., Walker R. M. and Wopenka B. (1987) 3.4 μ m absorption in interplanetary dust particles: evidence for indigenous hydrocarbons and a further link to comet Halley. *Meteoritics* (in press).
23. Kissel J., Sagdeev R. Z., Bertaux J. L., Angarov V. N., Audouze J., Blamont J. E., Büchler K., Evlanov E. N., Fechtig H., Fomenkova M. N., Langevin Y., Leonas V. B., Levasseur-Regourd A. C., Managadze G. G., Podkolzin S. N., Shapiro V. D., Tabaldyev S. R. and Zubkov B. V. (1986a) Composition of comet Halley dust particles from Vega observations. *Nature* **321**, 280-282.
24. Kissel J., Brownlee D. E., Büchler K., Clark B. C., Fechtig H., Grün E., Hornung K., Igenbergs E. B., Jessberger E. K., Krueger F. R., Kuczera H., McDonnell J. A. M., Morfill G. M., Rahe J., Schwehm G. H., Sekanina Z., Utterback N. G., Volk H. J. and Zook H. A. (1986b) Composition of comet Halley dust particles from Giotto observations. *Nature* **321**, 336-337.
25. Kissel J. (private communication).
26. Eberhardt P., Hodges R. R., Krankowsky D., Berthelier J. J., Schulte W., Dolder U., Lämmerzahl P., Hoffman J. H. and Illiano J. M. (1987) The D/H and $^{18}\text{O}/^{16}\text{O}$ isotopic ratios in comet Halley. *Lunar Planet. Sci. XVIII*, 252-253.
27. Solc M., Vanýsek V. and Kissel J. (1986) Carbon stable isotopes in comets after encounters with P/Halley. *Proc. 20th ESLAB Symposium on the Exploration of Halley's Comet I*, ESA SP-250, 373-374.
28. Flynn G. J. (1987) Earth encounter velocities and exposure ages of IDPs from asteroidal and cometary sources. *Lunar Planet. Sci. XVIII*, 294-295.
29. Flynn (private communication) points out that gravitational focussing by the Earth will be more effective, on the average, for particles derived from asteroids than those from comets.
30. Greenberg J. M. (1982) What are comets made of? In *Comets*, (L.L. Wilkening, ed.) Univ. Ariz. Press, Tucson, 131-163.
31. Seab C. G. and Shull J. M. (1986) Shock processing of interstellar grains. In *Interrelationships Among Circumstellar, Interstellar, and Interplanetary Dust*, eds. J. A. Nuth and R. E. Stencel, NASA Conf. Publ. 2403, pp. 37-53.

PIA UPDATE: CORRELATION ANALYSES OF MASS SPECTRA

L. W. Mason and B. C. Clark
Planetary Sciences Laboratory (0560)
Martin Marietta Astronautics
Denver, CO 80201

The PIA instrument aboard the Giotto spacecraft (a time-of-flight mass spectrometer) has been described elsewhere.¹ The mass spectra used in this analysis were decoded and mass numbers assigned according to the presence of carbon and silver, using the global values for these elements in their spectral absence.² The results presented here were obtained using a frequency of occurrence based analysis (similar to ref. 3) which correlates how often mass numbers appear in the mass spectra and which mass numbers tend to occur together in the same spectra; no amplitude information is utilized. The data are presented as plots of mass versus coincident mass for different subsets of the PIA data set, with both axes having units of atomic mass. Frequency contours are plotted at approximately five percent contour intervals, relative to the maximum AMU occurrence in that plot. The plots presented are symmetrical about the matrix diagonal, that is, every mass is coincident with itself in a given spectra. The plus marks indicate local maxima in the correlation profile.

Figure 1 shows the correlation plot for the entire compressed PIA data set consisting of 8030 mode 1, 2, and 3 individual mass spectra which were collected between 50 minutes before and 40 minutes after Giotto's closest approach to comet Halley. Carbon (mass 12) is the most frequently observed element, occurring in 74% of all spectra, as seen in the peak at coordinates 12,12 on the diagonal. The highest correlation which occurs between individual elements (off the diagonal) is seen at 12,16 (C and O). Combinations which occur less frequently are: O and Mg, Si and O, C and Mg, C and Si and so on. Mass 41 and mass 57 show similar patterns in their correlations with H (not shown), C, O, Mg, and Si.

When subsets of the total data set are defined and the resulting correlation matrices plotted, information about the specific relationships between simultaneously occurring mass units can be extracted. Figure 2 shows the profile resulting from all spectra containing Mg but not C. Mass 24 shows coincidence with all other masses by definition. Strong correlations (similar to the patterns seen in Fig. 1) between Mg and O, Si and O, O and 41, and O and 57 are also seen in this plot. Figure 3 shows the reciprocal data subset, that is, all spectra containing C without Mg. Strong correlations are seen between C and N, C and O, and C and Si, but the pattern seen in Fig. 2 at mass numbers 41 and 57 is absent. Two possible explanations for the appearance of these patterns with Mg, and the absence of these patterns without Mg have been postulated and are detailed as follows. The first involves the existence of molecular or cluster ions consisting of H, O and Mg in the mass spectra. The simplest plausible combinations of these elements which sum to the appropriate mass numbers are: $(\text{MgOH})^+$ for mass 41 and $(\text{MgOOH})^+$ for mass 57. The existence of molecular ions in the PIA mass spectra is not proven by this analysis, but the simplicity of the elemental formulas which sum to the appropriate mass numbers is compelling. The second explanation for the observed patterns is that mass 41 is in fact Ca^+ , and mass 57 is Fe^+ , with both either assigned to the wrong mass number (off by one), or occurring as the hydrides. The contours in Fig. 2 which range over mass 40 and 41 can be interpreted as support for the second explanation.

Molecular ion detection is indicated in other cases in the PIA data as shown in Figure 4, where all spectra having C but not O are plotted. Note the correlation between mass 26 and C and N (mass 14), allowing speculation that the CN^+ ion is present in a significant fraction of these spectra. PUMA data has shown significant occurrences at 24 major mass lines which were attributed to molecular ions.³ Of these, only masses 25, 26, and 29 are similar to frequent occurrences in the PIA data. It has been surmised, however, that two of the PIA amplifier stages were non-functional, possibly causing fewer mass lines to appear in these spectra than in the PUMA data.

This work was performed for the Jet Propulsion Laboratory, California Institute of Technology, sponsored by the National Aeronautics and Space Administration.

REFERENCES

- 1 Kissel, J. : ESA Spec. Publ. 1077, p.67-8, 1986.
- 2 Clark, B.C., Mason, L.W., & Kissel, J. : 20th ESLAB Symp., ESA SP-250, Vol III, p. 353-8, 1987.
- 3 Kissel, J., and Kreuger, F.R. : *Nature* 326:755-60 (1987).

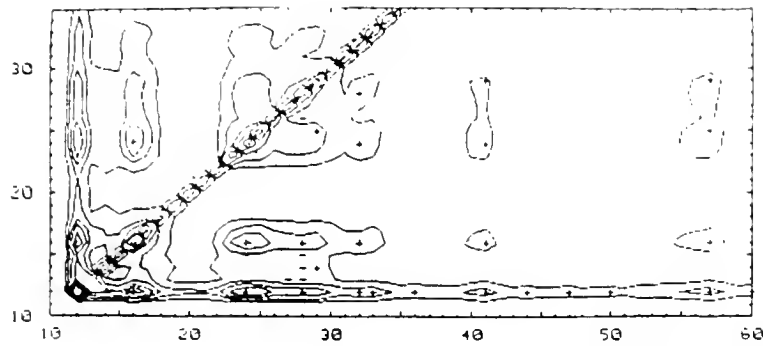


Figure #1 Frequency of occurrence contours for entire compressed PIA data set consisting of 8030 individual mass spectra. Axes are in units of atomic mass.

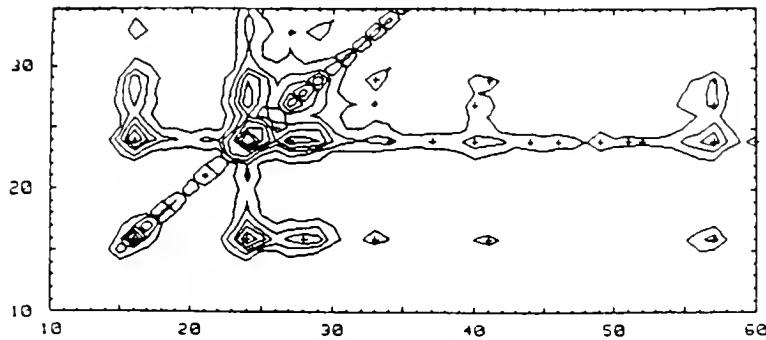


Figure #2 Subset of 321 spectra containing magnesium (mass 24) but not carbon (mass 12).

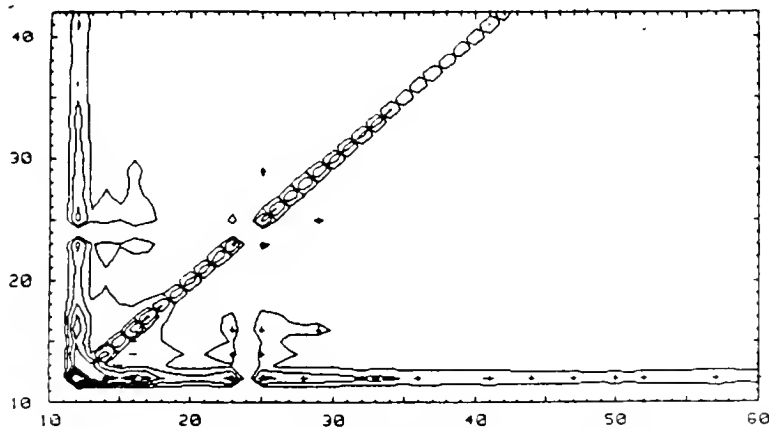


Figure #3 Subset of 4198 spectra containing carbon but not magnesium.

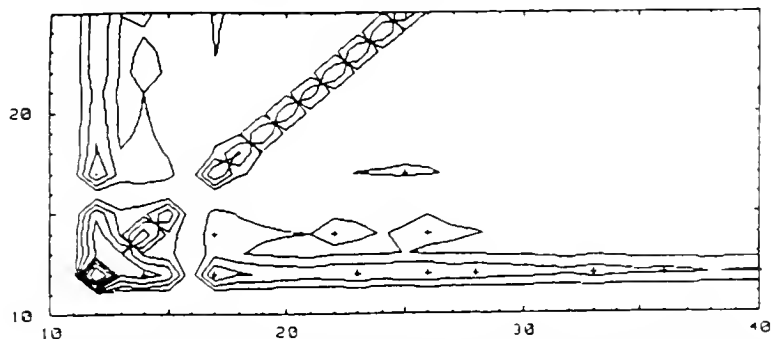


Figure #4 Subset of 3561 spectra containing carbon but not oxygen (mass 16). Presence of CN^+ ion may be indicated by correlations between mass 26 and carbon and nitrogen (mass 14).

A COMPARISON OF HALLEY DUST WITH METEORITES, INTERPLANETARY DUST AND INTERSTELLAR GRAINS

D. E. Brownlee
University of Washington
Dept. of Astronomy
Seattle, Washington 98195
U.S.A.

The Giotto, Vega 1 and Vega 2 spacecraft carried nearly identical instruments designed to measure the elemental and isotopic compositions of dust from comet Halley. The time-of-flight mass spectrometers measured mass spectra of positive ions generated during the hypervelocity impact of individual submicron particles. The thousands of spectra produced by the instruments provided a direct analysis of the bulk elemental composition of Halley solids and information on molecular and isotopic composition. The variations between spectra yielded an intimate view of the nature of Halley at the submicron scale.

The averaged composition of Halley is consistent with chondritic elemental abundances for elements heavier than sodium (Jessberger *et al.* 1986). The abundances of C and N in the Halley solids appear to be higher than those observed in the most carbon rich meteorites. Jessberger *et al.* estimate that carbon is enhanced by a factor of eight above its abundance in CI chondrites. The abundance of different types of carbon rich particles varied during the Giotto flyby indicating possible large scale heterogeneity in the nucleus (Clark *et al.* 1986). For the most part, molecules were disassociated during impact with the instruments but analysis of apparent molecular fragments has been used to estimate the molecular composition of the organic component in Halley (Kissel and Krueger 1987).

The variability of the mineral forming elements in the submicron Halley grains provides a powerful basis for comparison of Halley with the different classes of meteoritic materials that have been studied in the laboratory. The degree of variability in the Halley samples is larger than that seen in chondrites implying that Halley is more heterogeneous at the submicron scale. A critical distinction is that Halley contains abundant pure Mg silicates at this size scale while the carbon rich meteorites do not. The submicron compositional dispersion seen in Halley is dramatically different from the narrowly constrained compositions seen in the CI and CM (type 1 and 2) carbonaceous chondrites. These meteorites are carbon rich but are dominated by a serpentine-like hydrated silicate with a very narrow range of Mg/Si ratio. The Halley results are also unlike the compositional variations seen in the majority of interplanetary dust types that are dominated by hydrated minerals. The only known class of meteoritic material that appears to closely resemble the

Halley data is a class of interplanetary dust that is composed entirely of anhydrous minerals. These particles are black, porous aggregates of submicron grains. Some of the component grains in these aggregates are single minerals such as Mg_2SiO_4 , MgSiO_3 and FeS while others are compact masses of very small crystals and amorphous material imbedded in a low atomic weight matrix. If these particles are identical to Halley this would imply that Halley is dominated by olivine, pyroxene, iron sulfide, glass and amorphous carbonaceous matter. Carbon in these particles occurs as discrete grains and as films not generally exceeding 200 Å in thickness. As the minerals in these particles are anhydrous the only means of storage of water or OH in the material would be as ice filling the open voids. Because the pore spaces are submicron in size, ice and black dust should be intimately mixed even at the micron size scale.

A key issue in cometary studies is the relationship between comet dust and interstellar grains. Some authors (Kissel and Krueger 1987) have heavily interpreted the Halley results in favor of the Greenberg core-mantle model for interstellar grains. The Halley results do indicate high carbon abundances, consistent with the Greenberg model, but there is little definitive evidence to really substantiate the assertion that Halley is a mixture of preserved presolar grains that have silicate cores surround by thick radiation processed organic mantles. If Halley particles are identical to the anhydrous interplanetary particles, the core-mantle model does not describe their structure. These particles are more complex than an assemblage of elongated silicate cores mantled with thick organic films. An interesting approach for comparison of cometary, interstellar and interplanetary particles is the shape of the 10 μm silicate feature. Structure observed in the Halley 10 μm feature appears to correlate with that observed in the anhydrous interplanetary particles measured by Sandford and Walker (1987). Such measurements can distinguish materials dominated by low temperature minerals like hydrated silicates from high temperature minerals such as Mg silicates.

- Clark, B., Mason, L. W., and Kissel, J., *Eur. Space Agency Spec. Publ.* **250**, 353-358 (1986).
 Jessberger, E. K., Kissel, J., Fechtig, H. and Krueger, F. R., *Eur. Space Agency Spec. Publ.*, **249**, 27-20 (1986).
 Kissel, J. and Krueger, F. R., *Nature*, **326**, 755-760 (1987).
 Sandford, S. A. and Walker, R. M., *Ap. J.*, **291**, 838-851 (1985).

THE SPECTRAL PROPERTIES OF INTERPLANETARY DUST PARTICLES

Scott A. Sandford
NASA-Ames Research Center, M.S. 245-6
Moffett Field, CA 94035

The majority of the infrared transmission (absorption) spectra of individual interplanetary dust particles (IDPs) can be classified into one of three infrared classes based on the spectral profile of their $10\mu\text{m}$ silicate features (see Fig. 1). These three classes have been referred to as the olivines, the pyroxenes, and the layer-lattice silicates, after the terrestrial and meteoritic minerals that provide the best match to the observed $10\mu\text{m}$ band profiles (Sandford and Walker, 1985). Transmission electron microscopy and electron diffraction studies confirm that particles in the three infrared classes are, in fact, dominated by the appropriate mineral types (see Walker, Bradley, and Sandford, 1987, for a recent review of the properties of IDPs).

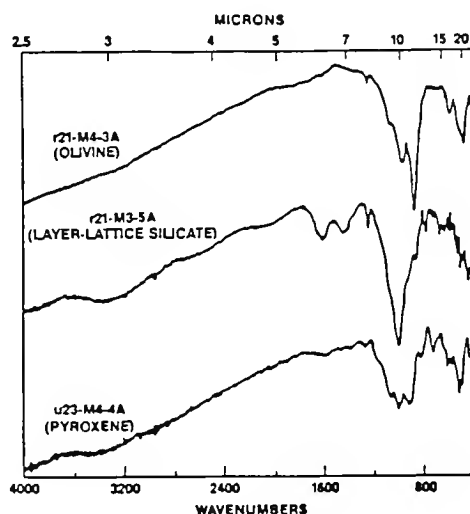


Figure 1. Representative spectra from IDPs in each of the three infrared classes. Figure adapted from Sandford and Walker, 1985.

Particles falling in the olivine and pyroxene infrared groups are dominated by the appropriate anhydrous mineral grains (Christoffersen and Buseck, 1986; Bradley and Brownlee, 1986). These particles are "coarse" grained in the sense that they contain mineral grains having diameters between 0.1 and 2 microns. These particles often have "fluffy" morphologies and consist primarily of single-mineral grains embedded in carbonaceous matrix. Diffraction studies show that the majority of the silicates are crystalline in nature, rather than amorphous. The carbonaceous material typically constitutes 2-8 percent of the particles by mass. The infrared spectra of these particles are dominated by the " $10\mu\text{m}$ " (Si-O-stretching mode) and " $20\mu\text{m}$ " (Si-O-Si-bending mode) features of crystalline silicates.

Particles in the layer-lattice silicate infrared class are usually dominated by smectic minerals (Tomeoka and Buseck; 1984, 1985) with a small minority containing primarily serpentines (Bradley and Brownlee, 1986). This is opposite of the case seen in meteorites where serpentines are observed to be the major layer-lattice silicates present. These particles represent the most common type of IDP in the stratospheric collections, and they tend to be more compact than the IDPs dominated by olivines and pyroxenes. Carbonates are

an important secondary mineral seen in most of the IDPs in this infrared class (Sandford and Walker, 1985; Sandford, 1986; Tomeoka and Buseck, 1986) are the source of the prominent $6.8\mu\text{m}$ feature seen in the spectra. Also apparent are the 3.0 and $6.0\mu\text{m}$ features due to adsorbed and absorbed water. As with the particles in the other two infrared classes, these particles contain about 5 percent carbonaceous material by mass.

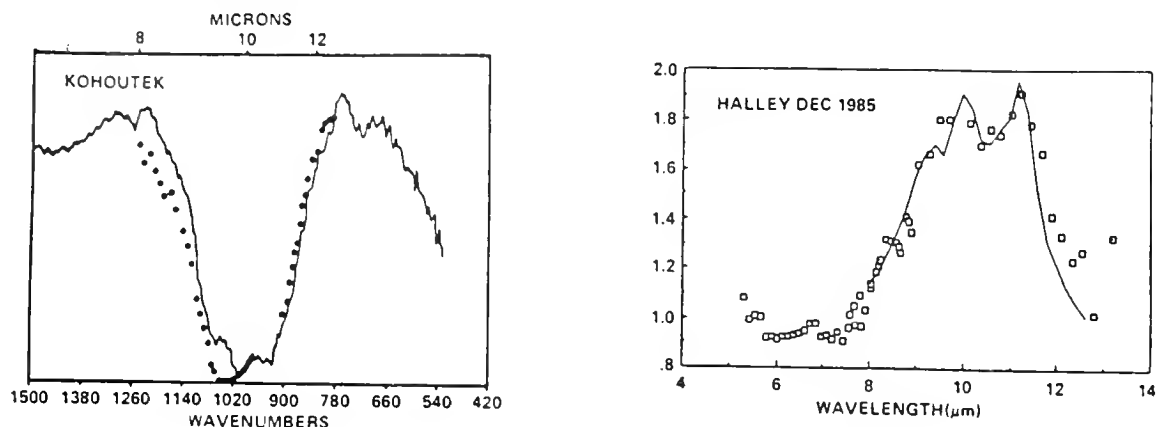


Figure 2. Comparison of the infrared emission from Comets Kohoutek and Halley with IDP spectral mixtures. The points are the cometary data; the solid lines are the IDP data. Figures adapted from Sandford and Walker, 1985, and Bregman *et al.*, 1987

To first order, the $10\mu\text{m}$ emission spectra of comets Kohoutek and Halley can be matched by combinations of these spectral types (see Fig. 2) (Sandford and Walker, 1985; Bregman *et al.*, 1987). In the case of comet Halley, a reasonable fit is provided by a combination containing approximately 55 percent olivines, 35 percent pyroxenes, and 10 percent layer-lattice silicates. In contrast, the comet Kohoutek silicate feature cannot be fit using mixtures that contain more than a few percent of the olivine-rich IDPs. This suggests that different comets may have different overall compositions. Given comet Halley's observed variability, we need to also consider the possibility that the relative mix of particle types ejected could vary from time to time within a single comet. It is interesting to note that the detailed features in the comet Halley $10\mu\text{m}$ data imply the presence of crystalline silicates, in contrast to the featureless interstellar 10-micron feature, which is generally thought to indicate the presence of amorphous silicates. The dominance of anhydrous minerals such as olivine and pyroxene in Halley (as inferred from the spectra) is consistent with the compositional constraints determined by the various Halley space-probe dust experiments (by Brownlee, this volume). The presence of at least some layer-lattice silicates in comet Halley is suggested, however, by the observation of a weak $6.8\mu\text{m}$ emission feature in the Halley data that has a strength consistent with the presence of carbonates in the abundance with which they are seen in IDPs.

Note from Figure 1 that the three different infrared types have " $20\mu\text{m}$ " features that fall at different spectral positions, and that in many cases this "feature" actually consists of several bands. These features are due to Si-O-Si-binding- and silicate-lattice-mode vibrations, and hence are more sensitive than the $10\mu\text{m}$ Si-O-stretching band to (i) cation substitution, (ii) crystalline order, and (iii) molecular symmetry. Thus, given that a combination of silicates is required to match the Halley $10\mu\text{m}$ data and the compositional information returned by the Halley space probes, we wouldn't expect a single " $20\mu\text{m}$ " band, but instead a series of overlapping features of varying widths and strengths. The net result should be a broadband excess near $20\mu\text{m}$ in which there may be no strong, obvious "narrow" features.

Despite the fact that the mass in IDPs is dominated by silicates, the interaction of the dust with visible photons is primarily mediated by the carbonaceous material (see Fig. 3). Intense bands in the Raman spectra of IDPs at 1350 and 1600 Δcm^{-1} and a broad feature between 2200 and 3300 Δcm^{-1} are characteristic of the presence of aromatic domains whose size scale is less than 25 Å (Allamandola, Sandford, and Wopenka, 1987). No spectral evidence exists for the presence of graphite within the IDPs. The absence of silicate bands in the Raman spectra demonstrates that the carbonaceous material effectively covers the silicates in the IDPs and "screens out" visible light through scattering and absorption before it reaches the silicates. This observation has important implications for the modeling of cometary thermal emission (see, for example, Krishna Swamy *et al.*, 1987, this volume). Little else is known about the composition of the carbonaceous component in IDPs except that the material contains C and H, with minor amounts of O and N (Bradley, Brownlee, and Fraundorf, 1984), and some small fraction of this material is the carrier of a phase enriched in deuterium (McKeegan, Walker, and Zinner, 1985). Presumably this material is similar to the polymeric phase seen in meteorites (Hayatsu and Anders, 1981), which consists of small aromatic domains randomly interlinked by short aliphatic bridges.

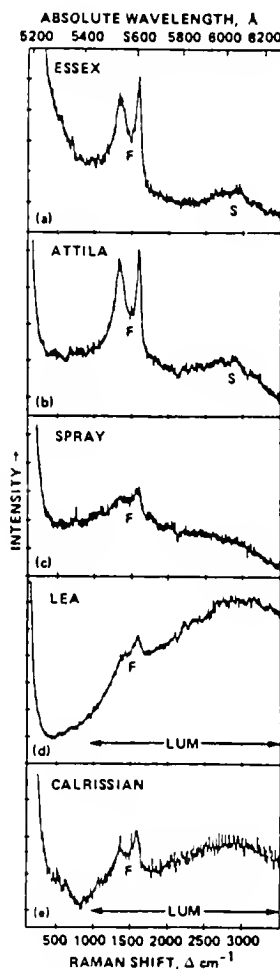


Figure 3. Raman spectra of five interplanetary dust particles.
Figure adapted from Allamandola, Sandford, and Wopenka, 1987.

In brief, the observed spectral and mineralogical properties of IDPs allow us to conclude the (i) the majority of IDP infrared spectra are dominated by olivine, pyroxene, or layer-lattice silicate minerals, (ii) to first order the emission spectra of comets Halley and

Kohoutek can be matched by mixtures of these IDP infrared types, implying that comets contain mixtures of these different crystalline silicates and may vary from comet to comet and perhaps even within a single comet, (iii) we probably do not expect to observe a single "20 μ m" feature in cometary spectra, (iv) carbonaceous materials dominate the visible spectra properties of the IDPs even though the mass in these particles consists primarily of silicates, and (v) the particle characteristics summarized in items (ii) and (iv) need to be properly accounted for in future cometary emission models.

References

- Allamandola, L. J., Sandford, S. A., and Wopenka, B., 1987, *Science*, **237**, 56-59.
 Bradley, J. P. and Brownlee, D. E., 1986, *Science*, **231**, 1542-1544.
 Bradley, J. P., Brownlee, D. E., and Fraundorf, P., 1984, *Science*, **223**, 56-58.
 Bregman, J. D., Campins, H., Witteborn, F. C., Wooden, D. H., Rank, D. M.,
 Allamandola, L. J., Cohen, M., and Tielens, A. G. G. M., 1987, *Astron. Astrophys.*,
 in press.
 Christoffersen, R. and Buseck, P. R., 1986, *Earth Planet. Sci. Lett.*, **78**, 53-66.
 Hayatsu, R. and Anders, E., 1981, *Topics Curr. Chem.*, **99**, 1-37.
 Krishna Swamy, K. S., Sandford, S. A., Allamandola, L. J., Witteborn, F., and Bregman,
 J. D., 1987, *Icarus*, submitted.
 McKeegan, D. K., Walker, R. M., and Zinner, E., 1985, *Geochim. Cosmochim. Acta*, **49**,
 1971-1987.
 Sandford, S. A., 1986, *Science*, **231**, 1540-1541.
 Sandford, S. A. and Walker R. M., 1985, *Astrophys. J.*, **291**, 838- 851.
 Tomeoka, K. and Buseck, P. R., 1984, *Earth Planet. Sci. Lett.*, **69**, 243-254.
 Tomeoka, K. and Buseck, P. R., 1985, *Nature*, **314**, 338-340.
 Tomeoka, K. and Buseck, P. R., 1986, *Science*, **231**, 1544-1546.
 Walker, R. M., Bradley, J. P., and Sandford, S. A., 1987, in *Meteorites and the Early Solar
 System*, (J. Kerridge, ed.), Univ. of Arizona Press, in press.

DISCUSSION

HUFFMAN: You can get a double-peaked Raman spectrum from many materials including graphite (well-ordered) that has simply been rubbed against a surface, not just from "amorphous" carbon.

SANDFORD: Yes, this is true. The presence of the double hump only tells you that the aromatic C-C bonds are present and the domains of order are limited in size (25 Å in IDPs). The ease with which the graphite spectrum (Raman) is altered and the lack of crystalline graphite seen in IDPs shows that the optical constants of graphite are not appropriate for cometary modeling.

RUSSELL: It appears to me that the difference between Halley and Kohoutek is that one is "processed" — heated to produce crystallinity — whereas the other is not. The nucleus of Halley is heated during each apparition, undergoes "night" and "day" thermal cycling, experiences pressure buildups and releases (jets and outbursts), and thus the top few meters (up to 100m, based on two outbursts observed in the infrared post-perihelion) are likely not "pristine."

SANDFORD: A smear of pyroxenes can mimic an amorphous 10 μm feature.

HANNER: We have been discussing comparisons between laboratory transmission spectra and comet emission spectra. One has to be a bit careful, for the shapes can differ, due to a scattering contribution in the transmission spectra and a range of grain sizes and temperatures contributing to the emission spectra.

AROMATIC COMPONENTS IN COMETARY MATERIALS

L. J. Allamandola¹, S. A. Sandford¹

and

B. Wopenka²

¹ NASA-Ames Research Center, MS 245-6
Moffett Field, CA 94035

²McDonnell Center for the Space Sciences
and Dept. of Earth and Planetary Sciences
Washington University, St. Louis, MO 63130

The Raman spectra of interplanetary dust particles (IDPs) collected in the stratosphere show two bands at about 1350 and 1600 Δcm^{-1} and a broader feature between 2200 and 3300 Δcm^{-1} that are characteristic of aromatic molecular units with ordered domains smaller than 25 Å in diameter (see Fig. 1 and reference 1). This suggests that the carbonaceous material in IDPs may be similar to the polymeric component seen in meteorites, where this material is thought to consist of aromatic molecular units that are randomly interlinked by short aliphatic bridges (cf. reference 2).

The features in the Raman spectra of IDPs are similar in position, and relative strength to interstellar infrared emission features that have been attributed to vibrational transitions in free molecular polycyclic aromatic hydrocarbons (PAHs) (see Fig. 2). The Raman spectra of some IDPs also show red photoluminescence (see Fig. 1) that is similar to the excess red emission from some astronomical objects and that has also been attributed to PAHs and PAH-related materials. Moreover, a part of the carbonaceous phase in IDPs contains deuterium-to-hydrogen ratios that are far greater than those found in terrestrial samples (3). Deuterium enrichment is expected in small free PAHs that are exposed to ultraviolet radiation in the interstellar medium (1, 4).

Taken together, these observations suggest that some fraction of the carbonaceous material in IDPs may have been produced in circumstellar dust shells and only slightly modified in interstellar space. Since many, if not most, IDPs come from comets, this supports the view that cometary material contains "primitive" components which can provide clues about early solar system (and perhaps even interstellar and circumstellar) processes.

References

1. L. J. Allamandola, S. A. Sandford, and B. Wopenka, 1987, *Science*, **237**, 56-59.
2. R. Hayatsu and E. Anders, 1981, *Top. Curr. Chem.*, **99**, 1-37.
3. K. D. McKeegan, R. M. Walker, and E. Zinner, 1985, *Geochim. Cosmochim. Acta*, **49**, 1971-1987.
4. L. J. Allamandola, A. G. G. M. Tielens, J. R. Barker, 1987, *Astrophys. J.*, submitted.
5. J. Bregman, L. J. Allamandola, J. Simpson, A. Tielens, and F. Witteborn, 1984, NASA/ASP Symposium on Airborne Astronomy, NASA Conf. Pub. 2353.

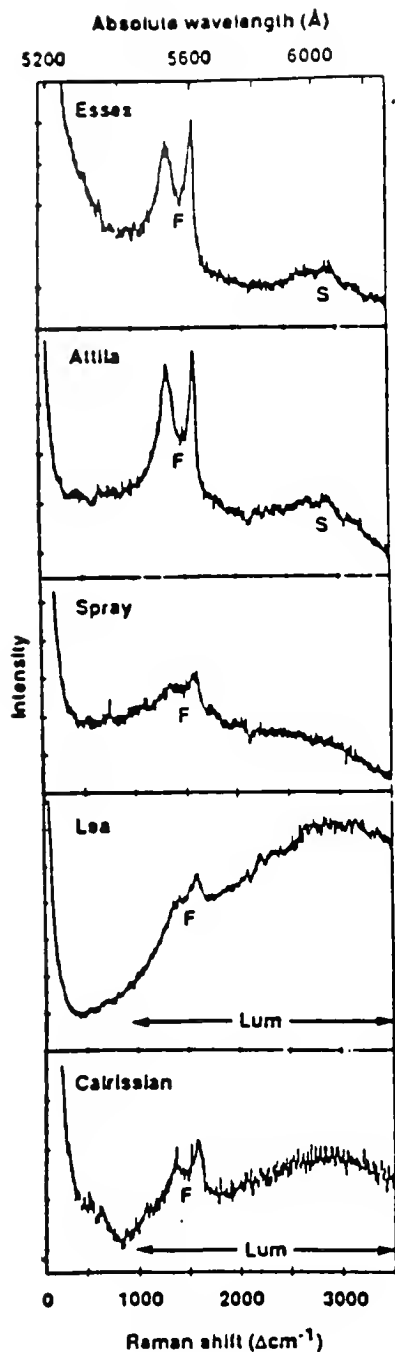


Figure 1 - Examples of the Raman spectra of IDPs. Many spectra are dominated by the Raman bands of disordered carbonaceous material (see the top two spectra), while others are dominated by red luminescence (see the bottom two spectra). The relative contribution from these two effects varies from particle to particle. The designations F, S, and Lum in the figure label the first- and second-order Raman bands and red luminescence, respectively. The large increase in counts near 0 cm^{-1} is from Rayleigh-scattered incident laser light. All the spectra shown were taken at a resolution of 5 cm^{-1} , and the sample was excited by the 5145 Å Ar^+ laser line. The upper axis indicates the absolute wavelength of the observed emission; the lower axis indicates the Raman shift (Stokes lines) with respect to the exciting-laser frequency. Figure adapted from reference (1).

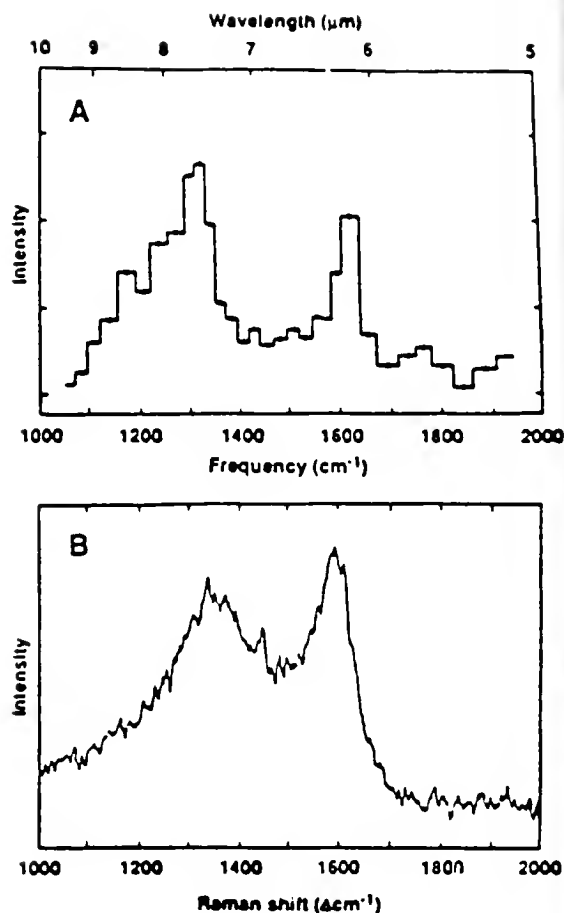


Figure 2 - Comparison between (A) the infrared emission spectrum of the Orion Bar [Orion data from reference (5)] and (B) the Raman spectrum of an IDP. Figure adapted from reference (1).

THE $3.4\mu\text{m}$ EMISSION FEATURE IN COMET HALLEY

T. Y. Brooke and R. F. Knacke

Astronomy Program

Department of Earth and Space Sciences
State University of New York at Stony Brook
Stony Brook, NY 11794

Several teams of ground-based observers reported observations of the emission feature centered at $3.36\mu\text{m}$ in comet Halley following its discovery by the Vega 1 spacecraft (Ref. 1-6). The position and shape of the band (Fig. 1) indicate a superposition of emissions by C-H groups. But the mechanism for the excitation of these C-H₃ groups is still not agreed upon. Three possibilities are summarized below. Elucidation of the emission mechanism is needed to determine whether the source is predominantly solid or gas. In addition, Table 1 shows that the derived carbon abundance in Halley depends strongly on the assumed mechanism.

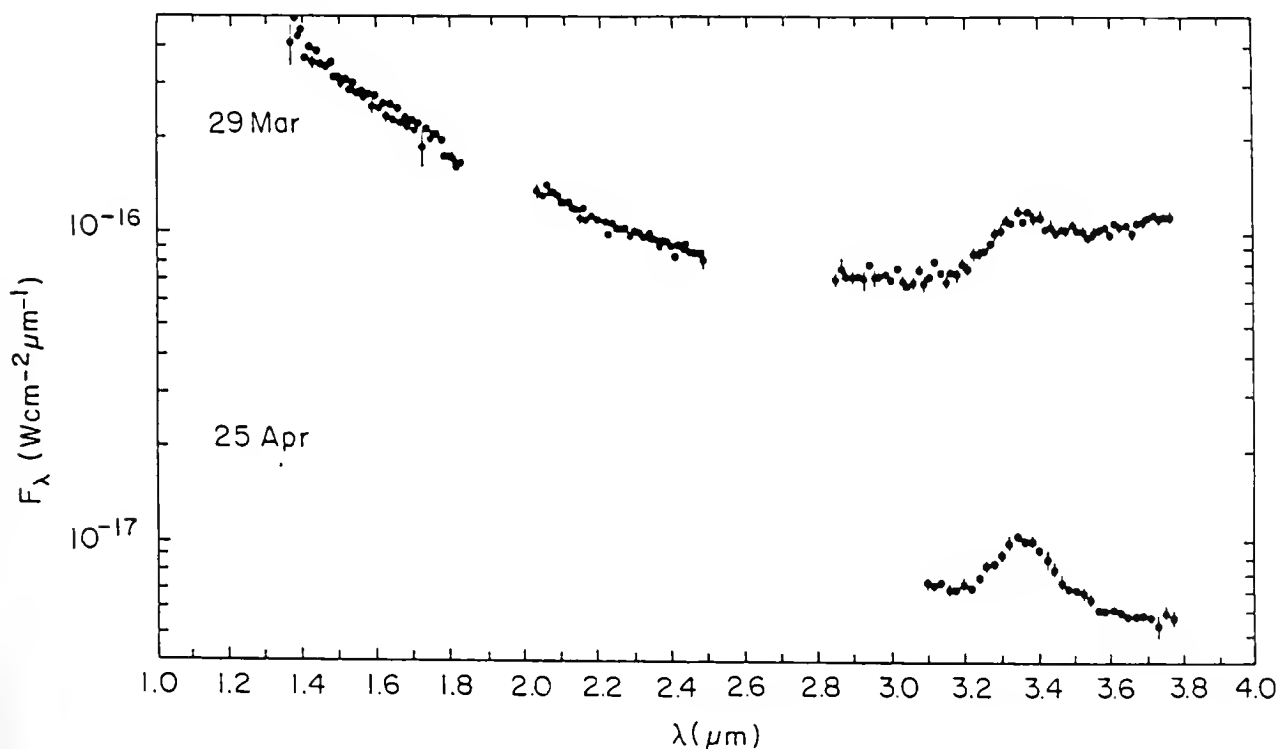


Figure 1. Spectra of comet Halley (Ref. 3)

1) THERMAL EMISSION FROM HOT GRAINS ($a < 0.1\mu\text{m}$)

Hydrocarbons in small grains could account for the observed $3.4\mu\text{m}$ flux if they were heated to $T > 500$ K, an equilibrium temperature for absorbing grains of radius $a < 0.1\mu\text{m}$ at 1 A.U. (Ref. 3). The required C-H production rate was ~ 1 percent of the water production on 26 Mar UT 1986 (Table 1).

One difficulty with ascribing the $3.4\mu\text{m}$ feature to thermal emission is that a relatively high-hydrocarbon band strength may be required to raise the feature above the observed continuum (Ref. 4). Another problem is the absence of strong emission features at longer

wavelengths (6-8 μ m) in comet Halley (Ref. 7, 8). These could be overwhelmed by the thermal emission from noncarbonaceous grains (Ref. 9).

TABLE 1
Relative Abundance of C-H in Comet Halley Derived from the 3.4 μ m Feature.

Mechanism	Ref	UT 1986	Q(C-H) (sec ⁻¹)	$\frac{Q(C-H)}{Q(H_2O)}$
1) Thermal emission from hot grains	3	26 Mar	2×10^{27}	~ 1%
2) UV-pumped IR fluorescence from large molecules	4	25 Apr	3×10^{26}	0.15%
3) Resonance scattering by molecules	3	26 Mar	4×10^{28}	30%
	6	28 Mar	2×10^{28}	10%
	8			20%

2) ULTRAVIOLET-PUMPED INFRARED FLUORESCENCE ($a \sim 5\text{\AA}$)

Large molecules or small clusters can absorb UV photons through electronic transitions and release the energy through excited vibrational transitions in the infrared. This mechanism has been invoked to explain the unidentified interstellar emission feature (Ref. 10, 11). All of the emission is in narrow bands so large line-to-continuum ratios are possible.

According to Reference 4, this fluorescence mechanism is efficient enough that the sun could have provided sufficient UV flux to excite the 3.4 μ m emission in comet Halley. They give a required molecular production of only 0.15 percent of the water production on 25 Apr UT 1986 (Table 1). While in principle the process may be highly efficient at converting UV photons to 3.4 μ m photons, considerable uncertainties do remain and a more detailed calculation for specific molecules in the solar radiation field is needed to test its applicability to the cometary emission.

3) RESONANCE SCATTERING BY MOLECULES

Simple infrared resonance scattering of sunlight by gas molecules could also explain the 3.4 μ m feature. Derived production rates depend on the assumed band strength, but are a few times 10 percent of the water production (Table 1).

The signature of resonance scattering would be the detection and measurement of relative intensities of vibration-rotation lines in the feature which would be absent in a solid. The highest resolution spectrum of Halley shows possible features in the band (Ref.

4), but there is no obvious candidate to date.

Resonance scattering provides a natural explanation for the absence of longer wavelength features since the solar flux drops with increasing wavelength (Ref. 8).

Even though the emission mechanism is still uncertain, some progress has been made at identifying the spectral groups responsible for the emission (Refs. 3, 4, 5, 8, 12). A feature at $3.52\mu\text{m}$ has been attributed to oxygen-containing molecules, possibly formaldehyde (Refs. 3, 5, 12). A feature at $3.28\mu\text{m}$ coincides with an interstellar emission feature and may be due to the $=\text{C-H}$ stretch in aromatic hydrocarbons. The bulk of the cometary emission, like the interstellar absorption feature, is at longer wavelengths where alkyl groups ($-\text{CH}_3$ and others), possibly attached to the ring molecules, can absorb. The presence of such side chains may be indicative of low-temperature formation environments (Ref. 13).

Further progress towards identifying the $3.4\mu\text{m}$ emitter lies in high signal-to-noise and higher spectral resolution observations of a bright comet. In May 1987, the $3.4\mu\text{m}$ emission feature was detected in comet Wilson (Ref. 14).

References

1. Combes, M., *et al.*, 1986, *Nature*, **321**, 266.
2. Wickramasinghe, D. T. and Allen D. A., 1986, *Nature*, **323**, 44.
3. Knacke, R. F., Brooke, T. Y., and Joyce, R. R., 1986, *Ap. J. (Letters)*, **310**, L49.
4. Baas, F., Geballe, T. R., and Walther, D. M., 1986, *Ap. J. (Letters)*, **311**, L97.
5. Danks, A. C., Encrenaz, T., Bouchet, P., Le Bertre, T., Chalabeav, A., 1987, *Astr. Ap.*, **184**, 329.
6. Tokunaga, A. T., Nagata, T., and Smith, R. G., 1987, *Astr. Ap.*, in **187**, 519.
7. Campins, H., Bregman, J. D., Witteborn, F. C., Wooden, D. H., Rank, D. M., Allamandola, L. J., Cohen, M., and Tielens, A. G. G. M., 1986, *20th ESLAB Symp. ESA SP-250*, Vol. II, p. 121.
8. Encrenaz, T., Puget, J. L., Bibring, J. P., Combes, M., Crovisier, J., Emerich, C., d'Hendecourt, L., and Rocard, F., 1987, *Symp. on the Diversity and Similarity of Comets, ESA SP-278*, in press.
9. Chyba, C. and Sagan, C., 1987, these proceedings.
10. Leger, A. and Puget, J. L., 1984, *Astr. Ap.*, **137**, L5.
11. Allamandola, L. J., Tielens, A. G. G. M., and Barker, J. R., 1985, *Ap. J. (Letters)*, **290**, L25.
12. Combes, M., *et al.*, 1986, *20th ESLAB Symp. ESA SP-250*, Vol. I, p. 353.
13. Knacke, R. F., Brooke, T. Y., Joyce, R. R., 1987, *Astr. Ap.*, **187**, 625.
14. Brooke, T., Knacke, R., Owen, T., and Tokunaga, A., 1987, *IAU Circ. No. 4399*.

DISCUSSION

SANDFORD: A nice talk! I think that we need to be careful not to present the thermal and resonance processes as exclusive as far as the source of the $3.4\mu\text{m}$ feature goes. I would expect that both processes are occurring. Certainly IDPs contain hydrocarbons and contributions from these would be predominantly thermal. On the other hand, these grains probably also shed hydrocarbons with intermediate velocities, and these should contribute via fluorescence (laboratory experiments on photolyzed ices show that these intermediate velocity hydrocarbons are easy to form and are likely to be common).

BROOKE: Thus, I expect that a truly satisfactory explanation of the $3.4\mu\text{m}$ feature will include a variety of thermal and fluorescence processes.

LYNCH: Have you looked at the dependence of the $3.4\mu\text{m}$ feature on heliocentric distance?

BROOKE: No, it should be done.

CAMPINS: The $3.4\mu\text{m}$ feature in Comet West may have been masked by the strong thermal continuum when the comet was at 0.3 AU.

BROOKE: If the $3.4\mu\text{m}$ -emitting material were present in abundance, we should see it even in the presence of a strong continuum; it should be enhanced close to the sun. It should be noted that Comet West showed the silicate feature, but did not show the $3.4\mu\text{m}$ feature. However, the apparent variability of the $3.4\mu\text{m}$ feature on the timescale of one day makes the prediction of when one should see the feature very difficult. The non-detection of the $3.4\mu\text{m}$ feature on one day does not imply that that comet does not have the $3.4\mu\text{m}$ feature at all other times. Clearly, more observations are required.

COMPARISON OF THE 3.36 μ m FEATURE TO THE ISM

A. T. Tokunaga and T. Brooke

It has been noted that the 3.36 μ m emission feature is not the same as that of any ISM band at 3.4 μ m (ref. 1,4,6,12,13,22). This short contribution documents this fact.

In Figure 1, the 3.36 μ m emission feature is compared to that of the 3.4 μ m absorption feature in the Galactic Center source IRS 7. The primary differences between the two features are the small shift in the maximum of absorption of emission and the somewhat broader width of the Galactic Center feature. While the similarity of the features is suggestive that they are the same type material, it is important to bear in mind that the Galactic Source IRS 7 absorption is unique. There is only one source in the Galaxy in which this feature is seen. This indicates that the material giving rise to the 3.4 μ m absorption feature in the Galactic Center may be rare and that it may not be abundant in comets.

Figure 2 shows infrared spectra of two protostellar sources (Mon R2 IRS-2 and IRS-3) and an evolved star with a circumstellar disk (OH 0739-14). The spectrum of the OH 0739-14 source shows that classical water ice band at 3.05 μ m which is well fitted by a model (the solid line). In contrast, the spectrum of Mon R2 IRS-2 is not fitted so well by the model and it also shows a weak absorption feature at about 3.42 μ m. The material giving rise to the 3.42 μ m feature is probably carbonaceous, but its precise composition is also unknown. (The spectrum of Mon R2 IRS-3 is not understood at all – it is unique.)

Figure 3 compares the emission feature in Comet Halley with the ISM emission features at 3.3-3.6 μ m. The peak of the 3.36 μ m feature in Halley does not correspond at all in wavelength to the emission features seen in the ISM. However, the emission features in the ISM have been identified with the polycyclic aromatic hydrocarbons ("PAHs," ref. 14) or similar material in composition such as "QCC" (ref. 18). If PAH material is present in Comet Halley, it is present in a relatively small amount compared to the material giving rise to the 3.36 μ m feature (ref. 1).

We list the comets for which both 3.4 and 10 μ m spectroscopy have been obtained in Table 1. There is no clear pattern to the presence or absence of the 3.4 μ m feature relative to the silicate feature or to whether the comet is new or old. Clearly, further spectroscopy of comets is needed. Also, some caution is required in the case of Comet Wilson, the 3.4 μ m feature was observed strongly but the silicate feature was weak (Gunych and Bregman, private communication).

In summary, there is no convincing analog to the cometary 3.36 μ m emission feature seen in the ISM. This fact suggests that if the carbonaceous material in comets came from the ISM, it was either further processed in the solar nebula or has a different appearance because of the different excitation environment of the sun and the ISM (as suggested by ref. 13).

References

1. Baas, F., Geballe, T. R., and Walther, D. M. 1986, *Ap. J. Lett.*, **311**, L97.
2. Brooke, this conference.
3. Butchart, I., McFadzean, A. D., Whittet, D. C., Geballe, T. R., and Greenberg, J. M. 1986, *Astron. Ap.*, **154**, L5.
4. Combes, M. *et al.* 1986, in *20th ESLAB Symp. on the Exploration of Halley's Comet*, Vol. 2, p. 353.
5. de Muizon, M., Geballe, T. R., d'Hendecourt, L. B., and Baas, F. 1986, *Ap. J. Lett.*, **306**, L105.
6. Encrenaz, Th., Puget, J. L., Bibring, J. P., Combes, M., Crovisier,

- J., Emerich, C., d'Hendecourt, L., and Rocard, F. 1987, in *Proceedings of the Brussels Conference*, in press.
7. Gehrz, R. D. and Ney, E. P. 1986, in *20th ESLAB Symp. on the Exploration of Halley's Comet*, Vol. 2, p. 101.
 8. Gehrz, R. D., this conference.
 9. Green, S. F., McDonnell, J. A. M., Pankiewicz, G. S. A., and Zarnecki, J. C. 1986, *20th ESLAB Symp. on the Exploration of Halley's Comet*, Vol. 2, p. 81.
 10. Hanner, M. S., Aitken, D. K., Knacke, R. F., McCorkle, S., Roche, P. F., and Tokunaga, A. T. 1985, *Icarus*, **62**, 97.
 11. Hanner, M. S., this conference.
 12. Knacke, R. F., Brooke, T. Y., and Joyce, R. R. 1986, *Ap. J. Lett.*, **310**, L49.
 13. Knacke, R. F., Brooke, T. Y., and Joyce, R. R. 1987, in *20th ESLAB Symp. on the Exploration of Halley's Comet*, Vol. 2, p. 95.
 14. Leger, A. and d'Hendecourt, L. 1986, *Polycyclic Aromatic Hydrocarbons and Astrophysics*, A. Leger, L. d'Hendecourt, and N. Boccara, ed.), p. 223.
 15. Lynch *et al.*, this report.
 16. Ney, E. P. and Merrill, K. M. 1976, *Science*, **194**, 1051.
 17. Oishi, M., Kawara, K., Kobayashi, Y., Maihara, T., Noguchi, K., Okuda, H., Sato, S., Iijima, T., and Ono, T. 1978, *Pub. Astron. Soc. Japan*, **30**, 149.
 18. Sakata, A., Wada, S., Tanabe, and Onaka, T. 1984, *Ap. J. Lett.*, **287**, L51.
 19. Smith, R. G., Sellgren, K., and Tokunaga, A. T. 1986, in *Summer School on Interstellar Processes: Abstr. of Contributed Papers*, NASA Tech. Mem. 88342, p. 127.
 20. Tokunaga, A. T., Golisch, W. F., Griep, D. M., Kaminski, C. D., and Hanner, M. S. 1986, *Astron. J.*, **92**, 1183.
 21. Tokunaga, A. T., this report.
 22. Wickramasinghe, D. T. and Allen D. A. 1986, , **323**, 44; Allen D. A. and Wickramasinghe, D. T. 1987, *Nature*, **329**, 615.

TABLE I
COMPARISON OF THE 3.4 μ M AND SILICATE FEATURES

Comet	Type	3.4 μ Feature Present?	r(AU)	Ref.	Silicate Present?	r(AU)	Ref.
West	New	No	0.5	17	Yes	0.2-1.0	16
IRAS-Araki-Alcock	Old	No	1.0	10	Yes(weak)	1.0	10
Halley	Old	Yes	0.9-2.0	1,4,6,12,13	Yes	0.6-1.3	7,9,20
Wilson	New	Yes	1.3	2	(weak)	1.3	11,15
Encke	Old	No	0.5	21	No	0.5	8

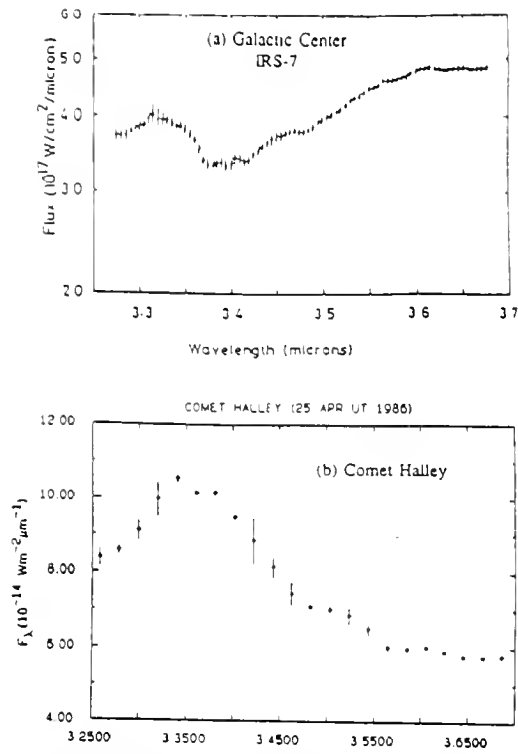


Figure 1. Comparison of the Galactic Center IRS-7 source (ref. 3) to Comet Halley (ref. 12). Note the slight offset in the maximum absorption in IRS-7 and the emission peak in Comet Halley.

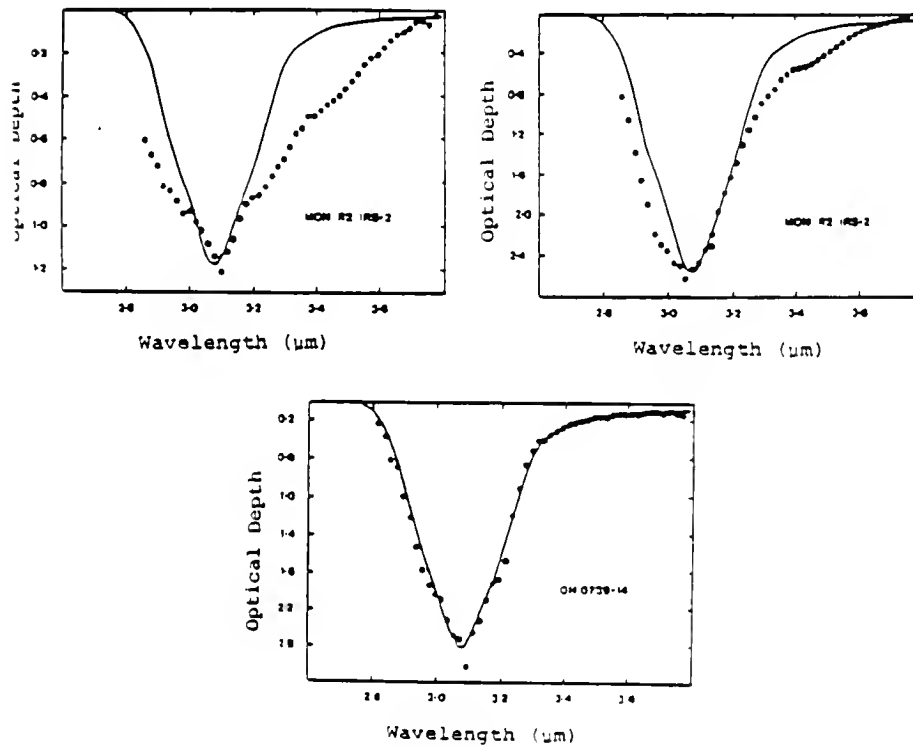


Figure 2. 3 μ m spectra of the interstellar ice band. Note the weak 3.4 μ m absorption band in Mon R2 IRS-2. The center of the absorption is approximately at 3.45 μ m. Spectra from ref. 18.

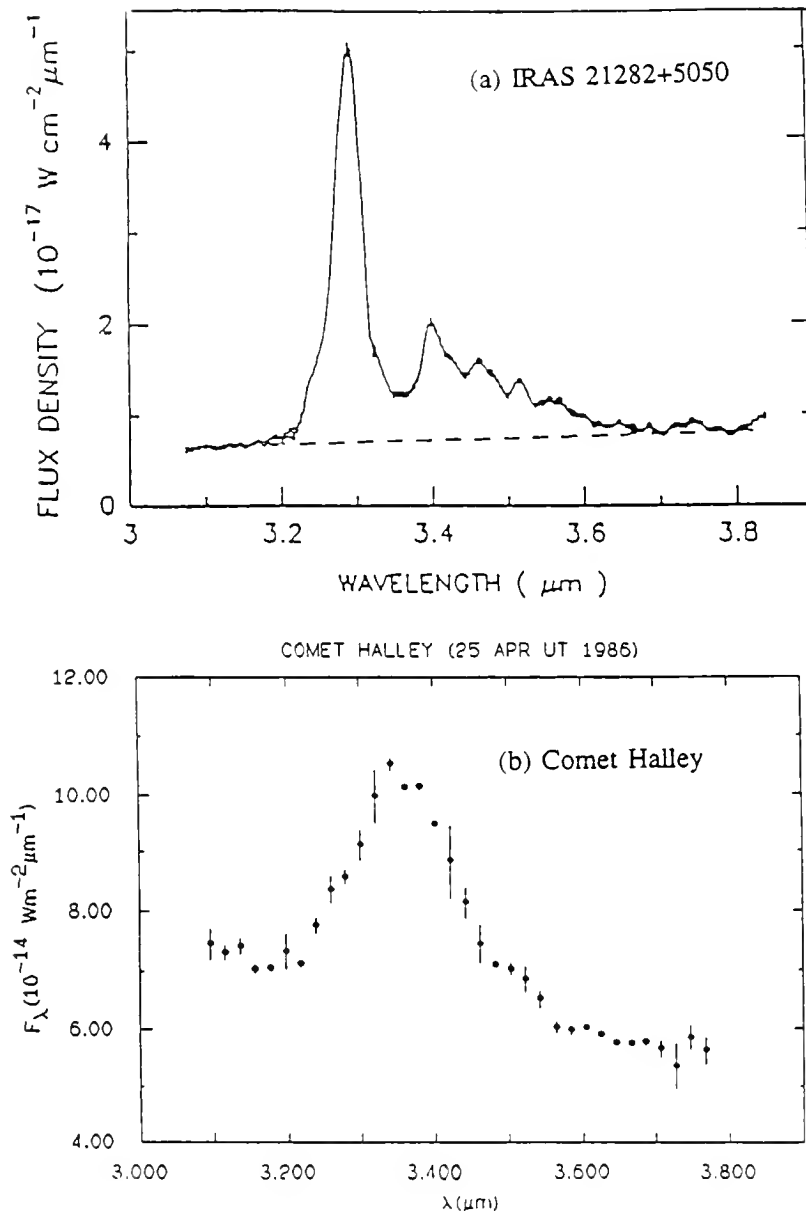


Figure 3. Comparison of the interstellar 3 μm emission features (ref. 5) with that of Comet Halley (ref. 12). Note that the peak of the Comet Halley feature is approximately at a *minimum* of series of emission features seen in IRAS 21282+5050.

A TWO COMPONENT MODEL FOR THERMAL EMISSION FROM ORGANIC GRAINS IN COMET HALLEY

Christopher Chyba and Carl Sagan
Laboratory for Planetary Studies
Cornell University
Ithaca, NY 14853-6801

Observations of Comet Halley in the near infrared reveal a triple-peaked emission feature near $3.4\mu\text{m}$, characteristic of C-H stretching in hydrocarbons (e.g., Wickramasinghe and Allen, 1986). A variety of plausible cometary materials exhibit these features, including the organic residue of irradiated candidate cometary ices (such as the residue of irradiated methane ice clathrate [Khare *et al.*, 1988]), and polycyclic aromatic hydrocarbons (Allamandola *et al.*, 1987). Indeed, *any* molecule containing $-\text{CH}_3$ and $-\text{CH}_2-$ alkanes will emit at $3.4\mu\text{m}$ under suitable conditions. Therefore tentative identifications must rest on additional evidence, including a plausible account of the origins of the organic material, a plausible model for the infrared emission of this material, and a demonstration that this conjunction of material and model not only matches the $3\text{--}4\mu\text{m}$ spectrum, but also does not yield additional emission features where none is observed. In the case of the residue of irradiated low-occupancy methane ice clathrate, we argue that the laboratory synthesis of the organic residue well simulates the radiation processing experienced by Comet Halley (We summarize the variety of post-accretion radiation environments experienced by the comet in Table 1; ultraviolet and charged particle irradiation of dust grains prior to cometary aggregation will also be of importance [Greenberg and Grim, 1986]). We use a simple two-component model for emission from dust in the Halley coma to predict an observed flux (heliocentric distance 1.16 AU, geocentric distance 0.549 AU) given by $F_\lambda = C_\lambda + \Omega\tau'_\lambda B_\lambda(T = 600\text{K}) + \Omega\tau B_\lambda(T = 350\text{K})$, where C_λ is the scattered solar flux, Ω is the telescope solid angle, τ is the optical depth of the blackbody continuum emitters ($T=350\text{ K}$), $\tau'_\lambda = \alpha(a/\lambda)\ln(t_\lambda^{-1})$ is the optical depth of the submicron (radius $a \sim 0.1\mu\text{m}$) organic emitters ($T=600\text{ K}$), and t_λ is given by the laboratory transmission spectrum of the residue of irradiated CH_4 ice clathrate (Fig. 1, after Khare *et al.*, 1988). We show that this model fits the $3.4\mu\text{m}$ feature (Fig. 2), provides optical depths in excellent agreement with those determined by spacecraft, and accounts for the absence of features at longer wavelengths (Figs. 3 & 4), despite the presence of such features in transmission spectra of typical laboratory-produced organics (e.g., as seen in Fig. 1).

REFERENCES

- Allamandola, L.J., Tielens, A.G.G.M, and Barker, J.R. (1987). *Polycyclic Aromatic Hydrocarbons and Astrophysics* (eds. A. Léger *et al.*), 255-271 (D. Reidel).
Greenberg, J.M., and Grim, R. (1986). *20th Esab Symposium on the Exploration of Halley's Comet 2*, 255-263.
Khare, B.N., Thompson, W.R., Murray, B.G.J.P.T., Chyba, C.F., Sagan, C., and Arakawa, E.T. (1988). *Icarus*, *in press*.
Wickramasinghe, D.T., and Allen, D.A. (1986). *Nature* **323**, 44-46.

TABLE 1 COMET HALLEY IRRADIATION HISTORY

ENVIRONMENT	DOSE (kev/cm ²)	DEPTH	REMARKS
INNER SOLAR SYSTEM Solar Wind, 1 Orbit	10 ²⁰	~0.1 μ m	Comet Shielded Within ~5 AU
Solar Wind, 10 ² -10 ³ Orbits	10 ²² -10 ²³	~0.1 μ m	
OORT CLOUD Solar Wind, 4.6 Gyr	10 ²¹	~0.1 μ m	
Cosmic Rays, 4.6 Gyr	10 ²¹ 10 ²⁰	~1 m ~10 m	
Radionuclides, 4.6 Gyr	10 ²⁰	Entire Comet	Assumes No Differentiation 26Al ~ 80%
INNER OORT CLOUD Solar Wind, ~1 Gyr	10 ²⁶	~1 μ m	Erosion?

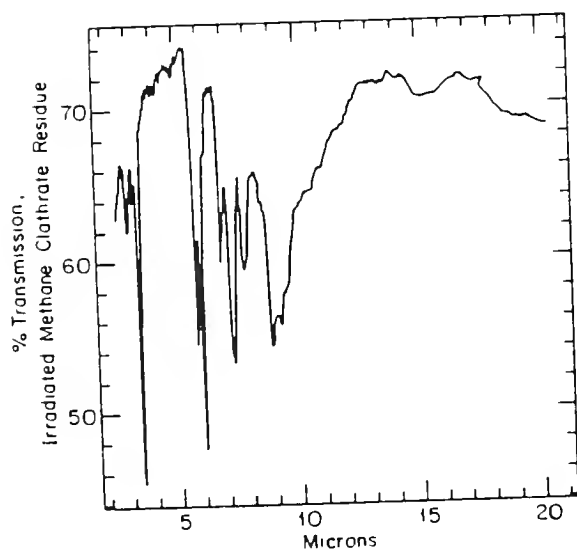


Fig. 1. Transmission spectrum of irradiated CH₄ clathrate residue (after Khare et al., *Icarus*, to be published [1987]).

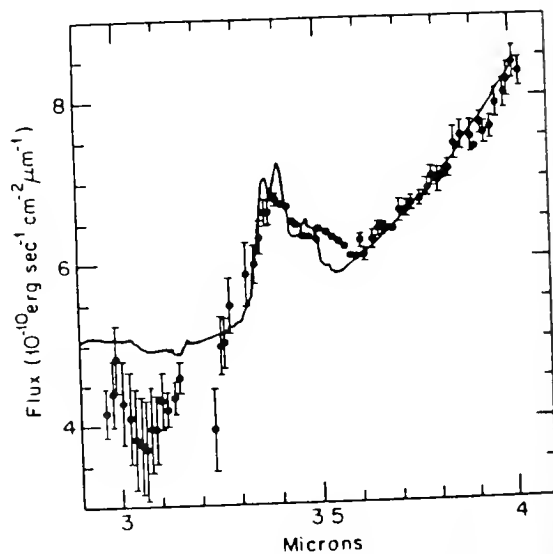


Fig. 2. Best fit (solid curve) to 3-4 μ m spectrum of Comet Halley observed by Wickramasinghe & Allen (*Nature* 323, 44-46 [1986]). The absorption feature at ~3.1 μ m, probably O-H stretch, is not modeled.

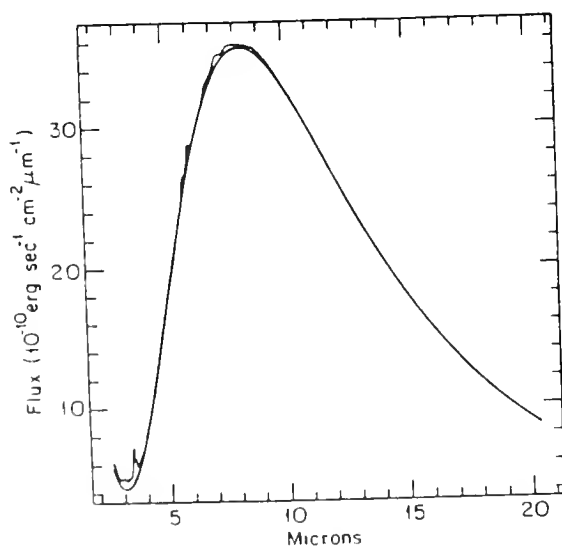


Fig. 3. The Comet Halley 2-20 μ m spectrum predicted by our model, compared to that of a 350 K blackbody.

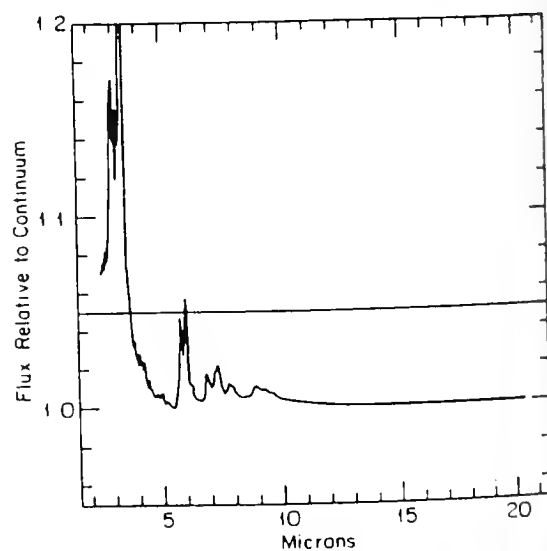


Fig. 4. The predicted 2-20 μ m spectrum, after dividing out the continuum. Only the 3.4 μ m feature rises above the 5%-above-continuum level (indicated by the solid line).

ON THE CARBON ABUNDANCE IN COMET HALLEY DERIVED FROM THE 3μ FEATURE: COMPARISON WITH INTERSTELLAR DUST

T. Encrenaz¹, J. L. Puget^{1,2}, L. d'Hendecourt³

¹Observatoire de Paris-Meudon, France

²Radioastronomie, Ecole Normale Supérieure, Paris, France

³Groupe de Physique des Solides, ENS, Paris France

ABSTRACT

In spite of some similarities with the infrared features observed in the interstellar medium, the 3μ signature observed in comet Halley's spectrum shows two distinct differences, (1) the 3.28μ and 3.37μ cometary features are both in emission, while the 3.37μ interstellar feature is most often observed in absorption; (2) there is no associated emission feature beyond 6μ in the cometary spectrum. These two facts can be simply explained if we assume that the excitation mechanism is resonance fluorescence by the solar IR radiation field. With this assumption, it is found that hydrocarbons are present in roughly equal quantities in both the saturated forms, with a total carbon abundance of about 30% of H_2O .

This carbon abundance can be compared with the abundances derived for the interstellar dust when all condensed (or condensable) components are considered. In comet Halley, from the gaseous phase, we find $H:C:N:O = 1.93:0.39<0.08:1.00$, while we have, for interstellar dust, $C:N:O = 0.50:0.14:1.00$, with the condensable hydrogen ranging from 1.4 to 2.2 according to the various models. Assuming that, in comet Halley, 20% of oxygen is trapped in grains (SiO , FeO , $MgO...$), this comparison suggests that about 40% of C and at least 50% of N is trapped in cometary grains.

Reference: Encrenaz *et al.*, Proceedings of the symposium "On the Diversity and Similarity of Comets," Brussels, April 6-9, 1987, ESA-SP, in press.

POSSIBLE IDENTIFICATIONS OF THE $3.4\mu\text{m}$ FEATURE

A. C. Danks
Applied Research Corporation
8201 Corporate Drive, Suite 920
Landover, MD 20785

and

D. L. Lambert
Department of Astronomy
University of Texas
Austin, TX 78712

INTRODUCTION

A feature at $3.4\mu\text{m}$ was first detected in Comet P/Halley by the IKS spectrometer on board the Vega 1 probe, Combes *et al.* (1986a,b); and subsequently from the ground by Danks *et al.*, Knacke *et al.* (1986), Wickramasinghe and Allen (1986) and Baas *et al.* (1986). The feature has since been reported in Comet Wilson (1986l), Tokunaga *et al.* (1987). The presence of the feature is of considerable interest for a number of reasons. First, it may represent the detection of a new parent molecule, and when combined with data from Giotto and Vega yield new information on cometary chemistry and the early solar system composition. Secondly, it may represent a link to the interstellar medium, the feature corresponds in wavelength and shape with an interstellar feature seen in absorption in a luminous star, towards the Galactic center known as GC-IRS7, Allen and Wickramasinghe (1981). The feature in turn is thought to be related with a growing family of unidentified infrared emission features seen in stellar objects, planetary nebulae, reflection nebulae, HII regions and extra galactic sources, Aitken (1981). These features occur at wavelengths 3.3, 3.4, 3.5, 6.2, 7.7, 8.6, and $11.25\mu\text{m}$.

IDENTIFICATION

Consider first the highest spectral resolution observation of the 3.4μ feature in Halley taken by Baas *et al.* (1986) shown in Figure 1. The spectrum has a resolution of $0.008\mu\text{m}$ and some structure can be seen in the profile. At first sight the structure corresponds remarkably well with the wavelengths of the rotation lines of the CH(1-0) ground electronic state. The R branch extends blueward from the band origin at $3.6\mu\text{m}$ to peak at approximately R12 at $3.4\mu\text{m}$, the short wavelength limit corresponding to the R-branch band head. The larger portion of the spectrum is shown in Figure 2 from Danks *et al.* and many P-branch lines can be seen to correspond with structure seen in the observed profile. However, peaking at R12 would imply a thermal-rotational temperature of approximately 300 K. At this temperature, the individual rotation line widths would be narrow and should be resolved by Baas *et al.* Although the temperature of the molecule could perhaps be explained by excitation processes during release of dust from the nucleus, how would the temperature be maintained? The molecule CH is seen in the visible and known to be excited by resonance-fluorescence; however, the dipole moment of CH is sufficiently large that it would be difficult to maintain a high J population. It is difficult to argue, then, that the feature arises from CH directly, although there is likely to be a small contribution.

The feature occurs at $3.4\mu\text{m}$ as a natural consequence of the vibrational energy or bond strength of the CH molecule. However, the bond strength can be modified by the near presence of other atoms, for instance when CH bonds occur naturally within larger molecular structures, i.e., polymers or cyclic molecules. These aspects are demonstrated

in Allamandola (1984). The region between 2-15 μm corresponds with energies typical of bond strengths which dictate the molecular vibrational frequencies, and this spectral region is known by chemists as the "fingerprint" region where particular groups of atoms give rise to "characteristic" absorption bands, e.g., C-H stretch olefinic 3.3 μm , C-H aromatic 3.4 μm , C-H-saturated 3.5 μm , C-C stretch 6.1 and 7.2 μm , C-C stretch 6.2 and 6.7 μm , =C-H out of plane bend 10 and 10.4 μm , etc. The width, shape and central wavelength of the C-H signature can be modified in a specific molecule depending on the structure and how many C-H bonds it has, but it essentially retains its personality. There are also abundance constraints which limit the choice of molecule; some favorite candidates based on models are CH_4 , NH_3 , CHN , H_2O , CO , CO_2 , etc. (Crovisier and Encrenaz 1983). The 3.4 μm emission is characteristic of the CH-stretching frequency (CH_3 , CH_2) of saturated hydrocarbons, while the 3.3 μm emission is characteristic of the CH stretching of unsaturated hydrocarbons – in particular alkenes ($-\text{CH}=\text{CH}-$, $\text{CH}=\text{CH}_2$) and aromatic compounds (Bellamy, 1975). But it is probably not possible to discriminate if the IR emission originates from a gaseous or solid phase, or uniquely identify the saturated H-C from the 3.4 μm feature.

An analogous situation exists for the UIBs which have been suggested to originate from polycyclic aromatic hydrocarbons (PAHs). As the name suggests these are cyclic molecules which can probably only form through condensation of grains. The argument is that once formed they are hard to destroy. Extinction in the interstellar medium tells us small grains exist, and depletion of C in the gas phase suggest the grains are made of graphite. Graphite, in turn, can give rise to the 2200Å feature. The graphite planes are held together by weak Van der Waals forces which are easily broken, providing PAHs in the gaseous- or single-molecule form. But many details are left unexplained. Donn *et al.* (1987) have addressed some objections, i.e., significant differences in wavelengths and intensities of the features, neglecting to take into account intramolecular vibrational relaxation in large molecules which can significantly change population distributions. Donn *et al.* agree, however, that hydrogen-rich carbonaceous material is probably responsible for the features based on laboratory data. The chemist would follow the same approach and would not make in identification of a sample based on an IR spectrum from the "fingerprint" region alone, but would also make a NMR measurement.

The 3.4 μm feature in Halley must be approached in the same way; identification will probably come only through a combination of spectroscopy with spacecraft data. For instance, data from PICCA (Positive Ion Cluster Composition Analyzer) on board Giotto has recently been analyzed by Huebner *et al.* (1987) who report mass peaks at 105, 91, 75, 61, and 45 at a regular spacing of approximately 15 amu. These data are consistent with decay products of a polymer, and by making up polymers from the most abundant elements H, O, C, and N, only a few possibilities exist – $(\text{NH})_n$ and $(\text{H}_2\text{CO})_n$. $(\text{H}_2\text{CO})_n$ is known as paraformaldehyde or as polyoxymethylene (POM), which was first predicted by Wickramasinghe (1974). It has an affinity for graphite and silicon and grows in whiskers on dust particles. It is stable to heating by solar radiation. In fact, in the spectrum of Danks *et al.* features are also seen at 3.3, 3.37, 3.51 and weakly at 3.58 μm . Features beyond 3.5 μm are easier to interpret in terms of gaseous emissions, as the number of candidates increases rapidly. Possible identifications of the 3.51 and 3.58 μm features are the fundamentals of H_2CO , ν_5 , and ν_1 , centered at 2843 cm^{-1} and 2783 cm^{-1} respectively. Gas phase chemistry of the interstellar medium predicts the abundances of diatomic molecules well, and also the formation of some linear molecules; certainly the molecules observed in the dark clouds at radio wavelengths are linear. In addition, Giotto and Vega both found large numbers of small grains rich in C, H, O, and N. All this re-enforces the hydrogenated, carbonaceous ideas, and we should probably concentrate on linear molecules in the gas phase. Some of this data lead Chyba and Sagan to propose small organic grains or grains with mantles of organic material formed from a methane clathrate bombarded by p^+ and γ rays to process the methane ice into an organic residue. The model fits the observations globally and could serve as a good basis for specifying what future space missions should look for.

CONCLUSION

In order to advance further, the identification of the $3.4\mu\text{m}$ feature and detection and identification of other parent molecules in general requires complementary probe data.

From the ground the $3.4\mu\text{m}$ feature should be re-observed in as many comets as possible. It has now been seen in Halley (old) and Wilson (new), but has not been detected in Enke (old), West (new), or IRAS (new). Technology is advancing fast, and it should be possible to obtain higher resolution observations and eventually mapping.

Observations from the KAO should be carried out in the $5\text{--}12\mu\text{m}$ region to search for the complementary bands of C-H, C=C, etc. The absence of features in this region to date is disquietening.

References

- Aitken, D. K., 1981, *Infrared Astronomy*, eds. Wynn-Williams, C. G.
 Chyba, C. and Sagan, C., 1987 (preprint).
 Allamandola, L. J., Sandford, S. A., Wopenka, B., 1987, *Science*, **237**, 56.
 Allamandola, L. J., 1984, *Galactic and Extragalactic Infrared Spectroscopy*, eds. Kessler, M. F. and Phillips, J. P., (D. Reidel Publishing Co., Dordrecht), p. 5.
 Allen, D. A. and Wickramasinghe, D. T., 1981, *Nature*, **294**, 239.
 Baas, F., Geballe, T. R., Walther, D. M., 1986, *Astrophys. J.*, **311**, L97.
 Bellamy, L. J., 1975, *The Infrared Spectra of Complex Molecules*, Vol. 1, Chapman and Hall, ed: London.
 Danks, A. C., Encrenaz, T., Bouchet, P., Le Bertre, T., and Chalabaev, A., 1987, *Astron. Astrophys.*, **184**, 329.
 Donn, B., Khanna, R., Salisbury, D., Allen J., and Moore, J., 1987, preprint.
 Combes *et al.*, 1986a, *Nature*, **231**, 266.
 Combes *et al.*, 1986b, ESA SP-250, in press.
 Crovisier, J. and Encrenaz, Th., 1983, *Astron. Astrophys.*, **126**, 170.
 Huebner, W. F., Boice, D. C., Sharp, C. M., Korth, A., Lin, R. P., Mitchell, D. L., and Reme, H., 1986, preprint.
 Knacke, R. F., Brooke, T. Y., and Joyce, R. R., 1986, *Astrophys. J.*, **310**, L49.
 Tokunaga, A. *et al.*, 1987, this conference.
 Wickramasinghe, D. and Allen D., 1986, *Nature*, **323**, 44.
 Wickramasinghe, N. C., 1974, *Nature*, **252**, 462.

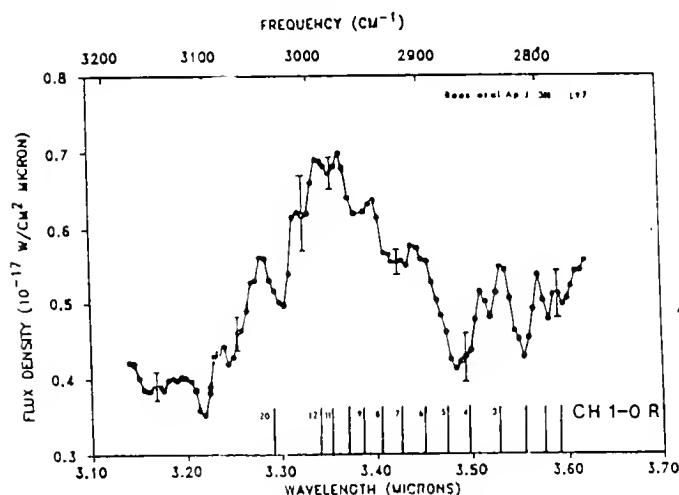


Fig (1) The $3.4\mu\text{m}$ feature in P/Halley taken from Beas et al (1986).

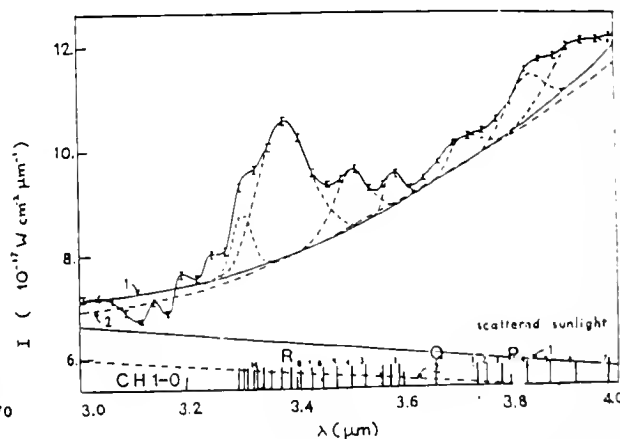


Fig (2) The spectrum of P/Halley from 3.0 to $4.0\mu\text{m}$ taken from Danks et al.

DISCUSSION AND RECOMMENDATIONS

Ground-based and space-probe measurements of P/Halley yielded a wealth of information about the chemical composition and size distribution of cometary grains.

The most important result to come from the PIA/PUMA data is the ground-truth demonstration that grains with chemical compositions similar to those seen in terrestrial, interplanetary interstellar grains exist in the nuclei of comets. It is evident, however, that many questions remain unanswered and new questions have been raised. We summarize the conclusions reached by the participants in this session, and outline their recommendations for future cometary investigations.

Spectroscopic Studies

The data returned during the Halley apparition provided a wealth of information about cometary dust grains. Realization of the potential of the data requires supplementary laboratory studies of grain materials. These should include experimental investigations of grain-processing mechanisms as well as laboratory spectroscopy of prospective grain constituents.

Spectroscopic studies of the emission features that appear in comets are extremely important to elucidate the origin of these features. Further observations of both new and evolved comets over a wide range in heliocentric distance are required. These should be supplemented by laboratory studies of materials thought to be similar to cometary constituents.

The detailed spectral shape of the $3.4\mu\text{m}$ feature in comets has yet to be well determined by observations at high-spectral resolution. Such observations, as well as comparative spectra of laboratory samples, will be necessary to distinguish between such mechanisms as emission by solid organic grains and resonance fluorescence by organic gases. Some of these models can be discriminated by documentation of temporal variations in the $3.4\mu\text{m}$ feature and by the presence or absence of features at other wavelengths as a function of heliocentric distance.

There are several broader questions that such observations of these emission features in a large sample of comets and stars can address. How do the comet features compare with those observed in circumstellar and interstellar dust? What are the connections between the hydrocarbon functional groups which produce the $3.36\mu\text{m}$ emission and those that produce the 3.29 and longer wavelength features in interstellar sources? Are the organic residues in comets formed after capture in the inner solar system, in the Oort cloud, or in the interstellar grains which were accreted into the comet nucleus?

Interplanetary Dust Particles

The interplanetary dust particles (IDPs) seem to be the closest analogue of comet dust accessible to laboratory study. At least one subset of IDPs, the anhydrous chondritic aggregates, are very likely to be comet dust, albeit "weathered" in the solar system for up to 10^4 years. It is important to study their physical structure, chemical and mineralogical make-up and to relate to these to physical and chemical processes in the comet. These data will form the basis for comparison with future *in situ* measurements of comet grains. An understanding of their alteration in the interplanetary medium and in the earth's atmosphere is also necessary.

It is also important to measure the optical properties of these IDPs, including their infrared emission features (if possible, as a function of temperature), for analogy with the

comet dust observed remotely. An attempt should then be made to model the optical properties, to test the adequacy of theoretical predictions for non-spherical particles.

Direct Sampling from Space Missions

It is apparent that the proposed space missions, such as the Comet Rendezvous Asteroid Flyby (CRAF), Comet Sample Return, and the Orbit Determination and Capture Experiment (ODACE) are of the highest priority for increasing our understanding of the composition and mineralogy of cometary grains and their relationship to interplanetary and interstellar grains. The results from PUMA/PIA and from analyzing IDPs show that much can be learned from the dust composition at the submicron level. From CRAF, dust samples can be analyzed by a variety of techniques including x-ray fluorescence, gas chromatography, secondary ion mass spectroscopy, and electron microscopy (see Chapter 5). These measurements can address the questions: Under what conditions did the mineral dust grains form? Have they been subjected to thermal and aqueous alteration? How do isotope ratios such as D/H and C_{12}/C_{13} compare with terrestrial vs. the ISM? What is the composition of the organic material in grains? By sampling the dust coma at different times, the heterogeneity of the nucleus can be investigated.

Earth-based remote sensing, however, will remain the bridge between the target comet, other new and evolved comets and the interstellar medium.

CHAPTER 4

LABORATORY INVESTIGATIONS

Ray Russell
Space Sciences Laboratory
The Aerospace Corporation

with contributions from B. Donn and L. Allamandola

1.0 INTRODUCTION

Laboratory studies related to cometary grains and the nuclei of comets can be broken down into three areas which relate to understanding the spectral properties, the formation mechanisms, and the evolution of grains and nuclei:

- 1) Spectral studies to be used in the interpretation of cometary spectra,
- 2) Sample preparation experiments which may shed light on the physical nature and history of cometary grains and nuclei by exploring the effects on grain emissivities resulting from the ways in which the samples are created, and
- 3) Grain processing experiments which should provide insight on the interaction of cometary grains with the environment in the immediate vicinity of the cometary nucleus as the comet travels from the Oort Cloud through perihelion, and perhaps even suggestions regarding the relationship between interstellar grains and cometary matter.

This summary will present a rather different view of laboratory experiments than is usually found in the literature, concentrating on measurement techniques and sample preparations especially relevant to cometary dust. In addition, it attempts to assimilate the information provided in B. Donn's talk at the workshop, some of his excellent, comprehensive references (Donn, 1985 and 1987), and the informal presentations by L. Allamandola, R. Thompson, T. Mukai, and the author. Another recent general overview of interstellar dust questions may be found in Tielens and Allamandola (1986). Extended abstracts of presentations made in this session are included in the Appendix.

Based on over two hours of animated discussion by the laboratory investigations working group on 10 August and numerous comments throughout the workshop, several areas of study were endorsed as important for furthering our understanding of cometary grains and nuclei. Some of these have been worked into the text in this chapter, and a summary of these recommendations is included in Chapter 5.

Laboratory studies of interplanetary dust particles were also recognized as important for our understanding of cometary dust. These particles were discussed in Session III and thus are not treated here (see paper by Walker, Chapter 3).

2.0 SPECTRAL STUDIES

Studies of infrared spectra of simulated cometary grains can lead to the identification of materials present in comets, shed light on the physical state and thermal history of the grain material using details of emission band structure, and aid the development of analytical treatments for predicting the emissivities of small particles near resonances in the optical constants of corresponding bulk samples. These studies can also be useful in planning future comet observations and instruments, for example, in the selection of spectral filters for CRAF and earth-orbiting instruments, by predicting where new spectral features may exist or elucidating what bandpasses would best improve our understanding of known features, and defining the spectral resolution necessary to resolve such band structures. This workshop focused on the mineral phase (primarily silicates) and hydrocarbons, but

ices and gas phase molecules (especially those such as CN which were shown to have been released by "parent" grains at a range of distances from the nucleus of Halley's Comet) are also important subjects of IR spectroscopic studies.

Spectral studies have been basically of three types; reflectance, transmittance, and emittance, and these are discussed in turn.

2.1 Reflectance

Reflectance measurements from polished surfaces can be used to derive optical constants of bulk samples. The optical constants can, in principle, be used to compute spectral emissivities of grains of the same precise composition as the bulk material but of arbitrary size, shape, and physical properties. However, as pointed out in Chapter 2, a comprehensive analytical treatment for the calculation of the scattering and emissivity as a function of wavelength for irregular, inhomogeneous particles is lacking. Thus, a complementary and perhaps more straightforward approach is to study the spectra of particulate samples which have some similarity to cometary grains, bearing in mind that particle size and shape, temperature, surface roughness, and even degree of aggregation of spherical particle samples ALL affect the resulting wavelength dependence of emissivity and scattering. Thus, this session focused on transmission and emission, and for a more complete discussion of optical constants we refer the reader to Chapter 2.

However, spectral reflectance studies (in some cases combined with transmission work) still seem to have a lot to offer in the study of thin films, such as those sputtered onto a surface (Day 1979 and 1980) or deposited onto a surface at low temperature. In both of these situations one attempts to measure spectral structure by reflectance not from a polished surface, but rather from an aggregate of material which, in practice, is likely to be a continuous, fairly smooth surface (although the surfaces so studied were not examined by SEM). Thin films are particularly useful for obtaining the spectra of volatiles or residues from processing of simple ices. In practice, this may be a reasonable way to create an analog for a cometary nuclear surface, but it has a limited application to the study of emitting and scattering particles seen in the visible and infrared.

Clearly, scattering from a single particle is an extreme case of reflectance. While one would ideally like to measure infrared scattering and emissivity of suspended, individual particles (preferably in a vacuum), relatively few studies of this type have been done at any wavelength (e.g., Ashkin 1970, Ashkin and Dziedzic 1971 and 1980, Hecht 1979a, b; Philip *et al.*, 1983; Marx and Mulholland 1983, and Arnold *et al.* 1982 and 1984) and can be prohibitively difficult experimentally. For example, it is very difficult to obtain single particles of volatiles, although they can be prepared as thin films or sputtered layers with comparative ease. The flux from a single particle at infrared or shorter wavelengths, especially at large scattering angles, is small and thus hard to measure. The forward scattering component can be lost in the incident (unscattered) flux.

One approach to investigating the scattering by single particles is to scale both particle dimensions and wavelength to the microwave region. Materials then have to be found with microwave optical constants matching those of interest for cometary grains at shorter wavelengths.

Two groups are pursuing this technique with application to astronomical grains. One group is now at the University of Florida (Schuerman 1980) the other is at the Ruhr University, Bochum FRG (Zerull *et al.* 1980). These facilities are valuable for studying effects of shape and roughness on the optical scattering. However, these experiments are not designed to derive emissivity functions so critical to compositional analysis based on infrared spectroscopy of cometary comae.

Weiss-Wrana (1983) suspended single particles electrostatically and measured the angular scattering of various silicate, carbonaceous, and meteoritic particles with a laser. Giese *et al.* (1986) have extended these measurements to three wavelengths. Some IDPs

have been studied by using advanced methods for thin sectioning in a support medium and clever optical enhancement techniques, but these experiments don't even attempt to simulate free particles in space.

Although some progress in this direction (which would even include zero g conditions) may be possible on the space station, we must push ahead in terrestrial labs now. Thus, measurements of ice films and residues, organic residues, and sputtered refractory films represent one of the active, productive areas of laboratory simulation going on today. Several groups (see below) are exploring the properties of ices and ice residues after a variety of methods of processing the films has been applied.

2.2 Transmittance

Perhaps the most abundant source of astrophysically relevant spectral information is the vast array of transmission measurements conducted on laboratory, lunar, terrestrial mineral, and meteorite samples, and even interplanetary dust particles. Because of the relative ease with which a sample can be put into a lab spectrometer and transmission (or more precisely, extinction = absorption + scattering) obtained, this has been a very productive survey technique. Good, comprehensive reference examples for minerals, etc., include, but by no means are limited to, Ferraro (1982), Hunt, Wisherd, and Bonham (1950), and Nyquist and Kagel (1971), and for IDPs, Sandford, Fraundorf, Patel, and Walker (1982), Sandford and Walker (1985), and Sandford (1985). A word of caution: One must be concerned about the fact that transmission data usually include the extinction due to scattering as well as the absorption which is of interest in the analysis of astronomical emission spectra. However, as was pointed out by Gehrz and Huffman, a further complication is that for some small lab instruments some of the radiation scattered out of the beam may still be detected if the sample and the light collector (or detector) are close enough together.

Even though one cannot be confident that all or none of the scattering effects are being measured, the technique is still very valuable for associating certain spectral features with specific groups, radicals, etc. in the samples. We simply point out that one can be misled in using pellet transmission spectra to identify the materials causing an emission spectrum, as the scattering wings on the sides of strong resonant features can make the features look very different from those seen in emission where only the absorption component of the transmission really applies.

To date, most of the transmission data have been obtained with "standard" lab instruments, such as those made commercially by Beckman and Perkin-Elmer. Recently, Fourier Transform interferometers for the IR (FTIRs) have become much more common, and machines by Nicolet and Mattson have permitted the computer controlled automatic acquisition of entire spectra from about $2.5\mu\text{m}$ to 25 or $40\mu\text{m}$. The use of the computer permits easy averaging of many spectra with the ability to print out the results in digital as well as graphic form. Data are typically saved on disk, and post-processing is frequently done. Few systems are currently used to acquire data beyond $40\mu\text{m}$, and there are not that many used regularly beyond $25\mu\text{m}$. The new devices have options allowing work all the way to the sub-millimeter, but these capabilities have not been exploited in lab studies such as we are discussing here.

The emissivity technique to be discussed below would allow the use of the same long wavelength spectrometers in the laboratory as are used for the astronomical observations. In principle, detectors from these spectrometers could also be used for transmission studies, as several of the new FTIR machines allow the user to provide the detector, and the output of the detector is fed into the computer that takes the interferogram and controls the mirror. The entire spectrometer could be used with more difficulty in conjunction with a Beckman or P-E, but the sensitivity would likely be lower and the aggravation factor much higher. However, all of these experiments which use the *same* instrument to take the astronomical and laboratory data have the advantage of producing spectra that are

much easier to compare. In view of the expected increase in number, quality, and spectral resolution of cometary spectra, the workshop participants recognized the need for long wavelength lab studies ($\lambda > 50\mu\text{m}$, out to $200\mu\text{m}$ or beyond).

2.3 Emittance

A very promising technique, based on the response of several attendees and the success of earlier published studies, is the use of actual emissivity measurements. This technique was pioneered by Lyon (1964) and Hunt (1976), who showed that the emissivity of a collection of small grains resting on a polished metal surface (usually copper to insure a single, uniform temperature) was the same as that of the grains floating in a vacuum, except for the addition of the grain emission reflected by the metal back toward the detector and the (easily subtracted) low, featureless background due to the polished metal. Thus, if one desired only to obtain the spectral shape and not the absolute grain emissivity, the technique was clean and fairly simple to use.

Rose (1977) utilized this technique in his thesis work analyzing meteorite samples, studying lunar samples, and exploring simulated astronomical grains produced by aqueous condensation (Day, 1976b). His apparatus used a chopping primary mirror to modulate the sample signal and remove the infrared background. He showed that the emission from amorphous silicates provided a good match to the spectral shape emitted by astronomical grains that had not been subjected to significant heating. Grains that had been heated or created with lattice structure showed spectral peaks characteristic of the mineral composition, similar to transmission spectra but with typically narrower peaks and, in some instances, at slightly different wavelengths.

Stephens and Russell (1979) and Nuth and Donn (1982, 1983b and references therein) used the techniques of laser vaporization and smoke condensation respectively, to produce similar amorphous silicate particles about 200 Å in size which stuck together in long, fractal-like chains and masses. The emissivity of such particles has been shown (Stephens and Russell 1979, and Cohen et al. 1980) to reproduce the shape and central wavelength of interstellar (Trapezium-like) silicate emission at both 10 and $20\mu\text{m}$ with a chi-squared per degree of freedom of 1-2, and to fit the broad, smooth $10\mu\text{m}$ feature in Comet Kohoutek

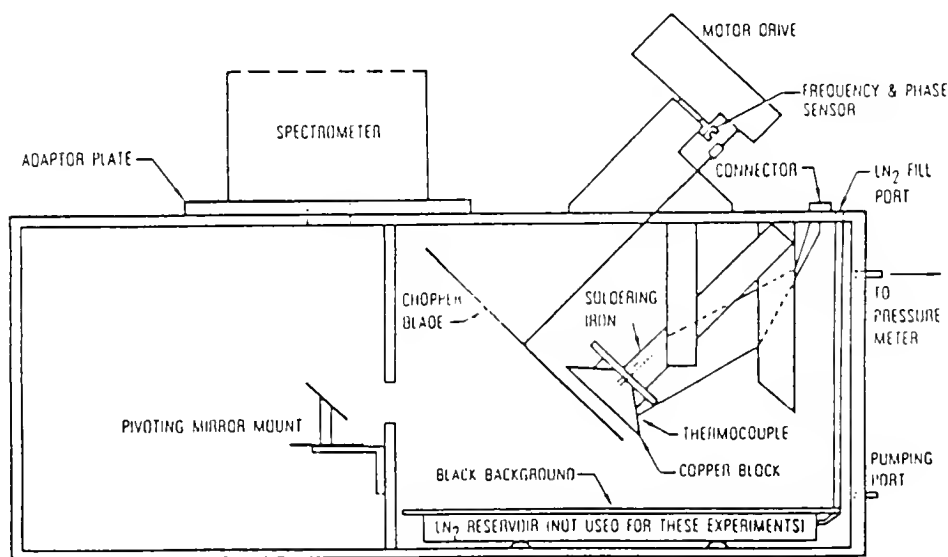


Figure 3.1 - Top schematic view of the emissivity chamber used to make the emission measurements. Sample typically covers $\leq 10\%$ of the surface of the copper block. The copper block is heated to either 42,77 or 127 C in making the measurements (from Hecht et al. 1986).

as well. Moreover, it was pointed out by Huffman that the ground enstatite and olivine spectra in Stephens and Russell looked remarkably similar to the Halley spectrum shown by Campins at the Workshop. The successful use of this emission study to match the spectra, and thus explain the nature, of two astronomical dust populations suggests that emissivity measurements are a very promising avenue for investigating cometary grain composition.

The schematic of the chamber used by Stephens and Russell is shown in Figure 3.1 as a simple, inexpensive way of obtaining such data. Figure 3.2 shows some of the data obtained with the chamber using the same CVF instruments as were used to obtain the comet data. Again, as was noted above but bears repeating again, having lab data taken with the *same* instruments as were used for the cometary studies greatly facilitates a clean, unambiguous comparison of the spectra.

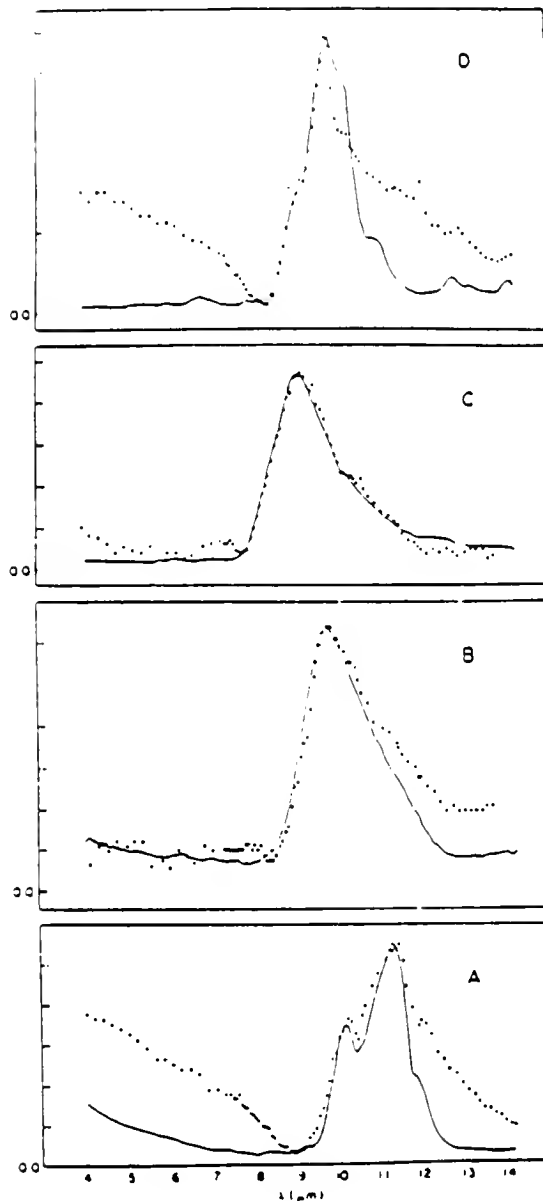


Figure 3.2 - Absorption (extinction spectra (*dots*) of A: ground olivine B: olivine condensate C: enstatite condensate; and D: ground enstatite, superposed on the corresponding emissivity data (*solid lines*) from Figure 3 (from Stephens and Russell 1979).

3.0 SAMPLE PREPARATION

In his recent review, "Experiments on the Formation, Properties and Processing of Cosmic Dust," Donn (1987) has provided a comprehensive reference list covering work on the physics and chemistry of working with dust samples which are designed to further our understanding of astronomical dust grains. Here, we will explore some of the practical considerations of producing collections of grains which we believe are related to those grains being observed by the "cometary spectroscopist," as well as some new lab efforts begun as a result of work on the identification of interstellar grains through infrared emission features.

3.1 Established Techniques for Producing and Studying Mineral Grains

Techniques for the preparation of cometary dust analogues include the grinding of mineral samples into micron or sub-micron size particles, deposition of dust samples on mirrored surfaces, condensation of smokes in an arc, condensation of laser-vaporized mineral material in a controlled atmosphere, pressing and grinding and re-pressing pellets (to get a uniform pellet sample), such as KBr, with a grain material present, collection of films both at warm temperatures and near 10 K, and collection of organic matter inside glass vessels with controlled atmospheres, just to name several. Each has inherent advantages and drawbacks, and thus the use of several approaches for the production of the same or similar samples probably gets us closest to the truth; deficiencies in each approach should become more apparent when the results, specifically the wavelength dependencies of the emissivity of the dust, from different experiments are compared.

An example familiar to the author of the added insight resulting from using two different experimental approaches relates to dust sample preparation via laser vaporization and condensation in a controlled atmosphere of a mineral sample of known composition (Stephens and Kothari 1978, Hecht *et al.* 1986) versus grinding up particles and pressing them in a KBr pellet versus using an arc to create a smoke. In the laser vaporization one can use a vast array of materials in different forms. The starting substance can be well characterized, and the atmosphere varied to simulate inert, O-rich, C-rich, or H-rich environments. However, as pointed out by Donn, the condensation is occurring at much higher densities than those found in astronomical situations, and we need to worry about what effect that will have on the resulting grain sample. In an arc, one is somewhat restricted in the materials that can be used and in the gas present during nucleation. Furthermore, one needs to worry about collection techniques that don't affect the sample.

Ground particles may be altered by the pressure used for the grinding and by contamination by the "mortar and pestle." Some of these concerns have been removed by the use of fluid air mills, where the "grinding" is accomplished by high speed impacts of grains with other grains in an inert gas flow inside a contained space, such as in a Trost Fluid Air Mill. The nature of the flow tends to avoid abrading the walls, as the fluid moves fastest at some distance away from the walls. Contamination is at a minimum, as the grinding is done by the material itself. The temperature is usually controlled by the temperature of the gas, and thus heating is minimized. However, it is difficult to collect the samples without the grains contacting room air (with the potential for chemical changes such as oxidation) and forming aggregates, although IDPs (and thus cometary grains by analogy) seem to be found in aggregates also; thus, this may actually be a positive aspect of the technique. One alternative sample production technique which attempts to minimize aggregation and thus determine the properties of separated grains is matrix isolation, which is discussed in Section 3.3.

Once the dust has been created by the technique of choice, the spectral dependence of emissivity (absorptivity) needs to be obtained by transmission or emission techniques. Although alluded to above, it will flesh out the example here to note specifically that a comparison of transmission and emission experiments has shown that using only the transmission through pressed KBr pellets containing ground samples will result in wavelength

shifts of the features (due to the refractive index of the pellet), as well as the inclusion of a strong scattering component near the edges of resonances which is inseparable from the absorptivity (emissivity). Allowing the dust to settle onto an already polished KBr window can alleviate the shift effect. However, one can only remove the scattering effect by measuring the emissivity directly, as discussed above.

In short, each method produces scientifically valuable samples worthy of study, but one must constantly be asking what effects may be attributable to the preparation and measurement techniques as opposed to the sample itself. In this example, the grains produced by the laser vaporization very strongly resemble IDPs in size, form, and amorphous nature, suggesting that, although they form faster than grains would in an astronomical environment, perhaps they do not form in a very different way, and we may use these results to further our understanding of the composition and structure of cosmic grains.

3.2 Hot Flow Grain Production

Another promising approach to the formation of cosmic grain analogues which is still under development involves the flow of gases through a series of furnaces resulting in nucleation and condensation of grains which can then be measured spectroscopically in situ. This technique is being pursued by, among others, Donn's group at Goddard and Arnold's group at the University of California at San Diego. In several respects these experiments will approximate the formation of grains in a proto-solar nebula or circumstellar shell. It will even be possible to add UV irradiation of the grains at a later time.

3.3 Organics and Low Temperature Volatiles

All of these techniques have been related to the grains known to be heated to, typically, over 300 K, and thus ignore the issue of the composition of the cometary nucleus where we believe ices play a predominant role. Based on cosmic abundance arguments, airborne measurements of water vapor in the coma, and now satellite fly-by experiments measuring the gas composition in situ, we now have strong support for the long-held belief that ices make up the major portion of the nucleus, with a significant dose of organic materials to help lower the albedo to less than 10%, perhaps less than 5%. This suggests that work on organics and ices will be critical to the success of future comet missions and our further understanding of comets, and that we should address sample preparations of this type here.

Chyba and Sagan (this meeting and 1987) and Khare, Sagan, Thompson, *et al.* (Sagan and Khare 1979, and Khare *et al.* 1987) have been experimenting with organic samples created under solar system-like conditions. These experiments have resulted in ice residues after irradiation and tholins created in a spark or UV-enriched environment which are promising analogues for cometary nuclear material. In particular, their fit to the 3.4/3.5 μm features in the spectrum of Comet Halley with their lab data on a methane ice-clathrate residue are quite good, and we look forward to the results of follow-on studies. Based on cosmic abundances, one would expect to find methane ice in comets, but it has not been seen so far. If the reaction products in methane clathrates are truly responsible for the observed 3.4/3.5 μm features, it would neatly explain the absence of the expected pure methane ice.

Unidentified IR emission features (UIR bands) are seen in many different astronomical objects at 3.3, 6.2, 7.7, 8.6, and 11.3 μm . It has recently been proposed that they may be carried by free, molecule-sized, polycyclic aromatic hydrocarbons (PAHs). As a class, PAHs are complex, planar, molecules made up of fused benzene rings which contain 20 to 50 carbon atoms and are extremely stable. Furthermore, model calculations suggest that these species, if present, would be as common as the most abundant, but far simpler polyatomic molecule, NH_3 . Alternative explanations include hydrogenated carbon-rich molecules or very small grains (molecular clusters) which are heated to high temperatures by absorption of a UV photon. The excess 12 μm flux correlated with galactic infrared

cirrus discovered with IRAS suggests the presence of a significant population of very small grains which are heated to high temperatures. Whatever the ultimate identification, in view of the ubiquity of the UIR bands in both galactic and extra-galactic sources, and the proposed link between interstellar and cometary dust particles, we expect this to be an important avenue of research in coming years.

In particular, there is some evidence for a weak $3.29\mu\text{m}$ feature in the spectrum of Halley, along with the stronger $3.36\mu\text{m}$ feature (the opposite of the situation in the spectra of most extra-solar system objects). This emphasizes our need to understand the emission mechanism in order to interpret correctly the spectra as we try to identify the composition and physical nature of the grains. Several proposed explanations for the $3.36\mu\text{m}$ feature are discussed in Chapter 3 of this report. Further laboratory tests of the viability of a fluorescence mechanism need to be conducted.

This new hypothesis of a previously unrecognized, but potentially very abundant component of the interstellar medium has important ramifications in many areas of astrophysics, and comets may eventually be our "laboratory" in which to test our models. For example, since the PAHs complexity and abundance would indicate a unique chemical history, not associated with the generally accepted ion-molecule interstellar chemistry models, they may well be the molecular progenitors of the larger carbonaceous dust grains (soot) which provide continuum emission and absorption in the infrared spectra of numerous astronomical sources. If this is the case, interstellar carbon particles may have PAHs in them, and if comets are related to interstellar grains, we would expect cometary "ices" to contain PAHs or PAH clusters.

Testing of the PAH/hydrogenated carbon/molecular cluster hypotheses and their impact on the larger astrophysical picture is severely hampered, however, by a general lack of knowledge of the physical and chemical properties of such grains in the forms they are likely to be in in space: ions, dehydrogenated radicals and free neutral species. Their spectroscopic properties are extremely important to know since virtually all observational data pertaining to this problem are spectroscopic in nature. At Goddard, the absorption, emission, and fluorescence spectra of PAHs are being measured, as well as those of amorphous hydrocarbons, by several techniques.

The NASA-Ames group is also undertaking a program to fill some of this gap by using another common preparation technique not yet discussed here, that of matrix isolation (see, e.g., Moskovits and Ozin 1976, Gole and Stwalley 1982, and Meyer 1971). In this approach, the species of interest is isolated by suspension in a frozen, solid, inert matrix at about 10 K. This has the advantage of maintaining the grains as separate entities (helping to prevent clumping and coagulation), but raises the question of how the interaction between the grains and the matrix may affect the observed spectrum.

Once the matrix, in this case containing PAHs, has been prepared, UV, visible, and IR absorption spectra are measured. Subsequently, exposure to a UV radiation field mimicking the solar or interstellar field, as appropriate, can produce ionized or partially dehydrogenated PAHs. The spectra of these species can then be measured. In addition to the spectroscopic studies of individual PAHs, the Ames group will also be focusing on the properties of small carbon clusters (20-30 Å in diameter) built up from PAHs. The laboratory data will then be used in theoretical modeling of UV-pumped IR fluorescence of PAHs and small amorphous carbon (soot) particles, and the possible application to understanding interstellar grains.

The pertinence to cometary grains will depend on further spectroscopic observation of comets at the wavelengths of the UIR bands; there is a possibility that the $11.3\mu\text{m}$ feature was seen in Halley (Campins, this meeting). In addition, as the molecules will emit differently when in a solid than when in a "gas" phase, further analysis of interplanetary dust particles and the results of a comet rendezvous will be needed before we can fully relate cometary and interstellar grains.

4.0 GRAIN PROCESSING

The section above treated the various ways one can create dust or grain samples in the lab which we believe simulate cosmic dust. However, as has already been mentioned above in passing, the astronomical grain is not created in the form in which it will live out its life; numerous forces act on a grain to alter it, including annealing, the passage of shock fronts which can actually cause vaporization and recondensation, the action of strong UV fields resulting in photolysis products and chemical reactions requiring an excitation energy suddenly becoming possible, sputtering by cosmic rays and ions and impacts among grains in denser environments, such as molecular clouds, and the addition of mantles through gas-grain collisions or hydration through grain contact with hydrogen and oxygen (or even water molecules) in the dark, cold, interior of these same dense clouds. As a result, laboratory simulations are not complete without addressing the effects of grain processing. Some grains, such as large silicate grains, may be strong enough to resist major change, and certainly several attempts to model warm interstellar/circumstellar dust with the Trapezium profile have met with success. However, the cometary environment shares with the dense, cold molecular clouds the strong probability that ices play a major role in determining the chemistry and physics of the solid phase, and in some instances the gas as well, and thus it is important to address processing of icy grains in particular.

We know from the measures of albedos that the surfaces of asteroids, the comae of several comets, and now the nucleus of Halley have remarkably low albedos, far too low to be ice as we are accustomed to seeing it. This suggests that contamination of the ice by dark material or processing of the ice by the environment is responsible for the dark appearance of the ice and that lab experiments to reproduce these low albedos are essential to our understanding of comets. Several groups have pursued and are continuing to conduct such experiments; these include the Leiden effort, Sagan and Khare's work, and, as noted below, the Ames effort.

4.1 Hydration

Some of the effects of hydration have been studied for silicates by, for example, Knacke and Kratschmer (1980) and Hecht *et al.* (1986), and for a variety of minerals which might have astronomical importance by Russell (1978). In each instance, spectral structure related to the amount of water of hydration could be reproducibly added to or removed from the spectrum by exposure to saturated water vapor or heat in a vacuum, respectively. Thus, the spectral shape, especially in the 5 to 8 μm region, is a fine diagnostic of the amount of hydration. Currently, additional studies on the effects of hydration for amorphous grains are underway at Goddard (Nuth *et al.* 1985).

4.2 Thermal Processing

The studies of amorphous vs. crystalline silicates (Donn *et al.* 1970, Day 1976a, Nuth and Donn 1983a and 1984, and Stephens and Russell 1979) have shown that the temperature history of the grain can be quite well assessed by the degree of structure present in the 10 μm spectra of (optically thin) silicate particles. Stephens was able to take amorphous olivine-composition glassy grains whose spectra matched the 10 and 20 μm interstellar features well, heat them up to temperatures in the 500 - 700 K range and recover the same spectral shape as seen for the original (crystalline) olivine sample. Thus, if a comet, like Halley, is observed to have a double-peaked structure in its 10 μm spectrum (Chapter 1), it is strong evidence for annealing of the cometary grains.

This is consistent with our picture of Halley material as having been heavily processed by multiple returns through the solar system, with repeated heating and cooling of the sticky, tough crust. Either heating portions of the crust to fairly high temperatures or irradiation processing (a combination of cosmic ray and UV-induced changes) in the surface could have altered the grain structure. The smooth spectra of the two first-time comets, Kohoutek and Wilson (Merrill 1974, Lynch *et al.* 1988 and abstract, this report), are also

consistent with this picture, as they would be expected to have unprocessed, primordial grains which would be amorphous in structure. On the other hand, we have no way of ruling out a different grain structure prior to the formation of Halley's Comet, or even precluding grain processing during the comet's formation.

Of course, we have a very limited data base of $10\mu\text{m}$ (much less $20\mu\text{m}$) cometary spectroscopy, and not a lot more lab data on dust samples specifically created to be cometary dust analogues (Hecht *et al.* 1986, is one exception). Workshop participants felt vigorous lab programs could provide several types of data (e.g. spectral data to guide filter selection and plan spectroscopy experiments, and physical data on nuclear surface materials to plan for penetrator experiments) in support of the NASA comet missions to maximize their scientific return (see below).

5.0 LABORATORY GROUPS

As so little information is available concerning the properties of ices and grains which are relevant to the low temperature, vacuum, UV-irradiated environment of comets (much less the poorly understood formation environment of cometary grains), a substantial, continuing laboratory program is clearly necessary to further our understanding of comets as they are today, how they formed, and their relation to the particles in the interstellar medium. This is a particularly urgent need for NASA to support the two comet missions being planned (CRAF and comet sample return). For example, combined analyses of the water and dust production rates, in concert with models of the icy and refractory grain components and the physical structure of the comet nucleus would enhance our understanding of the design requirements for probe and sampling instrumentation. Chapter 5 enumerates the specific areas of study endorsed by the workshop participants which were felt to be necessary to meet these requirements and to carry our understanding of comets forward.

Sometimes an example of a successful laboratory effort can be a valuable planning aid for future work. Furthermore, we know of no existing guide to the many scattered current laboratory efforts, and thought it might be helpful at least to provide a rough guide to the existing group efforts which were discussed at the workshop. In this spirit, brief summaries thereof are listed below in addition to our example. This will not, then, be a complete list, presenting as it does distillations of workshop discussions; my apologies to those who may have been left out — it is no assessment of the quality of such a program.

A good example of an ongoing effort is found in the well thought out and well funded Laboratory Astrophysics program begun in Leiden in 1976, sponsored by the Physics and Astronomy Departments at Leiden University and charged with carrying out experiments of direct relevance to astrophysics. It is indicative of the level of support and long-term commitment workshop participants felt are necessary for significant progress in the field. In addition to a chaired professorship for overall management of the Laboratory (J. M. Greenberg) and two assistant professor, tenure-track positions (to develop and direct the lab and theoretical programs, respectively), the start-up group also included four graduate student/post-doctoral positions as well as a very substantial laboratory start-up budget.

Combining astrophysical theoretical expertise with an on-going experimental program has proven to be a very successful approach to tackling many difficult, interdisciplinary programs. The principal theme of the research has been to shed light on the physical and chemical properties of interstellar and cometary ices by carrying out laboratory studies of astronomical ice analogues. During the past 12 years, the group has studied the spectroscopic properties, from the vacuum ultraviolet through the infrared, of ices made up of simple materials as well as mixtures and the results of different types of processing experiments, such as deposition at various temperatures, annealing, UV irradiation effects, and temperature cycling effects. In recent years, the Leiden group has started to address questions concerning the role sulfur plays in determining the properties of ices. The number of astronomers from the U.S. who have participated in the Leiden group at the doctoral or

post-doctoral level is further testament to the importance of this research group. That no laboratory of comparable scope exists in the U.S. is not for lack of talent or interest, but for lack of dollars.

The Cornell group has also worked for many years on studies of mixtures relevant to solar system environments, including the study of tholins, ices, frosts, and methane clathrates (see abstracts in the Appendix, and Sagan and Khare 1979), and elemental sulfur in solid and liquid form in view of its prevalence in solar system bodies (Sasson, Wright, Arakawa, Khare, and Sagan 1985). In view of the substantial amount of dark, organic material measured in Halley by the satellite fly-by experiments, and the large fraction of the bulk of the nucleus believed to be icy in nature, these are also particularly relevant projects to the study of comets.

In 1984, a modest effort was begun at the NASA Ames Research Center to foster close collaboration between laboratory experimentalists, astronomical observers, and theoreticians. During the past few years, tremendous progress has been made in IR spectroscopy of comets and galactic sources either known or believed to have ices present, resulting in some tight constraints on the physical and chemical properties of such grain materials. The approach taken at Ames will be to carry out experiments on samples comprised of materials thought to be present on or in grains in the interstellar medium. For example, IR observations have shown that CH_4 is not a major ice constituent but that something like CH_3OH is likely to be present in astronomical ices. Thus, an experimental program focused on the photolytic and physical properties of interstellar ice analogues containing CH_3OH is under way. Ices containing polycyclic aromatic hydrocarbons (PAHs) will also be studied at Ames in view of the suggestion that they may be a ubiquitous component of the interstellar medium and that interstellar and cometary grains may well be related.

A major laboratory program in support of the study of interstellar grains from many directions has been going on at the Goddard Space Flight Center for many years. This program has included (but certainly has not been limited to) investigations of condensation processes (see Donn 1987, for a review of this subject with an excellent reference list), hydration effects in silicates, sputtering processes, temperature dependence of the spectral transmission of silicates (annealing, Donn *et al.* 1970, and Day 1974 and 1976a), and currently the effects of aggregates through fractal analysis (Donn 1987). Lab equipment for studying cluster beams has been evolving at GSFC for several years, and is presently quite productive (Donn *et al.* 1981). Also, experiments on the scattering by fractal aggregates using microwaves and scaled-up simulated grains are being enhanced in collaboration with the microwave facility, Space Astronomy Laboratory, University of Florida (Schuerman 1980), and P. Meakin, J. Stephens, B. Gustofson, and R. Wang.

Another microwave laboratory for investigating the scattering by irregular, inhomogeneous particles is located at the Ruhr University, Bochum, FRG. The Bochum group has been active for more than 15 years, particularly in the study of the polarization by irregular grains. They demonstrated the importance of "fluffy" structure in producing the observed polarization and backscattering by interplanetary dust (Giese *et al.* 1978.)

A continuation of the emissivity studies cited above (Russell 1978 and Stephens and Russell 1979) with new materials and sample preparation techniques is being continued at The Aerospace Corporation in collaboration with J. Stephens of Los Alamos. Funded primarily on in-house research money, and using instrumentation built in-house for IR astronomical observations from 2-14 μm , this program has resulted in a promising match to some of the 6-8 μm absorption features seen in dense, cool sources using straight forward silicate samples modified by hydration (Hecht *et al.* 1986). Additional samples with totally different but interesting compositions have been measured and the results are being prepared for publication.

There are a number of other groups around the world studying various aspects of grain processing and grain optical properties. Since 1981, the group at Lecce, Italy has been investigating the ultraviolet and infrared optical properties of various forms of amorphous

and hydrogenated carbon, PAHs, and SiC (Borghesi *et al.* 1985, Bussoletti *et al.* 1986). Sakata *et al.* (1984) have been investigating the properties of quenched carbonaceous composite (QCC). Several groups have been studying sputtering and effects of ion irradiation, including the AT&T Bell Labs laboratory group (Lanzerotti *et al.* 1984) and the group at Catania, Italy (Strazzulla 1985).

6.0 ACKNOWLEDGMENTS

This report had its genesis in the presentation B. Donn gave at the meeting, but also draws heavily on his 1985 and 1987 reviews and several discussions. L. Allamandola kindly sent along several paragraphs on the Leiden and Ames work; the PAH discussion is my rewording of his input as applied more specifically to comets. J. Hecht set aside time to critically read and constructively comment on the draft of this chapter. Martha Hanner has, with the utmost of patience and kindness, shepherded me through to the completion of what was an even bigger task than I expected. I apologize to any groups that are left out of the discussion; it is not a comment on the value of work being done, but on the lack of time on my part to be complete. This work is supported at The Space Sciences Laboratory by The Aerospace Sponsored Research Program.

7.0 REFERENCES

- Arnold, S., Neuman, M., and Pluchino, A.B. 1984, *Optics Lett.*, **9**, 4.
- Arnold, S. and Pluchino, A. 1982, *Appl. Opt.*, **21**, 4194.
- Ashkin, A. 1970, *Phys. Rev. Lett.*, **19**, 283.
- Ashkin, A. and Dziedzic, J. M. 1971, *Appl. Phys. Lett.*, **24**, 586.
- 1980, in *Light Scattering by Irregularly-Shaped Particles*, D. W. Schuerman, ed., Plenum Press, NY, p. 233.
- Borghesi, A. Bussoletti, E., Colangeli, L. 1985. *A&A*, **142**, 225-231.
- Bussoletti, E., Borghesi, A., Colangeli, L. 1986, *Cosmic Dust Analogs: A Laboratory Approach*, in The Comet Nucleus Sample Return Mission Proc. Workshop ESA SP-249, p. 57.
- Chyba, C. and Sagan, C. 1987, *Nature*, submitted.
- Cohen, N. L., McCarthy, J. F., Russell, R. W., and Stephens, J. R. 1980, *B.A.A.S.*, **11**, 610.
- Day, K. L. 1974, *Ap. J. Lett.*, **192**, L15.
- 1976a, *Ap. J. Lett.*, **203**, L99.
- 1976b, *Icarus*, **27**, 561.
- 1979, *Ap. J.*, **234**, 158.
- 1980, *Ap. J.*, **246**, 110.
- Donn, B. 1985, *Experimental Investigations Relating to the Properties and Formation of Cosmic Dust Grains*, p. 109 in NASA Conference Publication 2403, Interrelationships Among Circumstellar, Interstellar, and Interplanetary Dust.
- Donn, B. 1987, September Capri Workshop Proceedings, *Experiments on Cosmic Dust Analogues*, preprint.

- Donn, B., Hecht, J., Khanna, R., Nuth, J., Stranz, D., and Anderson, A.B., 1981, *Surf. Sci.*, **106**, 576.
- Donn, B., Krishna Swamy, K. S., and Hunter, C. 1970, *Ap. J.*, **160**, 353.
- Ferraro, J. R. ed. 1982, *The Sadtler Infrared Spectra Handbook of Minerals and Clays*, Sadtler Res. Laboratories, Phil., Pa.
- Giese, R. H., Weiss, K., Zerull, R. H., Ono, T. 1978, *Astron. & Ap.*, **65**, 265-72.
- Giese, R. H., Killinger, R. T., Kneissel, B., Zerull, R. H. 1986, "Albedo and Colour of Dust Grains: Laboratory versus Cometary Results, in Vol II, 20th ESLAB Symposium on the Exploration of Halley's Comet, p.53.
- Gole, J. L. and Stwalley, W. C. 1982, *Metal Bonding and Interactions in High Temperature Systems (with emphasis on Alkali metals)*, American Chem. Soc., Washington, D.C.
- Hecht, J. H. 1979a, *J. Appl. Phys.*, **50**, 7186.
- 1979b, *J. Appl. Phys.*, **71**, 3132.
- Hecht, J. H., Russell, R. W., Stephens, J. R., and Grieve, P.R. 1986, *Ap. J.*, **309**, 90.
- Hunt, G. R. 1976, *J. Phys. Chem.*, **80**, 1195.
- Hunt, J. M., Wisherd, M. P., and Bonham, L. C. 1950, *Anal. Chem.*, **22**, 1478.
- Khare, B. N. *et al.*, 1987, *Icarus*, in press.
- Knacke, R. F. and Kratschmer, W. 1980, *Astron. Ap.*, **92**, 281.
- Lanzerotti, L. J., Brown, W. L., Johnson, R. E., *Laboratory Studies of Ion Irradiations of Water, Sulfur Dioxide, and Methane Ices*, Proc. NATO Workshop, Ices in the Solar System, ed. J. Klinger, D. Reidel, p. 1984.
- Lynch, D. K., Russell, R. W., Witteborn, F. C., Bregman, J. M., Rank, D. M., Cohen, M. C., and Campins, H. C. 1988, *B.A.A.S.*, **20**, abstract only, for Pasadena DPS Meeting, Nov. 13, 1987.
- Lyon, R. J. P. 1964, NASA Contractor Report CR-100, *Evaluation of Infrared Spectrophotometry for Compositional Analysis of Lunar and Planetary Soils, Part II: Rough and Powdered Surfaces*.
- Marx, E. and Mulholland, G. W. 1983, *J. Res. Nat'l. Bur. St.*, **88**, 321.
- Merrill, K. M. 1974, *Icarus*, **23**, 566.
- Meyer, B. 1971, *Low Temperature Spectroscopy*, Elsevier, NY.
- Moskovits, M. and Ozin, G. A. 1976, *Cryochemistry*, J. Wiley, NY.
- Nuth, J. A. and Donn, B. 1982, *J. Chem. Phys.*, **77**, 2639.
- 1983a, *J. Chem. Phys.*, **78**, 1618.
- 1983b, *J. Geophys. Res. Suppl.*, **88**, A847.
- 1984, *J. Geophys. Res. Suppl.*, **89**, B657.
- Nuth, J. A., Moseley, S. H., Silverberg, R. F., Goebel, J. H., and Moore, W. J. 1985, *Ap. J. Lett.*, **290**, L41.

- Nyquist, R. A. and Kagel, R. O. 1971, *Infrared Spectra of Inorganic Compounds*, Academic Press, NY.
- Philip, M.A., Gelbard F., Arnold, S. 1983, *J. Colloid and Interface Sci.*, **91**, 507.
- Rose, L. A. 1977, Ph.D. Thesis, U. of Minn., *Laboratory Simulation of Infrared Astrophysical Features*.
- Russell, R. W. 1978, Ph.D. Thesis, U. Ca. San Diego, *An Analysis of Infrared Spectra of Some Gaseous Nebulae, With Emphasis on the Planetary Nebula NGC 7027*.
- Sagan, C. and Khare, B. 1979, *Nature*, **277**, 102.
- Sakata, A. *et al.* 1984, *Astrophys. J.*, **287**, L51.
- Sandford, S. A. 1985, Ph.D. Thesis, Wash. U., *Laboratory Infrared Transmission Spectra from 2.5 to 25 μ m of Individual Interplanetary Dust Particles*.
- Sandford, S. A., Fraundorf, P., Patel, R.I., and Walker, R. M. 1982, *Meteoritics*, **17**, 276.
- Sandford, S. A. and Walker, R. M. 1985, *Ap. J.*, **291**, 838.
- Sasson, R., Wright, R., Arakawa, E. T., Khare, B. N., and Sagan, C. 1985, *Icarus*, **64**, 368.
- Schuerman, D. W. 1980, in *Light Scattering by Irregularly Shaped Particles*, D. W. Schuerman, ed., Plenum Press, NY, p. 227.
- Stephens, J. R. and Kothari, B. K. 1978, *The Moon and Planets*, bf 19, 139.
- Stephens, J. R. and Russell, R. W. 1979, *Ap. J.*, **228**, 780.
- Strazzulla, G. 1985, *Icarus*, **61**, 48-56.
- Tielens, A. G. G. M. and Allamandola, L. J. 1986, *Composition, Structure, and Chemistry of Interstellar Dust*, NASA Technical Memorandum 88350, and in *Interstellar Processes*, ed. by Hollenbach and Thronson, D. Reidel, Dordrecht.
- Weiss-Wrana, K. 1983, *A. & Ap.*, **126**, 240.
- Zerull, R. H., Giese, R. H., Schwill, S., and Weiss, K. 1980, in *Light Scattering by Irregularly-Shaped Particles*, D. W. Schuerman, ed., Plenum Press, NY, p. 273.

CHAPTER 5

FOCUS ON THE FUTURE

prepared by M. Hanner

with contributions from Panel Members and the Organizing Committee

INTRODUCTION

The third morning of the Workshop was devoted to a panel discussion (followed by general discussion) to assess what we have learned from Halley and to recommend future directions for infrared studies of comets and supporting laboratory investigations. Panel members were L. Allamandola, T. Encrenaz, R. Gehrz, M. Mumma and M. Hanner (moderator). The panelists were asked to address the following issues:

1. What steps can be taken to achieve consistent interpretation of Halley infrared data?
2. How successful has the Halley Watch been for infrared studies? Should some functions be extended to other comets?
3. What supporting laboratory research is needed?
4. What are the key infrared observations needed for future comets? Is new instrumentation required?
5. How do current and future NASA programs relate to comet studies?

1.0 ACHIEVING A CONSISTENT INTERPRETATION OF HALLEY DATA

1.1 Comparing Observations

- Observers should publish full details of their photometric system and calibration. Infrared photometric systems are not standardized among observatories; even "standard" infrared filters may have different effective wavelengths.
- Several groups carried out extensive photometric monitoring programs (Table 1-1). Efforts should be made to bring these basic data sets onto a common photometric system, so that they can be combined to give a synoptic history of the comet activity.
- Differences in beam size and sky chop amplitude have to be considered when comparing data sets. When jets were present in the coma, the brightness did not necessarily decrease inversely with distance from the nucleus.
- Whenever possible, intercomparisons should be done by the observers themselves.

1.2 Temporal Variability

- From November '85 through April '86, Halley displayed extreme variability. Not only did the amount of dust in the inner coma vary on timescales of a few hours, but also the size distribution apparently varied, so that the average optical properties changed.
- Thus it can be dangerous to combine data taken at different times (for example to extend spectral coverage) without taking this variability into account.
- Synoptic observations in the visible and ultraviolet spectral regions may be useful in charting the variability.
- Observers should *always* publish the UT times of their measurements.

1.3 Applying Models

- When interpreting data, it is a good idea to talk with the observers first!
- A complete, rigorous treatment of the scattering and emission from inhomogeneous, irregular grains does not exist; however, there are approaches to treat specific aspects of the problem.
- The limitations of the analytical methods for treating irregular particles have to be kept in mind when analyzing Halley data.
- Where high accuracy and detailed spectral fitting are not required (for example, estimating dust production rate and total emitting cross-section) the Q_{abs} computed from Mie theory may be adequate.
- The silicate grains in the coma may exhibit differing degrees of crystallinity. Structure in the spectral features will show up in the $10\mu\text{m}$ stretching mode for a lesser degree of crystallinity than in the $20\mu\text{m}$ bending mode vibration.
- Possible changes in grain properties during outburst need to be evaluated.
- Infrared data should not be interpreted without reference to data at other wavelengths.

2.0 INTERNATIONAL HALLEY WATCH/INFRARED NET

The International Halley Watch was established to advocate and coordinate worldwide observations of Halley and, thereafter, to prepare a permanent data archive. These roles were discussed specifically for the Infrared Net.

2.1 Coordination

Participants agreed that planning and coordination have been helpful:

- Many observers from other disciplines were encouraged to participate.
- Publicity from IHW facilitated allocation of observing time at large telescopes.
- Compiling and distributing observing schedules allowed observers to be aware of concurrent observations.
- Electronic hotline and mail system were useful for posting new observations and exchanging information quickly.

It was agreed that a permanent "comet hotline" for the purpose of exchanging observing schedules and new results would be useful.

However, a few desirable results were not realized:

- The $8\text{-}13\mu\text{m}$ spectral region was poorly observed, despite the fact that this could have been done from the ground with CVFs available at several telescopes.
- A common photometric system among observatories (filters, photometric standards) was not achieved, reflecting the larger problem of standardization in infrared astronomy.
- Coordination of KAO and ground-based observations proved to be difficult.
- In some cases, the Infrared Net has not been notified whether planned observations were actually obtained.

Participants expressed frustration over the dollars spent for coordination compared to the support available for actually carrying out the observations. However, most agreed that a continued, low-cost coordination effort for comet observations is desirable, and that this effort should include recommending the observations most needed. Some observers stated that they are now experiencing more difficulty than ever in obtaining telescope time for

comet observing, and they feel that there is a "backlash" resulting from the Halley effort.

2.2 The Archive

Software specialist B. McGuinness gave a status report on the archive for the infrared net (appended to this chapter). The Halley archive is designed to be a permanent, long-term database containing the original observations, without interpretation, and with sufficient information on instrument parameters that they can be re-evaluated by future researchers. Both an accessible CD-ROM and a printed version will be created. In addition, an archive is being prepared for Giacobini-Zinner.

Obviously, if the archive is to serve its purpose, all observers need to submit their data promptly. Final date for submission to the infrared net is June 30, 1988. All those who have contributed data will be offered a free copy of the completed archive.

The information to be placed in the header with each data set was discussed. In addition to instrument parameters such as beam size and chopping throw, comments on the weather and data quality should be included. An example of the header format is shown in Figure 5.1.

It was recommended that a bibliography of published papers related to the observations be appended to the archive.

Concern was expressed as to how the archive will be used after the considerable resources expended to create it. The recommendation was made that small grants be made available for utilizing the Halley and GZ data base.

Target publication dates are:

GZ printed archive - November 1988

GZ CD-ROM archive - May 1990

Halley printed archive - October 1989

Halley CD-ROM archive - July 1990

**** Final date for submitting data is June 30, 1988 ****

3.0 SUPPORTING LABORATORY STUDIES

This section draws on an evening of discussion by the laboratory investigations subgroup, as well as the discussions during Sessions III, IV and V.

Laboratory investigations can contribute to our understanding of comet grains in several ways, including:

- interpreting optical and infrared spectra obtained from Halley and other comets;
- supporting instrument design and measurement strategy for the CRAF mission;
- analyzing interplanetary dust particles;
- investigating the physical and chemical processes taking place on the nucleus and in the coma, as well as the processing of grains since their initial formation in the ISM.

Recommendations for specific measurements in these areas, directed toward the topics covered in this workshop, are summarized below.

3.1 Interpret Existing Infrared Observations

What types of silicates are present in comet dust and how do they compare to interstellar silicate grains?

What types of organic material are present in the grains?

NUMBER:
PREPARER:
FILE-NUM:

DATE:
RECD:
DISPOSITION:

OBSERVERS:

ADDRESSES:

TEL:

COMMENTS: Information above will not be archived.

SAMPLE = T:)
BITPIX = E:) Set by DS
NAXIS = O:)
EXTEND = T:)

OBJECT = comet e.g. "P/Halley," "P/Giacobini-Zinner"
FILE-NUM = : set by PS
DATE-OBS = Midpoint of observation (day/month/year)
TIME-OBS = : Midpoint of observation (decimal fraction of a day)
DATE-REL = Date observers allow data to be released to the public
DISCIPLN = 'IR STUDIES':
LONG-OBS = Longitude of observatory deg/min/sec
LAT--OBS = Latitude of observatory ± deg/min/sec
SYSTEM = Set by DS
OBSERVER = Names of observers (see COMMENT ADD. OBS. below)
SUBMITTR = 'KNACKE':
SPEC-EVT = Observation of a special event? - Yes (T) or No (F)
DAT-FORM = 'STANDARD':

DAT-TYPE = "Photometry, Filter Table, Spectroscopy, Polarimetry, Image"
OBSVTRY = Name of observatory
LOCATION = Location of observatory
TELESCOP = Telescope size in meters
INSTRUME = Instrument used to observe the comet, e.g. "InSb photometer," "2-banger photometer," "Bolometer," etc.

COMMENT General comments
COMMENT ADD.OBS. If more than 2 observers, all names after the first are placed here.
COMMENT NOTE Notes pertaining to rows in the table below
COMMENT OBSVRUN Observing period
COMMENT ORIGIN Location of beam center: coma, peak signal point, etc.
COMMENT REFERENCE Reference to a published paper
COMMENT SEEING Seeing in arcseconds
COMMENT WEATHER Weather conditions during the observation, e.g. cloudy, clear, marginal etc.
HISTORY STOSTARS Stars used as brightness standards

NLINES = :
END
Filter Mag Exp ApDiam TmUT InUT Airm ChpThrw BeamOffOrigin Or Filter Commented
arcsec hhmm hhmm Avg arcsec chp arcsec th Tabl
: : : : : : : : : : : :
: : : : : : : : : : : :
: : : : : : : : : : : :

Figure 5.1 - Sample Header Format for Halley Archive Infrared Net

Figure Explanation

TmUT: Time of midpoint of observation.

InUT: Duration of observation.

Beam Off Origin: Distance of beam from origin specified in comment.

Or: Number identifying one of the "origin" comments.

Filter Table: Number of specific table describing filter characteristics.

Comm Notes: Letter identifying one of the "Note" comments.

What is the carrier of the $3.36\mu\text{m}$ emission feature and what is the excitation mechanism?

Recommended Measurements

1. $10\mu\text{m}$ band shape versus physical and chemical properties of silicates (anhydrous/hydrated; degree of crystallinity; grain size and shape).
 2. $20\mu\text{m}$ band shape and 10 to $20\mu\text{m}$ band strength ratio in silicates.
 3. Temperature effects in spectral features.
 4. Complete spectra to $50\mu\text{m}$, and selected spectra to $200\mu\text{m}$.
 5. Spectra of appropriate organic materials, including PAHs and various forms of hydrogenated carbon.
 6. Optical constants for appropriate organic material in the $3\mu\text{m}$ region.
 7. Effects of grain size, from large molecules to small grains to grain aggregates.
 8. Resonant and non-resonant fluorescence - is this a viable excitation mechanism in solid grains?
 9. Microwave scattering on grain analogs: phase function, polarization, and Q_{scat} .
- (Spectral resolution of $\sim 5\text{cm}^{-1}$ is needed to support future comet observations.)

3.2 Provide Database in Support of CRAF

What are the most important wavelength bands to sample?

What gas/grain interactions take place in the inner coma?

What are the structural properties of the nucleus?

Recommendations

1. Identify and study position and width of spectral features to determine the required filters.
2. Study isotope effects, especially in CO_2 and ice bands, to define instrument and filter requirements.
3. Measure ions/radicals coming off well-defined surfaces to plan for measurements of the near-nucleus environment.
4. Study structural properties of ices, in preparation for penetrator experiment.

3.3 Analyze Interplanetary Dust Particles

What can the composition and structure of IDPs tell us about their origin and processing history?

What carbon compounds are present?

Can isotope anomalies identify remnant interstellar grains?

What are the optical properties of IDPs?

How do their infrared emission spectra compare with comet spectra?

Recommendations

1. Study the composition and mineralogy of units within grains to identify high and low temperature phases.
2. Identify the carbon-bearing materials within grains.

3. Measure key isotopes ratios, such as D/H, carbon.
4. Measure optical and infrared properties, if possible emission spectra.

3.4 Study Physical and Chemical Processes

How do grains form and how do they aggregate?

What dust structures result during the process of sublimation from the nucleus?

What are the structural properties of the nucleus?

Are there isotope fractionation effects during condensation and vaporization?

Is the hydrogen ortho/para ratio primordial?

How are cometary materials altered by irradiation?

Recommended Investigations

1. Structural properties of ices and heat conductivity.
2. Irradiation effects on simulated cometary nuclear surfaces.
3. Composition of residues produced by irradiation of ices, and their C:H:O ratio.
4. Outgassing of CN and other radicals from grains.
5. Isotope effects - fractionation during condensation and sublimation.
6. Ice sublimation and the expected ortho/para ratio.
7. Formation of dust structures, including clusters and "bucky- balls."
8. Energy storage mechanisms to drive outbursts and jets.

4.0 STRATEGY FOR FUTURE COMET OBSERVATIONS

4.1 Lessons from Halley

The infrared spectral region is the key to remote study of comet dust composition, as evidenced by the list of spectral features detected in Comet Halley (Table 1-2). Thus, infrared spectroscopy will be extremely important for future comet studies. However, without basic photometry to define the spectral energy distribution, the spectroscopy is often difficult to interpret; thus, coordinated programs covering a broad spectral range are vital.

Participants all agreed that the most serious omission from the Halley campaign is the lack of spectra across the 10-micron silicate feature. Moreover, only one spectrum of the 16-24 μ m region was obtained - at 1.3 AU pre-perihelion. It is not known whether the lack of identifiable silicate peaks in this spectrum was characteristic of the grains or was simply a result of temporal variability.

The Kuiper Airborne Observatory played a vital role in the Halley observations, providing the first ever cometary spectra at 5-8 μ m, 16-24 μ m, and 20-68 μ m, as well as direct detection of H₂O and upper limits to other parent molecules. It is crucial to cometary studies that NASA keep this facility operational.

The Lear jet observatory telescope can also be a valuable tool for comet observations, as evidenced by its role in the Halley program.

4.2 Science Rationale

As is often the case, new discoveries have created new puzzles about the nature of the material in comets. Scientific questions to be addressed by future observations include:

- How typical is Halley? Are the same spectral features, implying similar composition, seen in all comets, both new and evolved?
- What kinds of silicates are present in comets? Are hydrated silicates present as well as anhydrous forms (olivine, pyroxene)? Why did Halley show distinct peaks in the $10\mu\text{m}$ feature, indicative of crystalline grains while other astronomical sources do not? Where is the silicate bending mode vibration near $20\mu\text{m}$?
- How common is the $3.36\mu\text{m}$ emission in comets? What is the excitation mechanism, and are the carriers molecules or grains? Why is the strongest emission at $3.36\mu\text{m}$ in the comet and at $3.29\mu\text{m}$ in interstellar sources? Are there any emission features from organic material at longer wavelengths?
- What gaseous species originate from grains in the coma?
- What is the origin of the $12.2\mu\text{m}$ emission feature in Comet Wilson? Why was it not evident in Halley?
- Are emission features at $\lambda > 24\mu\text{m}$ present in other comets? What is their origin?
- How do the various spectral features vary with heliocentric distance, and what can this tell us about their excitation mechanism?
- Finally, how are cometary grains related to interstellar grains? Can we infer anything about their processing history?

4.3 Recommendations for Future Infrared Observations

The following recommendations for future observing of moderately bright comets were agreed upon:

- The 10 and $20\mu\text{m}$ silicate features should be observed with good spectral resolution ($\sim 1\%$) and with good temporal coverage.
- Synoptic $1\text{--}20\mu\text{m}$ filter photometry should be carried out with small or moderate-sized telescopes (≥ 75 cm), ideally telescopes dedicated for that purpose. Observations of bright comets at small angular distance from the sun are very desirable.
- The $2.7\text{--}5\mu\text{m}$ region should be observed with the maximum possible spectral resolution, not only to study the 3.29 and $3.36\mu\text{m}$ features, but also to confirm the presence of several other features tentatively detected in Halley spectra.
- Complete $5\text{--}13\mu\text{m}$ spectra and/or both 10 and $20\mu\text{m}$ spectra should be obtained during a KAO flight, in order to define the continuum level and to correlate spectral features. Lack of such coverage has complicated the interpretation of Halley data.
- The $2.65\mu\text{m}$ transition in the H_2O molecule should be observed in other comets, as a direct means of measuring the H_2O production rate and ortho/para ratio. Other parent molecules can also be searched for via their infrared transitions (e.g., HDO , H^{18}OH , CH_4 , CO_2 , H_2CO , CO); for this purpose, instrument sensitivities should be improved to permit detections at 1% of H_2O .
- The spectral region beyond $20\mu\text{m}$ needs further study, to confirm and identify the weak emission features discovered in Halley.
- Coordinated observations in different wavelength regions are needed, to correlate spectral variations and identify common carriers. For this purpose, two telescopes at the same site are very desirable, as is coordination of KAO, LJO, and ground-based measurements.
- Because bright comets appear unpredictably and often without sufficient warning to apply for observing time, let alone plan a coordinated campaign, we recommend that major observing facilities, including the KAO, have a target of opportunity plan,

whereby some observing time can be allocated on relatively short notice, to obtain key observations of new comets. Such a program already functions well on the IUE.

Comet P/Brorsen-Metcalf, with $P = 70$ years and $q = 0.48$ AU, has a favorable apparition in 1989, passing 0.4 AU from Earth about six weeks pre-perihelion. In contrast to Halley and Wilson, it will be favorably placed for Northern Hemisphere observers. An ephemeris for planning purposes is given in Table 5-1. Although brightness estimates are uncertain, it will be among the brighter periodic comets.

- We recommend that a coordinated program of ground-based and airborne observations be initiated to study P/Brorsen-Metcalf, during July - September 1989.
- There is also a need to study the class of fainter, short-period comets, to support NASA's CRAF mission.

4.4 Instrumentation

Specialized instrumentation for cometary observations is not required. Several new instruments under development for ground-based and airborne spectrophotometry and/or imaging will benefit cometary studies. Instruments which can operate in more than one spectral region are desirable, for the reasons discussed above.

5.0 RELATION TO NASA PROGRAMS

NASA-supported projects are an essential ingredient of infrared studies, since much of the infrared spectrum is accessible only from high altitude or from space. In the future, we can look forward to infrared spectroscopy with improved spatial and spectral resolution from several NASA projects. However, we stress that excellent science can be conducted with existing NASA facilities.

5.1 Ground-Based Support

- Grants to observers from NASA's Planetary Astronomy Program are needed to carry out the observational program outlined in Section 4.
- The large aperture and excellent sky at NASA's Infrared Telescope Facility (IRTF) on Mauna Kea make possible high-resolution spectroscopy of comets in the 3 and 10 μm atmospheric windows and also allow faint comets to be detected and bright comets to be followed over a wide range in heliocentric distance. Several of the 3 μm spectra of Halley and Wilson and one 10 μm spectrum were obtained at the IRTF with facility instruments.

5.2 Airborne Facilities

- The Kuiper Airborne Observatory will continue to be an important facility for comet observations. Many of the emission features detected for the first time in Halley spectra need to be confirmed in other comets and observed over a range in heliocentric distance to help identify their origin and excitation mechanism. Detection of emission bands from organic materials at 5 - 8 μm would greatly aid identification of the 3.36 μm carrier. Other parent molecules may be detected via infrared transitions. It is crucial that NASA keep the KAO flying, with a full schedule, and that comet observations be considered a bona fide part of the science program.
- The Lear Jet Observatory, equipped with a 30-cm telescope, complements the 91-cm KAO; both fly at similar altitude. The LJO, with its shorter flight times and more flexible schedule, is particularly suited for monitoring variability in the comet spectrum; a large dust outburst in Halley in April 1986 was successfully observed in this way. The telescope can point to elevations 0-30 degrees above the horizon; thus, comets can be followed near the sun. Simultaneous LJO and KAO flights can achieve desirable correlated observations in different spectral regions.

Table 5-1

EPHEMERIS (WITH PERTURBATIONS) FOR PARSORIEN-HEICALF - ORBIT BY D.K. YEOMANS																		
HR	HN	DT	HR	J.O.	R.A.	1950.0	DEC.	DELTA	DELGCT	R	ROOT	TMAG	MMAG	THETA	BETA	MODN	PSANG	PSAMV
-3	2447628.5	5	21	37.371	-15	41.64	3.4576	-41.2045	2.9819	-21.1910	-0.22.5	52.2	15.4	21.9	230.0	236.7		
-3	2447632.5	5	21	43.311	-15	3.99	3.3672	-42.0976	2.9894	-21.3311	-0.22.3	55.5	10.4	95.6	29.9	237.9		
-3	2447635.5	4	21	49.376	-14	72.97	3.2445	-42.8733	2.8573	-21.5279	-0.22.1	58.5	17.5	160.7	269.7	237.9		
-3	2447638.5	4	19	55.396	-13	41.49	3.1197	-43.5445	2.7946	-22.0111	-0.21.9	62.1	18.5	141.0	267.6	237.7		
-3	2447642.5	4	24	1.427	-12	58.42	2.9931	-44.1192	2.7533	-22.0324	-0.21.7	65.4	19.6	82.6	269.4	237.7		
-3	2447645.5	4	29	7.474	-12	13.62	2.8650	-44.6025	2.6674	-22.0674	-0.21.5	69.6	20.6	19.6	269.2	237.6		
-3	2447648.5	5	4	13.561	-11	20.94	2.7336	-45.0967	2.6027	-22.1297	-0.21.3	71.8	21.6	50.9	269.0	237.6		
-3	2447652.5	5	9	19.659	-10	33.91	2.6053	-45.2541	2.5374	-22.1979	-0.21.1	74.9	22.6	122.0	268.8	237.4		
-3	2447655.5	5	14	25.765	-9	47.17	2.4743	-45.6045	2.4713	-22.2674	-0.20.9	78.0	23.6	118.4	268.6	237.4		
-3	2447658.5	5	19	31.921	-8	52.52	2.3431	-45.8513	2.4343	-22.3381	-0.20.7	81.1	24.6	116.7	268.4	237.3		
-3	2447662.5	5	24	38.114	-7	56.85	2.2119	-46.0945	2.3370	-22.5361	-0.20.5	84.2	25.5	58.0	268.2	237.3		
-3	2447665.5	5	29	44.401	-6	56.70	2.0809	-46.3433	2.2895	-22.5835	-0.20.3	87.2	26.5	8.0	267.9	237.0		
-3	2447668.5	6	3	50.782	-5	42.59	1.9506	-46.5952	2.1994	-24.1183	-0.20.1	90.1	27.5	78.8	267.7	236.9		
-3	2447672.5	6	8	57.283	-4	33.40	1.8211	-46.8641	2.1293	-24.1294	-0.19.9	93.0	28.5	78.8	267.7	236.9		
-3	2447675.5	6	13	3.966	-3	26.77	1.6928	-44.1596	2.0582	-24.7674	-0.19.7	95.7	29.4	15.5	267.7	236.8		
-3	2447678.5	6	18	10.828	-2	7.03	1.5661	-43.5667	1.9863	-25.0281	-0.19.5	98.3	30.4	97.2	267.7	236.8		
-3	2447682.5	6	23	18.005	-1	16.66	1.4413	-42.8679	1.9134	-25.0914	-0.19.3	100.8	31.4	33.3	267.6	236.6		
-3	2447685.5	6	28	25.577	+1	4.47	1.3186	-42.4070	1.8394	-25.1708	-0.19.1	103.3	32.6	34.6	267.6	236.6		
-3	2447688.5	6	3	33.650	+2	59.14	1.1984	-41.0771	1.7644	-26.1605	-0.18.9	105.8	33.8	102.3	267.6	236.6		
-3	2447692.5	6	8	42.515	+3	45.16	1.0815	-39.9201	1.6922	-26.5561	-0.18.7	108.3	35.1	135.4	267.6	236.6		
-3	2447695.5	6	13	52.364	+4	11.37	0.9682	-38.5448	1.6110	-26.9599	-0.18.5	110.8	36.2	137.2	267.6	236.6		
-3	2447698.5	6	18	3.751	+5	50.53	0.8592	-36.8859	1.5325	-27.3730	-0.18.3	113.3	37.2	92.6	267.6	236.6		
-3	2447702.5	6	23	10.503	+6	33.59	0.7555	-36.8859	1.4529	-27.7956	-0.18.1	115.8	38.2	80.4	267.6	236.6		
-3	2447705.5	6	28	18.324	+7	13.24	0.6557	-32.1491	1.3722	-28.2213	-0.17.9	118.3	39.2	50.7	267.6	236.6		
-3	2447708.5	6	33	26.151	+8	30.99	0.5597	-28.4933	1.2893	-28.6814	-0.17.7	120.8	40.2	44.3	267.6	236.6		
-3	2447712.5	6	38	34.000	+9	11.57	0.4682	-23.1444	1.2065	-29.0645	-0.17.5	123.3	41.2	36.8	267.6	236.6		
-3	2447715.5	6	43	41.826	+10	4.98	0.3836	-16.1063	1.1221	-29.3979	-0.17.3	125.8	42.2	26.5	267.6	236.6		
-3	2447718.5	6	48	49.651	+11	45.30	0.3057	-16.0930	1.0368	-29.4717	-0.17.1	128.3	43.2	103.7	267.6	236.6		
-3	2447722.5	6	53	57.474	+12	13.62	0.2119	-14.6035	0.9509	-29.7966	-0.16.9	130.8	44.2	92.6	267.6	236.6		
-3	2447725.5	6	58	5.427	+11	11.57	0.1157	-14.2693	0.8650	-29.9074	-0.16.7	133.3	45.2	80.4	267.6	236.6		
-3	2447728.5	6	63	13.561	+10	4.98	0.0357	-12.3976	0.7800	-29.9074	-0.16.5	135.8	46.2	70.3	267.6	236.6		
-3	2447732.5	6	68	21.427	+9	3.99	0.0357	-10.4069	0.6977	-27.7601	-0.16.3	138.3	47.2	60.8	267.6	236.6		
-3	2447735.5	6	73	29.376	+8	3.99	0.0357	-8.4069	0.6150	-25.1716	-0.16.1	140.8	48.2	50.8	267.6	236.6		
-3	2447738.5	6	78	37.371	+7	3.99	0.0357	-6.4069	0.5325	-20.5788	-0.15.9	143.3	49.2	40.8	267.6	236.6		
-3	2447742.5	6	83	45.376	+6	3.99	0.0357	-4.4069	0.4492	-15.3721	-0.15.7	145.8	50.2	30.8	267.6	236.6		
-3	2447745.5	6	88	53.381	+5	3.99	0.0357	-2.4069	0.3657	-10.3721	-0.15.5	148.3	51.2	20.8	267.6	236.6		
-3	2447748.5	6	93	61.386	+4	3.99	0.0357	-0.4069	0.2822	-5.3721	-0.15.3	150.8	52.2	10.8	267.6	236.6		
-3	2447752.5	6	98	69.391	+3	3.99	0.0357	1.5931	0.1987	-0.3721	-0.15.1	153.3	53.2	0.8	267.6	236.6		
-3	2447755.5	6	103	77.396	+2	3.99	0.0357	3.5882	0.1152	3.3721	-0.14.9	155.8	54.2	-0.2	267.6	236.6		
-3	2447758.5	6	108	85.401	+1	3.99	0.0357	5.5833	0.0327	5.3721	-0.14.7	158.3	55.2	-1.2	267.6	236.6		
-3	2447762.5	6	113	93.406	0	3.99	0.0357	7.5784	0.0500	7.1721	-0.14.5	160.8	56.2	-2.2	267.6	236.6		
-3	2447765.5	6	118	101.411	-1	3.99	0.0357	9.5735	0.0673	8.9721	-0.14.3	163.3	57.2	-3.2	267.6	236.6		
-3	2447768.5	6	123	109.416	-2	3.99	0.0357	11.5686	0.0846	10.7672	-0.14.1	165.8	58.2	-4.2	267.6	236.6		
-3	2447772.5	6	128	117.421	-3	3.99	0.0357	13.5637	0.1019	12.5623	-0.13.9	168.3	59.2	-5.2	267.6	236.6		
-3	2447775.5	6	133	125.426	-4	3.99	0.0357	15.5588	0.1192	14.3574	-0.13.7	170.8	60.2	-6.2	267.6	236.6		
-3	2447778.5	6	138	133.431	-5	3.99	0.0357	17.5539	0.1365	16.1525	-0.13.5	173.3	61.2	-7.2	267.6	236.6		
-3	2447782.5	6	143	141.436	-6	3.99	0.0357	19.5490	0.1538	17.9476	-0.13.3	175.8	62.2	-8.2	267.6	236.6		
-3	2447785.5	6	148	149.441	-7	3.99	0.0357	21.5441	0.1711	19.7427	-0.13.1	178.3	63.2	-9.2	267.6	236.6		
-3	2447788.5	6	153	157.446	-8	3.99	0.0357	23.5392	0.1884	21.5378	-0.12.9	180.8	64.2	-10.2	267.6	236.6		
-3	2447792.5	6	158	165.451	-9	3.99	0.0357	25.5343	0.2057	23.3329	-0.12.7	183.3	65.2	-11.2	267.6	236.6		
-3	2447795.5	6	163	173.456	-10	3.99	0.0357	27.5294	0.2230	25.1280	-0.12.5	185.8	66.2	-12.2	267.6	236.6		
-3	2447798.5	6	168	181.461	-11	3.99	0.0357	29.5245	0.2403	26.9231	-0.12.3	188.3	67.2	-13.2	267.6	236.6		
-3	2447802.5	6	173	189.466	-12	3.99	0.0357	31.5196	0.2576	28.7182	-0.12.1	190.8	68.2	-14.2	267.6	236.6		
-3	2447805.5	6	178	197.471	-13	3.99	0.0357	33.5147	0.2749	30.5133	-0.11.9	193.3	69.2	-15.2	267.6	236.6		
-3	2447808.5	6	183	205.476	-14	3.99	0.0357	35.5098	0.2922	32.3084	-0.11.7	195.8	70.2	-16.2	267.6	236.6		
-3	2447812.5	6	188	213.481	-15	3.99	0.0357	37.5049	0.3095	34.1035	-0.11.5	198.3	71.2	-17.2	267.6	236.6		
-3	2447815.5	6	193	221.486	-16	3.99	0.0357	39.4999	0.3268	35.8986	-0.11.3	200.8	72.2	-18.2	267.6	236.6		
-3	2447818.5	6	198	229.491	-17	3.99	0.0357	41.4950	0.3441	37.6937	-0.11.1	203.3	73.2	-19.2	267.6	236.6		
-3	2447822.5	6	203	237.496	-18	3.99	0.0357	43.4901	0.3614	39.4888	-0.10.9	205.8	74.2	-20.2	267.6	236.6		
-3	2447825.5	6	208	245.501	-19	3.99	0.0357	45.4852	0.3787	41.2839	-0.10.7	208.3	75.2	-21.2	267.6	236.6		
-3	2447828.5	6	213	253.506	-20	3.99	0.0357	47.4803	0.3960	43.0790	-0.10.5	210.8	76.2	-22.2	267.6	236.6		
-3	2447832.5	6	218	261.511	-21	3.99	0.0357	49.4754	0.4133	44.8741	-0.10.3	213.3	77.2	-23.2	267.6	236.6		
-3	2447835.5	6	223	269.516	-22	3.99	0.0357	51.4705	0.4306	46.6692	-0.10.1	215.8	78.2	-24.2	267.6	236.6		
-3	2447838.5	6	228	277.521	-23	3.99	0.0357	53.4656	0.4479	48.4643	-0.09.9	218.3	79.2	-25.2	267.6	236.6		
-3	2447842.5	6	233	285.526	-24	3.99	0.0357	55.4607	0.4652	50.2594	-0.09.7	220.8	80.2	-26.2	267.6	236.6		
-3	2447845.5	6	238	293.531	-25	3.99	0.0357	57.4558	0.4825	52.0545	-0.09.5	223.3	81.2	-27.2	267.6	236.6		
-3	2447848.5	6	243	301.536	-26	3.99	0.0357	59.4509	0.5000	53.8496	-0.09.3	225.8	82.2	-28.2	267.6	236.6		
-3	2447852.5	6	248	309.541	-27	3.99	0.0357	61.4460	0.5173	55.6447	-0.09.1	228.3	83.2	-29.2	267.6	236.6		
-3	2447855.5	6	253	317.546	-28	3.99	0.0357	63.4411	0.5346	57.4398	-0.08.9	230.8	84.2	-30.2	267.6	236.6		

- SOFIA, a proposed 3-meter airborne telescope, would greatly aid the identification of fainter emission features in comet spectra, particularly those at $\lambda > 24\mu\text{m}$ and potentially other signatures of organic materials in the 5 - 8 μm region. It would bring into view a larger number of comets, over a wider range of heliocentric distance, including the important class of new comets, such as Bowell and Cernis, with perihelion at ~ 3 AU. Spatially resolved spectral observations would also be possible.

5.3 Telescopes in Earth Orbit

- The Infrared Astronomy Satellite (IRAS) observed at least 17 known comets in four bandpasses extending to $120\mu\text{m}$ during its 1983 sky survey. Many more comets are doubtless included in the asteroid catalogue. The high sensitivity, large field of view, and wide-wavelength coverage of the IRAS instrument affords an infrared view of comets, both spatially and spectrally, that will not be repeated within the next decade. Of particular interest are the dispersal of dust grains in the tail, the existence of dust comae at large heliocentric distance, and the formation of debris trails, such as that of Tempel 2. We recommend that NASA continue to support analysis of the IRAS comet data.

- The Space Infrared Telescope Facility (SIRTF) is a new space observatory in the planning stages. The present design goals are:

Facility lifetime: five years, with ten-year goal.

Spectral range: 1.8 to $700\mu\text{m}$

Aperture: 85 cm

Field of view 7 arcmin

Sensitivity: natural background-limited, 2 to $200\mu\text{m}$

Image quality: diffraction-limited for $\lambda > 5\mu\text{m}$

Three instruments have been selected for SIRTF, to provide photometric, imaging, and spectroscopic capability with the utmost sensitivity for infrared wavelengths. They are:

Infrared Array Camera - PI: G. Fazio, SAO

Multiband Imaging Photometer - PI: G. Rieke, Arizona

Infrared Spectrograph - PI: J. Houck, Cornell

These instruments will have the following capabilities:

Photometry with diffraction-limited beams from 2 to $700\mu\text{m}$ (beamsize 3 arcsec at $10\mu\text{m}$).

Low-resolution dispersive spectroscopy from 2.5 to $120\mu\text{m}$ (resolving power ~ 100).

Moderate resolution dispersive spectroscopy from 4 to $120\mu\text{m}$ (resolving power ~ 2000).

Wide-field and diffraction-limited imaging, mapping, and surveying at 2.5 to $200\mu\text{m}$, using arrays with at least 128×128 pixels.

Polarimetric capability for use in conjunction with both the imaging and photometric instrumentation.

SIRTF will provide unprecedented spectral coverage and sensitivity for the study of comets. Complete spectra can be obtained from 2.5 to $200\mu\text{m}$ at resolutions of 100 to 2000. With the continuum from 13- $16\mu\text{m}$ defined, the silicate features in the 16- $24\mu\text{m}$ region can be identified. Weak features at longer wavelengths can also be confidently detected. In addition, SIRTF will allow study of the shape of the $10\mu\text{m}$ silicate band

without interference from the $9.7\mu\text{m}$ ozone absorption, which now causes uncertainty in the definition of the peak near $9.8\mu\text{m}$. The coma can be spatially mapped in individual spectral features. The inactive nuclei of many short-period comets should be detectable in the thermal infrared.

- The Infrared Space Observatory (ISO) is a fully approved and fully-funded mission of ESA, which is scheduled for launch in 1992 - 1993. The expected lifetime is 18 months. ISO consists of a 60-cm telescope, cooled with a helium cryogenic system, and four focal plane instruments presently being built by European consortia. These instruments are summarized in Table 5-2. ISO is designed to be an observatory for the whole astronomical community. Two-thirds of the observing time will be made available to this community via submission and selection of proposals.
- We strongly recommend that NASA support guest investigators for comet studies on ISO.
- The Planetary telescope now under study in collaboration with FRG could greatly aid comet research. We strongly recommend that infrared instruments be considered for the payload.

6.0 THE COMET RENDEZVOUS/ASTEROID FLYBY MISSION

While there is much to be learned from remote sensing and laboratory studies, there are some questions that can only be answered with direct sampling. The Comet Rendezvous/Asteroid Flyby mission (CRAF) has the exciting prospect of sampling the composition of the solid grains with a variety of analysis techniques throughout the perihelion passage of the target comet.

Key element ratios can be measured, for comparison with meteorites, IDPs and the interstellar medium. Isotope anomalies that are tracers of interstellar grains can be detected, such as the D/H and $^{13}\text{C}/^{12}\text{C}$ ratios. The mineralogy of silicates can be studied and the composition of the organic material can be investigated.

Three dust analysis experiments have been selected for the payload:

The Cometary Matter Analyzer (COMA) will use secondary ion mass spectroscopy to measure the elemental and isotopic composition of the dust. The measurement technique is similar to that of the PIA/PUMA instrument on the Halley probes. (PI: J. Kissel FRG).

The Scanning Electron Microscope and Particle Analyzer (SEMPA) is a miniature scanning electron microscope with an energy-dispersive x-ray spectrometer. SEMPA will measure the elemental composition, dimensions, and surface morphology of individual micron-sized grains, from which the mineralogy and crystal form can be deduced. (PI: A. Albee).

The Cometary Ice and Dust Experiment (CIDEX) uses the techniques of x-ray fluorescence spectrometry and gas chromatography. The XRF can determine the bulk elemental composition of the dust (15 to 25 elements). The GC can study light gases, organics, and polar molecules; the volatiles can be released and analyzed stepwise at a series of temperatures from -90 to $+1000$ deg C. (PI: G. Carle).

In addition, the spacecraft will carry a complement of remote sensing instruments, gas mass spectrometers to measure the gas composition, and particles and fields instrumentation. Of particular relevance to this Workshop, a visual and near-infrared mapping spectrometer (VIMS) will survey the wavelength range from 0.35 to $5.2\mu\text{m}$, with a spectral resolution of 0.011 - $0.022\mu\text{m}$, while a thermal infrared radiometer (TIREX) will measure the emission from the coma and the nucleus through various filters at $\lambda \geq 5\mu\text{m}$.

- We strongly recommend that NASA fully support this important mission with a timely New Start and adequate funding.

Table 5-2
Instrument Payload for ISO

	Main Function	Wavelength (Microns)	Spectral Resolution	Spatial Resolution	Description
ISOCAM	Camera and Polarimetry	3 - 17	Broad-band, Narrow-band, and Circular Variable Filters	Pixel f.o.v.'s of 3, 6 or 12 arc/seconds	Two channels each with a 32x32 element array.
ISOPHOT	Imaging Photo- polarimeter	3 - 200	Broad-band and Narrow-band Filters. Near IR Grating Spectrometer with R=100	Variable (Diffraction - limited and wide beam)	Four sub-systems: .Multi-band, .Multi-aperture .Photo-polarimeter .Far-Infrared .Camera .Spectrophotometer .Mapping Arrays
SWS	Short-wavelength Spectrometer	3 - 45	1000 across wavelength range and 3×10^4 from 15-30 microns	14 and 20 arc sec.	Gratings, and Fabry-Pérot Interferometers
LWS	Long-wavelength Spectrometer	45 - 180	200 and 10^4 across wave- length range	1.65 arc minutes	Grating and Fabry-Pérot Interferometers

CURRENT STATUS OF THE INTERNATIONAL HALLEY WATCH INFRARED NET ARCHIVE

Brian B. McGuinness
Department of Earth and Space Sciences
State University of New York at Stony Brook
Stony Brook, NY 11794-2100

The primary purposes of the Halley Watch have been to promote Halley observations, coordinate and standardize the observing where useful, and to archive the results in a database readily accessible to cometary scientists. The intention of the IHW is to store the observations themselves, along with any information necessary to allow users to understand and use the data, but to exclude interpretations of these data. It is important to note that submission of observations to the IHW does not preclude the publication of these observations in journals. In fact, observers are urged to publish their data promptly in the open literature. Data submitted to the Infrared net of the IHW will not be released until the IHW archives are released.

Each of the archives produced by the IHW will appear in two versions: a printed archive and a digital archive on CD-ROMs. The CD-ROMs will contain everything submitted in digital form to JPL. Due to cost constraints, the printed archives will contain some, but not all, of the information in the digital archives for each of the observations. The printed versions will allow astronomers to quickly look up information and will give them an idea of what type of information is available on what dates. Each entry will contain the ID number of the corresponding file in the digital version, so the printed archives will be useful as indices to the CD-ROMs. The digital archives will allow the data to be easily accessed by computers for data reduction and analysis. CD readers for IBM PCs and other microcomputers are available to read the CD-ROMs. Thus, access to the digital archives will not be excessively expensive.

The archive is expected to have a very long lifetime. Experience indicates that magnetic tapes deteriorate to uselessness after only ten years or so. As CD-ROMs were developed relatively recently, their useful lifetimes are unknown, but they are expected to last at least 30 or 40 years. When they start to wear out, they can be copied onto newer CD-ROMs or other media. The archive is expected to be used at least up through the next apparition of Halley.

The IHW has already produced an archive for P/Crommelin. This consists of one printed volume and two 1600 bpi tapes. The CD-ROM version is contained in the Planetary Data System's (PDS) Interactive Data Interchange (IDI) disk. The Crommelin archive was created as a test of the Halley Watch. It enabled the IHW to determine what problems would be likely to appear during data collection for the creation of the other two archives. The proposed format for the printed versions of the G-Z and Halley archives has changed considerably based on experience gained from the Crommelin archive. Furthermore, the indexing scheme used for the G-Z and Halley digital archives will differ substantially from that used for Crommelin. Nonetheless, the Crommelin archive is a useful source of data, although its distribution in CD form has been far more limited than is planned for the Halley and G-Z disks.

The Halley archive will contain at least twenty gigabytes of information – possibly twice that. Recent estimates are that the printed version will consist of seven 500-page volumes and the digital version will consist of perhaps twenty CD-ROMs, depending on the data-compression techniques employed. This is obviously a large collection of cometary data.

The printed version of the Giacobini-Zinner archive will be published in November 1988, followed by the digital version in mid-1989. The printed Halley archive will be

published about October 1, 1989, and the digital version in mid-1990.

The IHW is subdivided into nine nets: Astrometry, Infrared Studies, Large-Scale Phenomena, Near-Nucleus Studies, Photometry and Polarimetry, Radio Studies, Spectroscopy and Spectrophotometry, Amateur Astronomers, and Meteor Studies. Each of these nets is headed by one or more Discipline Specialists, who decide what types of information to include in the archives and collect observations from the observers in their nets. Discipline Specialists for the Infrared net are R. Knacke and T. Encrenaz. The Discipline Specialists give the data they collect to their Software Specialists, who convert it to FITS [1,2] format and write it onto magnetic tapes. The tapes are then sent to the Lead Center at JPL in Pasadena, California, where the final editing and publication are done.

The IHW infrared center at Stony Brook has the task of deciding what types of infrared data to include in the archive, soliciting this information from the observers, determining the format for both the printed and digital versions of the archive, collecting and organizing the data, verifying that the data were received correctly, and converting the data to FITS format for submission to the Lead Center. From time to time the Discipline Specialists and the Software Specialist for the IR net meet with their counterparts from the other nets and personnel from the Lead Center to discuss the formats for the archives in order to achieve consistency across the nets. They also work on designing an indexing system to allow data on the CD-ROMs to be quickly and easily located.

Information submitted to the IR net is stored on a hard disk on an IBM PC/XT with a commercial database program. When complete, a printed copy is sent to the observer to be checked for errors and returned with corrections. It is then exported to ASCII text files and converted into FITS format. Once the FITS files have been checked for errors, they are uploaded at 9600 baud over a direct line to a DEC MicroVAX. From there they are written to tape and then mailed to the Lead Center.

Figures 1 and 2 show the general status of the IR net in April and August 1987. The proportion of the total data that has been received so far has increased, for two reasons. First, the IR net has received a large amount of information since April. Secondly, the estimated total amount of information expected has decreased as observers have reported that certain observations were not made due to bad weather or other problems. As information has been processed and submitted to JPL, more information has arrived, so the total amount of information in preparation has stayed fairly constant.

Figures 3 and 4 give a breakdown of the information by type. Infrared observations of Halley are dominated by photometry. The IR net has been processing Halley photometry and polarimetry data and has begun work on spectroscopy. There are still a few details about the digital format for images that need to be worked out before the images can be processed and submitted. Due to this and to the small amount of Giacobini-Zinner photometry and spectroscopy data received so far the G-Z data have not yet been fully processed. Processing of the G-Z photometry and spectroscopy data should be completed by the end of January 1988.

Figures 5 and 6 show the number of nights of observations made each month during the recent apparitions of Giacobini-Zinner and Halley.

The IHW infrared net needs the continued support of the observers. For the G-Z and Halley archives to be as useful as possible, observers must submit all available data so that the archives can be complete collections of the observations. It is also necessary for the IR center to be made aware of observations that were planned but not made in order for its calendar of observations to be updated. The Lead Center must operate with a continuous inflow of observational data. Each individual who contributes data will be given a free copy of the archives, both in the printed and digital forms.

The archive publication dates mentioned above set deadlines for data submission. The IR net needs time to organize and reformat the data. Extra time is required for dealing with unexpected problems such as hardware breakdown or difficulty in reading tapes. In

addition, the Lead Center needs time to organize the data received from the nine IHW nets. The Giacobini-Zinner data should have been delivered by December, 1987. Please contact us if you have data but could not meet the deadline. Halley observations should be submitted by June 1988.

Data may be submitted to the IHW infrared net in the form of tables, notes, computer printouts, or magnetic tapes mailed to either Dr. Roger Knacke or Brian McGuinness at the following address:

Department of Earth and Space Sciences
State University of New York at Stony Brook
Stony Brook, NY 11794

or to:

Dr. Therese Encrenaz
Observatoire de Paris
Section d'Astrophysique
92190 Meudon, France

We prefer that magnetic tapes be written in unlabelled form. Files on the tape should be written as ASCII text files or as FITS files. The tape density should be 1600 or 6250 bpi. When sending tapes, please indicate what format the tape is written in (plain unlabelled form, ANSI-D, or whatever) and what type of computer it was written on. Some computers, such as the Prime, have idiosyncrasies that affect tapes written by them. It would also be appreciated if the tape was accompanied by a list of what files it contains. This aids in the detection of errors during the process of reading the tape.

An alternative is to send the observations in the form of electronic mail on BITNET to BMCGUINESS@SBCCMAIL. This will cause them to be sent to the Stony Brook Computing Center's VAX 8600 computer system. From there they can be downloaded to the IBM PC/XT for processing.

REFERENCES

- [1] Griesen and Harten, 1981, *Astron. Astrophys. Suppl. Ser.*, **44**, 371-374.
- [2] Wells, Greisen, and Harten, 1981, *Astron. Astrophys. Suppl. Ser.*, **44**, 363-370.

IHW Infrared Network Data Reporting as of April 1987

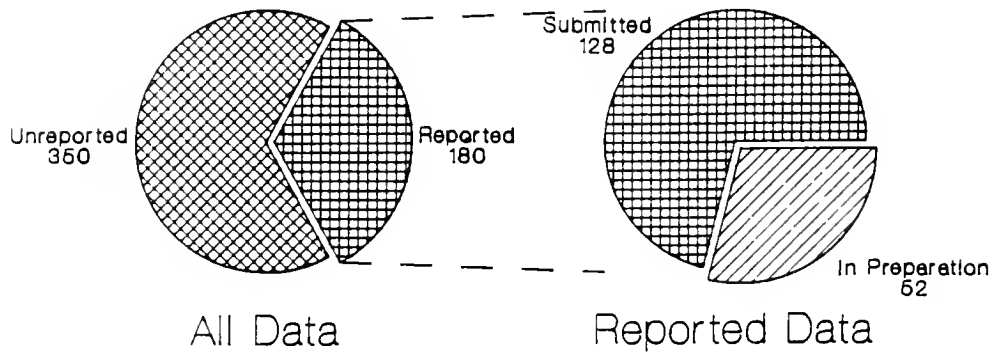


Figure 1.

IHW Infrared Network Data Reporting as of August 1987

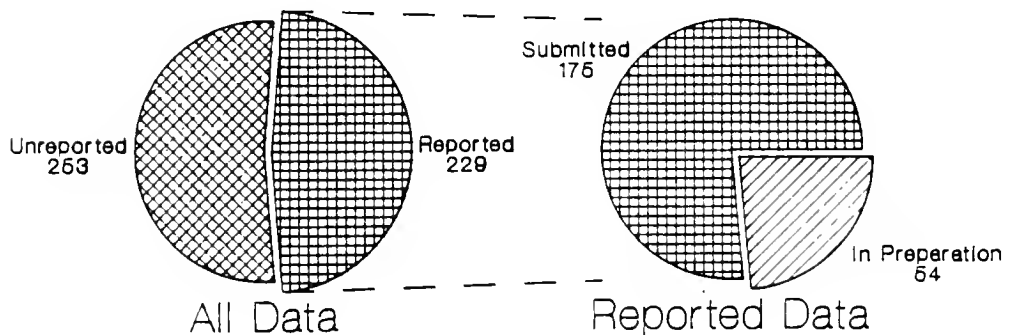
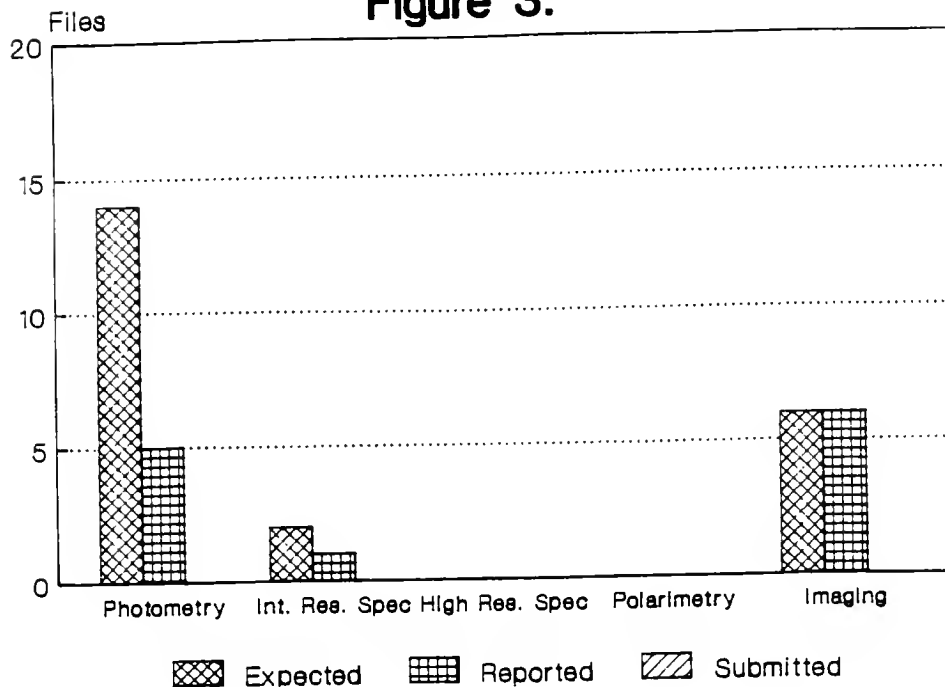


Figure 2.

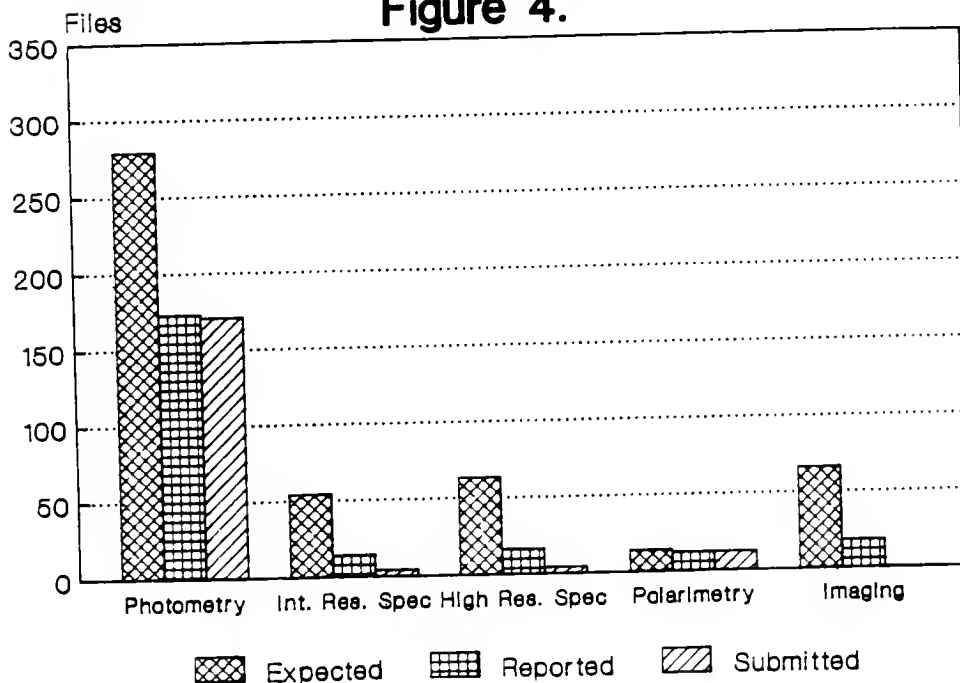
Infrared Data Status (G-Z)

Figure 3.



Infrared Data Status (Halley)

Figure 4.



Giacobini-Zinner Infrared Science Monthly Log of Observations

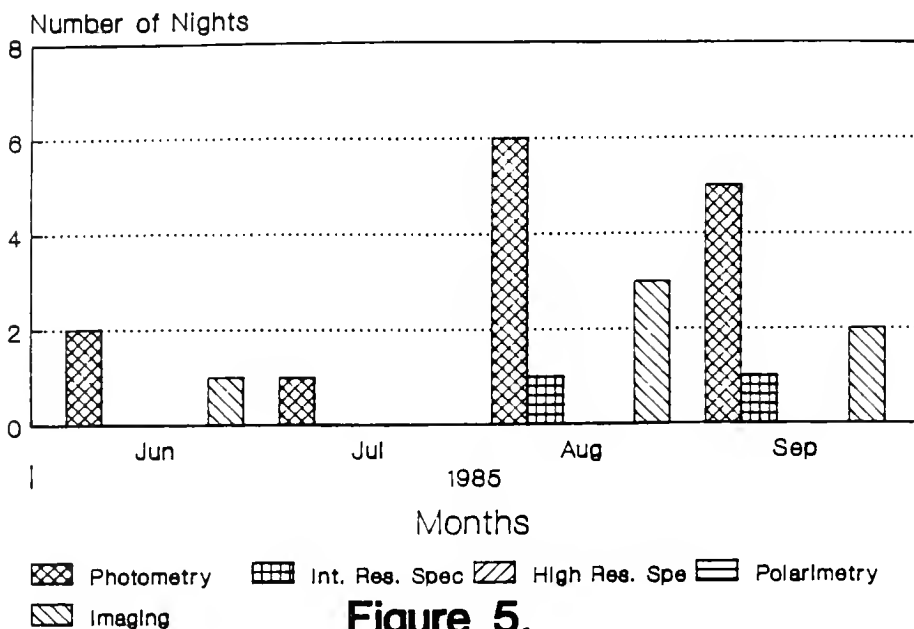


Figure 5.

Halley Infrared Science Monthly Log of Observations

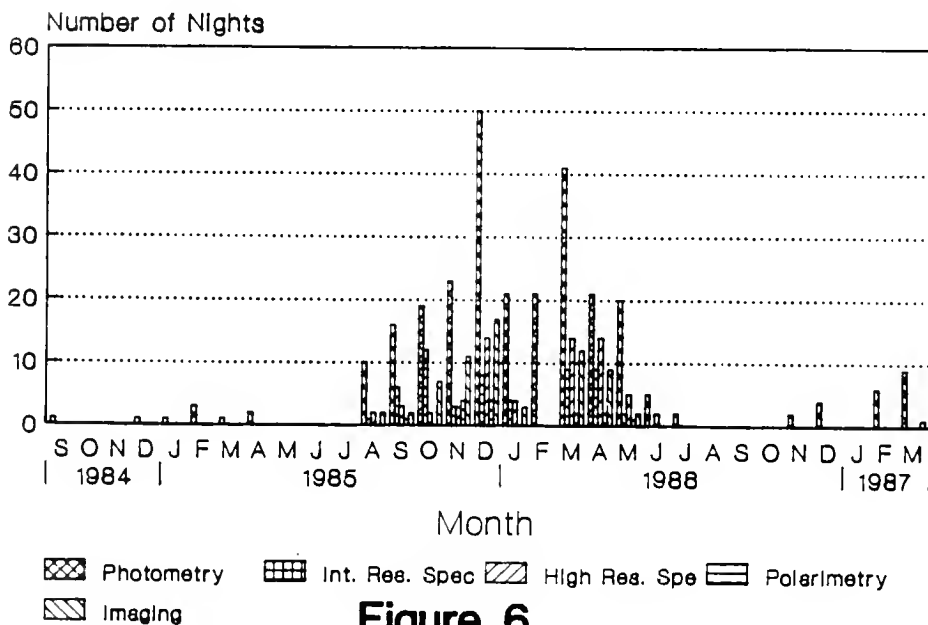


Figure 6.

E X T E N D E D A B S T R A C T S

ABSTRACTS

COMET DUST WORKSHOP

1. L. J. Allamandola, S. A. Sandford, and F. P. J. Valero - "Interstellar Grain Chemistry and the Composition of Comets"
2. Jesse D. Bregman - "The Spectral Appearance of Comets from the 5-20 μ m: A Survey of the Data"
3. T. Y. Brooke and R. F. Knacke - "The Near-Infrared Polarization and Color of Comet Halley: What Can we Learn About the Grains?"
4. M. R. Combi, T. B. McCord, J. F. Bell, R. H. Brown, R. N. Clark, D. P. Cruikshank, T. V. Johnson, L. A. Lebofsky, and D. L. Matson - "IR-Dust Observations of Comet Tempel 2 with CRAF VIMS"
5. Neil Divine - "Cometary Dust Size Distributions from Flyby Spacecraft"
6. N. Eaton, S. M. Scarrott, and R. F. Warren-Smith - "Polarization Images of Comet Halley"
7. Th. Encrenaz, J. Crovisier, M. Combes, V.I. Moroz, and A. Grigoriev - "Detection of Parent Molecules in the IR Spectrum of P/Halley with the IKS-Vega Spectrometer"
8. R. D. Gehrz and E. P. Ney - "Infrared Observations of P/Halley and P/Encke"
9. W. Glaccum, S. H. Moseley, H. Campins, and R. F. Loewenstein - "Airborne 20-65 Micron Spectrophotometry of Comet Halley"
10. Martha S. Hanner and Ray L. Newburn - "Infrared Observations of Comet Wilson"
11. Thomas L. Hayward, Gary L. Grasdalen and S. F. Green - "An Albedo Map of P/Halley on 13 March 1986"
12. Donald R. Huffman - "The Problem of Clustering in Laboratory Studies of Cometary Dust"
13. P. L. Lamy and J. M. Perrin - "Light Scattering of Large Rough Particles: Application to Cometary Grains"
14. David J. Lien - "Thermal Properties of Heterogeneous Grains"
15. David K. Lynch and Ray W. Russell - "Comet Halley's Colorful Outbursts"
16. D. K. Lynch, R. W. Russell, F. C. Witteborn, J. M. Bregman, D. M. Rank, M. C. Cohen, and H. C. Campins - "5-13 μ m Airborne Observations of Comet Wilson 1986: Preliminary Results"
17. P. Meakin and B. Donn - "Aerodynamical Properties of Fractal Grains: Implications for the Primordial Solar Nebula"
18. Karen J. Meech - "Color Gradients in the Coma of P/Halley"
19. Tadashi Mukai - "Optical Properties of Cometary Grains"
20. C. H. Perry, S. F. Green, J. A. M. McDonnell - "A Possible Explanation for the Inconsistency Between the Giotto Grain Mass Distribution and Ground-Based Observations"
21. K. Sellgren - "Properties of Interstellar Dust in Reflection Nebulae"
22. John R. Stephens and Bo A. S. Gustafson - "Laboratory Simulations of Comet Surfaces"

23. K. S. Krishna Swamy, S. A. Sandford, L. J. Allamandola, F. C. Witteborn, and J. D. Bregman - "A Multicomponent Model of the Infrared Emission from Comet Halley"
24. A. T. Tokunaga, W. F. Golisch, D. M. Griep, C. D. Kaminski, and M. S. Hanner - "The NASA Infrared Telescope Facility Comet Halley Monitoring Program II. Post-Perihelion Results"

INTERSTELLAR GRAIN CHEMISTRY AND THE COMPOSITION OF COMETS

L. J. Allamandola, S. A. Sandford, and F. P. J. Valero
NASA-Ames Research Center, Mail Stop 245-6
Moffett Field, CA 94035

During the past 15 years considerable progress in observational techniques has been achieved in the middle infrared ($5000\text{--}500\text{ cm}^{-1}$, $2\text{--}20\mu\text{m}$), the spectral region most diagnostic of molecular vibrations. Spectra of many different astronomical infrared sources, some deeply embedded in dark molecular clouds, are now available. These spectra provide a powerful probe, not only for the identification of interstellar molecules in both the gas and solid phases, but also of the physical and chemical conditions which prevail in these two very different domains.

By comparing these astronomical spectra with the spectra of laboratory ices, one can determine the composition and abundance of the icy materials frozen on the cold (10 K) dust grains present in the interior of molecular clouds (Tielens *et al.*, 1984; Tielens and Allamandola, 1987). These grains and their ice mantles may well be the building blocks from which comets are made. Thus, it is possible to learn something about the cometary materials by studying the photochemistry of interstellar ice analogs in the laboratory.

In the experiments described here we proceed with the assumption that cometary ices are similar to (and probably derived from) interstellar ices. As an illustration of the processes which can take place as an ice is irradiated and subsequently warmed, we present the infrared spectra of the mixture $\text{H}_2\text{O}:\text{CH}_3\text{OH}:\text{CO}:\text{NH}_3:\text{C}_6\text{H}_{14}$ (100:50:10:10:10). Apart from the last species, the ratio of these compounds is representative of the simplest ices found in interstellar clouds. The last component was incorporated into this particular experiment as a tracer of the behavior of a non-aromatic hydrocarbon. Figure 1 shows the change in the composition that results from ultraviolet photolysis of this ice mixture using a UV lamp to simulate the interstellar radiation field. Photolysis produces CO , CO_2 , CH_4 , HCO , H_2CO , as well as a family of moderately volatile hydrocarbons. As can be seen in Figures 2 and 3, less volatile carbonaceous materials are also produced.

Figure 2 shows the evolution of the infrared spectrum of the ice as the sample is warmed up to room temperature. We believe that the changes are similar to those which occur as ice is ejected from a comet and warmed by solar radiation. The warm-up sequence shows that the nitrile- or iso-nitrile ($-\text{CEN}$ or CEN)-bearing compound produced during photolysis evaporates between 200 and 250 K, suggesting that it is carried by a small molecular species. These molecules could be similar to the source material on comet Halley that is ejected in grains into the coma, freed by sublimation, and photolyzed by solar radiation to produce the observed CEN jets. The presence of several different types of $-\text{CH}_3$ and $-\text{CH}_2$ -bearing molecules in the residues is indicated by the spectral structure in the $3000\text{--}2700\text{ cm}^{-1}$ ($3.3\text{--}3.6\mu\text{m}$) region (Fig. 3). The profile and position of the " $3.4\mu\text{m}$ " emission feature in comet Halley indicates that the carrier of the cometary band is dominated by $-\text{CH}_3$ groups, while the band observed towards the galactic center and in this laboratory experiment indicates the presence of $-\text{CH}_2$ -dominated hydrocarbons (comet Halley: see papers by Danks, Tokunaga, and others in this report, as well as Baas, Geballe, and Walther, 1986; Galactic Center: see Allan and Wickramasinghe, 1981, and Jones *et al.*, 1983).

References

- Allen, D. A. and Wickramasinghe, D. T., 1981, *Nature*, **294**, 239.
Baas, F., Geballe, T. R., and Walther, D. M., 1986, *Astrophys. J.*, **311**, L97.
Jones, T. J., Hyland, A. L., and Allen, D. A., 1983, *Mon. Not. Roy. Soc.*, **205**, 187.
Tielens, A. G. G. M. and Allamandola, L. J., 1987, in *Physical Processes in Interstellar*

Clouds, eds. G. Morfill and M. Schaler, D. Reidel: Dordrecht, in press.
 Tielens, A. G. G. M., Allamandola, L. J., Bregman, J., Goebel, J., d'Hendecourt, L. B.,
 and Witteborn, F. C., 1984, *Astrophys. J.*, **287**, 697.

PHOTOCHEMICAL EVOLUTION OF
 $\text{H}_2\text{O} : \text{CH}_3\text{OH} : \text{NH}_3 : \text{CO} : \text{C}_6\text{H}_{14}$
 100 : 50 : 10 : 10 : 10

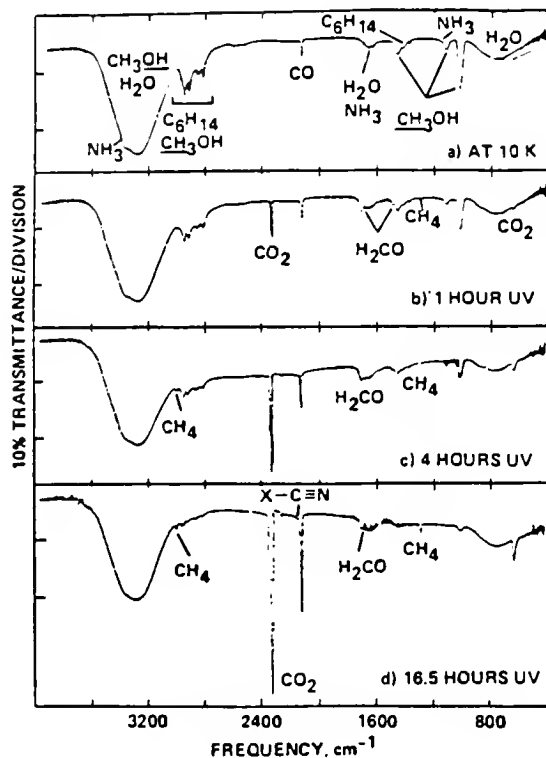


FIGURE 1

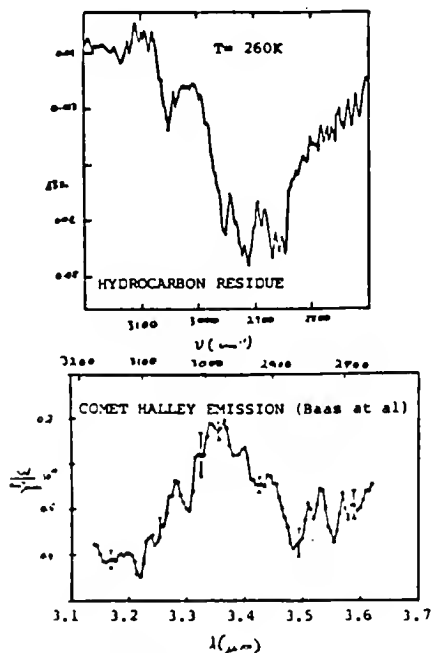


FIGURE 3

WARM-UP BEHAVIOR OF LOW VOLATILITY
 RESIDUE PRODUCED BY 15 HOURS
 PHOTOLYSIS OF $\text{H}_2\text{O} : \text{CH}_3\text{OH} : \text{CO} : \text{NH}_3 : \text{C}_6\text{H}_{14}$
 100 : 50 : 10 : 10 : 10

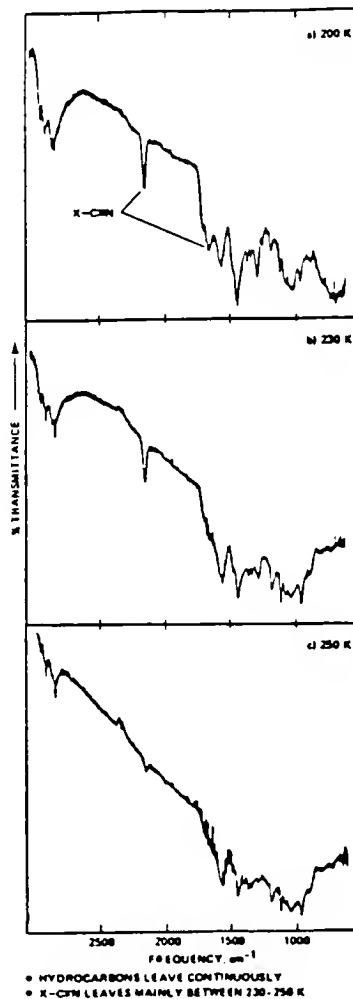


FIGURE 2

THE SPECTRAL APPEARANCE OF COMETS FROM 5-20 μ m: A SURVEY OF THE DATA

Jesse D. Bregman
NASA-Ames Research Center
Moffett Field, CA 94035

1. THE "EXPECTED" SPECTRAL APPEARANCE OF COMETS

Based on the concept of comets as being conglomerates of rocks and ices, we expect them to reflect these components in their emission spectra. Silicate materials (rocks) are common in many astronomical environments and show prominent features at about 10 and 18 μ m. Carbon, either in its amorphous or graphitic form, should be abundant, but is much more difficult to detect spectroscopically since it has no strong features (except for the hydrogenated forms). Ices are surely present in comets, but they are difficult to detect since they are volatile enough to dissipate when the comet is bright enough to be easily observed in the IR, with present equipment. There are certainly other materials present in comets, but the ones listed above should be the most common and thus dominate the thermal IR spectrum.

2. THE OBSERVATIONS

Table 1 summarizes most of the IR observations made on comets between 5 and 20 μ m. They fall into three broad categories: (1) filter photometry with spectral resolution $R \approx 10$, (2) CVF (circular variable filter wheel) spectroscopy with $R \approx 50$, and (3) spectra obtained with multi-detector grating spectrometers and $R \approx 50$ -100.

2.1 Filter Photometry

Photometry with narrowband ($R \approx 10$) or broadband ($R \approx 2$) filters has shown several important characteristics of cometary dust that are listed below.

1. Thermal emission is from dust at a temperature above that expected from a blackbody at the same distance from the sun (in some comets), indicating that the dust particles are small (Becklin and Westphal, 1966; Maas, Ney, and Woolf, 1970).

2. Silicates are a prominent component of comet dust since the spectra show a strong emission feature at 10 μ m (Maas, Ney, and Woolf, 1970).

3. Large particles, which are present along with small particles in cometary comae, do not show the 10 μ m silicate feature, and are not hotter than a blackbody. This effect was striking in comet Kohoutek which had hot dust with a silicate feature in the tail and coma, while the anti-tail dust was much cooler and did not show a silicate feature (Ney, 1974).

4. The apparent strength of the silicate feature varies with distance from the sun; and beyond about 1.5 A.U. there are no observations of a silicate feature in any comet (Rieke and Lee, 1974; Hanner *et al.*, 1987). This may in some part be due to the paucity of observations of comets at distances beyond 1 A.U. from the sun.

5. The data indicate that a single blackbody temperature does not completely describe the dust emission, but that a mixture of particle sizes (and thus emission from a range of temperatures) is needed to fit the spectra.

2.2 CVF Observations

Filter photometry has provided insight into the bulk nature of cometary dust and has even shown the broad emission features that identify silicates as a component material. To provide more detailed compositional information, higher resolution spectra are needed. The earliest of these spectra were obtained with single-detector systems using a continuously variable circular filter (CVF) and covered the wavelength range from 8-13 μ m. A spectrum of comet Bennet (Hackwell, 1971) had poor signal to noise, but still showed a strong silicate emission band at 10 μ m. Merrill (1974) obtained an excellent spectrum of comet Kohoutek, but had missing data in the 11 μ m region. It showed a smooth silicate emission, similar to that seen in stars.

2.3 Multi-Detector Grating Spectrometers

Since CVFs obtain data one point at a time, spectra can only be obtained of bright comets. Multi-detector spectrometers can cover the entire 8-13 μ m range simultaneously, thus providing the opportunity to obtain good quality spectra of considerably fainter comets. Hanner *et al.* (1984, 1985a, 1985b) observed three comets between 8-13 μ m which showed smooth spectra consistent with at most a 20 percent contribution from small silicate grains (comets Grigg-Skjellerup, Churyumov-Gerasimenko, and IRAS-Araki-Alcock). Feierberg *et al.* (1984) obtained similar results for comet IRAS-Araki-Alcock. Comet Halley was quite different, showing a strong silicate emission spanning the entire 8-13 μ m region, and it was the first comet to show structure in the 10 μ m silicate band indicative of a specific mineral type, olivine (Bregman *et al.*, 1987). The data also compared well with a spectrum generated from a combination of laboratory spectra of interplanetary dust particles as long as the mix was dominated by olivine-type material. Comet Giacobini-Zinner (Bregman, unpublished) shows similar structure, but the features are much weaker.

Details of the 20 μ m region are much less certain. Photometry shows excess emission consistent with silicate emission (when there is a 10 μ m silicate emission feature), but the single spectroscopic observation of a comet in this region (of Halley by Herter *et al.*, 1986) does not show the silicate feature at the expected strength.

TABLE 1
IR SPECTRAL OBSERVATIONS OF COMETARY DUST 5-20 μ m
(Through the 20th ESLAB Symposium on the Exploration of Halley's Comet)

COMET	TYPE OF OBSERVATION	REFERENCE
Ikeya-Seki	photometry	Becklin, E.E., and Westphal, J.A. 1966, <u>Ap.J.</u> , 145 , 445.
Bennet	photometry 2-20 μ m	Maas, R.W., Ney, E.P., and Woolf, N.J. 1970, <u>Ap.J.Lett.</u> , 160 , L101.
	CVF 8-13 μ m	Hackwell, J.A. 1971, <u>Observatory</u> , 91 , 33.
	photometry .5-18 μ m vs. R. Comets Enke, Bradfield, and Kohoutek too.	Ney, E.P. 1974b, <u>ICARUS</u> , 23 , 551.
Kohoutek	photometry .5-18 μ m nucleus, anti-tail	Ney, E.P. 1974a, <u>Ap.J.Lett.</u> , 189 , L141.
	photometry 2.2-22.5 μ m vs. R	Rieke, G.H. and Lee, T.A. 1974, <u>Nature</u> , 248 , 737.
	photometry 1-20 μ m vs. R, polarimetry 1.03, 1.65 μ m	Noguchi, K., Sato, S., Maihara, T., Okuda, H., and Uyama, K. 1974, <u>ICARUS</u> , 23 , 545.
	photometry .5-18 μ m vs. R. Comets Enke, Bradfield, and Bennet too.	Ney, E.P. 1974b, <u>ICARUS</u> , 23 , 551.
	photometry 1.25-12.5 μ m vs. R and aperture	Gatley, I., Becklin, E.E., Neugebauer, G., and Werner, M.W. 1974, <u>ICARUS</u> , 23 , 561.
	CVF 8-13 μ m	Merrill, K.M. 1974, <u>ICARUS</u> , 23 , 566.
	photometry 8.8-21 μ m vs. R.	Zeilik, M. and Wright, E.L. 1974, <u>ICARUS</u> , 23 , 577.
West	photometry .5-18 μ m vs. R.	Ney, E.P. and Merrill, K.M. 1976, <u>Science</u> , 194 , 1051.
		Kawara, K., Kobayashi, Y., Maihara, T., Noguchi, K. Okuda, H., Sato, S., Iijima, T., and Ono 1978, <u>PASJ</u> , 30 , 149.
Kobayashi-Berger-Milon	photometry .7-12.5 μ m also West and Bradfield	Ney, E.P. 1982, in <u>Comets</u> , ed. Wilkening, (The University of Arizona Press: Tuscon), 323.

Bradfield	photometry .7-12.5 μ m also West and K-B-M	Ney, E.P. 1982, in <u>Comets</u> , ed. Wilkening, (The University of Arizona Press: Tuscon), 323.
	photometry .5-18 μ m vs. R. Comets Enke, Kohoutek, and Bennet too.	Ney, E.P. 1974b, <u>ICARUS</u> , 23 , 551.
Stephen- Oterma	photometry 4.8-20 μ m	Hanner, M., Tokunaga, A.T., Veeder, G.J., and A'Hearn, M.F. 1984, <u>A.J.</u> , 89 , 162.
Swift- Gehrels	photometry 4.8-12 μ m	
Gunn	photometry 10&20 μ m	
Grigg- Skjellerup	photometry 3.5-20 μ m	
Grigg- Skjellerup	multichannel spectro- meter, 8-13 μ m	Hanner, M., Aitken, D., Roche, P. and Whitmore, B. 1984, <u>A.J.</u> , 89 , 170.
IRAS-Araki- Alcock	multichannel spectro- meter, 8-13 μ m	Feierberg, M.A., Witteborn, F.C., Johnson, J.R. and Campins, H. 1984, <u>ICARUS</u> , 60 , 449.
	multichannel spectro- meter, 8-13 μ m CVF 2.2-4.0 μ m	Hanner, M.S., Aitken, D.K., Knacke, R., McCorkle, S., Roche, P.F. and Tokunaga, A.T. 1985, <u>ICARUS</u> , 62 , 97.
	IRAS photometry	Walker, R.G., Aumann, H.H., Davies, J., Green, S., DeJong, T., Houck, J.R. and Soifer, B.T. 1984, <u>Ap.J.Lett.</u> , 278 , L11.
	photometry, 10 μ m	Brown, R.H., Cruikshank, D.P., and Griep, D. 1975, <u>ICARUS</u> , 62 , 273.
Crommelin	photometry 1.25-20 μ m	Hanner, M.S., Knacke, R., Sekanina, Z., and Tokunaga, A.T. 1985, <u>A&A</u> , 152 , 177.
Churyumov- Gerasimenko	photometry 1.25-20 μ m vs. R. Multichannel spectrometer 8-13 μ m	Hanner, M.S., Tedesco, E., Tokunaga, A.T., Veeder, G.J., Lester, D.F., Witteborn, F.C., Bregman, J.D., Gradie, J. and Lebofsky, L. 1985, <u>ICARUS</u> , 64 , 11.
Halley	photometry 1.25-20 μ m vs. R.	Tokunaga, A.T., Golisch, W.F., Griep, D.M., Kaminski, C.D. and Hanner, M.S. 1986, <u>A.J.</u> , 92 , 1183.
	photometry 2.2-20 μ m vs. R.	Hanner, M.S., Tokunaga, A.T., Golisch, W.F., Griep, D.M. and Kaminski, C.D. 1987, <u>A&A</u> , in press.

Halley (cont.)	multichannel spectrometer, 5-13 μ m	Bregman, J.D., Campins, H., Witteborn, F.C., Wooden, D.H., Rank, D.M., Allamandola, L.J., Cohen, M., and Tielens, A.G.G.M. 1987, <u>A&A</u> , in press.
	multichannel spectrometer, 5-10 μ m.	Campins, H., Bregman, J.D., Witteborn, F.C., Wooden, D.H., Rank, D.M., Allamandola, L.J., Cohen, M. and Tielens, A.G.G.M. 1986, in <u>Exploration of Halley's Comet</u> , Proc. 20 th ESLAB Symposium, ESA SP-250 II, 121.
	multichannel spectrometer, 16-30 μ m.	Herter, T., Gull, G.E., and Campins, H. 1986, in <u>Exploration of Halley's Comet</u> , Proc. 20 th ESLAB Symposium, ESA SP-250 II, 117.
	photometry 1.25-20 μ m	Gehrz, R.D. and Ney, E.P. 1986, in <u>Exploration of Halley's Comet</u> , Proc. 20 th ESLAB Symposium, ESA SP-250 II, 101.
	photometry 10 μ m	Russell, R.W., Lynch, D.K., Rudy, R.J., Rossano, G.S., Hackwell, J.A., and Campins, H.C. 1986, in <u>Exploration of Halley's Comet</u> , Proc. 20 th ESLAB Symposium, ESA SP-250 II, 125.
	photometry 1.25-19 μ m vs. R	Green, S.F., McDonnell, J.A.M., Pankiwicz, G.S.A., and Zarnecki, J.C. 1986, in <u>Exploration of Halley's Comet</u> , Proc. 20 th ESLAB Symposium, ESA SP-250 II, 81.

THE NEAR-INFRARED POLARIZATION AND COLOR OF COMET HALLEY: WHAT CAN WE LEARN ABOUT THE GRAINS?

T. Y. Brooke and R. F. Knacke
Astronomy Program
Department of Earth and Space Sciences
State University of New York at Stony Brook
Stony Brook, NY 11794

The near-infrared polarization and JHK colors of light scattered by dust grains in comet Halley were measured over a wide range in phase angle and heliocentric distance (Ref. 1). Colors were *redder* than solar with no statistically significant variation with phase angle, heliocentric distance, or pre- and post-perihelion. This suggests, but does not guarantee, that the grain population did not change drastically over time and that the data may be combined and modeled. However, short-term variations in visible polarization (Ref. 2) and dust albedo (Ref. 3) were seen in Halley. Also, near-infrared colors became systematically bluer after our observations were completed (Ref. 4).

The near-infrared colors of Halley fall in the range of those of other comets. Red JHK colors are typical of the scattering by size distributions of particles with effective size larger than a few microns for a wide range of materials, even for constant refractive index (Ref. 5). On the other hand comet nuclei may have similar near-infrared colors (Refs. 6, 7). So except for ruling out a significant cross section of small (Rayleigh) grains, JHK colors alone may not be particularly diagnostic of grain properties. Modeling of both polarization and color is *potentially* more powerful.

The near-infrared polarization is similar to the visible polarization of Halley and other comets in showing a negative branch at small phase angles and an approximately linear rise toward positive values at larger phase angles. This is qualitatively similar to low-albedo asteroid surfaces for which the negative branch is usually ascribed to double reflections with shadowing by rough surfaces (Ref. 8). However, the polarization of Halley *increases* with wavelength at large phase angles (Fig. 1), contrary to the available polarimetry of most asteroids (e.g., Ref. 9) and the interplanetary dust (Ref. 10). Future work should address this fact.

Mie theory calculations and a size distribution based on spacecraft data were used to model the near-infrared polarization and color of comet Halley (Ref. 11). Two components were needed: a "dirty" silicate and a more absorbing material similar to the composite material proposed to explain the thermal emission of several comets (Ref. 12). The silicate spheres, rather than rough surfaces, provided the negative branch. The model successfully reproduced the wavelength dependence of the polarization. This required wavelength-dependent refractive indices; in particular, the imaginary part of the index of refraction had to increase with wavelength, which is typical in absorbing materials at these wavelengths.

Numerous lines of evidence point to the presence of dark, absorbing, probably carbonaceous material in comets. Mie theory models of the near-infrared polarization and color tend to corroborate these results.

Models incorporating rough surfaces on the grains appear to be capable of matching both the negative branch of the visible polarization and the enhanced backscattering of cometary grains (Ref. 13).

One question is whether comet grains could be expected to scatter like spheres. The answer is probably not. Interplanetary dust particles are irregularly shaped aggregates with rough surfaces. Laboratory measurements and theoretical studies of rough particles show significant deviations from spheres both in phase function and the polarization. The

broader question is whether compositional implications derived from rough particle models will contradict those drawn from Mie theory calculations; i.e., how model-dependent are the results? An answer to this question will help determine what we can learn about cometary dust from remote measurements of polarization and color.

References

1. Brooke, T. Y., Knacke, R. F., and Joyce, R. R., 1986, *20th ESLAB Symp. ESA SP-250*, Vol. II, p. 87.
2. Mukai, T., Mukai, S., and Kikuchi, S., 1987, Symp. on the *Diversity and Similarity of Comets*, *ESA SP-278*, in press.
3. Gehrz, R. D. and Ney, E. P., 1986, *20th ESLAB Symp. ESA SP-250*, Vol. II, p. 101.
4. Tokunaga, A. T., 1987, these proceedings.
5. Jewitt, D. and Meech, K. J., 1986, *Ap. J.*, **310**, 937.
6. Hartmann, W. K., Cruikshank, D. P., and Degewij, J., 1982, *Icarus*, **52**, 377.
7. Brooke, T. Y. and Knacke, R. F., 1986, *Icarus*, **67**, 80.
8. Wolff, M., 1975, *Appl. Opt.*, **14**, 1395.
9. Zellner, B. and Gradie, J., 1976, *Icarus*, **28**, 117.
10. Leinert, C., *et al.*, 1981, *Astr. Ap.*, **103**, 177.
11. Brooke, T. Y., Knacke, R. F., and Joyce, R. R., 1986, *Astr. Ap.*, in press.
12. Hanner, M. S., 1983, in *Cometary Exploration*, ed. T. I. Gombosi, Hungar. Acad. Sciences, Budapest, **2**, 1.
13. Lamy, P. and Perrin, J., 1986, *20th ESLAB Symp. ESA SP-250*, Vol. II, p. 65.
14. Mukai, T., Mukai, S., and Kikuchi, S., 1986, *20th ESALB Symp. ESA SP-250*, Vol II, p. 59.

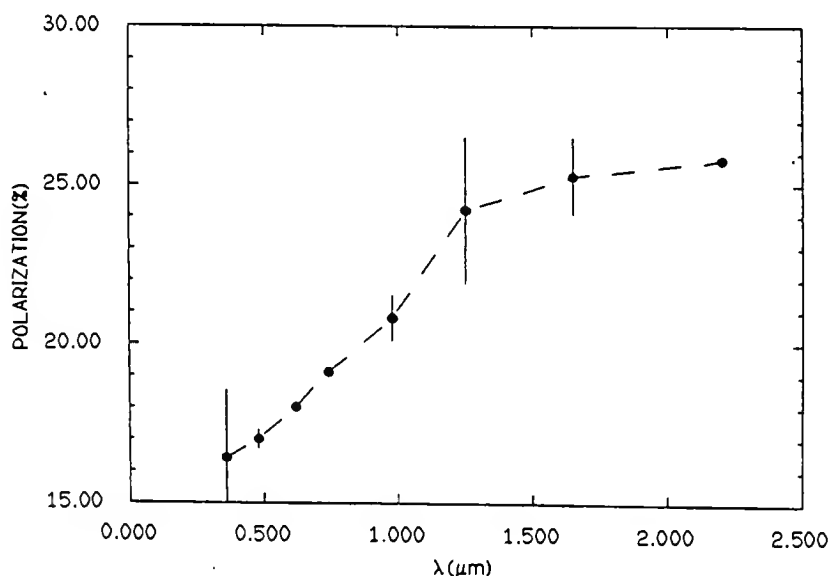


Fig. 1. Wavelength dependence of the polarization of the dust continuum of comet Halley at phase angle $\beta = 65^\circ$. Points below $1 \mu\text{m}$ are from Ref. 14, near-infrared points from Ref. 1.

IR-DUST OBSERVATIONS OF COMET TEMPEL 2 WITH CRAF VIMS

M. R. Combi¹, T. B. McCord², J. F. Bell², R. H. Brown³, R. N. Clark⁴,
D. P. Cruikshank⁵, T. V. Johnson³, L. A. Lebofsky⁶, and D. L. Matson³

¹Atmospheric and Environmental Research, Inc., Cambridge, MA 02139

²Hawaii Institute of Geophysics, U. Hawaii, Honolulu, HI 96822

³Jet Propulsion Laboratory, Pasadena, CA 91109

⁴U.S. Geological Survey, Denver, CO 80225

⁵Institute for Astronomy, U. Hawaii, Honolulu, HI 96822

⁶Lunar and Planetary Laboratory, U. Arizona, Tucson, AZ 85721

Measurement strategies are now being planned for using the Visual and Infrared Mapping Spectrometer (VIMS) to observe the asteroid Hestia, and the nucleus, and the gas and dust in the coma of comet P/Tempel 2 as part of the Comet Rendezvous Asteroid Flyby (CRAF) mission. The spectral range of VIMS will cover wavelengths from 0.35 to 5.2 μ m, with a spectral resolution of 11 nm from 0.35 to 2.4 μ m (192 channels) and of 22 nm from 2.4 to 5.2 μ m (128 channels). The instantaneous field of view (IFOV) provided by the foreoptics is 0.5 milliradians, and the current design of the instrument provides for a scanning secondary mirror which will scan a swath of length 72 IFOVs. The CRAF high-resolution scan platform motion will permit slewing VIMS in a direction perpendicular to the swath. This enables the building of a two-dimensional image in any or all wavelength channels. Important measurements of the dust coma will include the onset of early coma activity, the mapping of gas and dust jets and correlations with active nucleus areas, observations of the dust coma from various scattering phase angles, coverage of the low-wavelength portion of the thermal radiation, and the 3.4 μ m hydrocarbon emission. A basic description of the VIMS instrument, its general role in the CRAF mission, and in particular the important planned dust coma measurements, will be presented.

Cometary Dust Size Distributions from Flyby Spacecraft

Neil Divine

Jet Propulsion Laboratory, California Institute of Technology
 Pasadena, CA 91109, U.S.A.

Prior to the Halley flybys in 1986 the distributions of cometary dust grains with particle size were approximated using models which provided reasonable fits to the dynamics of dust tails, anti-tails, and infrared spectra. These distributions have since been improved using fluence data (i.e., particle fluxes integrated over time along the flyby trajectory) from three spacecraft. We fit these data using the dust particle mass m and the dummy variable

$$x = (m/m_t)^{1/\gamma}$$

in the form

$$F = F_t \left[(1+x)^{\beta-1} / x^{\beta} \right]^{\alpha\gamma}$$

for the cumulative fluence. Here the transition mass m_t separates sizes for which the relevant power law exponents have the values α , $\alpha+1$, 3α , and $3\alpha+1$ (for cumulative mass, incremental mass, cumulative radius, and incremental radius distributions, respectively, at large mass) from those for which they have the smaller values $\alpha\beta$, $\alpha\beta+1$, $3\alpha\beta$, and $3\alpha\beta+1$ (at small mass). Typical values of $\beta=0.2$ for the data (as contrasted with $\beta=0$ for the predicted model) reflect the rich abundance in the coma of particles smaller than several tenths of a micron diameter. This result is illustrated by the entries in the table below. The particle outflow velocities also play a role in deriving the production distribution of the grains at the nucleus surface. The fluence-derived distributions are appropriate for comparison with simultaneous infrared photometry (from Earth) because they sample the particles in the same way as the IR data do (along the line of sight) and because they are directly proportional to the concentration distribution in that region of the coma which dominates the IR emission.

Fluence	α	β	γ	m_t (kg)	F_t (m ⁻²)
Model	0.955	0.0	1.0	2.13×10^{-15}	2.9×10^8
<i>Giotto</i>	0.94	0.19	1.0	2.0×10^{-14}	8.07×10^6
VEGA-1	1.19	0.218	1.9	1.0×10^{-12}	1.43×10^6
VEGA-2	0.90	0.29	2.16	1.6×10^{-13}	9.8×10^5

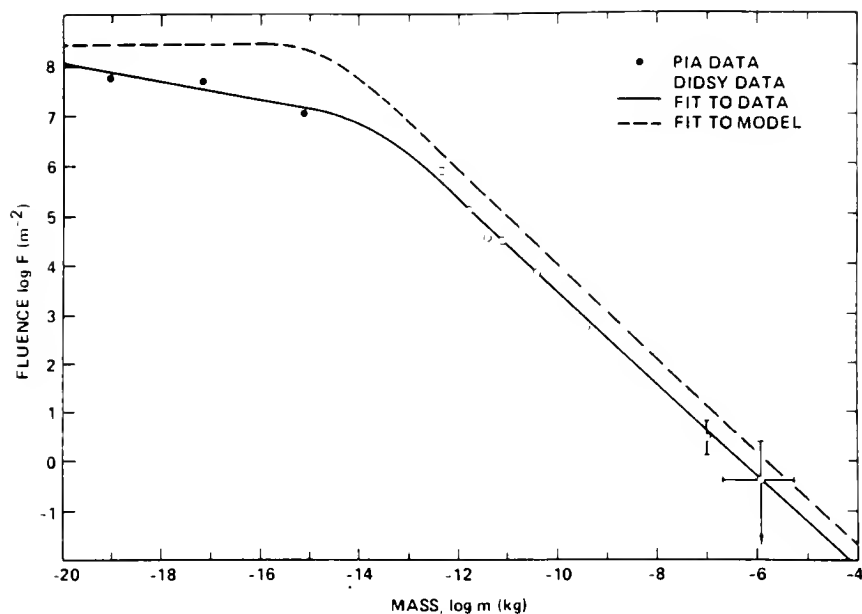


Figure 1. Sample cometary mass distributions from model and as fitted to fluence data from Giotto. Parameter values for the dashed and solid lines, respectively, appear in the first and second rows of the Table.

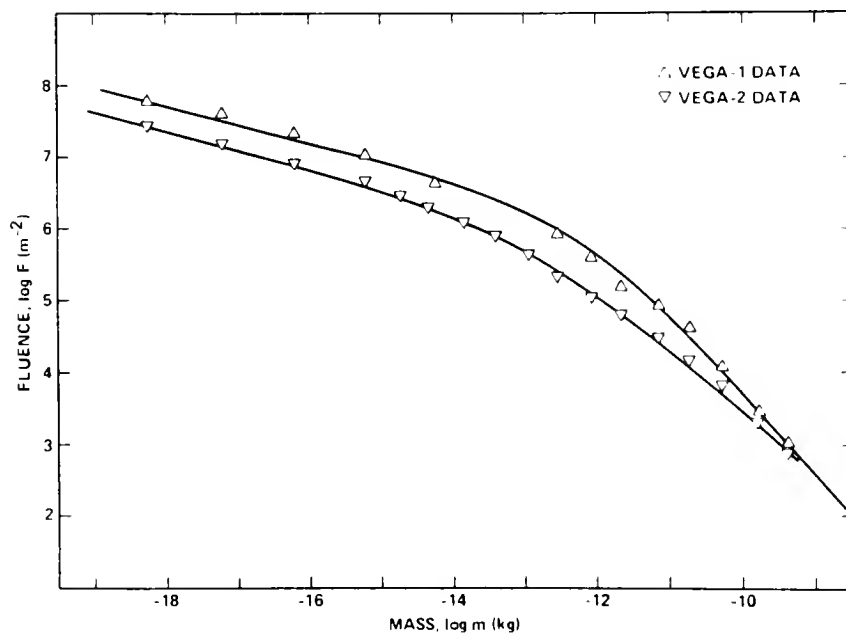


Figure 2. Sample cometary mass distributions fitted to fluence data from VEGA-1 and VEGA-2 SP-2. Parameter values appear in the third and fourth rows of the table.

POLZARIZATION IMAGES OF COMET HALLEY

N. Eaton, S. M. Scarrott and R. F. Warren-Smith
Physics Department, Durham University

Observations from two dates 16^h50^m GMT 5 January 1986 and 16^h10^m GMT 7 January 1986 are presented. The images were obtained with the Durham imaging polarimeter on the 1-m telescope of the Wise Observatory, Israel. The observations were made through a broad-band filter centered at 0.67 microns with a 0.17-micron effective bandwidth. This wavelength region should be dominated by continuum radiation. The intensity images cover 46 x 78 arcseconds.

Figure 1 shows the intensity image from 5 January in logarithmic form. A prominent anti-solar jet is readily seen. The polarization image (Fig. 2) shows that the linear polarization is higher on the whole of the sunward side of the nucleus. The jet shows up as a blob of increased polarization separated from the nucleus. There is no significant deviation of the direction of polarization from that expected from single scattering. The increase in percentage polarization could be due to a number of factors, smaller dust grains, increased dust-to-ratio, or a change in dust composition.

Figure 3 shows the intensity image from 7 January in logarithmic form. A number of dust features can be observed, with a major one pointing southeast. The percentage polarization image (Fig. 4) shows that this southeast jet produces a large excess of polarization.

If the period of rotation of dust features is taken to be 2.2 days, as is often suggested, then the two images differ by almost one complete rotation; yet the character of the two images is completely different.

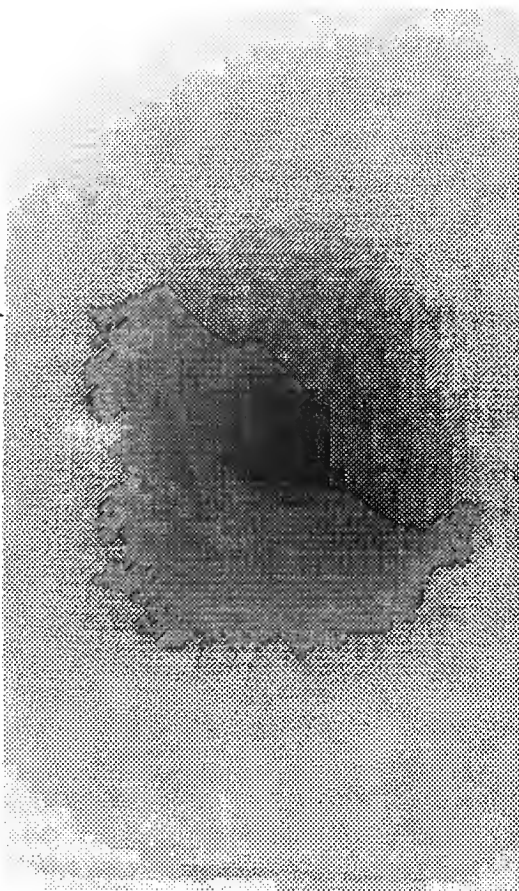


Figure 1. The intensity image from January is plotted in logarithmic form. North is up and east is to the left. The solar direction is southwest as indicated. The field is 46×78 arcseconds.



Figure 2. This shows the polarization image from 5 January. The percentage of linear polarization is plotted at each point. The gray-scale ranges from 5.9 (white) to 12.9% (black). Tick marks indicate the position of the nucleus seen in the intensity image. The scale is the same as in Figure 1. Edge effects are artifacts.

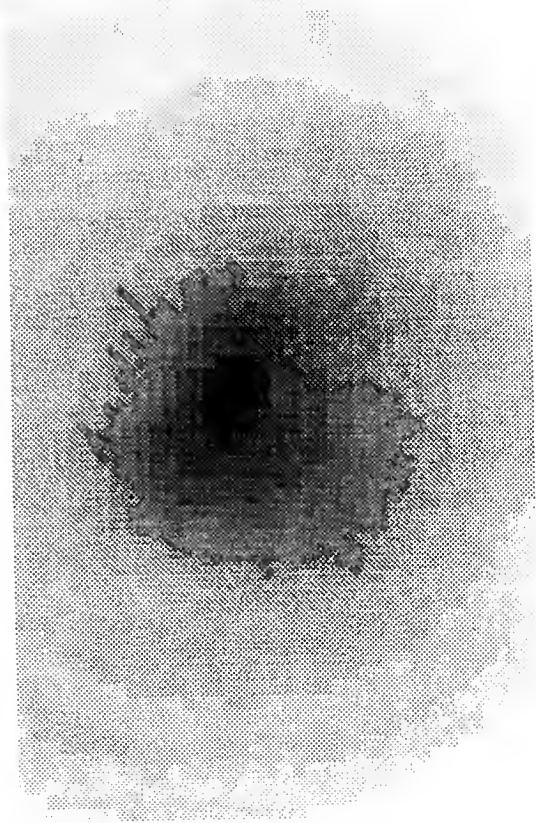


Figure 3. The intensity image from 7 January is plotted in logarithmic form. See Figure 1 for description.

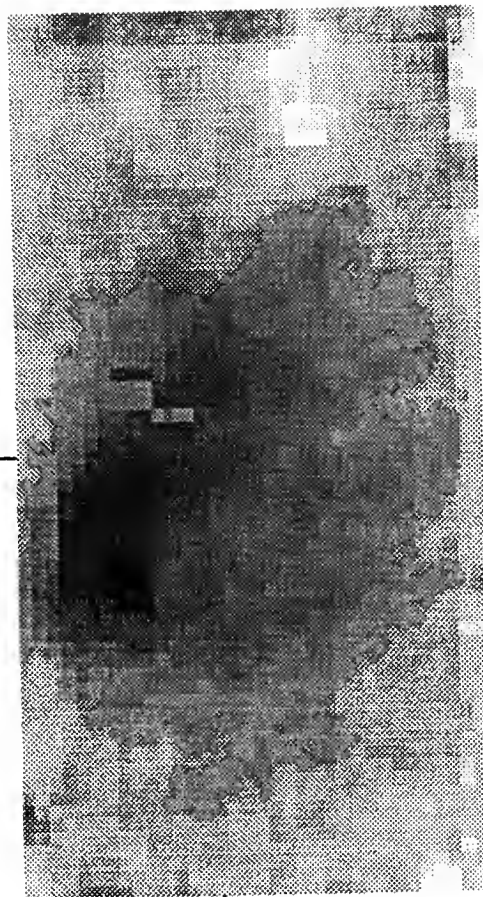


Figure 4. The polarization image from 7 January is shown. The gray-scale indicates the percentage linear polarization from 2.5 (white) to 18.4% (black). See Figure 2 for description.

DETECTION OF PARENT MOLECULES IN THE IR SPECTRUM OF P/HALLEY WITH THE IKS-VEGA SPECTROMETER

Th. Encrenaz, J. Crovisier, M. Combes
Observatoire de Paris

Meudon
France

and

V.I. Moroz, A. Grigoriev
IKI, Moscow
USSR

The two spectroscopic channels of the IKS experiment on board the VEGA probes were designed for the detection of emission bands of parent molecules and/or cometary dust, in the 2.5-5 μ m range and the 6-12 μ m range respectively. On VEGA 1, the experiment worked successfully, and cometary spectra were recorded at distances D from the comet nucleus ranging from about 250,000 to 40,000 km. The field of view was 1° and the spectral resolving power was about 50. On VEGA 2, no result could be obtained due to a failure of the cryogenic system.

The strong internal background signal caused by the (uncooled) instrument had to be eliminated. As it was not possible to use a sky chopper, the signal was only modulated by the rotation of the CVF wheel. In order to remove the background, we used the difference between the current spectrum and a reference spectrum with a very small cometary signal taken at the beginning of the sequence ($D \sim 200,000$ km). A good test of the reliability of a cometary feature is its evolution with distance D : the signal of a parent molecule, as well as the cometary dust, with a density distribution in r^{-2} , is in first order expected to vary as D^{-1} .

In the 2.5-5 μ m channel, strong emission features, which follow the expected D^{-1} variation, are attributed to parent molecules: H₂O, CO₂, and CH-bearing molecules, at 2.7, 4.3 and 3.3-3.4 μ m, respectively. Other weaker features also follow the D^{-1} law and are tentatively attributed to parent molecules: H₂CO at 3.6 μ m, CO at 4.6 and 4.7 μ m, and possibly OCS at 4.8 μ m and a CN-bearing molecule at 4.4 μ m. In addition, there is an emission feature at 2.8 μ m which does not follow the D^{-1} law but is stronger at the beginning of the sequence when the observed coma diameter is larger: it might be attributed to the daughter product OH. Finally, there is an absorption feature at 2.9 μ m which could be attributed to H₂O ice.

In the 6-12 μ m region, the cometary signal is dominated by the emission of dust, which is characterized by a blackbody emission at about 350K, with a strong and broad emission due to silicates between 8 and 12 μ m. This broad emission shows two distinct peaks at 9 and 11.2 μ m, which, as suggested by Bregman, can be well interpreted by the presence of olivine. The emission announced at 7.5 μ m in the preliminary reduction of the IKS data (Combes *et al.*, 1986) is now known to be of instrumental origin. The final IKS spectrum between 6 and 12 μ m is in very good agreement with the other spectra recorded from the KAO (Campins *et al.*, 1986; Bregman *et al.*, 1987) and from the ground (Bouchet *et al.*, 1987).

The derived production rates of H₂O and CO₂ are 10³⁰ and 2x10²⁸ respectively. Other production rates are indicated in Table 1. The 3.3-3.4 μ m feature is attributed to hydrocarbons in both the saturated (3.4 μ m) and unsaturated (3.3 μ m, alkenes and/or aromatics) forms. The fact that we see no associated features beyond 6 μ m can be simply interpreted if we assume the hydrocarbons are in the form of gaseous molecules, excited by resonant fluorescence as in the case of H₂O and CO₂. With this assumption, we derive

a total number of carbon atoms of about 30 percent of H₂O.

REFERENCES

Bregman, J. *et al.*, *Astron. Astrophys.*, in press, 1987.
 Campins, H. *et al.*, Proceedings of Heidelberg meeting, ESA, SP-250, Vol. 2, 121, 1986.
 Combes, M. *et al.*, *Nature*, 321, 266, 1986.
 Combes, M. *et al.*, proceedings of Heidelberg meeting, ESA, SP-250, Vol. 1, 353, 1987.
 Moroz, V. *et al.*, *Astron. Astrophys.*, in press, 1987.

TABLE I

Molecule	H ₂ O	CO ₂	Hydro-carbons	H ₂ CO	CO	OCS	CN-Mol
Wavelength(μm)	2.7	4.3	3.3-3.4	3.6	4.6-4.7	4.8	4.4
Production Rate (s ⁻¹)	10 ³⁰	2x10 ²⁸	2x10 ²⁹ *	5x10 ²⁸	5x10 ²⁸	5x10 ²⁷	?

*Total number of carbons.

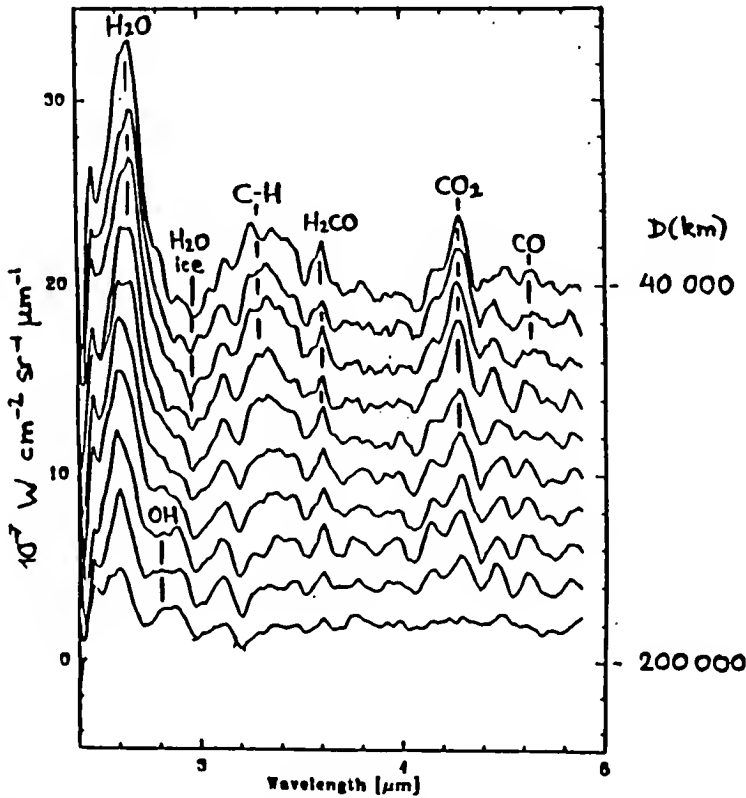


Figure 1 - Evolution of the cometary signal as a function of nucleus distance, as the spacecraft approaches the nucleus. Top: D=40,000 km; bottom: D=200,000 km.

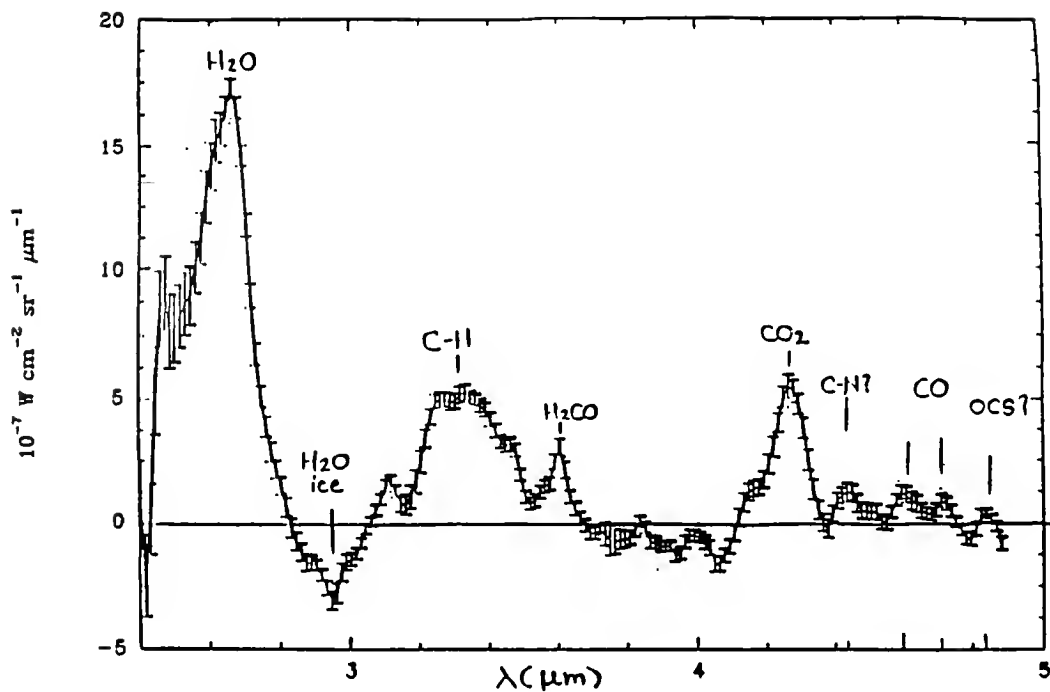


Figure 2 - Extraction of the 1/D part of the cometary signal between 2.5 and 5 μm. Signatures of secondary cometary products are eliminated in this procedure. The emissions are interpreted as the signatures of parent molecules. The vertical scale corresponds to a distance to the nucleus $D=40,000$ km.

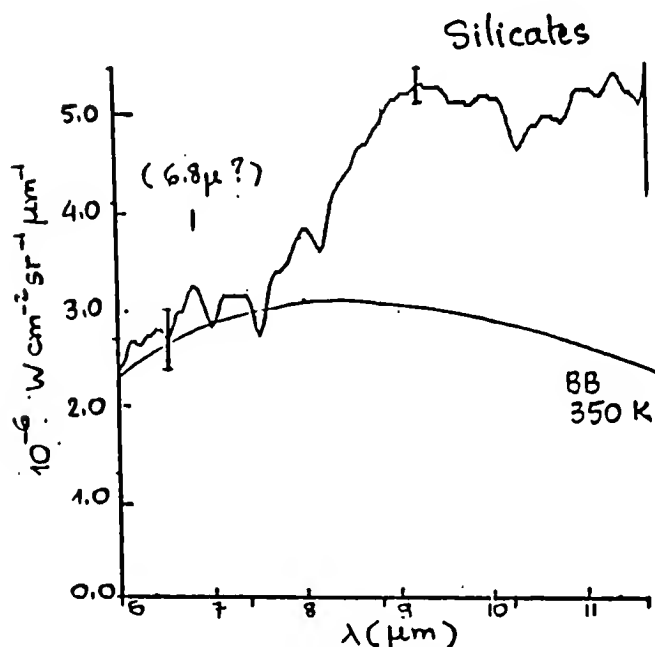


Figure 3 - The spectrum of the central coma (diameter of 700 km) between 6 and 12 μm. The broad emission between 8 and 12 μm is the silicate signature. The distance to the nucleus is 40,000 km.

INFRARED OBSERVATIONS OF P/HALLEY AND P/ENCKE

R. D. Gehrz and E. P. Ney
Astronomy Department
University of Minnesota

We used broadband optical/infrared photometers responding from 0.5 to 23 microns mounted on the University of Minnesota (UM) O'Brien 76-cm telescope, Wyoming Infrared Observatory (WIRO) 234-cm telescope, and UM's Mount Lemmon Infrared Observatory 152-cm telescope to measure P/Halley more than 30 times between 1985 December 12 and 1986 May 6. The Wyoming system was used to measure P/Encke on 1987 July 24. Our equipment and the observations of P/Halley have been more fully described by Gehrz and Ney (1986, Proc. 20th ESLAB Symposium, ESA SP-250). Conclusions based on a preliminary analysis of the P/Halley and P/Encke data are reported here.

Infrared energy distributions observed for P/Halley on several dates are shown in Figure 1. Halley showed the characteristic continuum dust emission that is probably caused by small iron and carbon grains. The continuum always was hotter than the black sphere temperature appropriate to the comet's heliocentric distance. This "superheat," which is characteristic of small comet grains because of their low emission efficiency, is a grain-size indicator. An important constituent of Halley's dust was silicate material as indicated by the presence of strong 10 and 20 μ m emission features on many occasions. The 10 μ m silicate signature was always present but varied in strength and shape for heliocentric distances within one AU. The feature was observed to be very weak for distances substantially greater than one AU. Halley's dust albedo appeared to decrease when the feature was weak. P/Encke, observed at a distance of 0.37 AU, showed very little continuum superheat and no appreciable silicate emission; the implication is that the grains in P/Encke are large.

Our observations of many comets thus far suggest a significant difference between comets which have primarily Type I (ion) tails and those which have prominent Type II (dust) tails in addition to Type I tails. P/Encke and Kobayashi/Berger/Milon are examples of the former which we shall designate IR Type I. West, Bennett, and P/Halley are examples of the latter and we designate these IR Type II. IR-Type I comets have muted or missing silicate signatures and weak superheating of the grains contributing to the continuum emission, while IR-Type II comets show strong silicate emission and continuum superheating. The silicate emission becomes weak or missing in some IR-Type II comets, like Halley, when they are at distances significantly greater than one AU. We conclude that the small grain component is severely depleted in IR-Type I comets, and that the small grain component in IR-Type II comets is incorporated into the nucleus in such a way that it can be frozen out for temperatures much lower than about 300K.

The research was supported by NASA, the University of Minnesota Graduate School, and the National Science Foundation.

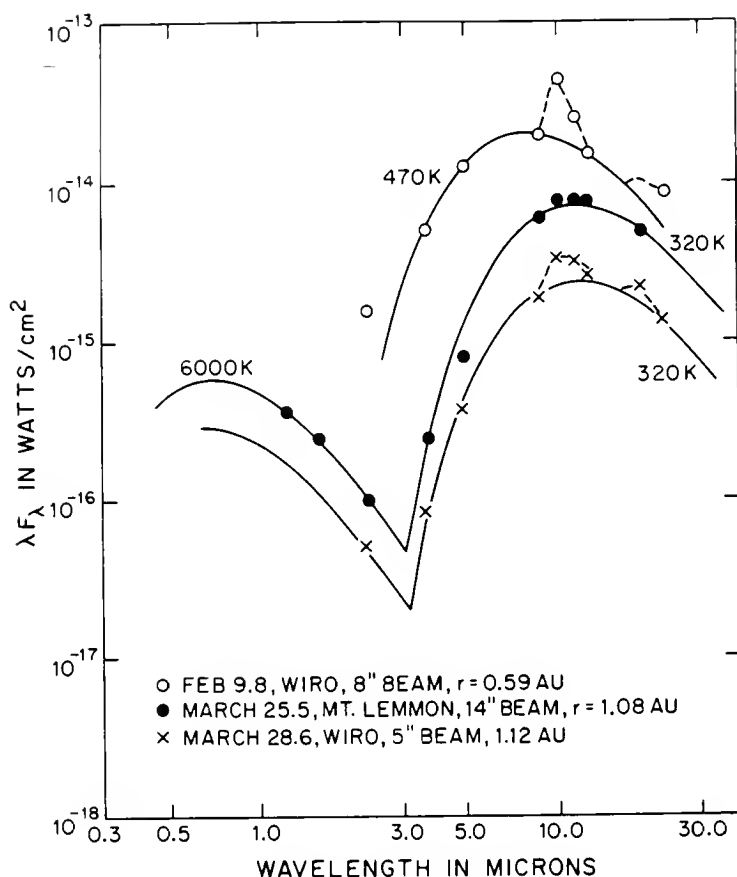


Figure 1 - The energy distribution of P/Halley on several dates showing the reflected solar and continuum thermal emission components as well as the 10 and 20 μ m silicate emission features. Typical variations observed in the contrast and shape of the silicate signature in P/Halley are represented. On 25.5 March, when the signature was absent, the albedo of P/Halley fell to about 5% suggesting that darker carbonaceous material was dominating the reflected light. Solar heating of localized jets coupled with rotation of the nucleus can account for the disappearance of the silicate feature of 25.5 March and its reappearance on 28.6 March. The continuum is superheated compared to the black grain temperature appropriate to the heliocentric distance ($T_{BB} = 356K, 270K, \text{ and } 265K$ for 0.59, 1.08, and 1.12 AU respectively) indicating that the grains producing the continuum emission are small. Values of delta (the earth-comet separation) were 1.55 AU on 9.8 February, 0.66 AU on 25.5 March, and 0.61 AU on 28.6 March.

AIRBORNE 20-65 MICRON SPECTROPHOTOMETRY OF COMET HALLEY

W. Glaccum^{1,2}, S.H. Moseley¹, H. Campins³, and R.F. Loewenstein²

¹ NASA Goddard Space Flight Center, Code 685, Greenbelt, MD 20771

² Yerkes Observatory, University of Chicago, Box 258, Williams Bay, WI 53191

³ Planetary Science Institute, SAIC, 2030 E. Speedway No. 201, Tuscon, AZ 85719

ABSTRACT

We report observations of Comet Halley with a grating spectrometer on board the Kuiper Airborne Observatory on four nights in December 1985 and April 1986. We obtained 20-65 μ m low-resolution ($R=24-40$) spectra of the nucleus with a 40 arcsec FWHM beam on 17 Dec. 1985, and on 15 and 17 Apr. 1986. On 20 Dec. 1985 we obtained only a 20-35 μ m spectrum. Most of the data have been discussed in a paper in press (Glaccum *et al*, 1987; see also Glaccum *et al*, 1986) where we dealt with the continuum. In that paper we fit models to the continuum that showed that more micron-size particles of grains similar to amorphous carbon were needed to fit the spectrum than were allowed by the Vega SP-2 mass distribution, or that a fraction of the grains had to be made out of a material (silicates, e.g.) whose absorption efficiency fell steeper than λ^{-1} for $\lambda > 20\mu$ m. We also presented spectra taken at several points on the coma on 15 Apr. which showed that the overall shape of the spectrum is the same in the coma. Tabulated values of the data and calibration curves are available from W. Glaccum. Here we discuss the spectral features.

The spectrum on 20 Dec. has an unresolved emission feature at $28.1 \pm 0.4\mu$ m, with a total flux of $(6.3 \pm 3.1) \times 10^{-14} \text{ Wm}^{-2}$. The uncertainty includes both the statistical noise and the uncertainty in atmospheric transmission. This is consistent with the 28.4 μ m feature seen by Herter *et al* on 14 Dec. 1985. We did not see the feature on the other nights. On all nights the spectrum can be fit by blackbodies with $T=360-400\text{K}$. On 15 April the spectrum has 4 broad ($\Delta\lambda=4\mu$ m) emission features centered at 23.5, 28.0, 34.5, and 45 μ m which peak about 7% above the continuum. The first 3 features are present in the spectra on the other nights, but to a lesser degree of confidence. The broad 28 μ m feature may be absent on 2 of the flights. The peak wavelengths of these features correspond closely with maxima in Q_{ext} of small olivine particles (Koike *et al*, 1981). Olivine has been proposed as a candidate material to explain the double-peaked structure of the 10 μ m feature (Campins and Ryan, 1987; Bregman *et al*, 1987).

References

- Bregman, J.D., Campins, H., Witteborn, F.C., Wooden, D.C., Rank, D.M., Allamandola, L.J., Cohen, M., and Tielens, A.G.G.M. 1987, *Astron. and Astrop.*, in press.
- Campins, H. and Ryan, E.V. 1987. Poster paper presented at this workshop.
- Glaccum, W., Moseley, S.H., Campins, H. and Loewenstein, R.F. 1986. *20th ESLAB Symp.*, ESA SP-250, Vol. II, 111.
- . 1987, *Astron. and Astrop.*, in press.
- Herter, T., Campins, H., and Gull, G.E. 1986, *20th ESLAB Symp.*, ESA SP-250, Vol. II, 117.
- Koike, C., Hasegawa, H., Asada, N., and Hattori, T. 1981. *Astrop. and Space Sci.* 79, 77.
- Wright, E.L. 1976. *Astrop. J.* 210, 250.

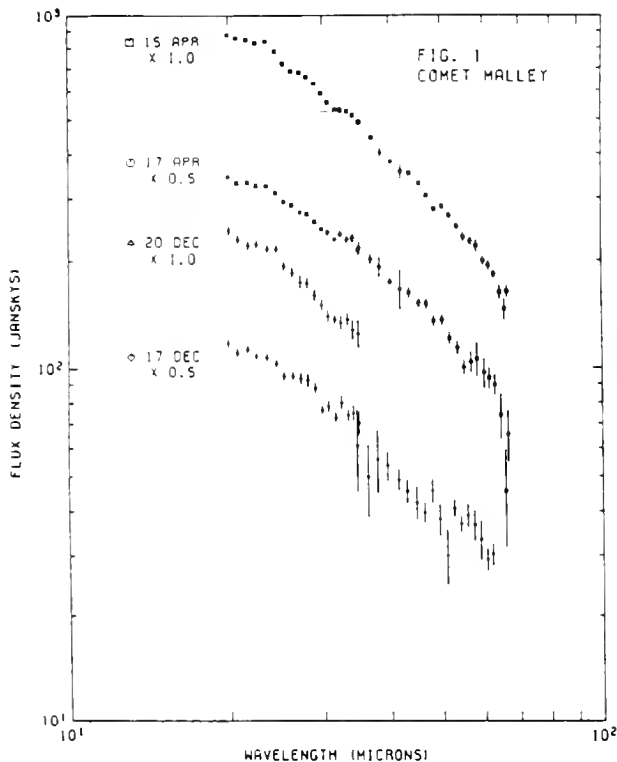


Fig. 1. The spectrum of Comet Halley on 4 nights with a 40 arcsec beam centered on the nucleus. All spectra are calibrated to Mars using the Wright model (Wright, 1976; S.F. Odenwald, 1983 private comm.); the April flights are calibrated directly, and for the December flights the calibration is transferred through α Ori. A new model for Mars by P. Christensen and B. Jakowsky (priv. comm.) would increase each spectrum uniformly by 10%. The spectra are corrected for telluric water vapor absorption by adjusting the amount of water vapor until the water lines disappear. Hence, the $28\mu\text{m}$ feature does not appear in the 20 Dec. spectrum. The dip at $65\mu\text{m}$ and the jump at $50\mu\text{m}$ are poorly corrected water lines. The structure in the 17 Dec. spectrum at $\lambda > 30\mu\text{m}$ is spurious and appears in other objects to a lesser degree. The spectra for 17 Apr. and 17 Dec. are slightly different than those shown in the two Glaccum et al references. The overlap of the 2 grating settings occurs at $35\mu\text{m}$. The agreement on all objects was excellent in April and good in December.

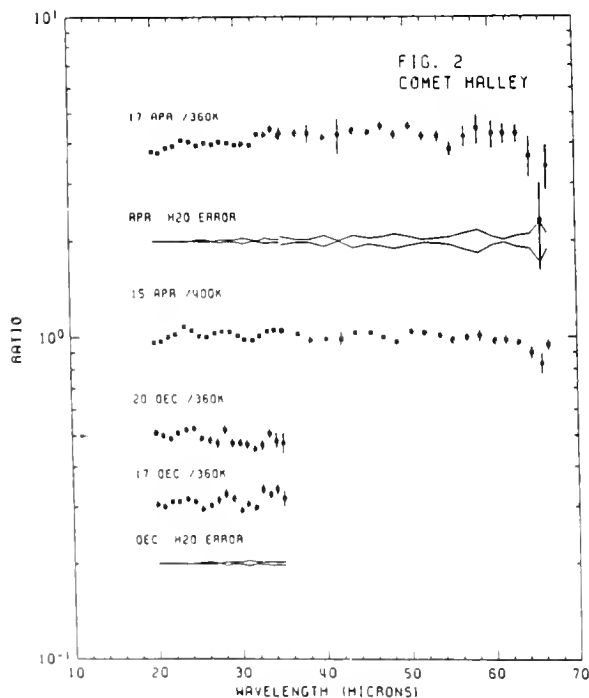


Fig. 2. Spectra of Comet Halley relative to blackbodies. To increase the contrast we have divided each spectrum by a blackbody which fits the overall 20-65 μm spectrum. Also shown are the effects on the spectra by a change of $\pm 20\%$ in the ratio of boresight water vapor on the comet and calibration legs. The data for the April flights is the same as in Fig. 1. For the December flights we have used a different calibration procedure. The comet data are calibrated to α Ori assuming it has a smooth spectrum and using values for water vapor from the on-board radiometers. The $28\mu\text{m}$ feature appears as a $9.5\% \pm 3.8\%$ excess in one channel; to remove it by adjusting water vapor requires a change by a factor of 3 in the ratio of boresight water vapor (as measured by the on-board radiometers) on the comet leg and the α Ori leg. Such a large error in the values obtained by the water vapor radiometers is unlikely, as this ratio has a standard error of 25% for the 5 other objects on the flight. If we assume that we can determine the ratio to $\pm 10\%$ on those objects by removing the water lines. The 25% standard error is typical. We cannot rule out the possibility of the feature being due to a change in sensitivity of that detector during the flight, but such changes are rare and have never been seen in that channel, and nothing was unusual about any other objects on that flight either before or after the comet.

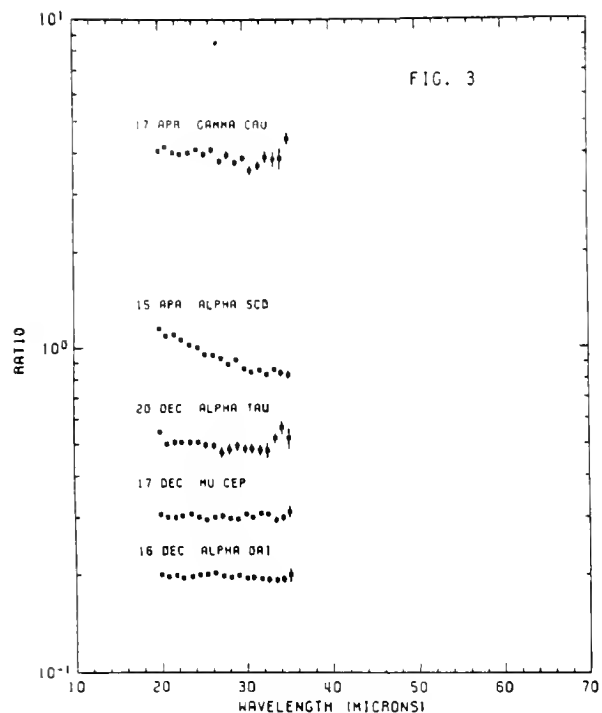


Fig. 3. Spectra of 5 representative stars relative to blackbodies (Glaccum, Ph.D. thesis, in preparation). To give the reader an indication of the noise in excess of "statistical" noise, we show representative stars from each flight, reduced in the same way as the comet (Fig. 2), and plotted to the same scale. Included is the spectrum of α Ori on 16 Dec., the night which Mars was observed. This has been divided by $B_{\lambda}(T=3500K) \cdot \lambda^{-0.155}$ so that the "smooth" spectrum used to reduce the December data in Figs. 2 and 3 is a straight line at $y=0.2$. The spectra of other stars are divided by a 3500K blackbody. The emission from γ Cru and α Tau is from their photospheres and should be featureless. We also expect α Sco and μ Cep to be featureless. The structure in the spectrum of γ Cru is due to a correction for a change of instrumental sensitivity during the flight and represents a worst-case example; the corresponding corrections for the comet are much smaller ($<2\%$).

INFRARED OBSERVATIONS OF COMET WILSON

Martha S. Hanner and Ray L. Newburn

Jet Propulsion Laboratory

Pasadena, CA 91109

Comet Wilson was observed from 1 - 20 microns with the NASA Infrared Telescope Facility May 29 - June 2, 1987, when the comet was at $R = 1.35$ AU post-perihelion. The spectral energy distribution is displayed in Figure 1. No silicate emission feature was evident in the spectrum. The color temperature of 264 K was 10 percent higher than the black body temperature. Near-infrared colors were $J-H = 0.42 \pm 0.03$ and $H-K = 0.15 \pm 0.03$, identical to the colors of Halley at 1.3 AU pre-perihelion. (Tokunaga *et al.*, *Astron. J.*, 92, 183, 1986). The 10-micron flux was 2.95×10^{-13} W/m² / μ m in a 7-arcsec beam on May 29.2.

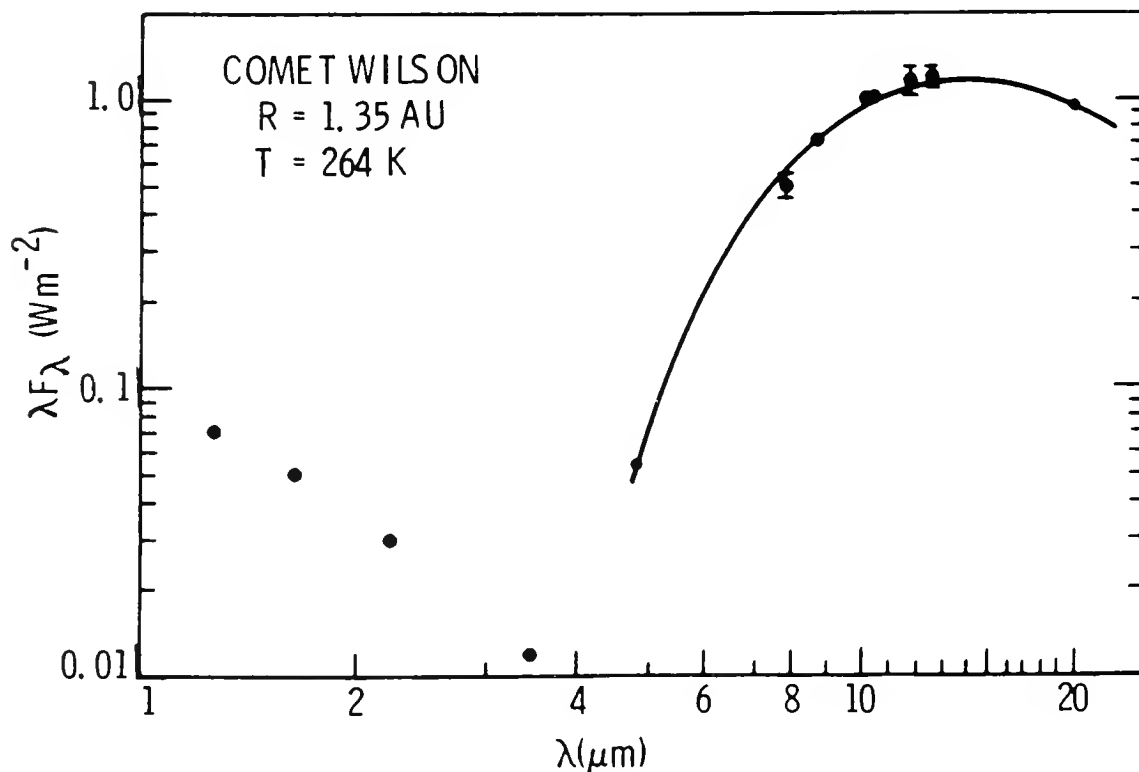


Figure 1. Relative spectral energy distribution of Comet Wilson 29.2 May and 1.2 June 1987.

An Albedo Map of P/Halley on 13 March 1986

Thomas L. Hayward and Gary L. Grasdalen

Wyoming Infrared Observatory, University of Wyoming

and

S. F. Green

Unit for Space Sciences, University of Kent, Canterbury, U. K.

We present in figure 1 an albedo map of comet Halley made from a $10\ \mu\text{m}$ image taken from the Wyoming Infrared Observatory at 16:56 UT on 13 March 1986 (Ref. 1), and a $7311\ \text{\AA}$ CCD image taken from the Anglo-Australian Telescope about an hour later (Ref. 2). To construct this map, the CCD image was first converted from 0.49 arcsec/pixel to 1 arcsec/pixel to match the scale of the $10\ \mu\text{m}$ image, then both were calibrated in λF_λ units. Because the peak of a black-body curve in these units is proportional to the area underneath, the albedo γ is:

$$\gamma = \frac{S}{S + 1},$$

where S is the ratio of the optical to infrared peak flux density (Ref. 3). Because $7311\ \text{\AA}$ and $10\ \mu\text{m}$ are near the peaks of the reflected and reradiated parts of the comet's spectrum, respectively, we simply divided the optical map by the infrared map to obtain S for each pixel. Errors due to the strong silicate feature and the poorly known $10\ \mu\text{m}$ background correction have not been fully evaluated at this time, but they should not affect the general appearance of figure 1.

According to our albedo map, most of the inner coma of Halley lies between $\gamma = 0.04$ and 0.08 . The overall smoothness of the map, especially near the nucleus, is remarkable considering the large dynamic range of the optical and IR maps, and the differences in spatial resolution and

image processing. The ridge near the south edge is due to the slight shifting of the IR image that was done to accurately register it with the optical image.

There is a fairly strong east-west slope in the albedo, almost parallel to the direction to the sun. Such a gradient along the solar direction has been reported for comet Giacobini-Zinner (Ref. 4), and for Halley (Ref. 5), and in both cases it has been attributed to the lower albedo of larger grains caused by multiple internal scattering. The larger grains are ejected more slowly from the nucleus; therefore they are more tightly confined to a line extending from the nucleus in the anti-solar direction. Figure 1 does not show the radial increase of albedo shown in the previous maps, but its small angular size and the background subtraction uncertainties make an exact comparison difficult. The albedo map of Halley presented by Hammel *et al.* (Ref. 5), taken when Halley was near opposition, exhibits a range of $\gamma = 0.2 - 0.3$ and higher, roughly three or four times the values in our map. Hammel *et al.* notes that the high albedos may be due to enhanced backscattering by dust grains at small phase angles. The lower values in our map, taken at the more moderate phase angle of 64° , are in excellent agreement with this conclusion.

REFERENCES

- ¹ Hayward, T. L., Gehrz, R. D., and Grasdalen, G. L. 1987, Ground-Based Infrared Observations of Comet Halley, *Nature* **326**, 55.
- ² Green, S. F., and Hughes, D. W. 1986, Near Nucleus CCD Imaging of Comet Halley at the Time of the Spacecraft Encounters, *20th ESLAB Symposium on the Exploration of Halley's Comet*, ESA SP-250, Vol II, 157- 161.
- ³ Ney, E. P. 1982, Optical and Infrared Observations of Comet in the Range $0.5 \mu\text{m}$ to $20 \mu\text{m}$., in *Comets* (ed. Wilkening, L. L. University of Arizona Press, Tucson), 323-340.
- ⁴ Telesco, C. M. *et al.* 1986, Thermal Infrared and Visual Imaging of Comet Giacobini-Zinner, *Astrophys. J. Let.*, **310**, L61-L65.
- ⁵ Hammel, H.B., Storrs, A. D., Cruikshank, D. P., Telesco, C. M., Decher, R. M., and Campins, H. 1986, Albedo Maps of Comets P/Giacobini- Zinner and P/Halley, *20th ESLAB Symposium on the Exploration of Halley's Comet*, ESA SP-250, Vol II, 73-77.

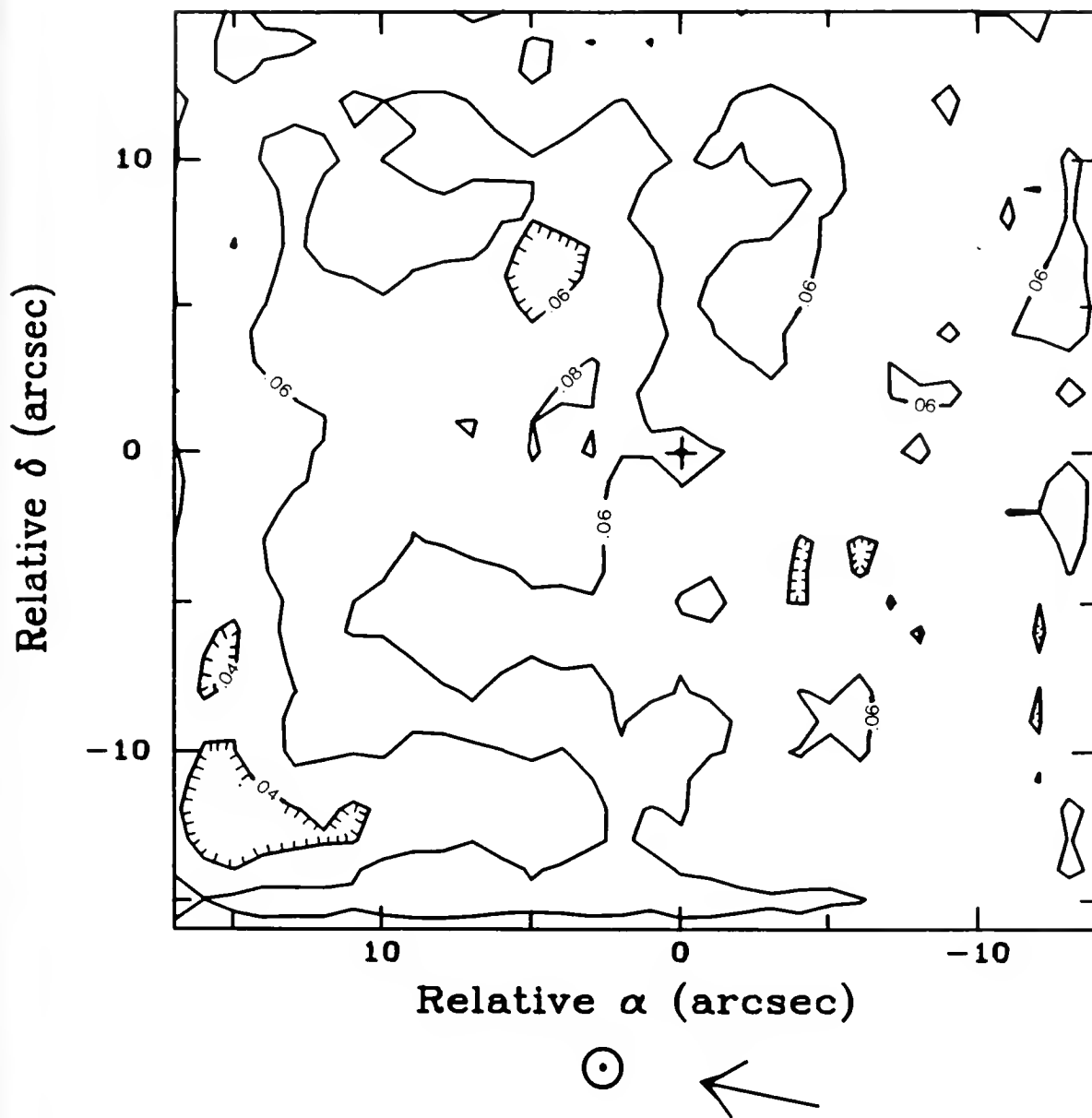


Figure 1: The albedo map derived from the IR and optical images. Contour levels are drawn at $\gamma = 0.04, 0.06$, and 0.08 . The central cross marks the position of peak optical and $10 \mu\text{m}$ emission.

THE PROBLEM OF CLUSTERING IN LABORATORY STUDIES OF COMETARY DUST

Donald R. Huffman

Department of Physics
University of Arizona
Tucson, AZ 85721

In trying to understand the nature of interstellar or interplanetary dust grains it is tempting to simply rely on direct laboratory measurements of grain properties such as extinction. However, until we are able to achieve agreement between directly measured extinction and the same property calculated from measured optical constants of the solid, application to astronomical observations is questionable. There are two major problems which we discuss here – the problem of what optical constants to use in the calculations, and the almost unavoidable problem of particle clustering in laboratory studies. Regarding the choice of optical constants, I personally do not believe one should use optical constants from rocks, lunar or terrestrial. It is not even clear how one properly defines optical constants for a heterogeneous aggregate such as a rock or an interplanetary dust aggregate. Regarding small particle measurements, a problem afflicting almost all laboratory measurements is the clustering of particles. Having failed in our considerable efforts to isolate particles (in infrared-transparent matrices and in low temperature solid argon, for example), we have tried to deal with the problem with a simple theory which seems to adequately describe the extinction by small, clustered particles in many cases. In terms of the relative complex dielectric function, the expression for volume-normalized extinction, averaged over orientation and ellipsoid shape factor is

$$\frac{\langle\langle C_{\text{abs}} \rangle\rangle}{v} = k \operatorname{Im} \left(\frac{2\epsilon}{\epsilon - 1} \operatorname{Log} \epsilon \right)$$

Details and examples of this treatment are given in the monograph by Bohren and Huffman, Chapter 12. An example of the improved agreement with experimental results achieved with the CDE calculation rather than sphere theory is shown in Figure 1, where measured and calculated extinction for sub-micron quartz particles are shown. With such successes as our basis, we can suggest applying the CDE and sphere theories using measured optical constants in cases that may apply to astronomical observations. Figure 2 shows such calculations using measured optical constants of glassy carbon from Edoh. One sees that shape effects induced by clustering become significant in the far infrared, leading to differences in both the slope and the magnitudes of extinction.

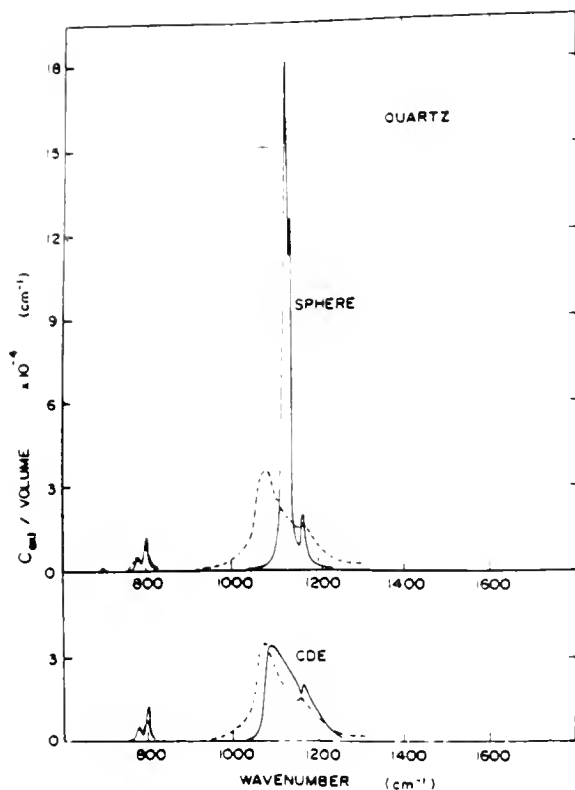


Figure 1: Measured extinction for crystalline quartz particles dispersed in KBr (dashed curves) compared with calculations for spheres (top) and for a continuous distribution of ellipsoidal shapes (bottom). From Bohren and Huffman (1983).

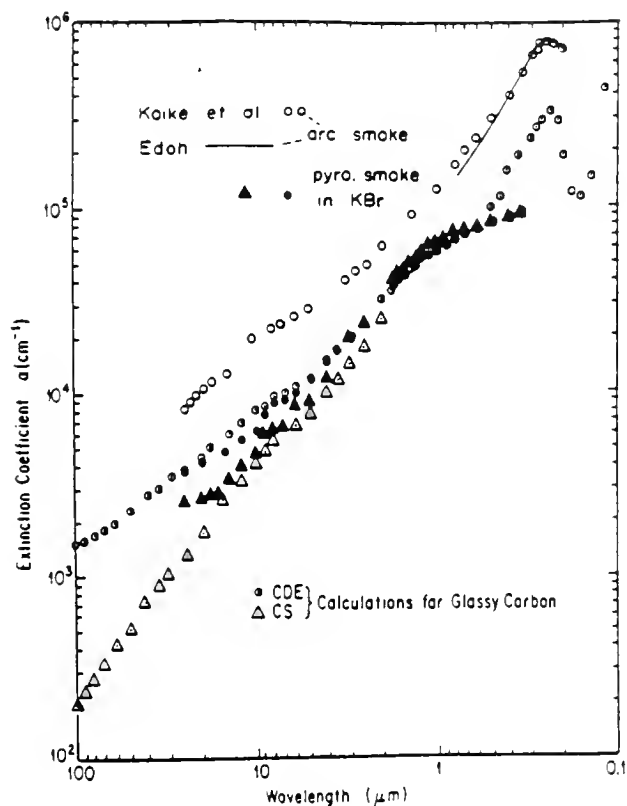


Figure 2: Comparison of various measured extinction values for carbon smoke with calculations based on optical constants for glassy carbon. Open circles are from Koike *et al.* 1980 on arc-condensed smoke. Solid circles and triangles are from Edon (1983) on smoke from acetylene pyrolysis, and the solid line is from Edon's measurements on arc-condensed smoke.

LIGHT SCATTERING OF LARGE ROUGH PARTICLES APPLICATION TO COMETARY GRAINS

P. L. Lamy and J. M. Perrin

Laboratoire d'Astronomie Spatiale
Marseille, France

While the electromagnetic field scattered by a spherical particle is classically obtained by the Helmholtz equation

$$\nabla^2 \varphi(r) + n^2 k^2 \varphi(r) = 0$$

where n is the complex index of refraction and k , the wave number, the general case of an arbitrary particle may be investigated in the general framework of the interaction of a wave with a scattering potential. The wave function $\varphi(r)$ then satisfies the Schrödinger equation

$$\nabla^2 \varphi(r) + k^2 (1 - V/E) \varphi(r) = 0$$

where $E = hc/\lambda$ is the energy. Note that the spherical case is recovered by taking $V = (1 - n^2)E$. This equality still holds for a rough particle, but the index of refraction n is modified, for instance, by introducing a distribution of the Fermi type (Chiappetta, 1980; Perrin and Lamy, 1986). The general solution of the Schrödinger equation is written

$$\varphi(r) = e^{ik \cdot r} + e/r^{ikr} f(\theta)$$

where the first term represents the incident wave and $f(\theta)$, the amplitude of the scattered wave. The main disadvantages of this approach are its restriction to large particles ($a \sim \lambda$; practically $a \geq 6 \lambda$) and its scalar nature preventing the calculation of the polarization. However, Perrin and Lamy (1986) have shown to avoid the second limitation and retrieve a vectorial description. They proved that in the case of large spheres when the ad hoc assumptions are satisfied, the expression of the scattering amplitude $f(\theta)$ may be approximated by an expansion series on a continuous basis which is analogous to the classical expansion series in partial waves, i.e., on a discrete basis. The analogy may be generalized, and the ratio of the two components $f_{||}(\theta)$ and $f_{\perp}(\theta)$ for a rough particle obtained by taking the ratio of the reflectivities for the two directions of polarization. These reflectivities involve the simple and double reflections calculated following the method developed by Wolff (1980) for rough surfaces. Figure 1 shows how well the model is able to reproduce the experimental result obtained on a rough particle of magnetite by Weiss (1981). In general, the intensity scattered by rough grains is characterized by a broad diffraction lobe, a flat behavior at intermediate scattering angles and backscattering enhancement. The polarization shows a broad maximum at θ equals 60 to 90° (its value depends upon the absorption) and a negative branch in the interval 160 to 180° approximately. This is most likely the correct explanation for the similar feature observed in comets in general and P/Halley in particular (Lamy *et al.*, 1987). More implications of rough particles, in particular in the infrared, are discussed in the summary section of this report.

References

- Lamy, P. L., Grün, E., and Perrin, J. M. (1987), *Astron. Astrophys.*, in press.
Perrin, J. M. and Lamy, P. L. (1986), *Optica Acta*, **33**, 1001.
Weiss, K. (1981), Ph.D. Thesis, Ruhr-Universität Bochum and Report BMFT-FB-W81-047.
Wolff, M. (1980), *Icarus*, **44**, 780.

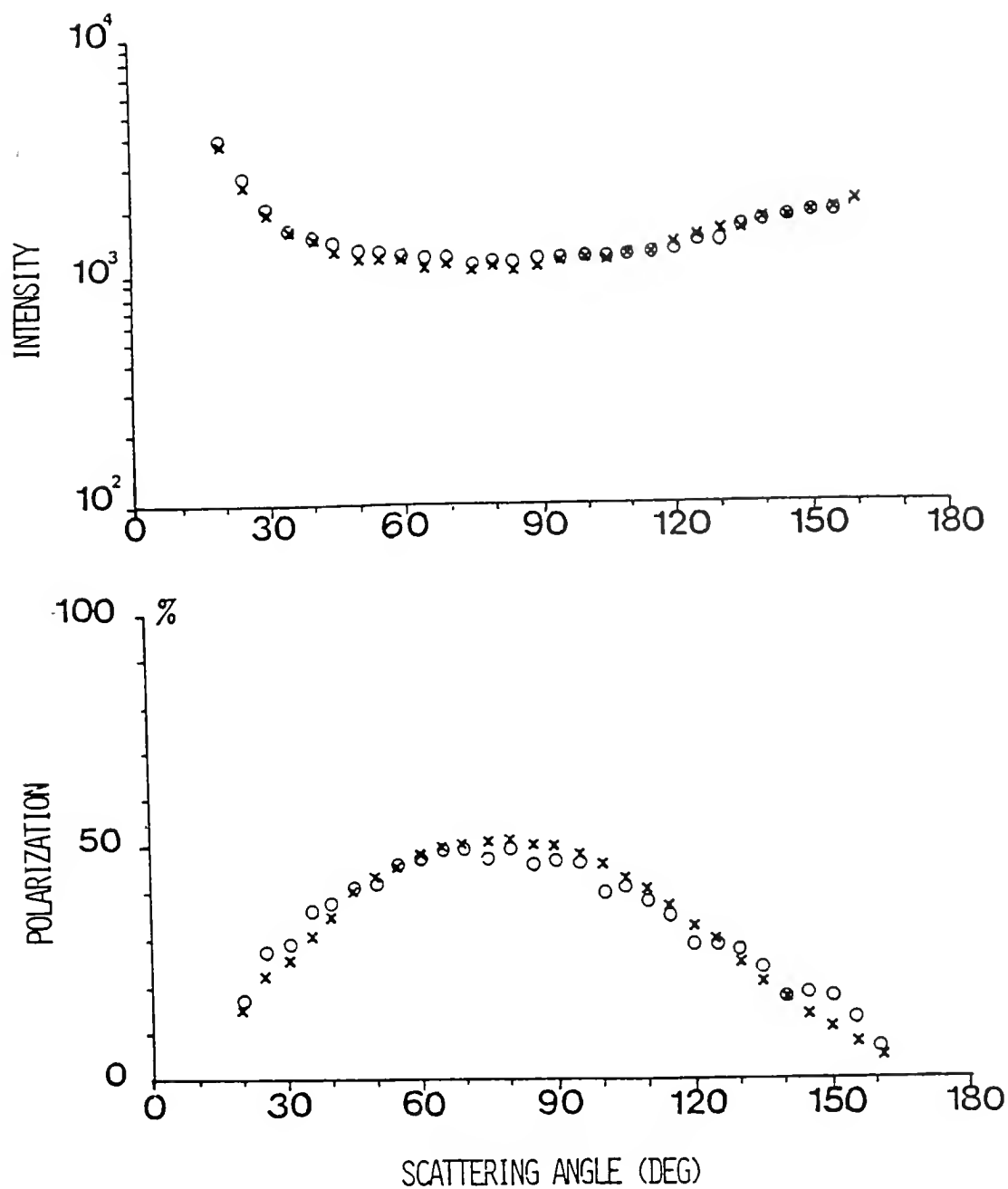


Figure 1. Total scattered intensity (top) and polarization (bottom) for a rough particle of magnetite: comparison of the experimental results (o) and the calculated results from the present model (x).

THERMAL PROPERTIES OF HETEROGENEOUS GRAINS

David J. Lien
Department of Physics
Kansas State University

Cometary dust is neither spherical nor homogeneous, yet these are the assumptions used to model the thermal, optical, and dynamical properties of cometary dust. To better understand the effects of heterogeneity on the thermal and optical properties of dust grains, the effective dielectric constant for an admixture of magnetite and a silicate were calculated using two different effective medium theories: the Maxwell-Garnett theory and the Bruggeman theory. Conceptually, the Maxwell Garnett (hereafter MG) theory describes the effective dielectric constant of a matrix material into which is embedded a large number of very small inclusions of a second material. The Bruggeman theory describes the dielectric constant of a well-mixed aggregate of two or more types of materials. Both theories assume that the individual particles are much smaller than the wavelength of the incident radiation.

The complex index of refraction (which is used as an input to Mie scattering calculations) for a heterogeneous grain using the MG theory is very similar to the complex index of refraction of the matrix material, even for large volume fractions of the inclusion. This is shown in Figure 1, where the real and imaginary parts of the complex index of refraction are plotted as a function of wavelength for magnetite, a silicate (*astronomical silicate*, Draine and Lee, 1984) and a 50-50 mix of these two minerals using the MG theory (both astronomical silicate and magnetite as the matrix material) and the Bruggeman theory. The Bruggeman theory retains the spectral features of both minerals. The thermal spectrum of a particle smaller than the wavelength of the incident radiation will show features similar to those seen in the imaginary component of the complex index of refraction.

The equilibrium grain temperature for spherical particles ranging in size from $.001\mu\text{m}$ to $100\mu\text{m}$ in radius at 1 astronomical unit from the sun was calculated for a range of particles which differ only in the volume fraction of astronomical silicate and magnetite (Figure 2). For the MG theory, magnetite is assumed to be the matrix. For most grains, the equilibrium grain temperature of a heterogeneous grain is intermediate between the grain temperatures of the homogeneous grains; however, the temperature is not equivalent to a volume-weighted average of the homogenous grain temperatures. There are large differences between the equilibrium grain temperatures for the small grains using the two effective medium theories. For large grains, the equilibrium grain temperature of all grains shown in the figure approach that of a blackbody (indicated in Figure 2).

The shape of the curves in Figure 2 is easily understood. For the smallest grains, the absorptivity in the visible and emissivity in the IR are constant with size, hence the lack of change in the equilibrium temperature. The IR emissivity is relatively small, yielding the high temperature (pure astronomical silicate is transparent in the visible and near-IR, causing the equilibrium grain temperature to be smaller for the smallest grains). As the grain size increases, the optical absorptivity first increases slightly, then reaches a constant

value. This causes the slight increase in the temperature around $0.1\mu\text{m}$. The IR emissivity increases for larger grain radii, causing a rapid decrease in the equilibrium temperature. As the size increases further, the IR emissivity and the optical absorptivity asymptotically approach a constant value, causing the equilibrium grain temperature to slowly increase with size.

The spectrum of heterogeneous grains in the thermal IR depends on the radius, the volume fractions of the materials, and the theory used. Figure 3 shows the thermal emission from $1\mu\text{m}$ and $10\mu\text{m}$ grains at 1 AU for homogeneous grains of magnetite and astronomical silicate and for a 50-50 admixture of these minerals using both the MG theory and the Bruggeman theory.

For the $1\mu\text{m}$ grains (Figure 3a and 3b), the spectral features observed are those seen in their respective imaginary index of refraction (Figure 1). Differences in the integrated emissivities are partly due to differences in the equilibrium grain temperature of each grain at 1 AU – ranging from 306 K for magnetite to 340 K for the 50-50 mixture calculated with the Bruggeman theory – and partly due to the total energy absorbed (and hence re-emitted) by the grain. For example, even though magnetite and astronomical silicate have nearly equivalent equilibrium grain temperatures (306 K and 307 K, respectively), astronomical silicate absorbs, and hence re-emits, much less energy than the grain of magnetite. The spectral features of the heterogeneous grains show the effect of the mixing theory used. For the MG theory, the spectral features are due primarily to the matrix material. For the Bruggeman theory, the spectral features of both materials are observed. In Figure 3b, this latter effect is seen as a strong absorption feature at $7.4\mu\text{m}$ and a strong emission feature at $10\mu\text{m}$ superposed on the near-blackbody spectrum of pure magnetite.

The spectrum of a $10\mu\text{m}$ grain is very different than that of a $1\mu\text{m}$ grain (Figures 3c and 3d). At $10\mu\text{m}$, the emissivity of the grain is almost constant as a function of wavelength; hence, the spectrum is close to that of a blackbody, regardless of the composition. The small differences in the spectra of the $10\mu\text{m}$ grains are due to differences in equilibrium grain temperatures and to differences in the composition. For larger grains, this latter effect becomes even less important.

The observational consequences of these results are the following. 1) the thermal spectrum seen in most comets is due primarily to large grains. The composition and sizes of these grains is almost impossible to determine. 2) The presence of the $10\mu\text{m}$ silicate feature indicates the existence of small grains ($< 1\mu\text{m}$). 3) The degree of heterogeneity of these grains can be determined somewhat by looking at the relative intensity and slope of the thermal emission from about 4 to $8\mu\text{m}$.

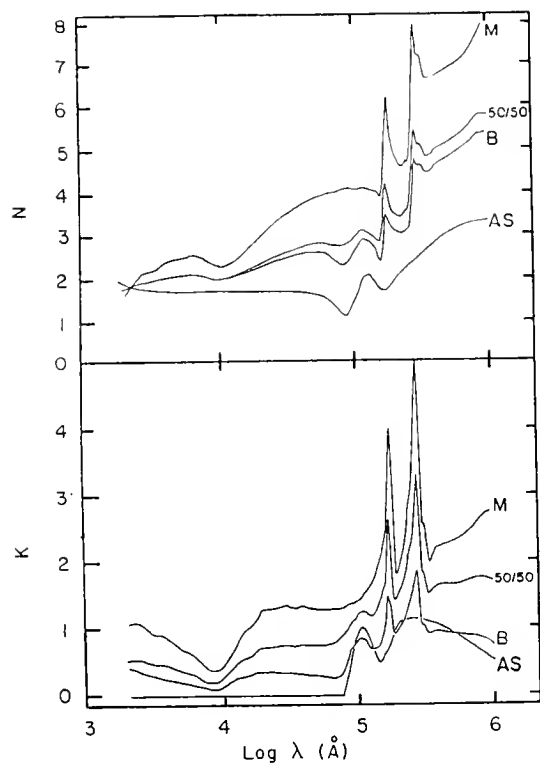


Figure 1

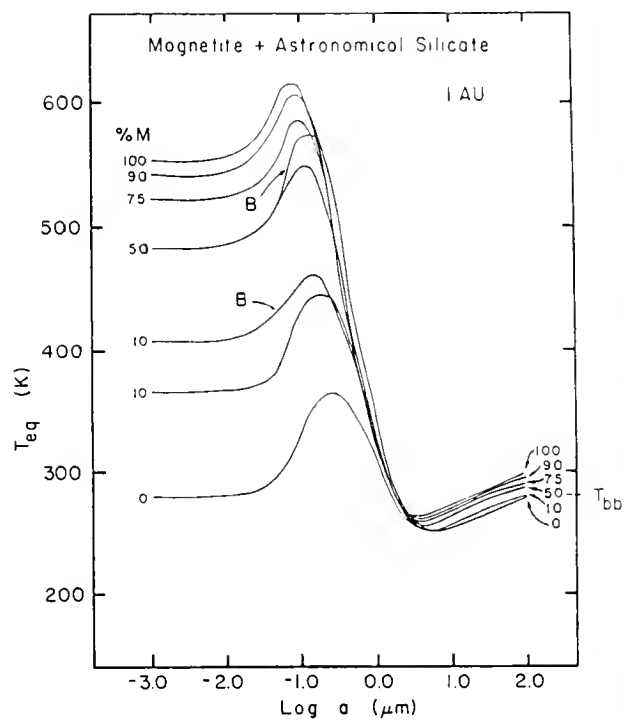


Figure 2

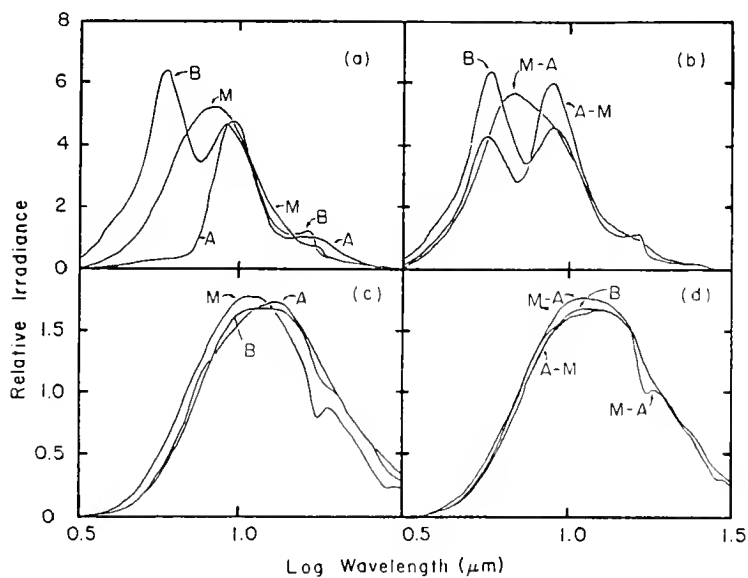


Figure 3

COMET HALLEY'S COLORFUL OUTBURSTS

David K. Lynch and Ray W. Russell
Space Sciences Laboratory, The Aerospace Corporation
Los Angeles, CA 90290

ABSTRACT

Two preperihelion outbursts by Comet Halley were observed, each showing different brightness changes at 2.3, 3.6, 4.6 and $10.3\mu\text{m}$. Neither event was observed from beginning to end. The first observation on November 8, 1985, lasted of the order of a day and was accompanied by a tail-like appendage recorded photographically. During the outburst the IR colors changed dramatically, showing no significant change at $10.3\mu\text{m}$ but showing progressively more change at shorter wavelengths over a time scale of a few hours. The second outburst measurement extended over several days (January 10-13, 1986) during which time the intensities at the four wavelengths increased by roughly the same amount. Although the outbursts were of different duration, the IR measurements suggest that the first event involved volatile ice particles that evaporated, while the second was associated with long-lived nonvolatile dust grains.

1. OBSERVATIONS

All observations were made using the 60-inch NASA/Steward telescope at Mt. Lemmon. A LHe-cooled CVF was used with a 15-arc sec aperture using conventional chopping/nodding techniques with a chopper throw of $210''$ N-S (Lynch *et al.* 1986). Three broadband filters were used with central wavelengths and half-power bandpasses of 2.3, 3.6, 4.6 and .5, .56, and $.28\mu\text{m}$, respectively. At $10.3\mu\text{m}$ the CVF defined the spectral band with a bandpass of $0.2\mu\text{m}$. The standard stars used were α Tau and β Peg, although the brightness changes observed are insensitive to the adopted fluxes of these stars.

2. OUTBURSTS

Figure 1 shows the time evolution of the outburst observed on November 8, 1985, UT. At $10.3\mu\text{m}$ the flux remained steady within the measurement uncertainties, but at $3.6\mu\text{m}$ the brightness dropped from magnitude 7.6 to 8.5, and at $2.3\mu\text{m}$ the change was from 6.2 to 9.4, more than 3 magnitudes. Clearly, the diminution increased toward shorter wavelength. Between the times of the two sets of observations a photograph was taken of the comet through the 6-inch finder telescope (Lynch and Russell, 1987), showing an irregular mass extending southward (p.a. 190°) by about 1 arc minute (Fig. 2). It is not known how long the feature endured.

The November 8, 1985, outburst occurred very near the ecliptic plane when the comet was 1.82 AU from the sun and only 17° from opposition. During this time many sporadic prototails formed and disappeared, and the properties of the outburst may well have been indicative of the rupture of the crust tail formation. The evident color changes are consistent with the behavior of ejected volatile material: ices show little absorption (and thus emission) at $10\mu\text{m}$, yet they would be expected to scatter solar radiation very efficiently at shorter wavelengths until the particles evaporated, typically with time scales of a few hours for $1\mu\text{m}$ -size particles. This ice hypothesis for the grain composition of the ejected material is supported by Bregman and Witteborn's report (1985) of a $3\mu\text{m}$ -ice feature.

Figure 1 also shows a very different type of color behavior during the much longer-lasting outburst occurring January 10-13, 1986. Here the brightness at all four wavelengths

increased by roughly the same amount, about 30 percent/night. Although the expulsion mechanism is not known, the time behavior of the dust emission can be understood if the ejected particles were nonvolatile, perhaps silicate particles which were known to be present during this time (Tokunaga *et al.* 1986; Gehrz and Ney, 1986). Such particles would show roughly similar brightness changes at all four wavelengths and would not evaporate. The persistence of the event suggests that the source of material endured for many days, because the transit time through the 10,000-km radius beam is roughly six hours for particles moving at velocities observed by spacecraft (Vaisberg *et al.*, typically 450 m/sec for grains of $1\mu\text{m}$ diameter).

Another outburst event occurred from approximately April 7 to 10, 1986 (Russell *et al.* 1986), and was more like the January outburst. Although no color information was obtained for that outburst, the large/small aperture observations required particles with lifetimes greater than a day, and a source of ejecta which seemed to continue for about two days. Spectral data obtained during this outburst did show a silicate feature near $10\mu\text{m}$.

3. CONCLUSIONS

Many outbursts occurred on comet Halley and the two discussed here show unequivocal evidence for two types of color changes during outbursts and for differentiation in particle composition or particle size distribution during outbursts. The first type discussed here is consistent with an anisotropic infusion of particles into the coma over a finite period of time, which were very efficient scatterers of shorter wavelength light but very poor emitters in the thermal IR ($\lambda > 5\mu\text{m}$). These particles must be quite volatile or traveling at larger speeds than observed by spacecraft to account for the observed factor of ~ 20 change at $2.3\mu\text{m}$ in ~ 6 hours.

The second type of outburst appears to be a much more steady, enduring (1 - few days) source of particles, and the particles are both longer-lived and show approximately a constant increase in emission/scattering from 2.3 to $10.3\mu\text{m}$.

Clearly, not all outbursts are the same. It is thus very important to chronicle and analyze time variability in both new and periodic comets in order to understand the mechanisms responsible for outbursts and to assess whether the mechanisms are common to both types of comets. Time-resolved spectroscopy of molecular emissions would be an ideal complement to IR observations of dust particles, especially if programs could be undertaken employing simultaneous observations of dust and gas through apertures with the same angular size. Visible imaging observations would provide, as they did for Halley, information on jets, particle trajectories, and rotation of the nucleus.

4. ACKNOWLEDGMENTS

We thank NASA and Steward Observatory for their generous granting of observing time and the organizers of this Workshop for the opportunity to participate in a valuable and timely meeting. This work was supported by NASA Contract No. NAS2-12370 and the Aerospace-Sponsored Research Program.

5. REFERENCES

1. Bregman, J. and Witteborn, F., 1985, IAU Circ. 4149.
2. Gehrz, R. and Ney E., 1986, *Proceedings of the 20th ESLAB Symposium on the Exploration of Halley's Comet*, Heidelberg, W. Germany, 27-31 October 1986, ESA SP-250, Vol. II, 101-105.
3. Lynch, D. K., Russell, R. W., Rettig, D. A., Rice, C. J., and Young, R. M., 1986, *Proceedings of the 20th ESLAB Symposium on the Exploration of Halley's Comet*,

4. Lynch D. K. and Russell, R. W., 1987, *Pub. A. S. P.*, in press.
5. Russell, R. W., Lynch, D. K., Rudy, R. J., Rossano, G. S., Hackwell, J. A. and Campins, H., 1986, *Proceedings of the 20th ESLAB Symposium on the Exploration of Halley's Comet*, Heidelberg, W. Germany, 27-31 October 1986, ESA SP-250, Vol. II, 125-128.
6. Tokunaga, A. T., Golisch, W. F., Griep, D. M., Kaminski, C. D., and Hanner, M. S., 1986, *Astron. J.*, **92**, 1183-1190.
7. Vaisberg, O. L., Smirnov, V. N., Gorn, L. S., Iovlev, M. V., Balikchin, M. A., Klimor, S. I., Savin, S. P., Shapiro, V. D., and Shevchenko, V. I., 1986, *Nature*, **321**, 274.

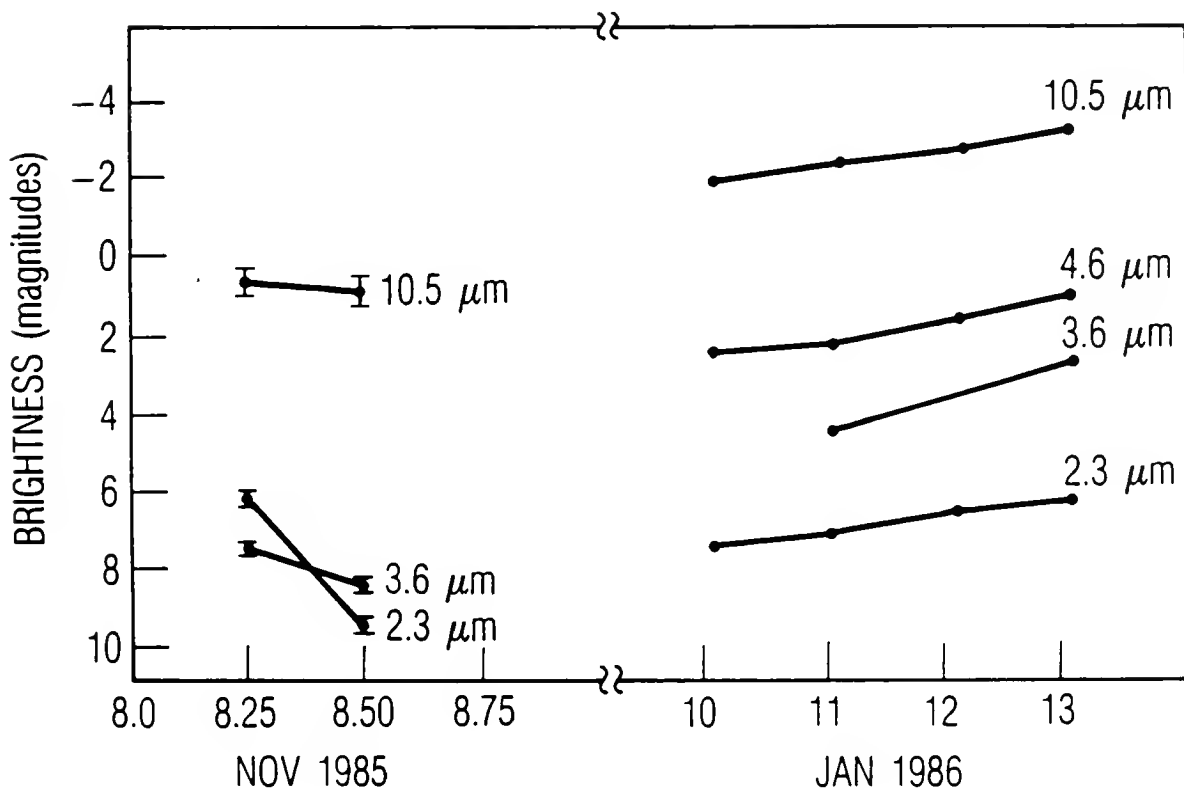


FIGURE 1

COMET HALLEY NOV 8.45, 1985 UT

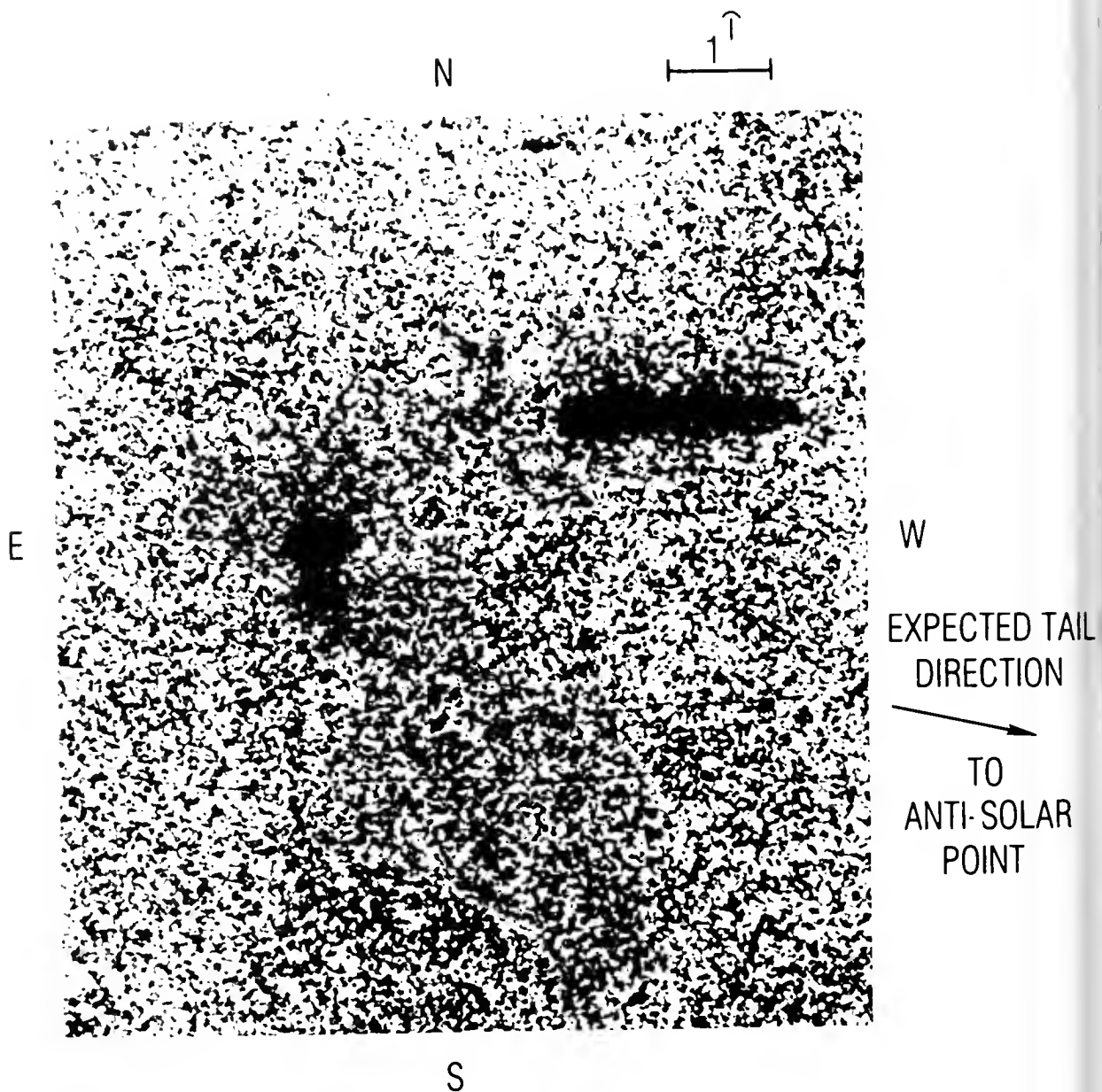


FIGURE 2

5-13 μ m AIRBORNE OBSERVATIONS OF COMET WILSON 1986 ℓ : PRELIMINARY RESULTS

D. K. Lynch and R. W. Russell
Space Sciences Laboratory
The Aerospace Corporation
Los Angeles, CA 90009

F. C. Witteborn and J. M. Bregman
Space Sciences Division, NASA-Ames Research Center
Moffett Field, CA 94035

D. M. Rank
Lick Observatory
University of California, Santa Cruz, CA 95064

M. C. Cohen
University of California, Berkeley, CA 94720

H. C. Campins
Planetary Sciences Institute
Tucson, AZ 85719

ABSTRACT

Comet Wilson was observed from the Kuiper Airborne Observatory approximately April 23.6 and 25.6, 1987, UT ($\simeq 3$ and 5 days after perihelion) using the NASA-Ames Faint Object Grating Spectrometer. Spectrophotometric data were obtained with a 21" aperture ($\simeq 10,000$ km at the comet) between 5 and 13 μ m and with a spectral resolution of 50-100. Spectra of the inner coma and nucleus reveal a fairly smooth continuum with little evidence of silicate emission. The 5-8 μ m color temperature of the comet was 300 ± 15 K, approximately 15 percent higher than the equilibrium blackbody temperature. All three spectra of the nucleus show a new emission feature at $\simeq 12.25\mu\text{m} \simeq$ two channels (.22 μm) wide. Visual and photographic observations made during the time of these observations showed a broad faint, possibly two-component tail. No outburst activity was observed.

This work was supported by NASA Contract No. NAS2-12370
and The Aerospace-Sponsored Research Program.

AERODYNAMIC PROPERTIES OF FRACTAL GRAINS: IMPLICATIONS FOR THE PRIMORDIAL SOLAR NEBULA

P. Meakin
Experimental Station
Central Research and Development Department
E. I. DuPont de Nemours & Company
Wilmington, DE 19898

and

B. Donn
Laboratory for Extraterrestrial Physics
NASA-Goddard Space Flight Center
Greenbelt, MD 20771

Full paper submitted to *Ap. J. Lett.*, December 1987

ABSTRACT

Under conditions in the primordial solar nebula and dense interstellar clouds, small grains have low relative velocities. This is the condition for efficient sticking and formation of fractal aggregates. A calculation of the ratio of cross-section, σ , to number of primary particles, N , for fractal clusters yielded $\ln \sigma/N = 0.2635 + 0.5189N^{(-0.1748)}$. This ratio decreases slowly with N and approaches a constant for large N . Under the usual assumption of collisions producing spherical compact, uniform density aggregates, σ/N varies as $N^{-1/3}$ and decreases rapidly. Fractal grains are therefore much more closely coupled to the gas than are compact aggregates. This has a significant effect on the aerodynamic behavior of aggregates and consequently on their evolution and that of the nebula.

It has been known for some time (Whitlaw-Gray and Patterson, 1932; Fuchs, 1964) that aerosols are fluffy, low-density aggregates. This is also true of particulate clouds in the laboratory (Stephens and Russell, 1979; Samson *et al.*, 1987) and is illustrated in Figure 1. Micrometer-size or smaller grains in the atmosphere (Fuchs, 1964) or solar nebula (Völk *et al.*, 1980; Weidenschilling, 1984) have relative velocities about one ms^{-1} . Therefore, similar structures should be found in each case.

Recent work, both experimental (Forrest and Witten, 1979; Martin *et al.*, 1986) and theoretical (Sutherland, 1967; Witten and Sander, 1981; Kolb *et al.*, 1983; Meakin, 1983, 1984a; Sander, 1984; Kolb; Samson *et al.*, 1987) has shown that these aggregates are fractals (Mandelbrot, 1982). Figure 2 compares a soot particle and a numerical simulation of cluster-cluster growth with linear trajectories. A principal characteristic of fractal aggregates is that the number of primary particles, N , within a radius r , measured from randomly selected particle, is given by

$$N(r) = Ar^D. \quad (1)$$

A is some constant dependent on the system and D is the fractal dimension which depends upon the accretion process. For aerosols the primary process would be cluster-cluster accretion (Meakin *et al.*, 1985). This process leads to a value of D with $1.7 < D < 2.1$ (Meakin, 1984b; Julien *et al.*, 1984). For a fractal, the density $\rho(r)$ decreases with size according to the relation

$$\rho(r) \propto r^{D-3}. \quad (2)$$

For aerosol aggregates, therefore, $\rho(r)$ varies approximately as r^{-1} .

This result will have a significant effect on the aerodynamic behavior of fractal aggregates. In the usual treatments of the grain collisions where it has been assumed that collisions produce compact bodies with a constant density, the gas drag decreases rapidly with size. For fractals on the other hand, drag decreases very slowly, as we now show.

We report here the first step towards a quantitative analysis of the aerodynamic behavior of fractal aggregates. A calculation of the projected cross-section as a function of size has been carried out. Numerical simulations were performed using the cluster-cluster aggregation model (Meakin *et al.*, 1985). A gas-kinetic velocity distribution in which velocities are proportional to $N^{-1/2}$ was adopted. Nine simulations were carried out starting with 200,000 particles and continued until the maximum size first exceeded 10,000 particles.

After each cluster (containing N particles) had been generated, the projected area was obtained by projecting the cluster onto a plane and picking $5N$ points at random in a circle of radius R_{max} enclosing the projected cluster (here R_{max} is the maximum radius of the cluster measured from its center of mass). If M of these points are in the region containing the projection, then an estimate of the projected cluster area, σ , is given by

$$\sigma = \pi R_{max}^2 \frac{M}{5N} \quad (3)$$

For each cluster this procedure was repeated for two other projections in directions mutually perpendicular to the first.

The continuous line in Figure 3 shows the dependence of $\ln(\sigma/N)$ on $\ln(N)$. Since the fractal dimensionality (D) is less than 2, we expect that in the asymptotic limit ($N \rightarrow \infty$) that σ/N should be independent of N (perhaps σ could depend on some power of $\ln(N)$, but not on a power of N). Consequently, the data shown in Figure 1 have been fitted to the form

$$\sigma = AN + BN^\beta. \quad (4)$$

For clusters in the size range $N = 5-100$ a nonlinear least squares fit give $A = 0.2635$, $B = 0.5189$ and $\beta = 0.8252$. This curve is represented by the upper line in Figure 3 which has been displaced to distinguish it from the simulation data. It is apparent that this fits the simulation results very well for all values of N . Even for single particles ($N = 1$) the dashed curve gives a projected area of $A+B$ or 0.782 compared to a value of $\pi/4$ or 0.785 expected for a sphere of unit diameter. For clusters in the size range 1-2500 particles, the same procedure gave $A = 0.2403$, $B = 0.5172$ and $\beta = 0.8465$. Again, $A+B = 0.768$ is quite close to the expected values of $\pi/4$. These results suggest that in the limit $N \rightarrow \infty$ the projected area approaches a value of about 0.24.

For comparison, in Figure 3, we include the curve for $\sigma/N \propto N^{-1/3}$, appropriate for a compact body. This curve has been set to $\sigma = \pi/4$ at $N = 1$ and thus matches the fractal curve at $\ln N=0$. Note the steep decrease in the $\ln \sigma/N$ compared to the fractal curve. As σ/N is the ratio of gas drag-to-particle mass, it is the dominant factor in establishing the gas-grain interaction. With the gas velocity field, it determines the motion of the aggregate.

For fractal grains, the near constancy of this ratio means that aggregates will have similar aerodynamic behavior over a wide range of sizes. In particular, larger fragments will not settle much faster than smaller ones nor will they interact very differently with turbulent eddies leading to large relative velocities (Völk *et al.*, 1980; Weidenschilling, 1984).

The optical properties of fractals also differs from those of compact particles (Berry and Percival, 1986).

References

- Berry, M. V. and Percival, I. C., 1986, *Optica Acta*, **33**, 577.
- Forrest, S. R. and Witten, T. A., 1979, *J. Phys.* **A12**, L109.
- Fuchs, N. A., 1964, *Mechanics of Aerosols*, McMillan, N.Y., Ch. 1.
- Julien, R., Kolb, M. and Botet, R., 1984, in *Kinetics of Aggregation and Gelatin*, eds. F. Family and D. P. Landau, Elsevier, p. 101.
- Kolb, M., Botet, R. and Julien, R., 1983, *Phys. Rev. Lett.*, **51**, 1123.
- Mandelbrot, B., 1982, *The Fractal Geometry of Nature*, W. H. Freedman, N.Y.
- Martin, J. E., Schaeffer, D. W. and Hurd, A. J., 1986, *Phys. Rev.*, **A33**, 3540.
- Meakin P., 1983, *Phys. Rev. Lett.*, **51**, 1119.
- Meakin, P., 1984a, *J. Coll. Interface Sci.*, **102**, 505.
- Meakin, P., 1984b, *Phys. Rev.*, **A29**, 997.
- Meakin, P., 1988, in *Phase Transitions and Critical Phenomena*, C. Domb and J. L. Lebowitz, eds., Academic Press, N.Y.
- Meakin, P., Vicsek, T. and Family, F., 1985, *Phys. Rev.*, **B31**, 564.
- Samson, R. J., Mulholland, G. W. and Gentry, J. W., 1987, *Langmuir*, **3**, 272.
- Sander, L. M., 1984, in *Kinetics of Aggregation and Gelation*, eds. F. Family and D. P. Landau, Elsevier, p. 13.
- Stephens, J. R. and Russell, R., 1979, *Ap. J.*, **228**, 780.
- Sutherland, D. N., 1967, *J. Colloid Interface Sci.*, **25**, 373.
- Völk, H. J., Jones, F. C., Morfill, G. E. and Röser, R., 1980, *Astron. Astrophys.*, **85**, 316.
- Weidenschilling, S. J., 1984, *Icarus*, **60**, 553.
- Whitlaw-Gray, R. and Patterson, H. S., 1932, *Smoke*, Edward Arnold & Co., London, Chs. 8, 10.
- Witten, T. A. and Sander, L. M., 1981, *Phys. Rev. Lett.*, **47**, 1400.

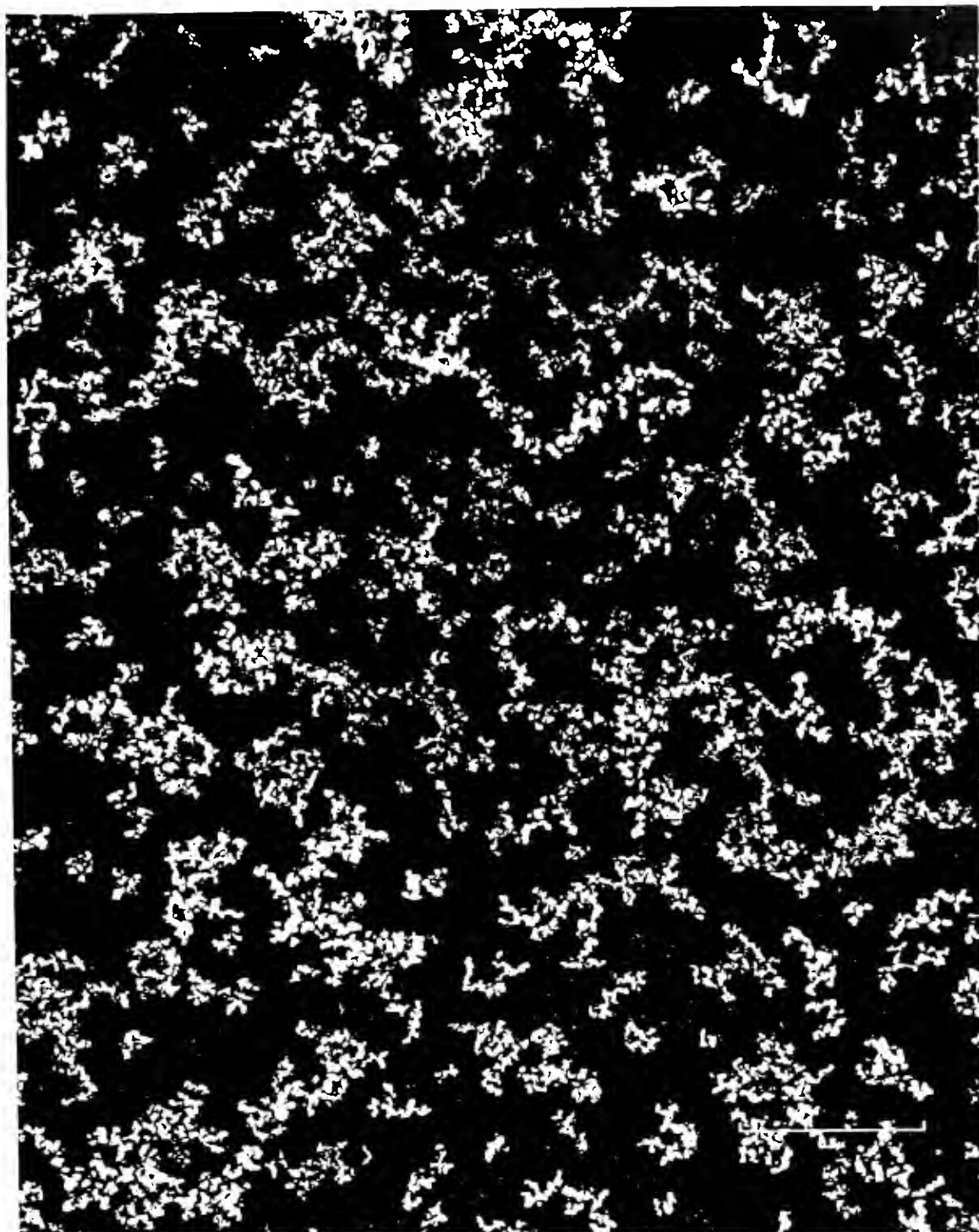
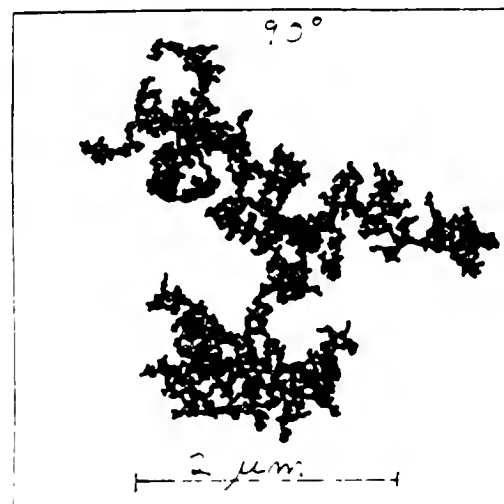
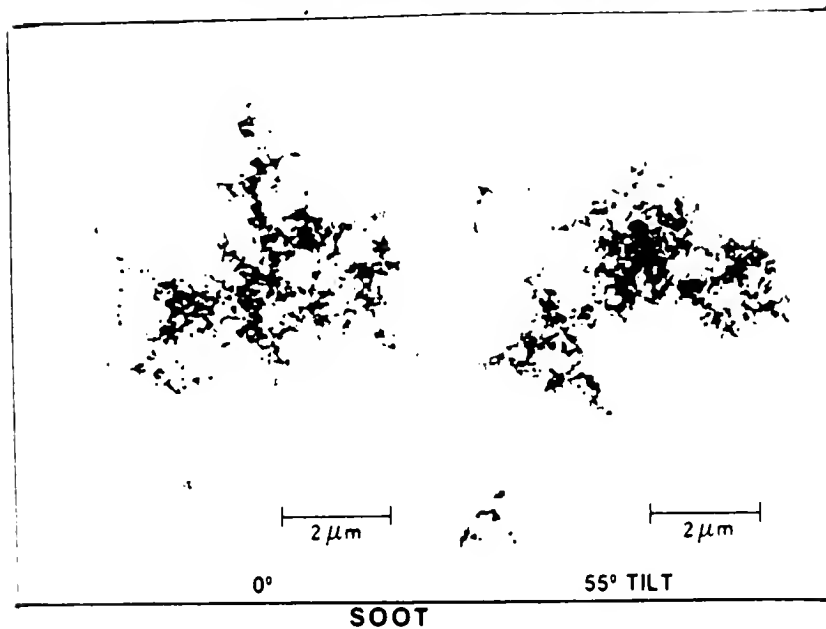


Figure 1 - Fused Silica clusters. Primary particles are $\sim 10\mu$. Because of high-formation temperature, particles are molten and fuse on contact. (Courtesy of Cab-O-Sil Division, Cabot Corp.).

AGGLOMERATE VIEWED AT TWO ANGLES



COMPUTER SIMULATION

Figure 2 - Comparison of soot particle and numerical simulation at two angles of view showing fractal structure. (Soot-structure courtesy of G. W. Mulholland, National Bureau of Standards).

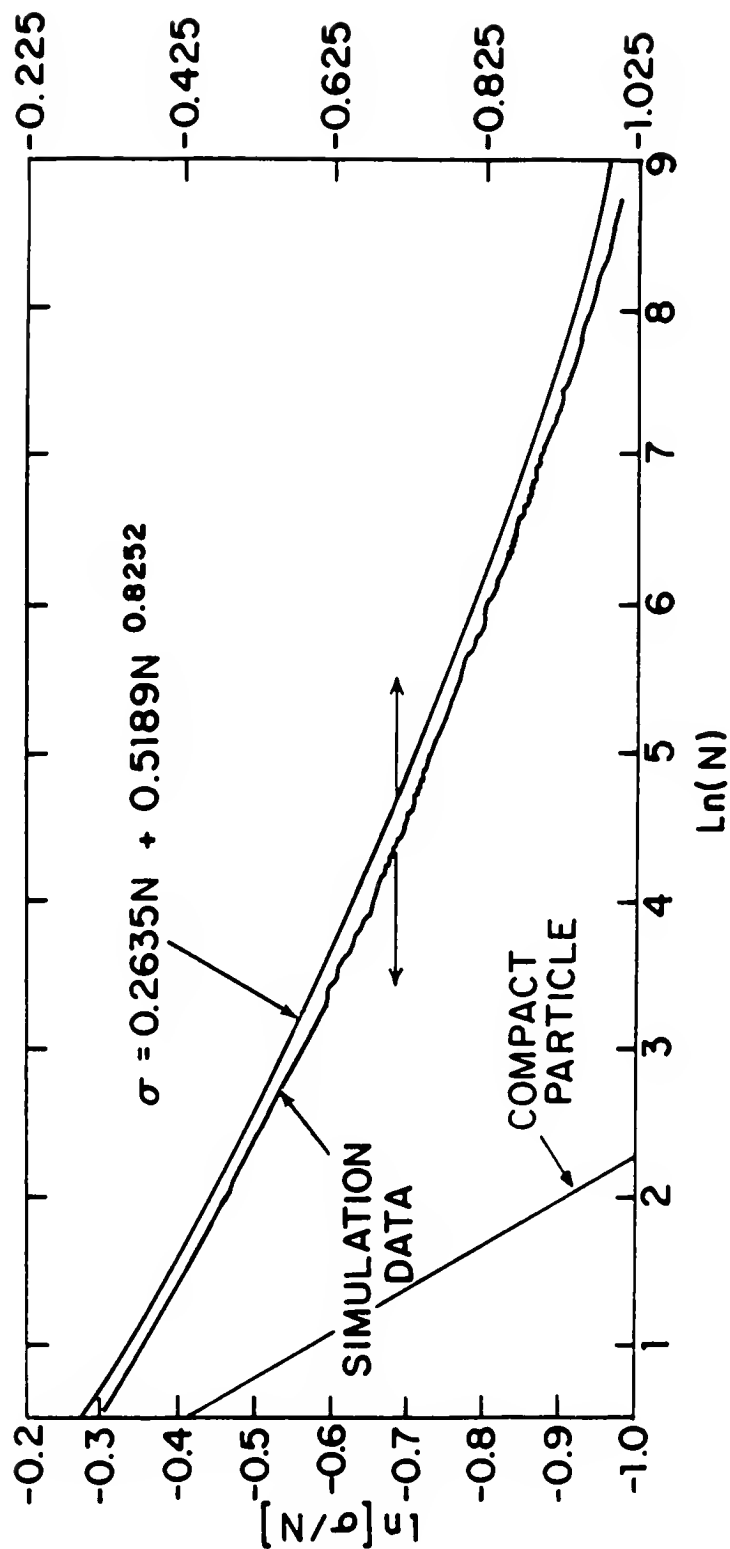


Figure 3 - Projected cross-section of fractal aggregates. Cross-section, σ , measured in terms of particle of unit diameter, $\sigma = \pi/4$. N is number of particles in aggregate. For fractal aggregate, $(\sigma/N)_{\infty} = 0.24$, $\ln \sigma/N_{\infty} = 1.43$. Curve for compact object decreases without limit. The two fractal curves have been displaced 0.025 units in the abscissa of clarity.

COLOR GRADIENTS IN THE COMA OF P/HALLEY

Karen Meech
Institute for Astronomy
University of Hawaii at Manoa
Honolulu, HI 96822

Some important information relevant to the understanding of the gas/dust dynamics near the surface of a comet nucleus concerns knowledge of the grain composition and scattering properties as well as the particle size distribution of dust in the coma. Ground-based measurements of light scattered from the dust comae can provide some information about the physical grain properties, in particular about the mean optically dominant grain size (Jewitt and Meech, 1986, hereafter JM86). Optical spectra of continua of nine comets presented in the paper show that all of the scattered light is reddened with respect to the Sun.

There is, in addition, significant scatter in the amount of reddening seen for different comets. In the near-IR regions, the reddening decreases until near $2\text{-}3\mu\text{m}$ where the reflectivity is nearly neutral. Beyond $2\text{-}3\mu\text{m}$ the scattered radiation is somewhat blue with respect to the sunlight. Figure 1 (Fig. 4 from JM86) illustrates the change in reflectivity (expressed as percent per 10^3Å) as a function of wavelength. The trend is consistent with: (1) scattering from \approx micron-sized and larger slightly absorbing spheres, (2) scattering from power law grain-size distributions where the mean grain size is a $\geq 1\mu\text{m}$, or (3) scattering from the surfaces of macroscopic grains (which cannot be treated by Mie theory). Therefore, the slope of the continuum reflectivity may be used as a diagnostic of the mean optical sizes of grains in the comae of comets.

It is of particular interest to see if there are any observable changes in the grain-size distribution during outbursts. Time series spectrophotometric observations were made of P/Halley during 15-22 November 1985 using the McGraw-Hill 1.3m telescope at Kitt Peak (Meech and Jewitt, 1987). The effective spectrograph resolution was $\approx 15\text{Å}$ in the wavelength range $3700 \leq \lambda (\text{Å}) \leq 6900$. Two outbursts of about 0.6 mag and 0.4 mag occurred near 15 November 1985 at $\sim 10\text{ UT}$, and 21 November 1985 at 4:30 UT, respectively. Although the dust continuum level increased by nearly a factor of two during the outbursts, the continuum color, measured as a reflectivity gradient, remained essentially constant during the entire eight-day observation interval. The reflectivity gradient found for P/Halley was $S' = (9 \pm 2)\%$ per 10^3Å in the wavelength interval $4390 \leq \lambda (\text{Å}) \leq 6820$. This is consistent with the optical reflectivity gradients found for other comets (see Fig. 1).

Although no coma color changes were observed during the November 1985 outbursts, a color gradient within the coma has been observed in P/Halley. Observations were obtained by D. Jewitt with the IIDS spectrograph using the Kitt Peak 2m telescope on 2 May 1986. Spectra were obtained at 12 different positions in the coma along the projected sun-comet line. The continuum reflectivity gradients computed from the spectra as a function of distance from the nucleus are shown in Figure 2. It is clear from the figure that the dust is all reddened with respect to the sunlight (neutral scattering has $S'=0$). However, the grain color becomes systematically bluer in the anti-solar direction (negative displacement from the nucleus) as compared to the solar direction. The color gradient indicates a change in the mean optically dominant grain size in the coma. A plausible explanation is that grains with a large radiation pressure factor, β , ejected in the sunward direction are decelerated and turned around by solar radiation pressure much sooner than are the grains with small β . Since β is a function of particle size, the radiation pressure introduces a grain-size sorting in the coma.

Radial color gradients in J, H, and K images of P/Halley such as reported by Campins

(1987) have not been observed by us. We have found no difference between the optical V and R profiles in a sample of ten comets observed with high-precision CCDs (Jewitt and Meech, 1987). However, we have found that focus differences between filters can cause apparent color gradients on scales a few times the seeing disk, qualitatively similar to the gradients reported by Campins.

REFERENCES

- Campins, H., 1987, this volume.
Jewitt, D. C. and K. J. Meech, 1986, *Astrophys. J.*, **310**, 937-952.
Jewitt, D. C. and K. J. Meech, 1987, *Astrophys. J.*, **317**, 992-1001.
Meech, K. J. and D. C. Jewitt, 1987, *Astron. Astrophys.*, **187**, 585- 593.

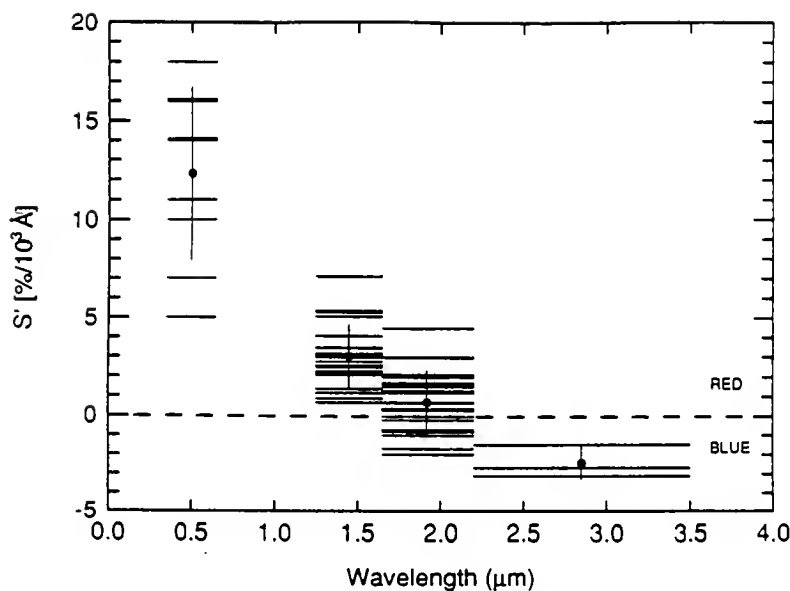


Figure 1. The normalized reflectivity gradient, $S'(\lambda_1, \lambda_2)$, measured in $\%/10^3 \text{ Å}$, is shown as a function of the wavelength of observation λ (in μm). Each comet is represented by a horizontal bar connecting the end point wavelengths λ_1 and λ_2 . Neutral scattering is indicated by the dashed horizontal line at $S'(\lambda_1, \lambda_2) = 0$. Reddening of the scattered radiation is indicated by $S' > 0$ while enhanced blue scattering is indicated by $S' < 0$. The mean S' within each measured wavelength interval is plotted with a black dot and the 1σ standard deviation on the mean is shown with a vertical line. The figure shows that the color of the scattered radiation varies systematically with the wavelength of observation.

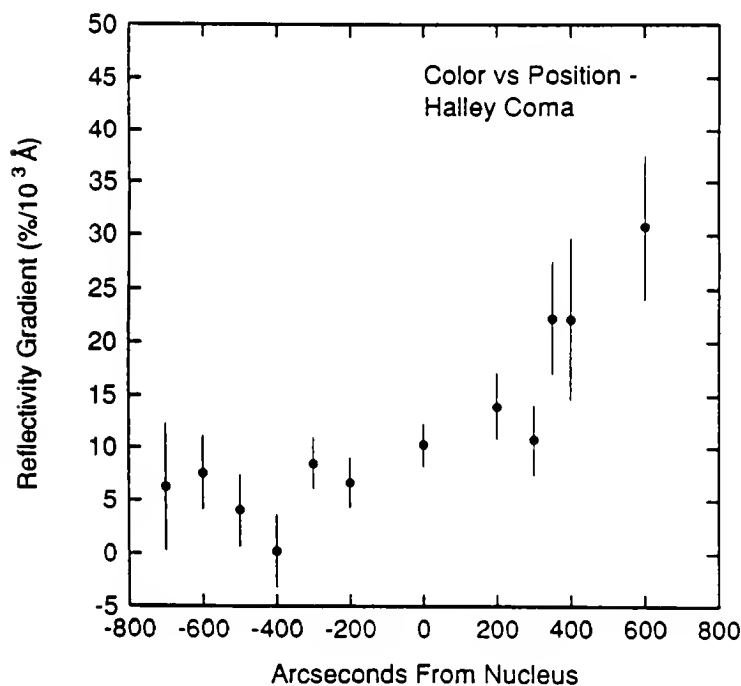


Figure 2. The reflectivity gradient in the grain coma of comet P/Halley versus distance along the projected sun-comet line, measured in arcseconds from the nucleus. Positive units on the x-axis indicate displacement towards the sun. The graph shows that the reflectivity gradient is a weak function of position on the coma. The approximate gradient is $dS'/dx = 0.01\%$ per 10^3 Å per linear arcsecond. The observations were obtained on UT 1986 May 3, when the comet was at $R = 1.6 \text{ AU}$, $\Delta = 0.7 \text{ AU}$.

OPTICAL PROPERTIES OF COMETARY GRAINS

Tadashi Mukai
Kanazawa Institute of Technology
Nonoichi, Ishikawa 921, Japan

An analysis of visible/near-infrared polarimetry of Comet Halley¹ leads to a variation of the complex refractive index $m=n-i-k$ of grain material with wavelength, i.e., a slight decrease of n from 1.39 at $\lambda=0.37\mu\text{m}$ to 1.37 at $\lambda=2.2\mu\text{m}$, in contrast to an increase of k from 0.024 at $\lambda=0.37\mu\text{m}$ to 0.042 at $\lambda=2.2\mu\text{m}$. The mass distribution of grains reported by Mazets *et al.* from *in situ* measurements of Vega 2 was applied in the analysis.

Combining these optical constants with those of "astronomical silicate" proposed by Draine², we present "cometary silicate" as a candidate for cometary grains. Figure 1 shows the complex refractive index of the proposed "cometary silicate."

Based on the Mie theory, an emission efficiency of each of the grains is computed, as well as its temperature, as functions of grain radius and sun-comet (grain) distance r (see Fig. 2).

It is found (Fig. 3) that the tentative thermal spectrum from these "cometary silicates," where the mass distribution of grains reported by Mazets *et al.*³ from Vega 2 was applied, fits very well to the infrared spectrum of Comet Halley at $r=1.3$ AU detected by Tokunaga *et al.*⁴ and Herter *et al.*⁵

This means that "cometary silicate" can explain not only the phase angle (sun-comet-observer angle) and wavelength dependences of visible/near-infrared polarization, but also the thermal emission spectrum of Comet Halley.

REFERENCES

1. Mukai, T., Mukai, S., Kikuchi, S., 1987, *Astron. Astrophys.*, in press.
2. Draine, B. T., 1985, *Ap. J. Suppl.*, **57**, 587-594.
3. Mazets, E. P. *et al.*, 1986, *Nature*, **321**, 276-278.
4. Tokunaga, A. T. *et al.*, 1986, *Astron. J.*, **92**, 1183-1190.
5. Herter, T. *et al.*, 1986, ESA SP-250, Vol. 1, 117-120.

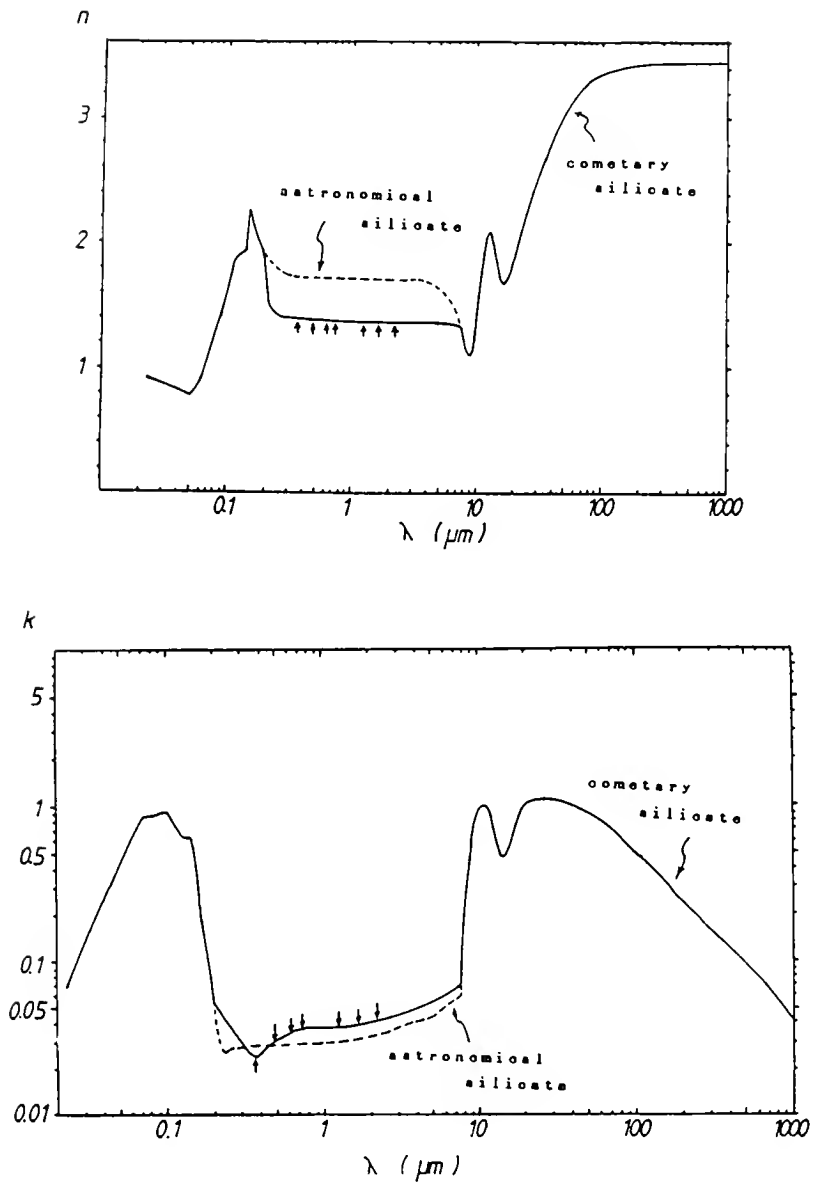


Figure 1. Refractive index n and absorption coefficient k of the proposed "cometary silicate," as a function of wavelength λ . Seven arrows indicate the values deduced from an analysis of polarimetry of Comet Halley.¹⁾

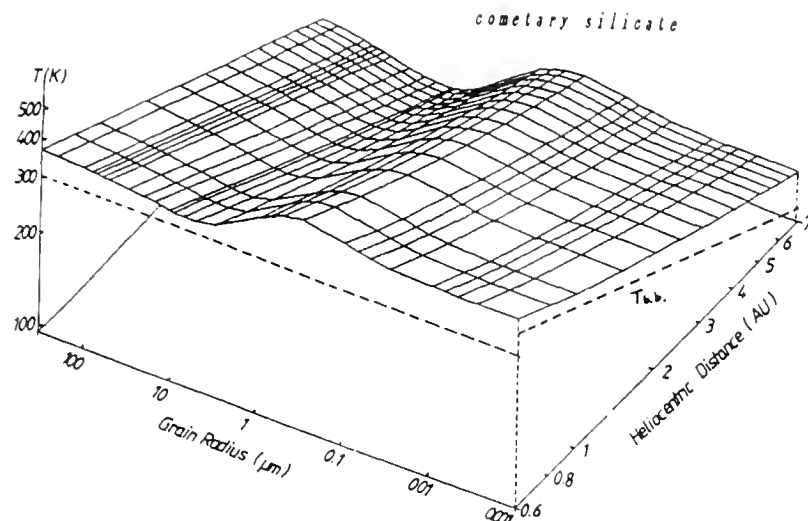


Figure 2. Temperature T , in units of K, of the proposed "cometary silicate." $T_{b.b.}$ denotes the temperature of a black body, which is independent of grain radius.

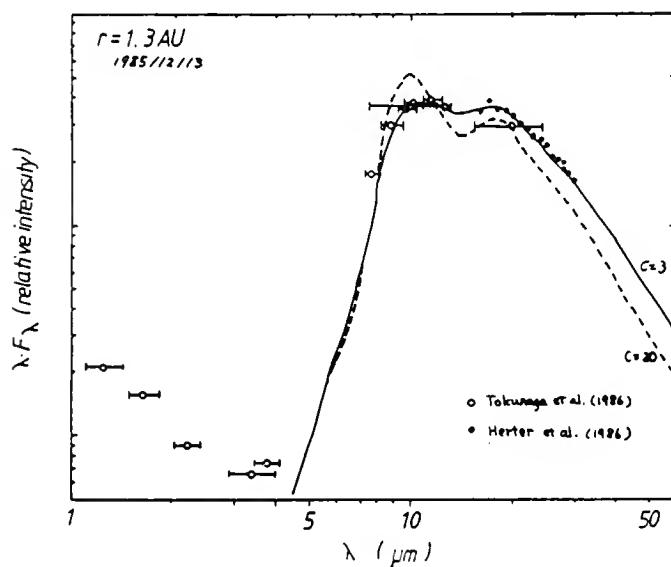


Figure 3. The energy distribution of Comet Halley λF_λ vs. λ . Computed curves (thermal emission alone) are normalized to the observed data of Tokunaga *et al.* (1986) at $\lambda = 12.5 \mu\text{m}$. The data of Herter *et al.* (1986) have been scaled to match a value computed at $\lambda = 20 \mu\text{m}$. In order to demonstrate a variation of spectrum due to an increase of smaller grains with radii less than $0.1 \mu\text{m}$ by a factor c in number, two computed results are illustrated based on dust distribution by Mazets *et al.* (1986). $c=3$ leads negligible changes in brightness and polarization in visible (scattered light), but $c=20$ produces significant variations in both.

A POSSIBLE EXPLANATION FOR THE INCONSISTENCY BETWEEN THE GIOTTO GRAIN MASS DISTRIBUTION AND GROUND-BASED OBSERVATIONS

C. H. Perry, S. F. Green, J. A. M. McDonnell
Unit for Space Sciences
University of Kent
Canterbury, UK

The Problem:

Giotto measured the *in situ* Halley dust grain mass distribution with two instruments, PIA (Particle Impact Analyzer) and DIDSY (Dust Impact Detection System), as well as the total intercepted mass from the deceleration of the spacecraft (Giotto Radio-Science Experiment, GRE). The mass distribution for $m < 10^{-10}$ kg is dealt with elsewhere (McDonnell *et al.*, 1987, *Astron. & Astrophys.*, in press) and was measured by the Vega spacecraft with similar results. DIDSY was, however, the only experiment to measure individual grain masses for $m > 10^{-9}$ kg. This "discrete" data was transmitted for an unbiased sample of grains large enough to excite more than one sensor on the front shield. Preliminary analysis of these discrete data (McDonnell *et al.*, 1987) indicated a mass distribution index $\alpha' \cong 0.5$ (where $N(>m) = K \cdot m^{-\alpha}$), significantly lower than for the lower mass grains. A consequence of this low slope is that the contribution to the total cross-sectional area of grains (upon which ground-based observations of scattered and thermal radiation depend), and the total grain mass, is dominated by these large grains.

Ground-based observations made shortly before encounter (Hanner *et al.*, 1987, *Astron. & Astrophys.*, in press) (Hayward *et al.*, 1987, *Nature*, **326**, 55-57 and this report) have fluxes much higher than would be predicted from Giotto data. In addition, the observed silicate emission around $10\mu\text{m}$ cannot be fitted with models based on the Giotto mass distribution, due to suppression of the feature by the dominant large-mass grains (Crifo 1987, ESA SP-278, in press). Thus some explanation must be found for the discrepancy between the Giotto mass distribution and ground-based observations.

The Solution:

Interpretation of DIDSY data depends on the momentum transfer to the front shield, rather than the momentum actually possessed by the grains. For impacts which do not penetrate the shield, the momentum transfer is greater than that carried by the particle itself, since shield material is also vaporized and ejected. As the penetration mass is reached ($\cong 3 \times 10^{-9}$ kg), this enhancement must be derated to allow for ejecta continuing through the rear of the 1 mm shield. Figure 1 shows the DIDSY discrete data for a realistic range of values for this derating factor (γ). Two points in particular should be noted:

- 1) The region of overlap with the binned data at $\cong 5 \times 10^{-10}$ kg shows the same mass distribution index $\cong 0.9$.
- 2) For any reasonable value of γ the large-mass slope is shallower up to the limit of data ($\cong 10^{-6}$ kg) and lies in the range $0.3 \leq \alpha' \leq 0.6$.

The GRE total spacecraft deceleration is a measure of the average mass distribution up to the largest impacting particle. The average large grain mass index which satisfies both the DIDSY data and GRE total mass is $\alpha' = 0.54 \pm 0.02$ up to $m \cong 5 \times 10^{-4}$ kg. (This assumes a r^{-2} cometocentric density distribution for the time near closest approach when telemetry was lost.) This is only an average value; if the slope is shallower (say

$\alpha' \cong 0.4$) for $10^{-9} < m < 10^{-6}$ kg, then it would be steeper ($\alpha' = 0.85$) above 10^{-6} kg to satisfy the GRE total mass. Herein lies a possible explanation for the inconsistency between observations and spacecraft data.

Giotto encounter lasted only a few minutes, but grains which were encountered took between one and six or more hours to arrive from the nucleus, with the largest mass grains having the lowest velocities (e.g., Gombosi, 1986, ESA-SP-250, Vol. II, 167-172). Thus, if the level of activity from the region of the nucleus surface that was sampled changed during this period, the observed mass distribution would not be representative of that near the nucleus. Figure 2 shows the mass distribution that would be observed for a model with high activity six hours before encounter, falling by a factor of 30 one hour before. This model satisfies both the observed DIDSY and GRE data and the ground-based observations, since the latter, made $\cong 6$ hours pre-encounter, would sample the small grains emitted from the high activity region.

Conclusions:

1) Giotto DIDSY and GRE data represent observations of dust originating from a narrow track along the nucleus. They are consistent with ground-based data (which measure the average coma properties), if assumptions are made about the level of activity along this track.

2) The actual size distribution that should be used for modeling of the whole coma should not include the large mass excess actually observed by Giotto. Extrapolation of the small grain data ($\alpha \cong 0.9$) should be used, since for these grains the velocity dispersion is low and temporal changes at the nucleus would not affect the shape of the mass distribution.

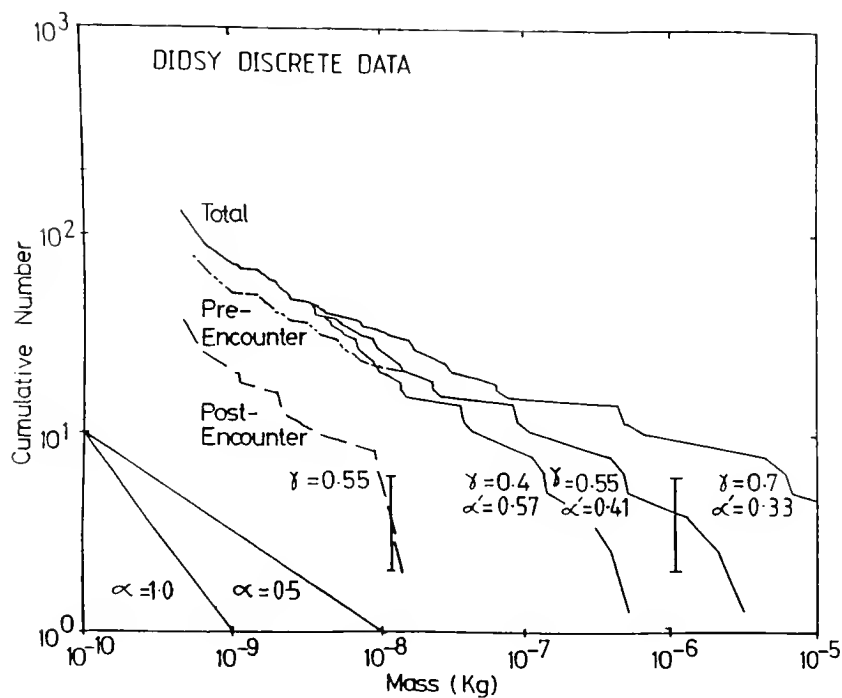


Figure 1. Relative fluence for DIDSY discrete data. The performance limit of the front shield is taken as 3×10^{-9} kg. The different curves correspond to different values of the momentum derating exponent (see text).

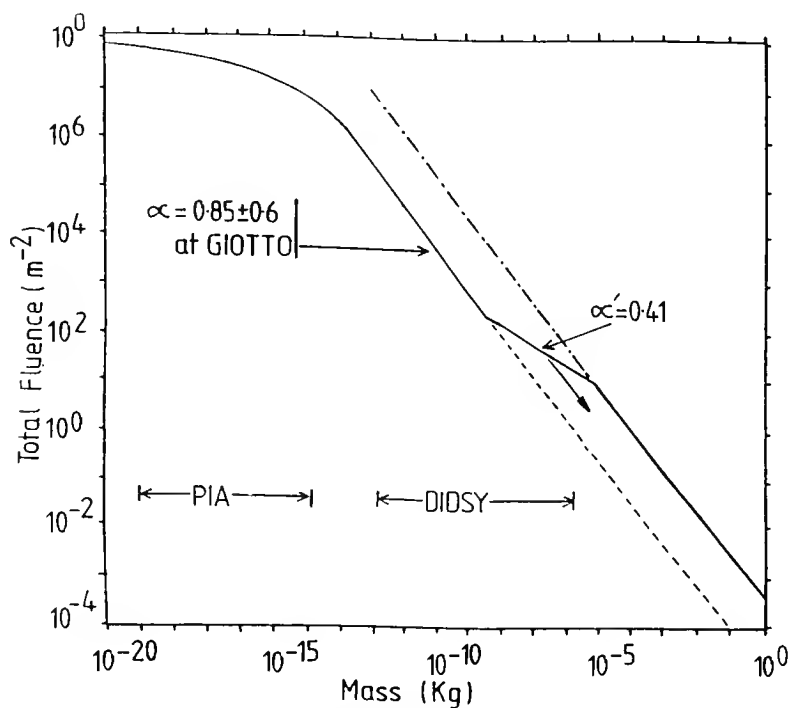


Figure 2. A fluence plot (solid line) which satisfies the Giotto data and represents an intermediate stage between an outburst (chain line) and an inactive period some time later (dotted line). The arrow shows how the distribution would change with time. In addition α' would increase with time. See text for details.

PROPERTIES OF INTERSTELLAR DUST IN REFLECTION NEBULAE

K. Sellgren
Institute for Astronomy
University of Hawaii
Honolulu, HI 96822

Observations of interstellar dust in reflection nebulae are the closest analog in the interstellar medium to studies of cometary dust in our solar system. The presence of a bright star near the reflection nebula dust provides the opportunity to study both the reflection and emission characteristics of interstellar dust. At $0.1\text{--}1\mu\text{m}$, the reflection nebula emission is due to starlight scattered by dust. The albedo and scattering phase function of the dust is determined from observations of the scattered light. At $50\text{--}200\mu\text{m}$, thermal emission from the dust in equilibrium with the stellar radiation field is observed. The derived dust temperature determines the relative values of the absorption coefficient of the dust at ultraviolet wavelengths where the stellar energy is absorbed and at far infrared wavelengths where the absorbed energy is reradiated. These emission mechanisms directly relate to those seen in the near- and mid-infrared spectra of comets. In a reflection nebula, however, the dust is observed at much larger distances (0.1 pc) from the star than in our solar system (1 AU), so that the equilibrium dust temperature is 50 K rather than 300 K . Thus, in reflection nebulae, thermal emission from dust is emitted at $50\text{--}200\mu\text{m}$.

At $1\text{--}25\mu\text{m}$ in reflection nebulae, non-equilibrium emission from small particles ($a\sim 10\text{ \AA}$) is observed in excess over scattered light and equilibrium thermal emission from dust. These small particles, which may be either small grains or large molecules such as polycyclic aromatic hydrocarbons, have low enough heat capacity that when they absorb a single ultraviolet photon, they are temporarily heated to high temperatures ($\sim 1000\text{ K}$). This theory has been proposed to explain the $1\text{--}25\mu\text{m}$ continuum and unidentified emission features (at $3.3, 3.4, 6.2, 7.7, 8.6$, and $11.3\mu\text{m}$) observed in reflection nebulae and elsewhere in the interstellar medium.

The IRAS survey is ideal for studying the excitation of these small particles, as it is very sensitive to low-surface brightness emission and its $12\mu\text{m}$ band in reflection nebulae is dominated by small particle emission. Detailed spatial studies of the Pleiades reflection nebulae, illuminated by B stars, show that the 12 and $25\mu\text{m}$ emission is mostly non-equilibrium emission, while the 60 and $100\mu\text{m}$ emission is mostly equilibrium thermal emission from dust. The $12/25\mu\text{m}$ color temperature is independent of distance from the star, as predicted by non-equilibrium emission models, while the $60/100\mu\text{m}$ color temperature decreases with distance from the star, as expected for equilibrium thermal emission. The $60/100\mu\text{m}$ color temperature observed in other reflection nebulae, whose stars range in temperature from $3,000$ to $21,000\text{ K}$, implies that 60 and $100\mu\text{m}$ emission from these reflection nebulae is also primarily due to equilibrium thermal emission. The $12/100\mu\text{m}$ ratio should therefore be a measure of the relative amount of non-equilibrium and equilibrium thermal emission from dust in reflection nebulae. We have observed the $12/100\mu\text{m}$ ratio to be roughly constant for stellar temperatures of $5,000$ to $21,000\text{ K}$. This implies that the excitation of the small grain emission must occur over a broad range of visual and ultraviolet wavelengths, rather than at a specific visual or ultraviolet wavelength. The $12\mu\text{m}$ emission also accounts for a large fraction ($\sim 25\text{--}40\%$) of the total infrared emission from dust. Because it radiates such a large fraction of the total reradiated stellar energy, it therefore must contribute a similarly large fraction of the visual and ultraviolet absorption from dust. This again suggests a broad band absorption, as there are few or no visual or ultraviolet absorption features capable of accounting for such a large fraction of the total absorption by dust.

LABORATORY SIMULATIONS OF COMET SURFACES

John R. Stephens
Los Alamos National Laboratory
Los Alamos, NM

Bo A. S. Gustafson
Space Astronomy Laboratory
University of Florida
Gainesville, FL

The geometric albedos of frozen mixtures consisting of colloidal silica and carbon black mixed with water have been measured over the wavelength range of 400 to 800 nm to compare with recent observations of Comet Halley. Data were obtained as a function of sample temperature, scattering angle, and wavelength as the frozen samples warmed to 0 degrees C in a vacuum. Scattering from water ice, flat black paint, and Kodak white reflectance paint were also measured.

A schematic of the apparatus is shown in Figure 1. The sample is frozen onto a quartz plate in thermal contact with a copper block that has been cooled with liquid nitrogen. The front surface of the deposit is warmed and allowed to freeze again to provide a smooth surface and a uniform 2 mm sample thickness. The assembly was placed in a vacuum chamber with the deposit surface vertical and the surface normal 20 degrees from the incident source beam. The chamber vacuum and sample temperature are monitored throughout the experiment. The intensity of the source is monitored prior to the experiment. The deposit is illuminated using a Xe arc lamp, and the scattering intensity measured, over the spectral range of 400-800 nm, as a function of scattering angle as the sample is warmed to 0 degrees C.

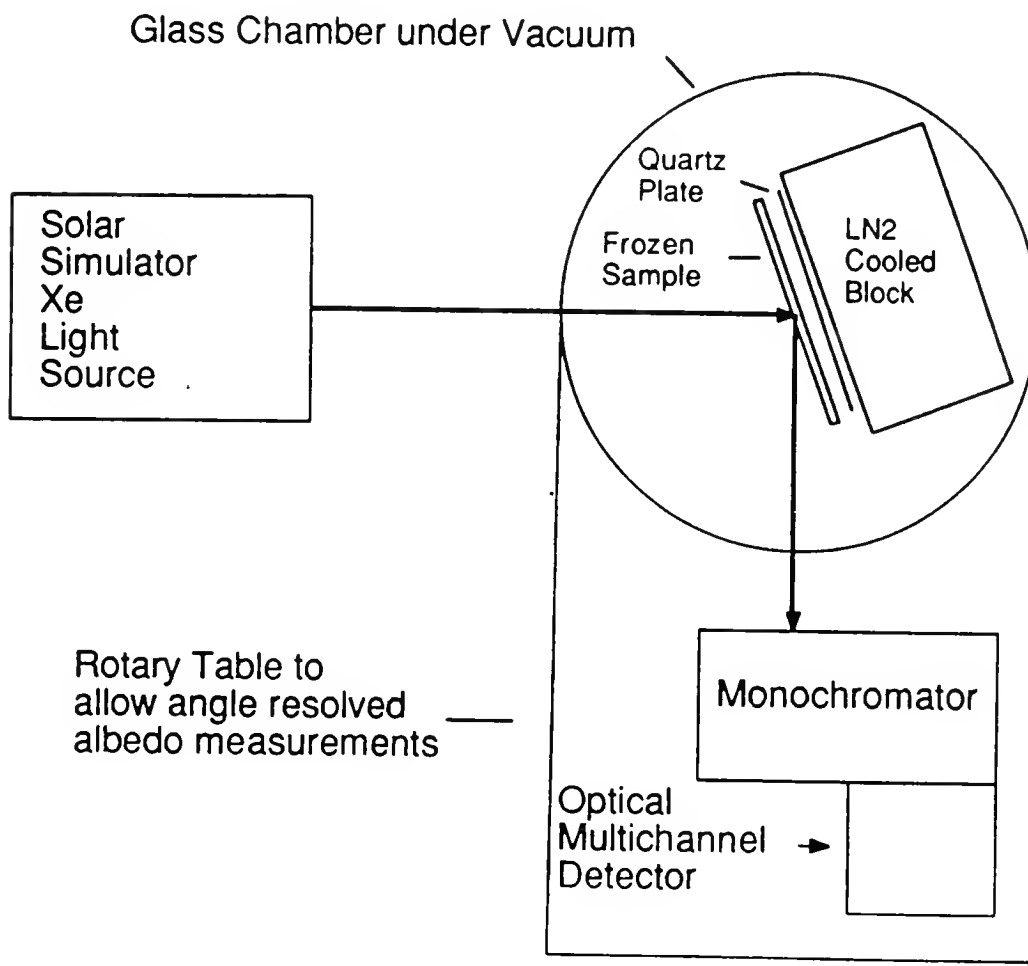
The albedo of pure water, mixtures of 1% carbon plus 10% colloidal silica in water, and 10% colloidal in water were measured. The generalized geometric albedo at each angle is calculated by normalizing the intensity of scattered light at each angle to the source intensity and dividing the result by the intensity of light scattered from a lambert surface. Kodak white reflectance paint, which has a published reflectance of greater than 98% from 200 to 2500 nm, was used as the lambert surface in calculating the geometric albedos. Since the angular dependence of the generalized geometric albedos was small, the albedos were averaged over all angles to yield an average (angle integrated) general geometric albedo for each sample.

The geometric albedos were only weak functions of scattering angle and were flat from 400 to 800 nm within the 15% precision of the experiments. The apparent angle integrated albedo for the water ice sample was 0.05. The low apparent albedo for the water ice sample was 0.05. The low apparent albedo resulted from the high transmission of the sample. Angle integrated albedos were 0.05 for the C/SiO₂/H₂O mixture and from 0.3 to 0.6 for the SiO₂/H₂O mixtures. Flat black paint had an albedo of 0.05. Due to transmission of the SiO₂/H₂O mixture, the albedo of an optically thick deposit may be as much as 30% higher than the above figures. The C/SiO₂/H₂O mixture showed less than a 20% increase in albedo as the sample warmed from -60 C, while the albedo the SiO₂/H₂O mixture increased from 0.3 to 0.6 while warming from -40 to -20 C. In the SiO₂/H₂O deposit, a highly reflective layer of SiO₂ formed on the surface as the ice sublimed, leading to an increase in albedo and decrease in transmitted light.

The change in albedo of the samples show that sublimation of the water from the sample surfaces can have a major effect on the albedo of a particle/ice sample in the visible. Such processing may have a marked effect on the visible albedo of comet surfaces as well.

Figure 1

Schematic of Apparatus to Measure Surface Albedos



A MULTICOMPONENT MODEL OF THE INFRARED EMISSION FROM COMET HALLEY

K. S. Krishna Swamy, S. A. Sandford, L. J. Allamandola,
F. C. Witteborn, and J. D. Bregman
NASA-Ames Research Center, M.S. 245-6
Moffett Field, CA 94035

We have tried to construct a coherent and consistent model to explain the observed infrared radiation from comet Halley from 3 to $160\mu\text{m}$ based on information available from collected interplanetary dust particles (IDPs) and the recent Halley flybys. We have considered carbonaceous materials as well as silicates in modeling cometary comae spectra. We used the optical constants of an α :C-H film (1) to represent the carbonaceous material and optical constants from lunar sample 12009.48 (a sample rich in olivines) to represent the silicates (2). While the carbonaceous component in comets is probably not identical to α :C-H films, the properties of the films should provide a representative behavior. An olivine-rich silicate mixture was chosen since spectral matches to the Halley $10\mu\text{m}$ silicate feature indicate that crystalline olivine is a major component of the Halley dust (3). In the visible spectral region we used $m = 1.38 - 0.039i$ for the silicates and data from reference (4) for the carbonaceous component. We have used both the dust grain-size distribution inferred for comet Halley (5) and a simple power law ($n \propto a^\alpha$) distribution in our calculations. The absorption cross-sections for spheres and core-mantle grains were done using Mie theory (6) and Guttler's theory (7) respectively. Several possible cases have been considered which can explain the observed strength of the 3.4 and $10\mu\text{m}$ features relative to the adjacent continuum and the slope of the continuum in the $4\text{--}8\mu\text{m}$ region.

Mixture of Independent Silicate and Carbonaceous Grains

The ratio of mass fraction of silicates to amorphous carbon ratio (X) of about 40 is required for the Halley dust-size distribution to fit the observations. The same is true of the power law-size distribution when $\alpha = -3.5$ (Fig. 1). The $10\mu\text{m}$ feature flattens as the size of the particles increases. The presence of weak features can be seen between 6.1 and $7.1\mu\text{m}$ in the model spectra. These are due to the amorphous carbon and are present even at high values of X . The Halley spectra show that features in this spectral region may be present (3).

Composite Grains

Most of the mineral grains in IDPs are covered with a thin layer of carbonaceous material (8). We have done a number of calculations in which we take this observation into account. If we add a thin carbonaceous coating to the model silicate grains, we find that a good match can be obtained for $X \sim 8$. If the coatings are assumed to be thick, then we require $X > 1$ to produce the observed $3.4\mu\text{m}$ feature. Such a low X value is probably unreasonable given the much higher value seen in IDPs and the rarity of thickly mantled silicate grains in IDPs. Figure 2 shows the model spectrum resulting from a mixture of silicate and amorphous carbon grains ($X=40$, $\alpha=-3.5$) compared with the observational data. The match is quite good over the entire wavelength range.

Conclusions

A model based on a mixture of coated silicates and amorphous carbon grains produces a good spectral match to the available Halley data and is consistent with the compositional and morphological information derived from IDP studies and Halley flyby data. The dark

appearance of comets may be due to carbonaceous coatings on the dominant (by mass) silicates. The lack of a $10\mu\text{m}$ feature may be due to the presence of large silicate grains. The optical properties of pure materials apparently are not representative of cometary materials. The determination of the optical properties of additional silicates and carbonaceous materials would clearly be of use.

A detailed description of the model and results will appear in a forthcoming issue of *Icarus*.

References

1. Angus, J. C., et al., 1986, in *Plasma Deposition Films*, eds. Mort and Jansen, CRC, Press, Boca Raion, 89.
 2. Perry, C. H., et al., 1972, *Moon*, **4**, 315.
 3. Bregman, J. D., et al., 1987, *Astron. Astrophys.*, in press.
 4. Arakawa, T., et al., 1985, *Phys. Rev.*, **31B**, 8097.
 5. Mazets, E. P., et al., 1986, *Nature*, **321**, 276.
 6. van de Hulst, H. C., 1957, *Light Scattering by Small Particles*, John Wiley and Sons, NY.
 7. Guttler, A., 1952, *Ann. Physik*, **6**, 5.
 8. Allamandola, L. J., et al., 1987, *Science*, **327**, 56.
- References from Figure 2.
9. B. Baas, R., et al., 1987, *Astrophys. J.*, **311**, L97.
 10. C. Campins, H., et al., 1986, *ESA SP-250*, Vol. II, 107.
 11. G. Glaccum, W., et al., 1986, *ESA SP-250*, Volumes I, II, and III.
 12. H. Herter, T., et al., 1986, *ESA SP-250*, Vol. II, 117.
 13. K. Knacke, R. F., et al., 1986, *ESA SP-250*, Vol. II, 95.
 14. W. Wichramasinghe, D. T. and Allen D. A., 1986, *Nature*, **323**, 44.

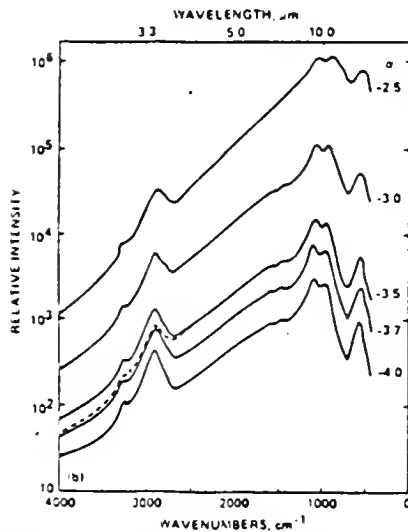


Figure 1. Emission curves for silicate and amorphous carbon mixtures for various values of α . The solid lines are for $X=40$; the dashed line is for $X=80$.

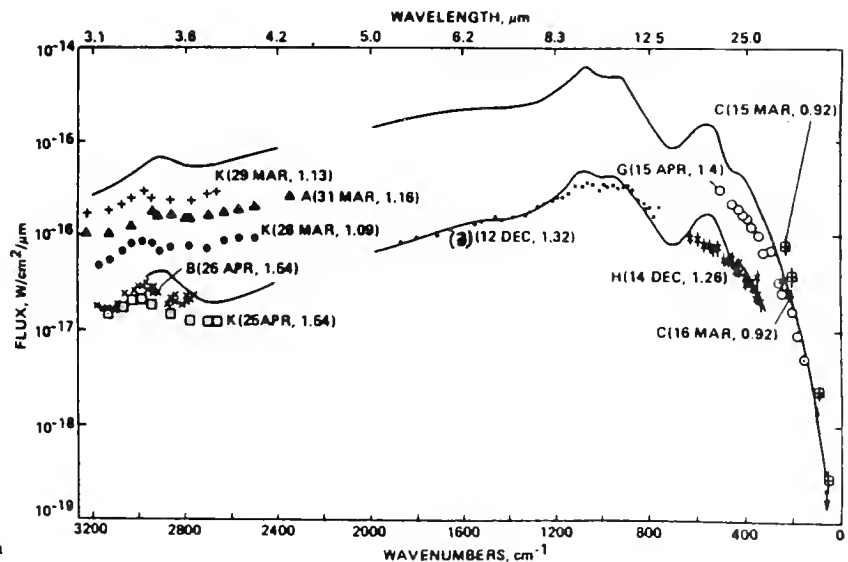


Figure 2. Comparison of the calculated and observed infrared emission from 3 to $160\mu\text{m}$ for Comet Halley. The solid curves are for $r=1.32$ and 0.92 AU with $\alpha = -3.5$ and $X=40$. The observational data are from the numbered and lettered references in the reference list.

THE NASA INFRARED TELESCOPE FACILITY COMET HALLEY MONITORING PROGRAM II. POST-PERHELION RESULTS

A. T. Tokunaga

Institute for Astronomy, University of Hawaii

W. F. Golisch, D. M. Griep and C. D. Kaminski

Infrared Telescope Facility

M. S. Hanner

Jet Propulsion Laboratory

The post-perihelion results of a 1-20 μ m infrared monitoring program of Comet Halley are presented. These results complement previous observations of the pre-perihelion passage of Halley (Tokunaga *et al.* 1986). The observations cover the time period of March 1986 to the present time. During the time the comet was observable, we obtained two or more observations per month. The most interesting results were (1) a detectable change in the J-H and H-K colors of Halley, and (2) a search for a nuclear rotation at J during 20 February to 10 March was unsuccessful.

The perihelion J-H and H-K colors were constant at 0.48 ± 0.01 and 0.17 ± 0.01 , respectively. A preliminary reduction of the data shows that the post-perihelion colors were:

	J-H	H-K
20 Apr. - 12 June 1986	0.43 ± 0.03	0.15 ± 0.01
6 July - 21 Dec. 1986	0.40 ± 0.02	0.06 ± 0.02
26 Feb. - Mar. 1987	0.36 ± 0.05	0.07 ± 0.04

Thus the colors were at first similar to pre-perihelion and then changed from July onward to be bluer and more similar to the solar colors. This suggests that a change may have occurred in the composition of the dust coma of Halley in July 1986.

Reference

Tokunaga *et al.* 1986, *Astron. J.*, **92**, 1183.



Report Documentation Page

1. Report No. NASA CP-3004	2. Government Accession No.	3. Recipient's Catalog No.	
4. Title and Subtitle Infrared Observations of Comets Halley and Wilson and Properties of the Grains		5. Report Date September 1988	6. Performing Organization Code EL
		8. Performing Organization Report No.	
7. Author(s) Martha S. Hanner,*editor		10. Work Unit No.	
		11. Contract or Grant No.	
9. Performing Organization Name and Address NASA Office of Space Science and Applications Solar System Exploration Division Planetary Astronomy Program		13. Type of Report and Period Covered Conference Publication	
		14. Sponsoring Agency Code	
12. Sponsoring Agency Name and Address National Aeronautics and Space Administration Washington, DC 20546			
15. Supplementary Notes *Jet Propulsion Laboratory, California Institute of Technology, Pasadena, CA 91109			
16. Abstract <p>This report summarizes the presented papers and discussions at a workshop held at Cornell University, August 10-12, 1987 to review the infrared observations of Comet Halley and Comet Wilson and to relate them to optical properties and composition of cometary grains. Relevant laboratory studies are also discussed. Recommendations are made for future infrared comet observations and supporting laboratory investigations.</p>			
17. Key Words (Suggested by Author(s)) comets Comet Halley Comet Wilson cometary grains infrared		18. Distribution Statement Unclassified - Unlimited Subject Category 89	
19. Security Classif. (of this report) Unclassified	20. Security Classif. (of this page) Unclassified	21. No. of pages 204	22. Price A10

3 5002 03034 4498

[illegible]

qQB 723 .H2 I54 1988

- Infrared observations of
comets Halley and Wilson
ASTRON

qQB 723 . H2 I54 1988

Infrared observations of
comets Halley and Wilson

National Aeronautics and
Space Administration
Code NTT 4

Washington, D C
20546 0001

Official Business
Penalty for Private Use: \$100

SPECIAL FOURTH-CLASS RATE
POSTAGE & FEES PAID
NASA
Permit No. G 27

NASA

POSTMASTER

If Undeliverable (Section 158
Postal Manual) Do Not Return
